

Dissertation zur Erlangung des Doktorgrades  
der Fakultät für Chemie und Pharmazie  
der Ludwig-Maximilians-Universität München

**Functional Characterization of  
the Presenilin Homologue SPE-4**

Aya Yamasaki-Meythaler  
aus  
Tokyo, Japan

2006

## Erklärung

Diese Dissertation wurde im Sinne von § 13 Abs. 3 bzw. 4 der Promotionsordnung vom 29. Januar 1998 von Herrn Prof. Dr. Christian Haass betreut und von Herrn Prof. Dr. Ralf-Peter Jansen vor der Fakultät für Chemie und Pharmazie vertreten.

## Ehrenwörtliche Versicherung

Diese Dissertation wurde selbständig, ohne unerlaubte Hilfe erarbeitet.

München, am 2.11.2006

.....  
(Aya Yamasaki-Meythaler)

Dissertation eingereicht am 5.11.2006

1. Gutachter: Prof. Dr. Ralf-Peter Jansen

2. Gutachter: Prof. Dr. Christian Haass

Mündliche Prüfung am 5.12.2006

For my parents and Tobi,  
who always believed in me.

The results in this dissertation are partially presented in the following publication:

**The GxGD Motif of Presenilin Contributes to Catalytic Function and Substrate Identification of  $\gamma$ -Secretase**

Aya Yamasaki, Stefan Eimer, Masayasu Okochi, Agata Smialowska, Christoph Kaether, Ralf Baumeister, Christian Haass, and Harald Steiner

*The Journal of Neuroscience*, April 5, 2006 • 26(14):3821–3828 • 3821

This publication is enclosed in the end of this dissertation.

## Abbreviations

<b>AD</b>	Alzheimer's Disease
<b>A<math>\beta</math></b>	Amyloid- $\beta$ peptide
<b>ADAM</b>	a disintegrin and metalloproteinase
<b>AICD</b>	APP intracellular domain
<b>APH-1</b>	anterior pharynx-defective phenotype
<b>APLP</b>	APP like protein
<b>APP</b>	$\beta$ -amyloid precursor protein
<b>BACE</b>	$\beta$ -site APP-cleaving enzyme
<i>C. elegans</i>	<i>Caenorhabditis elegans</i>
<b>CD44</b>	Cluster of differentiation 44
<b>CTF</b>	C-terminal fragment
<b>Egl</b>	egg laying defective
<b>FAD</b>	familial AD
<b>F-NEXT</b>	Flag tagged NEXT
<b>F-N<math>\beta</math></b>	Flag tagged N $\beta$
<b>GLP-1</b>	germ-line proliferation defective
<b>HEK</b>	human embryonic kidney
<b>HOP-1</b>	homologue of PS
<b>LIN-12</b>	abnormal cell lineage-12
<b>MEF</b>	mouse embryonic fibroblast
<b>N<math>\beta</math></b>	Notch $\beta$ peptide
<b>NCT</b>	Nicastrin
<b>NEXT</b>	Notch extracellular truncation
<b>NICD</b>	Notch intracellular domain
<b>NTF</b>	N-terminal fragment
<b>PEN-2</b>	PS enhancer-2
<b>PS</b>	Presenilin
<b>RNAi</b>	RNA interference
<b>S1, S2, S3, S4</b>	site 1, site 2, site 3, site 4
<b>sAPP</b>	soluble APP
<b>SEL-12</b>	suppressors and/or enhancers of lin-12
<b>SPE-4</b>	spermatogenesis defective-4
<b>SPP</b>	signal peptide peptidase
<b>SPPL</b>	SPP like protein
<b>sw</b>	Swedish mutant
<b>TACE</b>	TNF- $\alpha$ convertase

## Abbreviations

<b>TMD</b>	transmembrane domain
<b>TMIC</b>	transmembrane-intracellular
<b>TNF-<math>\alpha</math></b>	tumor necrosis factor- $\alpha$
<b>wt</b>	wild type

# Contents

<b>Abbreviations .....</b>	<b>5</b>
<b>Contents .....</b>	<b>7</b>
<b>1. Introduction.....</b>	<b>13</b>
<i>1.1 Histopathology of Alzheimer's disease .....</i>	<i>13</i>
<i>1.2 Genetics of Alzheimer's disease.....</i>	<i>15</i>
<i>1.3 Molecular biology of Alzheimer's disease .....</i>	<i>18</i>
1.3.1 $\beta$ -Amyloid precursor protein processing .....	18
1.3.2 $\gamma$ -Secretase.....	20
1.3.2.1 Notch and other substrates of $\gamma$ -secretase .....	21
1.3.2.2 Presenilin.....	23
1.3.2.3 Nicastrin.....	25
1.3.2.4 APH-1 and PEN-2.....	26
1.3.2.5 Assembly of the $\gamma$ -secretase complex .....	27
1.3.2.6 Substrate recognition of $\gamma$ -secretase.....	28
<i>1.4 The presenilin homologues in C. elegans .....</i>	<i>29</i>
<i>1.5 Aim of the study.....</i>	<i>30</i>
<b>2. Materials and Methods.....</b>	<b>31</b>
2.1 <i>Machines, hardware and software.....</i>	<i>31</i>
2.1.1 Equipment and instrument .....	31
2.1.2 Recombinant DNA techniques.....	32
2.1.3 Cell culture .....	32
2.1.4 Protein analysis .....	32
2.1.5 Immunofluorescence microscopy .....	33
2.2 <i>Recombinant DNA techniques .....</i>	<i>34</i>
2.2.1 Constructs and vectors .....	34
2.2.2 PCR.....	35
2.2.2.1 Primers and template cDNAs.....	35

## Contents

2.2.2.2 Reaction mixture .....	36
2.2.2.3 PCR program .....	37
2.2.2.4 Two-step PCR .....	37
2.2.3 Isolation and purification of PCR products .....	37
2.2.3.1 Materials .....	37
2.2.3.2 Agarose gel electrophoresis .....	38
2.2.3.3 Isolation and purification of PCR products from agarose gels .....	38
2.2.4 Enzymatic modification of cDNA fragments .....	38
2.2.4.1 Enzymes .....	38
2.2.4.2 Restriction enzyme treatment .....	39
2.2.4.3 Alkaline phosphatase treatment .....	39
2.2.4.4 Ligation of cDNA fragments .....	39
2.2.5 Transformation of <i>E. coli</i> .....	40
2.2.5.1 Materials .....	40
2.2.5.2 Preparation of competent cells .....	40
2.2.5.3 Transformation of <i>E. coli</i> .....	40
2.2.6 Preparation of plasmid DNA from <i>E. coli</i> .....	41
2.2.6.1 Materials .....	41
2.2.6.2 Small-scale plasmid DNA preparation (mini-prep) .....	41
2.2.6.3 Mini-prep DNA analysis .....	42
2.2.6.4 Large-scale plasmid DNA preparation (maxi-prep) .....	42
2.2.7 DNA sequencing .....	42
2.3 Cell culture and cell lines .....	43
2.3.1 Materials .....	43
2.3.2 Cell lines and medium .....	43
2.3.3 Cell culture .....	44
2.3.4 Transfection of mammalian cells .....	44
2.3.4.1 Materials .....	44
2.3.4.2 Transfection mixture .....	44
2.3.4.3 Transient cotransfection .....	44
2.3.4.4 Stable transfection .....	45
2.4 Antibodies .....	46
2.4.1 Monoclonal antibodies .....	46

2.4.2 Polyclonal antibodies .....	46
2.4.3 Secondary antibodies .....	47
2.5 Protein analysis.....	47
2.5.1 Total cell lysate .....	47
2.5.1.1 Materials.....	47
2.5.1.2 Cell lysate preparation .....	47
2.5.1.3 Protein quantitation .....	48
2.5.2 Membrane lysate .....	48
2.5.2.1 Materials.....	48
2.5.2.2 Preparation and solubilization of membrane .....	48
2.5.3 Immunoprecipitation.....	49
2.5.3.1 Materials.....	49
2.5.3.2 Co-immunoprecipitation from total cell lysate .....	49
2.5.3.3 Immunoprecipitation from conditioned medium .....	50
2.5.4 Cell-free AICD assay .....	51
2.5.4.1 Materials.....	51
2.5.4.2 Membrane preparation .....	51
2.5.4.3 AICD assay .....	52
2.5.5 In vitro $\gamma$ -secretase assay with C100.....	52
2.5.5.1 Materials.....	52
2.5.5.2 In vitro $\gamma$ -secretase assay.....	52
2.5.6 Sample preparation for SDS-PAGE.....	53
2.5.6.1 Materials.....	53
2.5.6.2 Sample preparation .....	53
2.5.7 SDS-Polyacrylamide gel electrophoresis (PAGE).....	54
2.5.7.1 Tris-Glycine gel .....	54
2.5.7.1.1 Materials.....	54
2.5.7.1.2 Gel preparation.....	55
2.5.7.1.3 Electrophoresis.....	55
2.5.7.2 Tris-Tricine gel .....	55
2.5.7.2.1 Materials.....	55
2.5.7.2.2 Electrophoresis.....	55
2.5.7.3 Modified Tris-Bicine urea gel.....	56

## Contents

2.5.7.3.1 Materials .....	56
2.5.7.3.2 Gel preparation.....	56
2.5.7.3.3 Electrophoresis.....	57
2.5.8 Western blotting.....	57
2.5.8.1 Materials .....	57
2.5.8.2 Blot.....	57
2.5.8.3 Blocking procedure.....	58
2.5.8.4 Primary antibody incubation.....	58
2.5.8.5 Secondary antibody incubation.....	58
2.5.8.6 Detection.....	58
2.6 Immunofluorescence microscopy.....	59
2.6.1 Cell preparation and transient cotransfection .....	59
2.6.2 Slide preparation .....	59
2.6.2.1 Materials .....	59
2.6.2.2 Cell fixation and permeabilisation .....	59
2.6.2.3 Antibody incubation and mounting .....	60
2.6.2.4 Microscopic analysis.....	60
2.7 Transgenic lines of <i>C. elegans</i> and rescue assays .....	60
<b>3. Results .....</b>	<b>62</b>
3.1 Functional characterization of SPE-4 .....	62
3.1.1 SPE-4 is the most distant PS homologue.....	62
3.1.2 SPE-4 wt is not incorporated to the $\gamma$ -secretase complex .....	63
3.1.3 SPE-4 does not process an APP-based substrate <i>in vitro</i> .....	65
3.1.4 The C-terminus of PS1 is required for $\gamma$ -secretase complex assembly.....	66
3.1.4.1 SPE-4 can undergo a partial $\gamma$ -secretase complex assembly by exchanging its C-terminus with that of PS1 .....	66
3.1.4.2 SPE-4/PS1c does not support $\gamma$ -secretase activity .....	68
3.1.4.3 Cells expressing SPE-4/PS1c are deficient in NCT maturation .....	69
3.1.4.4 Cells expressing SPE-4/PS1c show strongly decreased PEN-2 levels .....	71
3.1.5 The putative active site domain of SPE-4 may have proteolytic activity .....	74
3.1.5.1 Construction of an active site chimeric protein .....	74
3.1.5.2 PS1/SPE-4 <sub>6/7</sub> forms a $\gamma$ -secretase complex in PS1/2 <sup>-/-</sup> MEF cells .....	74

3.1.5.3 PS1/SPE-4 <sub>6/7</sub> supports $\gamma$ -secretase-mediated APP processing .....	78
<b>3.2 Identification of sequence requirements of PS for the <math>\gamma</math>-secretase substrate selectivity</b> .....	<b>80</b>
3.2.1 PS1/SPE-4 <sub>6/7</sub> does not support Notch processing in PS1/2 <sup>-/-</sup> MEF cells .....	80
3.2.2 TMD7 is the responsible domain for the Notch cleavage deficiency of PS1/SPE-4 <sub>6/7</sub> .....	84
3.2.2.1 Construction of PS1/SPE-4 <sub>6</sub> and PS1/SPE-4 <sub>7</sub> .....	84
3.2.2.2 PS1/SPE-4 <sub>6</sub> and PS1/SPE-4 <sub>7</sub> support processing of APP .....	85
3.2.2.3 PS1/SPE-4 <sub>7</sub> is inactive in Notch processing .....	88
3.2.3 A single amino acid at position x of the GxGD motif contributes to the Notch processing deficiency of PS1/SPE-4 <sub>7</sub> .....	89
3.2.3.1 The GxGD active site motif of SPE-4 contains a phenylalanine residue at position x instead of leucine.....	89
3.2.3.2 PS1/SPE-4 <sub>7</sub> F392L and PS1/SPE-4 <sub>7</sub> F392M support APP processing .....	90
3.2.3.3 PS1/SPE-4 <sub>7</sub> F392L and PS1/SPE-4 <sub>7</sub> F392M support Notch processing .....	92
3.2.4 Leucine at the position x of the GxGD motif is important for Notch processing in PS1 .....	93
<b>4. Discussion.....</b>	<b>96</b>
4.1 <i>A proteolytic function of SPE-4</i> .....	96
4.1.1 SPE-4 does not undergo $\gamma$ -secretase complex formation.....	96
4.1.2 The active site domain of SPE-4 supports APP processing.....	98
4.2 <i>Identification of sequence requirements of PS for <math>\gamma</math>-secretase substrate cleavage</i> ...	99
4.2.1 The active site of SPE-4 discriminates APP and Notch substrates.....	99
4.2.2 Identification of a critical amino acid within TMD7 at position x of the GxGD motif.....	99
4.2.3 Putative molecular basis of substrate discrimination by the GxGD motif.....	102
4.3 <i>Putative function of SPE-4 in C. elegans</i> .....	105
4.4 <i>Outlook</i> .....	106
<b>5. Summary.....</b>	<b>109</b>
<b>6. References.....</b>	<b>111</b>

Contents

**Acknowledgements ..... 122**

**Curriculum vitae ..... 123**

**Appendix: Publications ..... 125**

## 1. Introduction

### 1.1 Histopathology of Alzheimer's disease

Alzheimer's disease (AD) is the most common neurodegenerative disease in the world (Selkoe, 2001). It is estimated that about 18 million people worldwide are currently affected with AD. Since the major risk factor of AD is ageing, the number of patients is projected to be doubled by 2025 due to the prolongation of life expectancy. ([http://w3.whosea.org/en/Section1174/Section1199/Section1567/Section1823\\_8066.htm](http://w3.whosea.org/en/Section1174/Section1199/Section1567/Section1823_8066.htm))

The first AD patient, Auguste D., was reported by a German psychiatrist, Alois Alzheimer, in 1907 (Figure 1A and B). The symptoms described were progressive memory impairment, disordered cognitive function, altered behavior including paranoia, delusions, loss of social appropriateness and a progressive decline in language function (Alzheimer, 1907; Alzheimer et al., 1995).

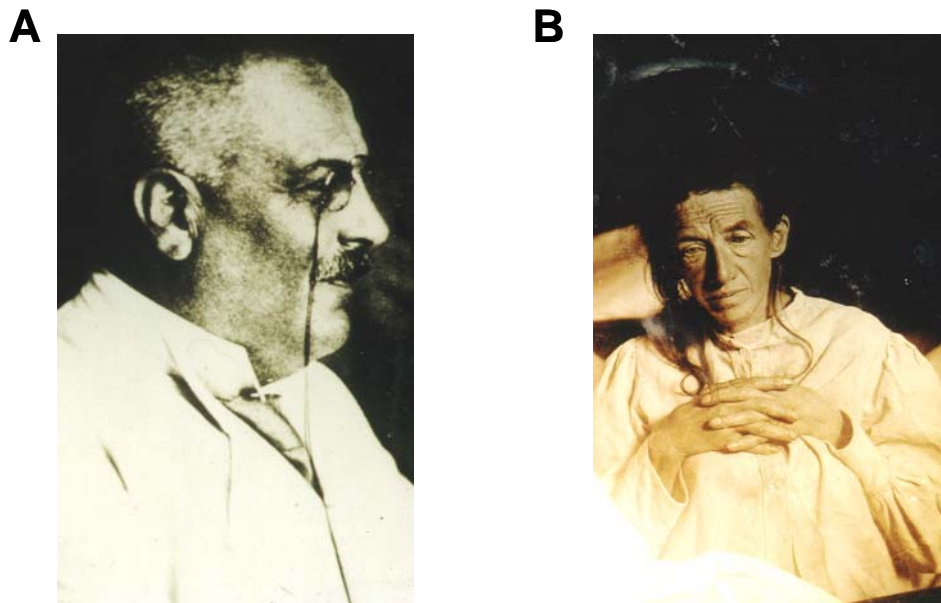


**Figure 1: Alois Alzheimer and the first AD patient, Augste D.**

Photographs showing Alois Alzheimer (A) and the first reported AD patient Augste D. (B).

## Introduction

Postmortem, the brain of the patient showed atrophy and “*many fibrils*” in the cell and “*military foci*” all over the cortex, especially in the upper layers, which were observed by silver staining. These lesions, that Alzheimer reported 100 years ago, are the pathological hallmarks of AD, which today are described as neuronal cell loss, the intracellular accumulation of neurofibrillary tangles and the extracellular deposition of senile plaque (Figure 2). The neurofibrillary tangles are composed of hyperphosphorylated forms of the tau protein (Grundke-Iqbal et al., 1986), which assembles into arrays of paired helical filaments (Figure 2A). Normally, tau is a soluble protein that promotes microtubule assembly and stabilization. In contrast, the pathological tau protein shows altered solubility properties, forms filamentous structures, is abnormally phosphorylated and has less affinity for microtubules (Grundke-Iqbal et al., 1986; Goedert et al., 1992). The neurofibrillary tangles are also observed in other neurodegenerative disorders, such as frontal temporal dementia or Pick’s disease. The second characteristic pathology of AD are the extracellular deposited senile plaques, which are usually found in brain regions such as hippocampus, amygdala, cortical and subcortical areas (Selkoe, 2001; LaFerla and Oddo, 2005). These plaques are primarily composed of A $\beta$  (amyloid  $\beta$ -peptide) (Glennner and Wong, 1984).

A $\beta$  is a highly hydrophobic peptide that aggregates to form oligomers. Several A $\beta$  species of 37 to 43 amino acids in length are found. Among those, the one ending at amino acid 42 (A $\beta$ 42), that is two amino acid residues longer than the much more abundantly produced A $\beta$ 40 species, is more hydrophobic and particularly prone to aggregation (Jarrett et al., 1993). Most plaques in the AD brain are “diffuse” plaques, in which the amyloid core is surrounded by few dystrophic dendrites and axons. There are also less frequent “neuritic” plaques (Figure 2B), in which dystrophic neurites are a prominent and commonplace feature. Since diffuse plaques are also found frequently in healthy aged brains, it is hypothesized that diffuse plaques are the precursor of neuritic plaques (Selkoe, 2001; LaFerla and Oddo, 2005).

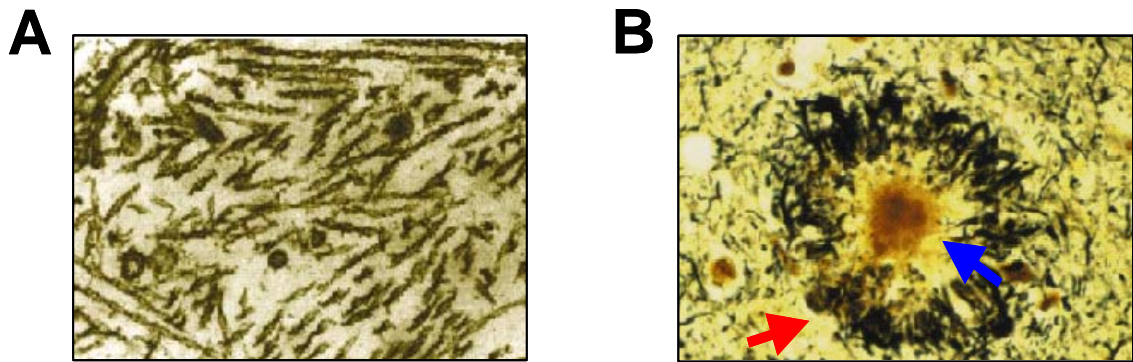


**Figure 2: Histopathology of Alzheimer's disease**

Typical histopathological hallmarks of AD. A: Neurofibrillary tangles. The hyperphosphorylated tau protein is assembled into paired helical filaments. B: Amyloid plaque. A $\beta$  deposition in the core of the plaque (blue arrow) and the dystrophic nerve terminals filled with deposits of hyperphosphorylated tau (red arrow). (Photos from Sisodia and St George-Hyslop, 2002)

## 1.2 Genetics of Alzheimer's disease

5-10% of AD cases are genetically inherited as familial AD (FAD) while the majority of the cases are sporadic (Selkoe, 2001). The onset age of the disease is earlier in FAD than the sporadic AD. Genetical analysis of pedigrees with FAD has revealed at least three AD-causing genes, APP ( $\beta$ -amyloid precursor protein), PS (presenilin) 1 and 2 (Goate et al., 1991; St George-Hyslop et al., 1992; Levy-Lahad et al., 1995; Rogaev et al., 1995; Sherrington et al., 1995). Most FAD cases are caused by mutations in the *PS1* gene whereas *APP* and *PS2* mutations are rather rare.

The APP gene is located on chromosome 21 and encodes for a protein of 770 amino acids. The gene can be alternatively spliced to encode for the protein of 695 or 751 amino acids APP variants. Both the 770 and 751 amino acids APP splice variants are ubiquitously expressed. Compared to these two splice variants, the 695 amino acid isoform is expressed at higher levels in neurons (Haass et al., 1991). APP is a type I transmembrane glycoprotein, which harbors the A $\beta$  peptide. Three different enzymes termed  $\alpha$ -,  $\beta$ -, and  $\gamma$ -secretase (see also chapter 1.3.2) process APP (Figure 3 and Figure 4). Interestingly, all the FAD missense mutations found in APP are located near to the three secretase-cleavage

## Introduction

sites suggesting that they cause AD by an alteration of the APP cleavage. The mutations predominantly localize close to the  $\gamma$ -secretase cleavage site and cause an increase in the production of A $\beta$ 42 peptides. There is also a rare mutation in a Swedish family that localizes to the  $\beta$ -secretase cleavage site. This mutation causes an increase in the production of all A $\beta$  peptides. Mutations in the vicinity of the  $\alpha$ -secretase cleavage site do not influence the processing of APP but rather alter the aggregation properties of A $\beta$  (Selkoe, 2001). The alteration of the normal APP expression is also known to cause AD as in Down's syndrome patients. These patients exhibit AD pathology due to the overexpression of APP because they possess three copies of chromosome 21, on which the APP gene is found (Head and Lott, 2004).

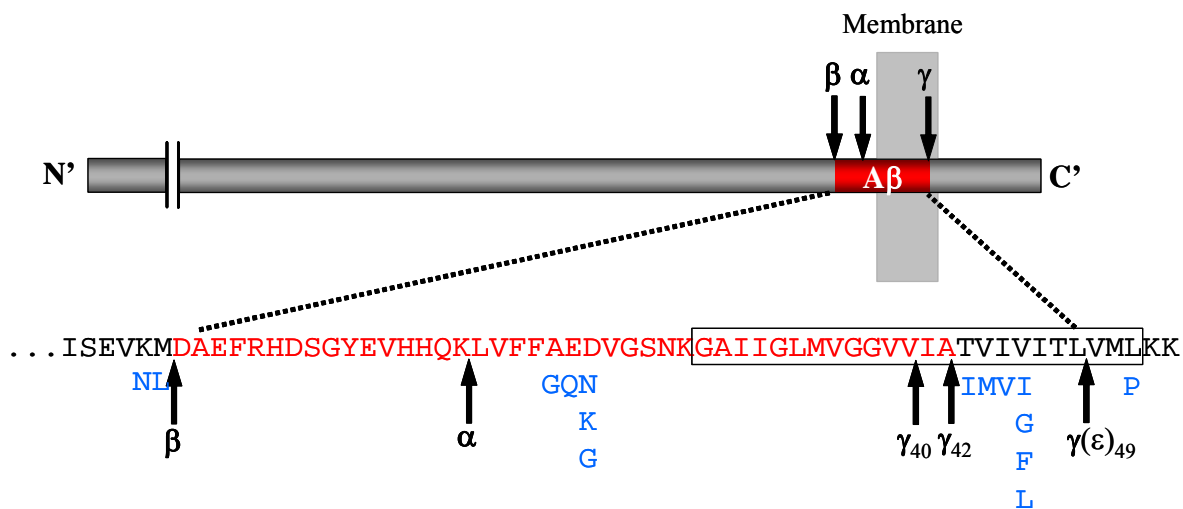


**Figure 3: Schematic representation of APP and the A $\beta$  domain**

The secretase cleavage sites of APP and the FAD mutations (indicated in blue) are shown. The predicted TMD is boxed. The A $\beta$  domain is displayed in red.

The genes encoding PS1 and PS2 are located on chromosome 14 and 1 respectively (Levy-Lahad et al., 1995; Sherrington et al., 1995). PS1 and PS2 are polytopic membrane proteins that share about 63% of sequence identity. To date, more than 150 of missense mutations are found in PS1 and 11 in PS2 (Alzheimer's Disease and Frontotemporal Dementia Mutation Database: <http://www.molgen.ua.ac.be/ADMutations/>). All the mutations lead to an increase in the production of A $\beta$ 42.

Apart from the three genes described above, the  $\epsilon$ 4 allele of apolipoprotein E has been identified as a major genetic risk factor for late-onset AD. Genetic analysis indicate that the inheritance of one or two  $\epsilon$ 4 alleles will increase the likelihood of developing AD leading to an earlier onset age compared to subjects harboring  $\epsilon$ 2 and/or  $\epsilon$ 3 alleles (Corder et al., 1993).

In contrary to the FAD cases, the reasons for the development of sporadic AD, which forms the majority of all AD cases, are unclear. The greatest risk factor of AD is ageing. However, the mechanism how ageing contributes to A $\beta$  deposition in the brain is not well established. It is discussed that a deficiency in A $\beta$  degradation (Yasojima et al., 2001) or an increase in  $\beta$ -secretase cleavage of APP (Holsinger et al., 2002; Yang et al., 2003) might cause sporadic AD. These observations suggest that the balance between generation and clearance of A $\beta$  is altered by ageing. This may result from an alteration of gene expression or from unknown factor(s) involved in A $\beta$  generation and clearance. Such alteration could also cause an acceleration of the A $\beta$  aggregation rate in the brain. In addition, if for example the  $\gamma$ -secretase activity was altered during ageing, it would surely influence not only A $\beta$  secretion but also intracellular signaling mediated by the intracellular domains that are generated by  $\gamma$ -secretase of all other  $\gamma$ -secretase substrates (see 1.3.2.1). Moreover, the difference in the levels of alteration of A $\beta$  generation and clearance may account for the difference in the onset age of the disease. As described above (see 1.1), diffuse senile plaques, which also exist in healthy-aged brains, are suggested to be precursors of neuritic senile plaques. If that was the case, all persons developing diffuse plaques in their brains would eventually get AD if they lived long enough (Thal et al., 2002). Further investigations are required for understanding the cause of sporadic AD.

## 1.3 Molecular biology of Alzheimer's disease

### 1.3.1 $\beta$ -Amyloid precursor protein processing

Cleavage of APP within the ectodomain by either  $\alpha$ - or  $\beta$ -secretase generates the membrane-bound APP C-terminal fragments, APP-CTF $\alpha$  or CTF $\beta$  (Figure 4). Following ectodomain shedding by  $\alpha$ - or  $\beta$ -secretase, the membrane-bound APP-CTFs are subsequently processed by  $\gamma$ -secretase within the transmembrane domain. The  $\alpha$ -secretase cleavage processes APP within the A $\beta$  domain between residues 16 and 17 of the A $\beta$  domain and thus precludes A $\beta$  generation. Therefore, this process is referred to as the “non-amyloidogenic pathway”. The combination of  $\alpha$ - and  $\gamma$ -secretase cleavage generates the AICD (APP intercellular domain) and releases soluble APP $\alpha$  (sAPP $\alpha$ ) and the p3 peptide. On the other hand,  $\beta$ -secretase cleaves APP at the beginning of the A $\beta$  domain resulting not only in AICD and sAPP $\beta$  but also in A $\beta$  peptide generation. Therefore this process is referred to as the “amyloidogenic pathway” (Figure 4). The  $\gamma$ -secretase cleavage site is located in the middle of APP transmembrane domain at the end of the A $\beta$  domain. Besides the  $\gamma$ -secretase cleavage site, there is another  $\gamma$ -secretase dependent cleavage site close to the end of the transmembrane domain of APP, which is referred to as the  $\epsilon$ -cleavage site (Weidemann et al., 2002) (Figure 3 and Figure 4). This  $\epsilon$ -cleavage site is analogous to the S3 cleavage site of another  $\gamma$ -secretase substrate, Notch (see also 1.3.2.1 and Figure 6). The AICD species starts from the  $\epsilon$ -cleavage site. So far, AICD starting from the  $\gamma$ -secretase cleavage site has not been found, whereas the longer intracellular A $\beta$  can be isolated from mammalian cells (Zhao et al., 2004; Qi-Takahara et al., 2005; Zhao et al., 2005; Kakuda et al., 2006). Thus,  $\epsilon$ -cleavage may precedes  $\gamma$ -cleavage. This hypothesis however is still under debate.

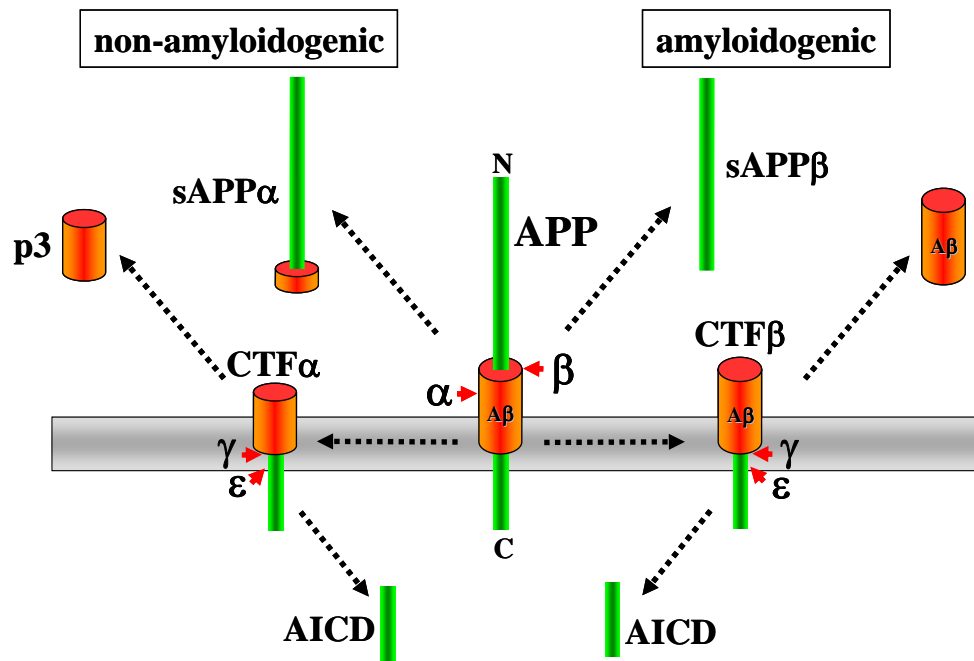


**Figure 4: APP processing**

In the non-amyloidogenic pathway, the large ectodomain of APP is cleaved by  $\alpha$ -secretase within the A $\beta$  domain that releases sAPP $\alpha$ . The membrane-bound APP-CTF $\alpha$  is further cleaved by  $\gamma$ -secretase within the transmembrane domain. This cleavage results in p3 and AICD generation. In the amyloidogenic pathway, APP is cleaved by the combination of  $\beta$ - and  $\gamma$ -secretase. These cleavages result in the generation of sAPP $\beta$ , A $\beta$  and AICD.

Ectodomain shedding of APP occurs primarily by  $\alpha$ -secretase, a type I membrane protein. Studies with protease inhibitors revealed that  $\alpha$ -secretase is a zinc metalloproteinase, and several members of ADAM (a disintegrin and metalloproteinase) family proteins, ADAM9, ADAM10 and ADAM17, which is also known as TACE (tumor necrosis factor- $\alpha$  convertase), were identified as  $\alpha$ -secretase (Buxbaum et al., 1998; Koike et al., 1999; Lammich et al., 1999).

BACE ( $\beta$ -site APP-cleaving enzyme)-1 has been identified as  $\beta$ -secretase. BACE-1 is a type I transmembrane protein, with aspartyl protease activity (Hussain et al., 1999; Sinha et al., 1999; Vassar et al., 1999; Yan et al., 1999; Lin et al., 2000). The BACE-1 knock out shows a complete absence of A $\beta$  generation suggesting that BACE-1 is the only protease mediating  $\beta$ -secretase activity (Cai et al., 2001; Luo et al., 2001).

### 1.3.2 $\gamma$ -Secretase

After ectodomain shedding of APP by either  $\alpha$ - or  $\beta$ -secretase, the resultant membrane-bound APP-CTF is cleaved by  $\gamma$ -secretase within the transmembrane domain.

$\gamma$ -Secretase is an unusual aspartyl protease occurring as a high molecular weight complex (Figure 5). PS was the first complex component to be identified in  $\gamma$ -secretase. The first hint that  $\gamma$ -secretase may be a complex was obtained from the observation that overexpression of PS in mammalian cells, causes a replacement of endogenous PSs, i.e. they disappear and cannot be detected anymore. It was speculated that there is a competition between exogenous and endogenous PS for limiting factors interacting with PS (Thinakaran et al., 1996; Thinakaran et al., 1997). Moreover, glycerol gradient experiments demonstrated that PS1 NTF and CTF co-fractionate in high molecular weight fractions (Capell 1998, Yu 1998). In addition, it has been found that  $\gamma$ -secretase activity is present in a high molecular weight fraction in a PS-dependent manner (Li 2000). Indeed, three proteins NCT (nicastrin) (Yu et al., 2000), APH (anterior pharynx-defective phenotype)-1 and PEN (PS-enhancer)-2 were identified as  $\gamma$ -secretase complex components (Francis et al., 2002; Goutte et al., 2002; Lee et al., 2002; Steiner et al., 2002) (Figure 5). Notably, it is known that PS1 and PS2 do not occur in the same complex (Yu et al., 1998; Steiner et al., 2002; Shirotani et al., 2004b). Edbauer et al (Edbauer et al., 2003) showed that when all four components were expressed together in yeast, which has no homologues of  $\gamma$ -secretase components and thus lacks  $\gamma$ -secretase activity, active  $\gamma$ -secretase was reconstituted. This suggests that these four components are necessary and sufficient for the activity of the enzyme. The apparent molecular mass of the complex is approximately 200 kDa. However, different molecular weights of the  $\gamma$ -secretase complex have been reported ranging from 250 to 2000 kDa, most likely depending on the analytical methods used (Capell et al., 1998; Yu et al., 1998; Li et al., 2000a; Steiner et al., 2002; Kimberly et al., 2003; Nyabi et al., 2003). It is still unclear which molecular mass an active  $\gamma$ -secretase complex has.

Because of the existence and requirement of four components for the  $\gamma$ -secretase activity, it is very difficult to analyze the individual function of the components of the complex. PS contains the catalytic center of  $\gamma$ -secretase with two critical aspartate residues (Wolfe et al., 1999a), and NCT was recently reported as the initial substrate recognition molecule (Shah

et al., 2005). Compared to PS and NCT, very little is known about the roles of APH-1 and PEN-2 in the complex in the mechanism of  $\gamma$ -secretase cleavage.

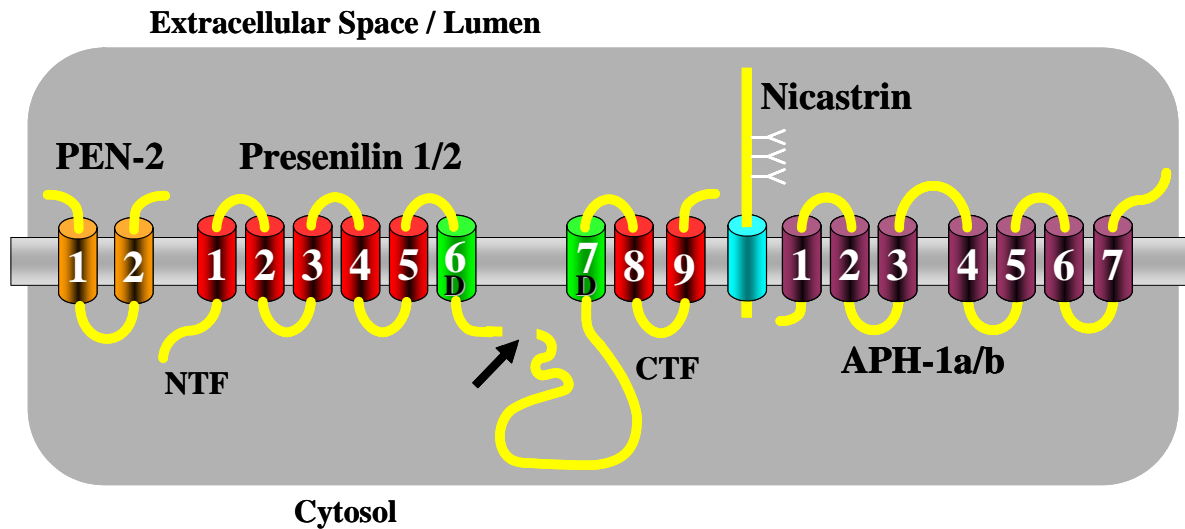


**Figure 5: The  $\gamma$ -secretase complex**

A schematic model of the  $\gamma$ -secretase complex composed of PS, NCT, APH-1 and PEN-2 is shown. TMDs 6 and 7 of PS, which harbor the two critical aspartates, are shown in green. The endoproteolytic cleavage site of PS is indicated with an arrow.

### 1.3.2.1 Notch and other substrates of $\gamma$ -secretase

Apart from APP, there is a growing number of type I transmembrane proteins that has been identified as substrates of  $\gamma$ -secretase such as APLP (APP like protein) 1 and 2 (Scheinfeld et al., 2002), Notch (1-4) receptors (Wong et al., 1997; Davis et al., 1998; Levitan and Greenwald, 1998; Qian et al., 1998; Berezovska et al., 1999; De Strooper et al., 1999; Donoviel et al., 1999; Herreman et al., 1999; Herreman et al., 2000; Nakajima et al., 2000; Struhl and Greenwald, 2001), Delta and Jagged (Ikeuchi and Sisodia, 2003; LaVoie and Selkoe, 2003), N- and E-cadherin (Georgakopoulos et al., 1999; Baki et al., 2001; Marambaud et al., 2002), ErbB4 (Ni et al., 2001), CD44 (Cluster of differentiation 44) (Lammich et al., 2002). Among these proteins, Notch is one of the most important and

## Introduction

well-studied substrate of  $\gamma$ -secretase. Notch functions as a receptor at the cell surface and mediates cell-cell signaling interactions to specify cell fates during development (Bray, 2006). The evidence that  $\gamma$ -secretase is involved in Notch processing was first indicated by genetic studies in *C. elegans* and *Drosophila* that showed the requirement of Notch signal transduction (Levitan and Greenwald, 1998; Struhl and Greenwald, 2001). Importantly, PS1 knockout mice or PS1/2 double knockout mice have defects reminiscent of Notch knockout phenotypes (Shen et al., 1997; Wong et al., 1997; De Strooper et al., 1998). The lethality of the PS knockout mice can be rescued by re-introduction of PS1 (Davis et al., 1998; Qian et al., 1998). Furthermore, PS-deficient cells show defects Notch processing (De Strooper et al., 1998; Song et al., 1999), and in addition,  $\gamma$ -secretase inhibitors block Notch processing (De Strooper et al., 1999). Moreover, it has been demonstrated that Notch interacts with PS (Ray et al., 1999).

Notch undergoes a proteolytic cascade like APP for its activation (Figure 6). Notch is first cleaved by furin in the *trans*-Golgi network at S1 during transport. The S1 cleavage generates a TMIC (transmembrane-intracellular) Notch, which interacts with ligands, Jagged and Delta. Upon the ligand interaction, TMIC undergoes a second cleavage at S2 mediated by TACE. Upon S2 cleavage, the ligand-bound ectodomain region is endocytosed into the ligand expressing cell and the NEXT (Notch extracellular truncation) fragment remains embedded in the membrane at the cell surface (Parks et al., 2000). NEXT is subsequently cleaved by  $\gamma$ -secretase at two sites S3 and S4. The cleavage at S3 releases the NICD (Notch intracellular domain) from the membrane. NICD translocates to the nucleus and interacts with transcription factors to regulate target genes (Jarriault et al., 1995; Schroeter et al., 1998). The S3 cleavage resembles the  $\epsilon$ -cleavage of APP, whereas the cleavage at S4, which occurs in the middle of the transmembrane domain and release N $\beta$  (Notch- $\beta$ ), an A $\beta$  like peptide, is analogous to the  $\gamma$ -cleavage site of APP (Okochi et al., 2002). Interestingly, similar to the processing of APP, an alteration of S4 cleavage is also observed in PS1 FAD mutant expressing cells and causes an increase of the ratio of longer species of N $\beta$  (N $\beta$ 25) against the major shorter N $\beta$  species (N $\beta$ 21), (Okochi et al., 2006).

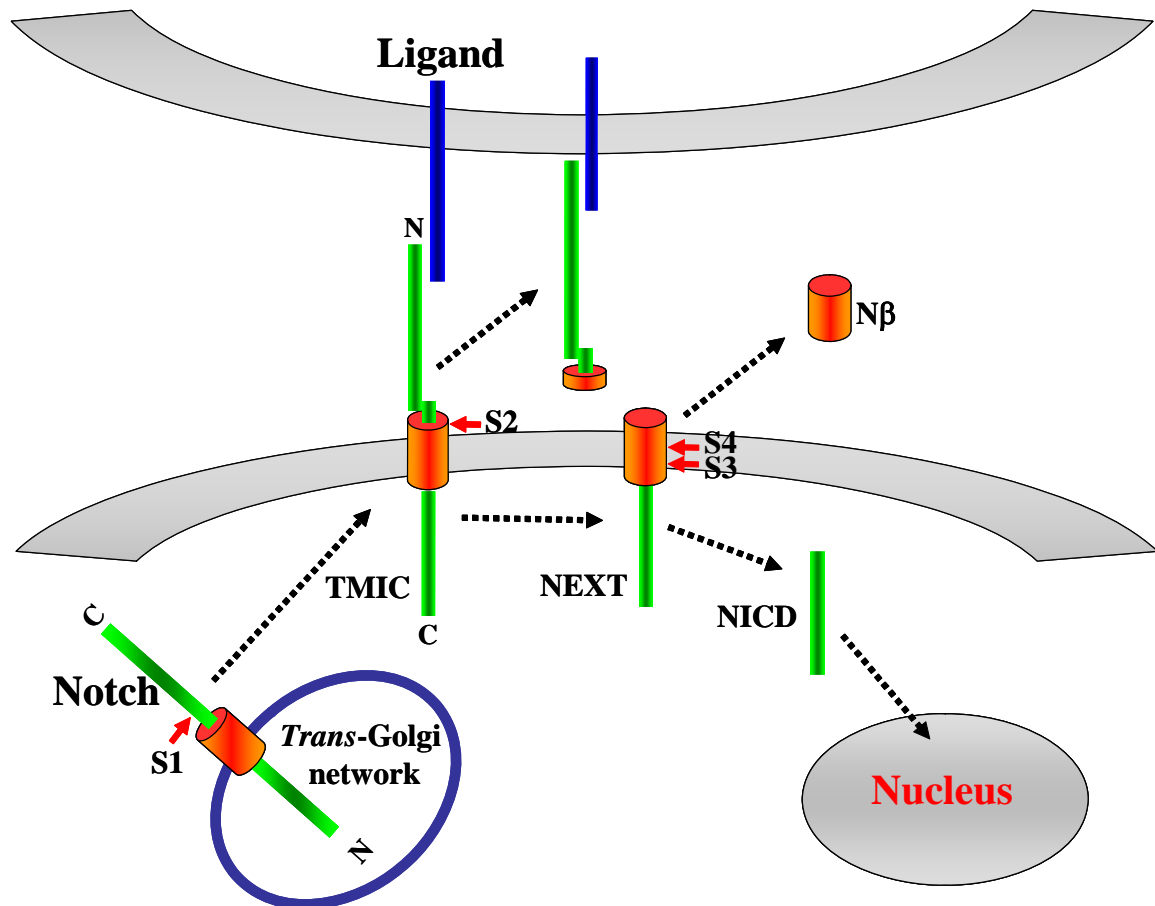


**Figure 6: Notch processing**

Notch is cleaved at four different cleavage sites, S1-S4. The cleavage at S1 takes place in the *trans*-Golgi network, and the subsequent cleavages occur upon the interaction between TMIC and ligand that is presented by neighboring cell. The S3 and S4 cleavages are dependent on  $\gamma$ -secretase. The S3 cleavage product, NICD, translocates to the nucleus where it is involved in transcriptional regulation. The N $\beta$  peptide, the analogue of A $\beta$ , is produced by S4 cleavage.

### 1.3.2.2 Presenilin

PSs (PS1 and PS2) are polytopic transmembrane proteins (Figure 5) that span the membrane 9 times (Kaether et al., 2004; Henricson et al., 2005; Laudon et al., 2005; Oh and Turner, 2005). PSs are endoproteolyzed within the large cytoplasmic loop (Figure 5, arrow) and exist as N-terminal fragment (NTF) and C-terminal fragment (CTF) in the cell (Thinakaran et al., 1996). These NTF and CTF form a heterodimer (Capell et al., 1998; Yu

## Introduction

et al., 1998; Saura et al., 1999), and this heterodimer form of PSs are more stable compared to the holoprotein (Ratovitski et al., 1997; Steiner et al., 1998). Endoproteolysis of PS is most likely an autocatalytic event. It was reported that endoproteolysis of PS1 or PS2 is blocked when one of its active aspartate is inactivated (Steiner et al., 1999b; Wolfe et al., 1999a). Because of the apparent correlation between endoproteolysis and proteolytic activity, it was further suggested that PS is a protease that activates itself by auto-cleavage. The observation that endoproteolysis of PS may be an auto-cleavage is further supported by the study of Edbauer and colleagues showing  $\gamma$ -secretase complex reconstitution in yeast, which has no homologues of  $\gamma$ -secretase complex components and lacks  $\gamma$ -secretase activity (Edbauer et al., 2003). Edbauer and colleagues demonstrated that PS1 NTF and CTF were generated by endoproteolysis upon co-expression with the other three components NCT, APH-1 and PEN2 in yeast. However, it was demonstrated that endoproteolysis of PS is not required for  $\gamma$ -secretase activity because there is a FAD deletion mutant that lacks exon 9 domain ( $\Delta$ exon9) of PS1 which encodes the endoproteolysis and which displays  $\gamma$ -secretase activity (Steiner et al., 1999a). In addition, other artificial mutations in PS such as several mutants of G384 undergo endoproteolysis but do not support proteolytic activity of  $\gamma$ -secretase (Steiner et al., 2000). Thus, the endoproteolysis of PS is most likely an auto-cleavage but does not initiate its catalytic activity.

The FAD mutations in PSs lead a small shift of APP cleavage at the  $\gamma$ -secretase cleavage site, which results in an increase in the ratio of A $\beta$ 42 to A $\beta$ 40 (Selkoe, 2001). Together with these findings, the severe impairment of A $\beta$  generation in cells derived from PS1 knockout mice (De Strooper et al., 1998) as well as the complete absence of A $\beta$  generation in PS1 and PS2 double knockout (Herreman et al., 2000; Zhang et al., 2000) suggested that PSs are directly involved in the  $\gamma$ -secretase cleavage or are the  $\gamma$ -secretase itself. Furthermore, studies with peptidomimetic inhibitors designed to mimic the A $\beta$ 42 cleavage site to inhibit the  $\gamma$ -secretase activity suggested that the  $\gamma$ -secretase is an aspartyl protease (Wolfe et al., 1999b). It was supported by the finding of two completely conserved aspartate residues within transmembrane domains (TMD) 6 and TMD7 in all PSs (Figure 5). The functional importance of these aspartate residues in PS1 and PS2 was demonstrated by Wolfe et al for PS1 and Steiner et al for PS2 (Steiner et al., 1999b; Wolfe et al., 1999a), showing that A $\beta$  generation was abolished when either of the two aspartates was mutagenized. Furthermore, it was shown that PS1 has sequence homology particularly

around the second aspartate in TMD7 with bacterial type 4 prepilin peptidase and contains a novel GxGD motif instead of the classical aspartyl protease consensus sequence D(T/S)G(T/S). This GxGD active site motif is very well conserved in all PSs (Steiner et al., 2000). Moreover, a cross-linking study and a pulldown assay using aspartic protease transition state analogue inhibitors that inhibit  $\gamma$ -secretase activity demonstrated a direct interaction between the inhibitor and PS (Esler et al., 2000; Li et al., 2000b; Beher et al., 2003). Taken together, these data provide strong evidence that PS is a novel GxGD-type aspartyl protease. Subsequent studies identified SPP (signal peptide peptidase) and SPPL (SPP-like peptidase) (Weihofen et al., 2002) apart from the type 4 prepilin peptidases (LaPointe and Taylor, 2000; Steiner et al., 2000; Weihofen and Martoglio, 2003) as members of GxGD-type aspartyl protease family. SPP catalyzes intramembrane proteolysis of signal peptides liberated from secretory preproteins. In humans, besides the clearance of signal peptides, SPP is also required for processing of the hepatitis C virus core protein (Weihofen et al., 2002). Recently, TNF $\alpha$  has been identified as a substrate for the SPP homologues SPPL2a and SPPL2b. Release of the TNF $\alpha$ -ICD triggering expression of interleukin-12 (Friedmann et al., 2004; Fluhrer et al., 2006; Friedmann et al., 2006). Interestingly, the membrane topology of SPP and SPPL are diametrical from that of PS. Therefore, their substrates are as well diametrical, i.e. type II instead of type I transmembrane proteins as in PS. Also, unlike PS, SPP and SPPL are not endoproteolysed and moreover function by themselves, whereas PS requires complex formation to become active. Thus, the GxGD active site motif defines a novel class of protease, cleaving its substrates within the membrane (PS, SPP, SPPLs) or at the cytosolic region near the membrane (type 4 prepilin peptidases).

### 1.3.2.3 Nicastrin

NCT is a type I transmembrane glycoprotein (Figure 5). It was identified as a protein that interacts with PS by co-immunoprecipitation studies in the mammalian cells (Yu et al., 2000). In addition, genetic studies in nematode *Caenorhabditis elegans* (*C. elegans*) showed that NCT is involved in the Notch signaling pathway (Goutte et al., 2000) and genetically interacts with SEL-12 (suppressor and/or enhancer of lin-12), a *C. elegans* PS homolog (Levitan et al., 2001). NCT has also been shown to interact with both  $\gamma$ -secretase

## Introduction

substrates, APP and Notch (Yu et al., 2000; Chen et al., 2001). NCT undergoes glycosylation within the secretory pathway to yield the mature complex-glycosylated form, which exists in the active  $\gamma$ -secretase complex (Edbauer et al., 2002; Leem et al., 2002; Tomita et al., 2002; Yang et al., 2002). The NCT function was not clear until recently, when Shah and co-workers (Shah et al., 2005) showed that the ectodomain of NCT can bind to ectodomain-shedded APP and Notch. This suggests that after the ectodomain shedding of the substrate, which is necessary for the further processing by  $\gamma$ -secretase (Struhl and Adachi, 2000), the stubs are recognized by NCT before  $\gamma$ -secretase cleavage occurs.

### 1.3.2.4 APH-1 and PEN-2

APH-1 and PEN-2 were identified by genetic screening for mutants which enhance the Notch signaling defect phenotype in *C. elegans* (Francis et al., 2002; Goutte et al., 2002). APH-1 is a multitransmembrane protein, which is predicted to span the membrane seven times (Fortna et al., 2004) (Figure 5). Co-immunoprecipitation and pull-down approaches revealed that APH-1 interact with PS NTF/CTF heterodimer and NCT in mammalian cells and *in vivo* (Lee et al., 2002). In humans, there are two homologues APH-1, APH-1a and APH-1b. Furthermore, there are two APH-1a splice variants reported, APH-1aL and APH-1aS. Like PS1 and PS2, the different APH-1 species do not occur in the same complex (Hebert et al., 2004; Shirotani et al., 2004b) suggesting that there are six distinct  $\gamma$ -secretase complexes with every possible combination of PS and APH-1 variants in human cells. In mice, which contain a third APH-1 homolog, APH-1c, there are eight complex possibilities (Hebert et al., 2004). However, whether there are any differences on the  $\gamma$ -secretase activity or any substrate preference of an individual  $\gamma$ -secretase complex is not well understood.

It has been demonstrated that the absence of APH-1 causes a decrease in the levels of the other  $\gamma$ -secretase complex components (Takasugi et al., 2003; Shirotani et al., 2004b; Ma et al., 2005; Serneels et al., 2005). This observation suggests that APH-1 stabilizes the  $\gamma$ -secretase complex. However, the APH-1 function for cleavage within an assembled complex is still unclear.

PEN-2 is a small (~10kDa) membrane protein with two transmembrane domains (Figure 5). It has been demonstrated that PEN-2 is involved in the initiation of PS endoproteolysis (Takasugi et al., 2003) and that is required for the stabilization of PS NTF and CTF (Hasegawa et al., 2004; Prokop et al., 2004) within the  $\gamma$ -secretase complex. However, it is still unclear whether and how PEN-2 contributes to the catalytic function of  $\gamma$ -secretase. Further studies are required to elucidate the functions of APH-1 and PEN-2.

### **1.3.2.5 Assembly of the $\gamma$ -secretase complex**

RNA interference (RNAi) studies have revealed that PS is stabilized as an un-cleaved holoprotein in the absence of PEN-2 (Luo et al., 2003; Takasugi et al., 2003; Prokop et al., 2004). Unlike nascent PS holoprotein, which is degraded rapidly (Steiner et al., 1998), the accumulated PS holoprotein under PEN-2-limiting conditions forms a stable high molecular weight complex together with NCT/APH-1. This indicates that PEN-2 is required to initiate the endoproteolysis of PS. The PS holoprotein accumulation is abolished when NCT or APH-1 has been knocked down together with PEN-2 suggesting that NCT and APH-1 function upstream of PEN-2. On the other hand, an overexpression of APH-1 increased the level of PS holoprotein, which was augmented by co-expression of APH-1 and NCT (Takasugi et al., 2003). This suggests that PS holoprotein is stabilized by APH-1 and NCT. Moreover, there is an evidence for a NCT/APH-1 subcomplex formation early during assembly (LaVoie et al., 2003; Morais et al., 2003; Shirotani et al., 2004a). These observations led to a model of  $\gamma$ -secretase complex assembly. According to this model, first NCT and APH-1 form a subcomplex that binds to the PS holoprotein and thereby stabilizes it. Then, PEN-2 elicits the final step of  $\gamma$ -secretase complex maturation by facilitating the endoproteolysis of PS (Figure 7). In addition, it has been demonstrated that the assembly of the  $\gamma$ -secretase complex is completed within the ER/early secretory compartments of the cells. Immediately after assembly of the last component, PEN-2, PS is endoproteolyzed, and the complex is released from the ER and targeted to late secretory compartments, including the plasma membrane, where it cleaves its substrates (Kaether et al., 2002; Capell et al., 2005).

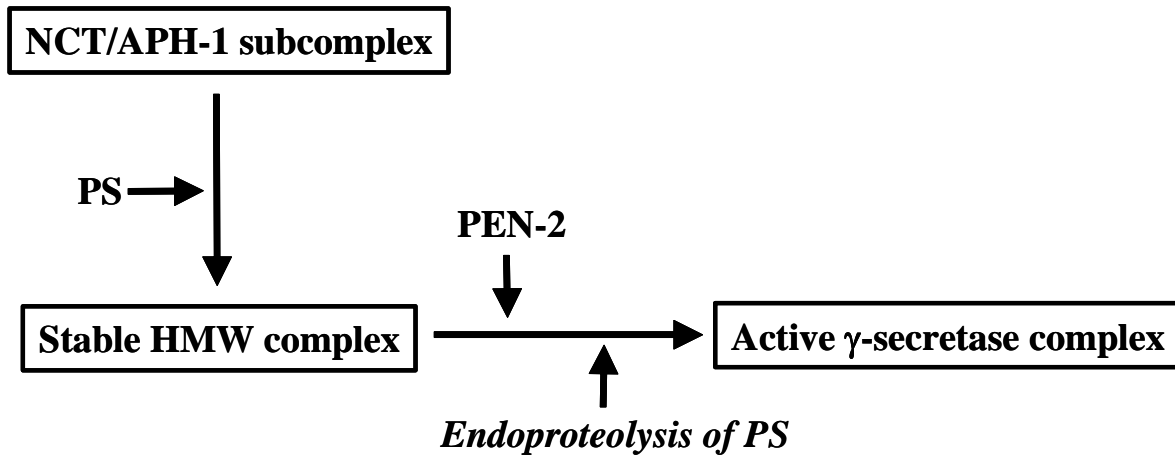


**Figure 7: Schematic model of  $\gamma$ -secretase assembly**

Schematic model of  $\gamma$ -secretase assembly and activation is shown. First, a NCT/APH-1 subcomplex is formed that stabilizes the PS holoprotein. In the next assembly step, PEN-2 binds to initiate PS endoproteolysis.

### 1.3.2.6 Substrate recognition of $\gamma$ -secretase

It has been demonstrated that ectodomain shedding of the substrate is required for the subsequent  $\gamma$ -secretase cleavage (Struhl and Adachi, 2000). In addition, a recent finding has demonstrated that the large ectodomain of NCT recognizes the ectodomain shedded-substrate (Shah et al., 2005). Furthermore, before the substrate cleavage occurs at the active site of  $\gamma$ -secretase, the substrate binds to the so-called “docking site”, which is different from the active site. The existence of such a binding site was shown by coisolation of APP-CTFs with  $\gamma$ -secretase using immobilized active site-directed inhibitors (Esler et al., 2002; Tian et al., 2002; Beher et al., 2003; Tian et al., 2003). It was shown recently that the docking site is located in PS very close to the active site within a distance of three amino acids (Kornilova et al., 2005). Together with the finding that NCT functions as an initial substrate receptor, the existence of the docking site at the PS NTF/CTF suggests a model of stepwise substrate transfer to the active site (Figure 8).

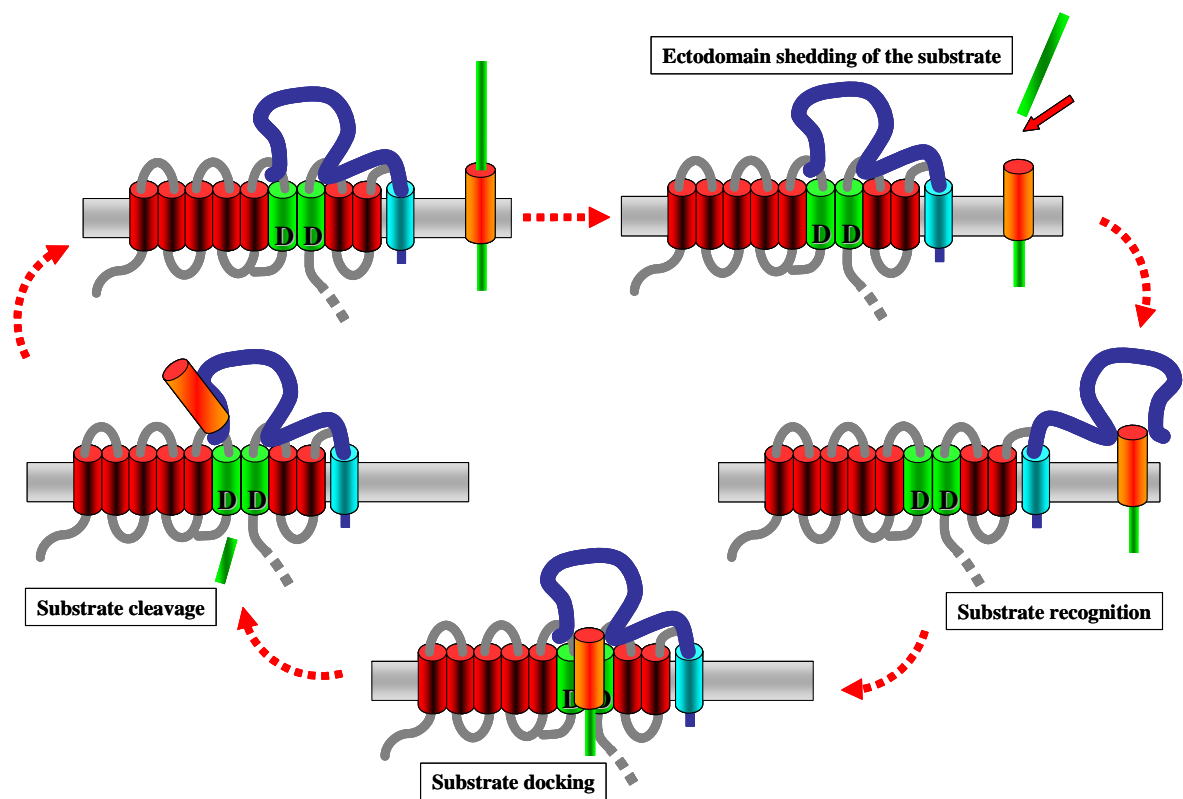


**Figure 8: The substrate recognition and docking sites of the  $\gamma$ -secretase complex**

The ectodomain-shedded substrate (for example APP-CTF $\beta$ ) is recognized first by NCT. It is subsequently bound at the docking site that exists in PS before it proceeds to the active site to get cleaved. This figure is modified from Shah et al., 2005.

#### 1.4 The presenilin homologues in *C. elegans*

Three PS homologues, SEL-12, HOP (homologue of PS)-1, and SPE (spermatogenesis defective)-4 have been identified in the nematode *C. elegans* (L'Hernault and Arduengo, 1992; Levitan and Greenwald, 1995; Li and Greenwald, 1997). It has been shown that *sel-12* activity facilitates the activity of LIN (abnormal cell lineage)-12 and GLP-1 (germ-line proliferation defective-1), the *C. elegans* Notch receptors. (Levitan and Greenwald, 1995; Baumeister et al., 1997). Genetic analysis showed that reducing or eliminating SEL-12 function causes an egg-laying defective (Egl) phenotype due to an abnormal vulva muscle development caused by a defect of Notch signaling. Interestingly, this Egl defect

## Introduction

phenotype can be rescued by human PS1 or PS2 (Levitan et al., 1996) suggesting that SEL-12 is a bona fide PS. The second PS homologue in *C. elegans*, HOP-1, has been shown to have a similar function in Notch signaling like SEL-12 (Li and Greenwald, 1997). HOP-1 is also able to rescue the Egl defect phenotype in the SEL-12 mutant worms. This observation suggests the functional redundancy of SEL-12 and HOP-1 like PS1 and PS2 in human. In contrast to the other two homologues, which are expressed somatically during all developmental stages in nearly all tissues (Levitan and Greenwald, 1995; Baumeister et al., 1997; Westlund et al., 1999), the third PS homologue in *C. elegans*, SPE-4, has a characteristic expression pattern. After hatching from the egg, *C. elegans* proceeds through four larval stages, which end in a molt, before it reaches adulthood. The *spe-4* gene is exclusively expressed during the larval stage 4 (L4) in spermatogenesis in the spermatheca, and it is involved in spermatogenesis where it is required for protein transport or sorting (L'Hernault and Arduengo, 1992; Arduengo et al., 1998). However, it has not been investigated whether SPE-4 functions as a protease like PS and whether it is involved in Notch signaling.

### 1.5 Aim of the study

The first aim of this study was to investigate the putative proteolytic function of *C. elegans* SPE-4, the most distant PS homologue. Despite its low homology to PS, the two functional aspartates within TMDs 6 and 7 and the GxGD active site motif as well as the PALP motif are conserved. These motifs are characteristic for PS-type aspartyl proteases and thus indicated that SPE-4 functions as a protease. Because it is difficult to analyze SPE-4 function directly in *C. elegans* due to its temporally and spatially limited expression and therefore low abundance, mammalian cells were employed to address the first aim. In addition, it was reasoned that, if SPE-4 had a proteolytic function, it might influence the substrate cleavage of  $\gamma$ -secretase due to its sequence differences to PS. The second aim of the study was therefore to investigate whether SPE-4 could be used as a tool to identify putative sequence requirements, in particular at the active site domain in TMDs 6 and 7 of PS, for  $\gamma$ -secretase activity by a domain-swapping approach.

## 2. Materials and Methods

### 2.1 Machines, hardware and software

#### 2.1.1 Equipment and instrument

Shaker (KM2)	Edmund Buhler
Rotator	Scientific Industries
Thermo-shaker (Thermomixer compact)	Eppendorf
Magnet stirler (IKAMAG RCT basic)	IKA Labortechnik
Vortex (Vortex Genie 2)	Scientific Industries
Microwave	Bosch
Heatblock	Liebig
Centrifuge for Eppendorf tubes (Biofuge pico)	Heraeus, Kendro
Centrifuge for Eppendorf tubes / 4°C (Biofuge pico)	Heraeus, Kendro
Centrifuge / 4°C / swing rotor (Megafuge 1.0R)	Heraeus, Kendro
Centrifuge / 4°C / swing rotor (Multifuge 3 L-R)	Heraeus, Kendro
Centrifuge (J2-21)	Beckman
Rotors: Type JA10, Type JA 20	Beckman
Ultracentrifuge (L7-55)	Beckman
Rotors: Ti 50, Ti 70	Beckman, Sorvall
Table ultracentrifuge (Optima Ultracentrifuge)	Beckman
Rotor: TLA-55	Beckman
pH-Meter (Inolab pH Level 1)	WTW
Scale (Analytical+ 200 g – 0,0001 g)	Ohaus
Scale (Standard 2000 g – 0,01 g)	Ohaus
Photometer (SmartSpec™ 3000)	Bio-Rad
Disposable cuvette (10 x 11x 45 mm)	Sarstedt
Quarz cuvette (10 x 10 x 45 mm)	Hellma
Incubator 37°C (Function line)	Heraeus
Incubator 56°C	Heraeus
Freezer -20°C	Elektrolux
Fridge 4°C	Elektrolux
Autoclave (Tuttnauer 3850 EL)	Systec
Water deionizing machine (Milli-Q academic)	Millipore
Pipettier (Accu-Jet)	Brand
Disposable pipets (25 ml, 10 ml, 5 ml)	Sarstedt
Pipette tips (1 ml, 200 µl, 20 µl, 2 µl)	Sarstedt
Disposable tubes (50 ml, 15 ml, 2 ml, 1,5 ml, 0,5 ml, 0,2 ml)	Sarstedt

### 2.1.2 Recombinant DNA techniques

PCR-machine (Mastercycler personal)	Eppendorf
37°C incubator (Function line)	Haereus
37°C shaker (Certomat BS-1)	B. Braun Biotech International
Elektrophoresis chamber (Model: B1; Model: B2)	Owl Separation Systems, Inc.
UV-Lamp (White/ Ultraviolet Transilluminator)	UVP
Camera (CCD Video Camera Module)	
Software (Quickstore pluss II)	MS Laborgeräte
Printer (p91)	Mitsubishi

### 2.1.3 Cell culture

Clean bench (Hera Safe HS12)	Heraeus, Kendro
CO <sub>2</sub> -Incubator (Hera cell)	Heraeus, Kendro
Gas burner (Vulcan)	Heraeus, Kendro
Centrifuge (Megafuge 1,0)	Heraeus, Kendro
Water bath (Typ 1002 ; Typ 1003)	GFL
Microscope (Wiloverts 10x 4/10/20)	Hund
N <sub>2</sub> -Tank (Chronos)	Messer Griesheim
Freezer -80°C (HFU 80)	Heraeus, Kendro
Cloning ring (8x8 mm)	Bellco
Sterile disposable pipettes (2 ml, 5 ml, 10 ml, 25 ml)	Sarstedt
Disposable tubes (15ml, 50ml)	Sarstedt
Pasteur pipettes	Sarstedt
Disposable culture dish (60 x 15 mm, 100 x 17 mm, 24 well, 12 well)	Nunc

### 2.1.4 Protein analysis

<b>Electrophoresis chambers:</b>	
Mini-PROTEAN 3 electrophoresis cell	Bio-Rad
X Cell Sure Lock™ Mini Cell	Novex, Invitrogen
Transfer chamber: Mini Trans-Blot transfer cell	Bio-Rad
Power supply (Power Pac 300)	Bio-Rad
Scanner: Epson Perfection 4870 Photo	Epson
Scanner: Umax Astra 1220S	
Film developer (Curix 60)	Agfa

### **2.1.5 Immunofluorescence microscopy**

Axioskop2 plus	Zeiss
63X/1.25 oil Plan-NEOFLUAR objective lens	Zeiss
Standard FITC und TRITC Fluoreszenzse filter sets	
AxioCam HRm camera	Zeiss
Software: Axio Vision Software Images	Zeiss
Adobe Photoshop 6.0	Adobe

## 2.2 Recombinant DNA techniques

### 2.2.1 Constructs and vectors

Constructs	Cloning sites	Vector	
PS1 wt	SmaI / NotI	pBY895	§1
PS1 wt	EcoRI	pcDNA3.1 zeo(+)	§2
His-PS1 wt	BamHI / XhoI	pcDNA4/His C	§3
PS1 D385N	EcoRI / BamHI	pcDNA3.1 zeo(-)	§4
PS1 D385A	BamHI / XhoI	pcDNA3.1 zeo(+)	§5
His-PS1 D385A	BamHI / XhoI	pcDNA4/His C	§6
SEL-12	SmaI / NotI	pBY895	§7
HOP-1	SmaI / NotI	pBY895	§8
SPE-4	SmaI / NotI	pBY895	§9
SPE-4 wt	HindIII / XhoI	pcDNA3.1 zeo(+)	
His-SPE-4 wt	EcoRV / XhoI	pcDNA4/His B	
SPE-4/PS1c	HindIII / XhoI	pcDNA3.1 zeo(+)	
His-SPE-4/PS1c	EcoRV / XhoI	pcDNA4/His B	
SPE-4/PS1 loop/PS1c	HindIII / XhoI	pcDNA3.1 zeo(+)	
His-PS1/SPE-4 <sub>6/7</sub>	EcoRI / XhoI	pcDNA4/His C	
His-PS1/SPE-4 <sub>6/7</sub> D394A	BamHI / XhoI	pcDNA4/His C	
His-PS1/SPE-4 <sub>6</sub>	BamHI / XhoI	pcDNA4/His C	
His-PS1/SPE-4 <sub>7</sub>	BamHI / XhoI	pcDNA4/His C	
His-PS1/SPE-4 <sub>7</sub> F392L	BamHI / XhoI	pcDNA4/His C	
His-PS1/SPE-4 <sub>7</sub> F392M	BamHI / XhoI	pcDNA4/His C	
His-PS1 L383F	BamHI / XhoI	pcDNA4/His C	
APPsw-6myc	Clal	pCS2	§10
F-NEXT		pcDNA3 hygro(+)	§11

**Table 1: cDNA constructs**

The overview of the constructs and the vectors. Restriction enzyme sites which were used to clone the constructs into the respective vectors are also indicated.

§1, 7, 8 and 9: The *sel-12* cDNA (GenBank accession number AF171064) was amplified by PCR from a *C. elegans* mixed stage cDNA library (provided by Bob Barstead) and subcloned as a SmaI/NotI fragment under the control of a 2.8 kb *sel-12* promoter fragment starting at the translational start ATG of *sel-12* to generate pBY895 (Wittenburg et al., 2000). PCR-amplified cDNAs encoding HOP-1 (amplified from the *C. elegans* mixed stage cDNA library), SPE-4 (provided by Dr. Steve L'Hernault) and PS1 were subcloned into pBY895 as SmaI/NotI fragments replacing the *sel-12* cDNA thus placing them under the control of the *sel-12* promoter. Those constructs were provided by Dr. Stefan Eimer.

§2~6: These constructs were provided by Dr. Harald Steiner.

§10: This construct was provided from Dr. Alison Goate (Hecimovic et al., 2004).

§11: NEXT construct, which was provided from Dr. Raphael Kopan (Kopan et al., 1996), was modified by Dr. Masayasu Okochi (Okochi et al., 2002).

## 2.2.2 PCR

Each cDNA fragment was amplified by PCR. Template cDNA, forward and reverse primers (Table 1) and dNTPs were mixed together with PCR reaction buffer and Pwo DNA polymerase (see 2.2.2.2), and the PCR was carried as described in 2.2.2.3.

### 2.2.2.1 Primers and template cDNAs

Construct	Primer pairs	cDNA template
SPE-4 wt	F: 5' CCAAGCTTTGTCTAAAAATGGACACC CTTCGATCGATTTCTAGCGAATTAG-3' R: 5' -CCGCTCGAGTCATCCGTAAAGTTGCTC-3'	SPE-4
His-SPE-4 wt	F: 5' -GATATCGACACCCCTTCGATCGATTTCT-3' R: 5' -CCGCTCGAGTCATCCGTAAAGTTGCTC-3'	SPE-4
SPE-4/PS1c	F: 5' -CCAAGCTTTGTCTAAAAATGGACACC TTCGATCGATTTCTAGCGAATTAG-3' R: 5' -GGTGATGGAGATCGGCAGAGCAGG-3'	SPE-4 wt
	F: 5' -CCTGCTCTGCCGATCTCCATCACC-3' R: 5' -CGCCTCGAGCTAGATATAAAATTG-3'	PS1 wt
His-SPE-4/PS1c	F: 5' -GATATCGACACCCCTTCGATCGATTTCT-3' R: 5' -CCGCTCGAGTCATCCGTAAAGTTGCTC-3'	SPE-4/PS1c
SPE-4/PS1 loop/PS1c	F: 5' -CCAAGCTTTGTCTAAAAATGGACACC TTCGATCGATTTCTAGCGAATTAG-3' R: 5' -GTGGACCTTTTCGGACATAAAAACGGCAAAGAG-3'	SPE-4/PS1c
	F: 5' -CTCTTTGCCGTTTTATGTCCGAAAGGTCCAC-3' R: 5' -CTCCAAAGCCGAGACGTACTCCCTTTTCCTC-3'	PS1 wt
	F: 5' -GAGGAAAGGGGAGTACGTCTCGGCTTTGGAG-3' R: 5' -CGCCTCGAGCTAGATATAAAATTG-3'	SPE-4/PS1c
His-PS1/SPE-4 <sub>6/7</sub>	F: 5' -CCGAATTC AAGAAAGAACCCTCAA-3' R: 5' -CAATCCAGAGAACAACCACGCAGTCCATTC-3' F: 5' -GAATGGACTGCGTGGTTTTGTCTCTGGATTG-3' R: 5' -CTGTTGCTGAGGCTTTACCAATCAGAAGACTG-3'	PS1 wt SPE-4/PS1 loop/PS1c
	F: 5' -CAGTCTTCTGATTGGTAAAGCCTCAGCAACAG-3' R: 5' -CGCCTCGAGGCAAATATGCTAGATATA-3'	PS1 wt
His-PS1/SPE-4 <sub>6/7</sub> D394A	F: 5' -CCGGATCCACAGAGTTACCTGCACC-3' R: 5' -GAAGACGAAAGCTCCAAAGC-3' F: 5' -GCTTTGGAGCTTTTCGTCTTC-3' R: 5' -CGCCTCGAGGCAAATATGCTAGATATA-3'	His-PS1/SPE-4 <sub>6/7</sub>
His-PS1/SPE-4 <sub>6</sub>	F: 5' -CCGGATCCACAGAGTTACCTGCACC-3' R: 5' -GTGGACCTTTTCGGACATAAAAACGGCAAAGAG-3' F: 5' -CTCTTTGCCGTTTTATGTCCGAAAGGTCCAC-3' R: 5' -CGCCTCGAGGCAAATATGCTAGATATA-3'	His-PS1/SPE-4 <sub>6/7</sub> PS1 wt

Construct	Primer pairs	cDNA template
His-PS1/SPE-4 <sub>7</sub>	F: 5' -CCGGATCCACAGAGTTACCTGCACC-3'	PS1 wt
	R: 5' -CTCCAAAGCCGAGACGTACTCCCCTTTCCTC-3'	
	F: 5' -GAGGAAAGGGGAGTACGTCTCGGCTTTGGAG-3'	His-PS1/SPE-4 <sub>6/7</sub>
	R: 5' -CGCCTCGAGGCAAATATGCTAGATATA-3'	
His-PS1/SPE-4 <sub>7</sub> F392L (§1)	F: 5' -CCGGATCCACAGAGTTACCTGCACC-3'	His-PS1/SPE-4 <sub>7</sub>
	R: 5' -GAAATCTCCAAGCCGAGACGTACTCCCCTTTC-3'	
	F: 5' -CGTCTCGGCTTGGGAGATTTTCGTCTTCTACAGT-3'	
	R: 5' -CGCCTCGAGGCAAATATGCTAGATATA-3'	
His-PS1/SPE-4 <sub>7</sub> F392M (§2)	F: 5' -CCGGATCCACAGAGTTACCTGCACC-3'	His-PS1/SPE-4 <sub>7</sub>
	R: 5' -GAAATCTCCCATGCCGAGACGTACTCCCCTTTC-3'	
	F: 5' -CGTCTCGGCATGGGAGATTTTCGTCTTCTACATG-3'	
	R: 5' -CGCCTCGAGGCAAATATGCTAGATATA-3'	
His-PS1 L383F	F: 5' -CCGGATCCACAGAGTTACCTGCACC-3'	PS1 wt
	R: 5' -GAAAATGAAATCTCCAAATCCAAGTTTTACTCC-3'	
	F: 5' -GGAGTAAACTTGGATTTGGAGATTTTCATTTTC-3'	
	R: 5' -CGCCTCGAGGCAAATATGCTAGATATA-3'	

**Table 2: Primers and cDNA templates used**

Primer pairs, forward primer (F) and reverse primer (R), and cDNA templates, which were used for PCR to generate the constructs, are shown.

§1 and 2 were generated by Dr. Stefan Eimer.

### 2.2.2.2 Reaction mixture

cDNA template	1µl
Forward primer (1 µg/µl)	1µl
Reverse primer (1 µg/µl)	1µl
10xPCR reaction buffer complete (Peq Lab)	10µl
dNTPs (10 mM, Roche)	2µl
PWO DNA polymerase (1 U/µl, Peq Lab)	2.5µl
dH <sub>2</sub> O	82.5µl
Final volume:	100µl

### 2.2.2.3 PCR program

94°C	2 min	
94°C	15 seconds	10 cycles
48°C	30 seconds	
72°C	1 min	
94°C	15 seconds	15 cycles
55°C	30 seconds	
72°C	1 min	
72°C	7 min	
4°C	∞	

### 2.2.2.4 Two-step PCR

Two-step PCR was performed to introduce mutation or to replace domain(s) in the construct. The first PCR was performed using indicated primer pairs (see 2.2.2.1). The PCR products were isolated and purified as described in 2.2.3. Aliquot of purified PCR products were mixed (1:1) and this mixture was used as the cDNA template for the second PCR. The second PCR was performed using the outer primer pairs.

## 2.2.3 Isolation and purification of PCR products

### 2.2.3.1 Materials

**TBE-buffer:**

9 mM Tris-base, 2 mM EDTA in dH<sub>2</sub>O

**6x DNA-loading buffer:**

30% Glycerol, 0.25% Bromophenolblue and 0.25% Xylenecyanol FF in dH<sub>2</sub>O

Agarose NA

Amersham Biosciences

1 kb DNA ladder

Gibco Invitrogen Corporation

Nucleo Spin Extraction Kit

Macherey-Nagel

### 2.2.3.2 Agarose gel electrophoresis

20  $\mu$ l of 6x DNA-loading buffer was added into 100  $\mu$ l PCR products, loaded on 1% Agarose in TBE-buffer and 0.2  $\mu$ g/ml Ethidiumbromide, and were separated by electrophoresis. 1 kb DNA ladder was applied in parallel to the PCR products. Electrophoresis was carried out by constant voltage at 150 volt.

### 2.2.3.3 Isolation and purification of PCR products from agarose gels

The expected size of cDNA band was confirmed under the UV lamp, cut out and transferred into an Eppendorf cup. cDNA fragments were extracted and purified from agarose gel using Nucleo Spin Extraction Kit at final volume 20-30  $\mu$ l. Isolated and purified cDNA fragments were either used as template cDNA for the second PCR, if necessary, or proceeded to the enzyme treatment steps.

## 2.2.4 Enzymatic modification of cDNA fragments

### 2.2.4.1 Enzymes

#### **Restriction enzymes:**

HindIII (10 U/ $\mu$ l)	MBI Fermentas
XhoI (10 U/ $\mu$ l)	MBI Fermentas
EcoRI (10 U/ $\mu$ l)	MBI Fermentas
BamHI (10 U/ $\mu$ l)	MBI Fermentas

#### **Alkaline phosphatase:**

Shrimp alkaline Phosphatase (SAP; 1 U/ $\mu$ l, )	Roche
---	-------

#### **Ligase:**

T4 DNA ligase (5 U/ $\mu$ l)	Roche
------------------------------	-------

#### **2.2.4.2 Restriction enzyme treatment**

Purified cDNA fragments were digested by the indicated restriction enzymes (see 2.2.1). Total amount of cDNA fragment (20 µl), 10 U of each enzyme and reaction buffer from the manufacture, adjusted the volume to 30 µl with dH<sub>2</sub>O, were mixed and incubated overnight at 37°C. 5 µg of vectors were also digested by the corresponding enzymes for 2 h at 37°C. After the reaction, cDNA fragments were isolated by agarose electrophoresis (see 2.2.3.2) and purified with Nucleo Spin Extraction kit (see 2.2.3.3).

#### **2.2.4.3 Alkaline phosphatase treatment**

To avoid self-ligation, the linearized vectors were dephosphorylated by SAP (see 2.2.4.1) before ligation. 1 U of SAP per 10-15 µg of vector fragment was added with reaction buffer from the manufacture. The mixture was incubated at 37°C for 1 h and SAP was deactivated by boiling the mixture at 65°C for 10 min.

#### **2.2.4.4 Ligation of cDNA fragments**

Ligation was performed to insert cDNA fragments into a vector. 200-300 ng vector, 0.5-1 µg cDNA fragment, 5 U T4 ligase and reaction buffer from the manufacture were mixed with dH<sub>2</sub>O at the final volume of 20 µl. The ligation mixture was incubated for 1 h at room temperature. 10 µl of the ligation mixture was used for *E. coli* transformation (see 2.2.5).

## 2.2.5 Transformation of *E. coli*

### 2.2.5.1 Materials

**LB medium (Low Salt Luria-Bertani Medium):**

1% Tryptone, 0.5% Yeast Extract, 0.5% NaCl in dH<sub>2</sub>O (adjust pH to 7.0)  
(Autoclaved at 120°C/1.2 bar for 20 min)

**LB agarose plates with or without ampicillin:**

LB medium, 1.5% Agarose, (100 µg/ml ampicillin)  
(Autoclaved at 120°C/1,2 bar for 20 min)

**Transformation buffer:**

50 mM CaCl<sub>2</sub>, 15% Glycerol, 10 mM PIPES pH 6.6

**Competent *E. coli* strain:**

DH5α

### 2.2.5.2 Preparation of competent cells

Overnight DH5α culture in LB medium was adjusted to OD<sub>600</sub>=0.2 by dilution with fresh LB medium. 5 ml of OD adjusted DH5α was added into 400 ml fresh LB medium and further cultured for 2-3 h at 37°C by shaking. When the density of the cells become OD<sub>600</sub>=0.2, the culture was chilled on ice for 10 min, then centrifuged at 1500xg for 10 min at 4°C. The cell pellet was suspended in 200 ml of transformation buffer (see 2.2.5.1), and was centrifuged again at 1500xg for 10 min at 4°C after chilled on ice for 20 min. The cell was suspended once again in 20 ml of transformation buffer. Aliquots of the suspension were frozen in liquid N<sub>2</sub> and stored at -80°C in the freezer.

### 2.2.5.3 Transformation of *E. coli*

100 µl of competent cells were added to the ligation mixture (see 2.2.4.4) and incubated for 20 min on ice. Heat shock treatment of the *E. coli* / ligation mixture was done at 42°C for 1 min. 1 ml of fresh LB medium was added into the mixture and incubated at 37°C for 1 h with shaking. The mixture was centrifuged at 16,000xg for 1 min and the pellet was re-suspended with 100-200 µl of LB medium and was plated onto LB-agarose plate containing 100 µg/ml ampicillin. After incubation at 37°C overnight, colonies were picked,

inoculated into 2 ml of fresh LB medium containing ampicillin and incubated overnight at 37°C. 1.5 ml of the overnight culture was used for mini prep (see 2.2.6.2).

## 2.2.6 Preparation of plasmid DNA from *E. coli*

### 2.2.6.1 Materials

**LB medium:**

See 2.2.5.1

**TENS buffer:**

10 mM Tris pH 8.0, 1 mM EDTA pH 8.0, 0.1N NaOH, 0.5% SDS in dH<sub>2</sub>O

**NaOAc buffer:**

3 M NaOAc in dH<sub>2</sub>O (adjust pH to 5.2)

**RNAse (DNAse-free):**

10 mg/ml RibonucleaseA (RNAse; Sigma) in 10 mM Tris pH 7.5, 10 mM NaCl  
Solved for 15 min at 100°C and cooled down slowly to room temperature.

Stored at -20 °C.

**TE buffer**

10 mM Tris pH7.6, 1 mM EDTA pH8.0 in dH<sub>2</sub>O

Nucleobond AX 500 Kits

Macherey-Nagel

### 2.2.6.2 Small-scale plasmid DNA preparation (mini-prep)

Plasmid DNA transformed in *E. coli* was isolated by the alkaline-lysis method from *E. coli*. 1.5 ml of overnight *E. coli* culture in LB medium (see 2.2.5.3) was collected into Eppendorf tube and centrifuged for 1 min at 16,000xg. The supernatant was gently discarded leaving 50-100 µl with cell pellet. The *E. coli* pellet was resuspended with leftover supernatant by vortexing, mixed well with 300 µl TENS buffer (see 2.2.6.1) and incubated for 5 min on ice. The suspension was neutralized by adding 150 µl 3 M NaOAc (see 2.2.6.1), and the insoluble fraction was removed by centrifugation for 5 min at 16,000xg. Supernatant was transferred into a fresh tube and plasmid DNA and RNA was precipitated by mixing with ice-cold 100% ethanol. Precipitated plasmid DNA and RNA was centrifuged for 10 min at 16,000xg. The pellet was rinsed once with ice-cold 70% ethanol, dried and solved in 27 µl TE buffer (see 2.2.6.1) with 3 µl RNAse solution.

### **2.2.6.3 Mini-prep DNA analysis**

3 µl of mini-prep DNA was treated with restriction enzymes as described above (see 2.2.4.2) to identify positive clones. After the restriction digest, the DNA fragments were separated by agarose electrophoresis (see 2.2.3.2). One of typically several positive clones containing the predicted size of insert cDNA fragment was selected and used for large-scale DNA preparation (see 2.2.6.4).

### **2.2.6.4 Large-scale plasmid DNA preparation (maxi-prep)**

5-10 µl of the leftover overnight culture from a positive *E. coli* clone was inoculated in 200 ml of fresh LB ampicillin medium (see 2.2.5.1), and cultured at 37°C overnight by shaking. Plasmid DNA was isolated and purified from the *E. coli* overnight culture using Nucleobond AX 500 Kits following the protocol from the manufacture. Plasmid DNA was resuspended in 200 µl TE buffer (see 2.2.6.1). 2 µl of aliquot was diluted in 600 µl TE and carried out for measurement of DNA concentration by photometer at OD260.

### **2.2.7 DNA sequencing**

All cDNA constructs were confirmed by sequencing by GATC Biotech AG (Konstanz, Germany).

## 2.3 Cell culture and cell lines

### 2.3.1 Materials

**Medium:**

Dulbecco's modified Eagle's medium (DMEM) Gibco Invitrogen Corporation

**Supplements:**

Fetal bovine serum Gibco Invitrogen Corporation

Glucose Gibco Invitrogen Corporation

**Antibiotics:**

Penicillin/streptomycin (PS) Gibco Invitrogen Corporation

G418 Gibco Invitrogen Corporation

Zeocin invitrogen

Hygromycin B invitrogen

**Trypsin-EDTA** Gibco Invitrogen Corporation

**PBS:**

140 mM NaCl, 10 mM Na<sub>2</sub>HPO<sub>4</sub> 2H<sub>2</sub>O, 1.75 mM KH<sub>2</sub>PO<sub>4</sub>, 2.7 mM KCl

### 2.3.2 Cell lines and medium

Cell lines	Antibiotics
PS1/2 <sup>-/-</sup> MEF	PS/G418
HEK293/sw	PS/G418
PS1 wt/HEK293/sw	PS/G418/zeocin
PS1 D385N/HEK293/sw	PS/G418/zeocin
SPE-4 wt/HEK293/sw	PS/G418/zeocin
His-SPE-4 wt/HEK293/sw	PS/G418/zeocin
SPE-4/PS1c/HEK293/sw	PS/G418/zeocin
His-SPE-4/PS1c/HEK293/sw	PS/G418/zeocin
His-PS1 wt/HEK293/sw	PS/G418/zeocin
His-PS1 L383F/HEK293/sw	PS/G418/zeocin
F-NEXT/His-PS1 wt/HEK293/sw	PS/G418/zeocin/hygromycin B
F-NEXT/His-PS1 L383F/HEK293/sw	PS/G418/zeocin/hygromycin B

### 2.3.3 Cell culture

Mouse embryonic fibroblast (MEF) cells derived from PS1/2 double knockout (PS1/2<sup>-/-</sup>) mouse (Herreman et al., 1999) were cultured in DMEM supplemented with 10% fetal bovine serum, 2 mM glucose, 1% of penicillin/streptomycin and 200 µg/ml G418, under 5% CO<sub>2</sub> at 37°C. For inoculation, the cells were washed once with autoclaved PBS, trypsinized for 5 min and an appropriate amount of cells was spread in fresh medium.

Human embryonic kidney (HEK) 293 cells stably expressing human APP carrying the Swedish mutation (HEK293/sw) (K595N and M596L double mutations in APP<sub>695</sub> variant) (Citron et al., 1992) were cultured and spread as MEF cells.

### 2.3.4 Transfection of mammalian cells

#### 2.3.4.1 Materials

**Medium:**

OptiMEM

Gibco Invitrogen Corporation

**Transfection reagent:**

Lipofectamine 2000

Invitrogen

#### 2.3.4.2 Transfection mixture

<b>Culture plate</b>	<b>Volume of plating medium</b>	<b>Total cDNA and dilution volume</b>	<b>Lipofectamine 2000 and dilution volume</b>
24 well	1 ml	1 µg and 50 µl	2 µl and 50 µl
10 cm	15 ml	16 µg and 1.5 ml	40 µl and 1.5 ml

#### 2.3.4.3 Transient cotransfection

One tenth of PS1/2<sup>-/-</sup> MEF cells from a confluent 10 cm culture dish were spread into a 10 cm dish containing 15 ml of culture medium without antibiotics. On the next day, cells were transiently cotransfected with the respective combinations of two cDNAs using lipofectamine 2000 In total 16 µg of cDNAs (8 µg/cDNA) and 40 µl of lipofectamine 2000

per dish were used. First, cDNAs and lipofectamine 2000 were mixed with 1.5 ml of OptiMEM and incubated for 5 min at room temperature. Both solutions were mixed, incubated for 20 min at room temperature and then gently added onto the cells. 24 h after transfection, the medium was replaced with 4.5 ml of fresh medium and conditioned for 16 h.

#### **2.3.4.4 Stable transfection**

To establish stable cell lines, HEK293/sw cells were transfected with cDNA as described above (see 2.3.4.3). A day after transfection, cells were split 1:10~1000. Two days after the transfection, zeocin at final concentration 0.2 mg/ml was added and the zeocin-resistant cells were selected under the zeocin containing medium for 2-3 weeks. Single cell clones were isolated using cloning-cylinders, transferred to 24 well plate and cultured. The appropriate clone was selected as working clone based on a robust expression level of transfected cDNA (see 2.5). Pool stable cell lines were generated by hygromycin B selection, at final concentration at 0.5 mg/ml, for F-NEXT stably expressing cells. The cells were transfected as described above (see 2.3.4.3), and split 1:10 in 4-5 of 10 cm dishes for selection. After 2-3 weeks, all hygromycin B-resistant single cell clones were collected all together, transferred into fresh 10 cm dish and further cultured.

## 2.4 Antibodies

### 2.4.1 Monoclonal antibodies

Antibody	Epitope	Reference / supplier	IP <sup>1</sup>	Blot	IF <sup>2</sup>
PS1N	PS1 N-terminus	(Capell et al., 1997)		1: 5000	
3D7	PS1 aa 263-407	(Steiner et al., 1999b)		1:2000	
HF5C	PS2 aa 297-356	(Steiner et al., 1999b)		1:10000	
6E10	A $\beta$ aa 1-17	Signet Laboratories		1: 10000	
M2	FLAG-tag	Sigma		1: 1000	
9E10	Myc-tag	Santa Cruz Biotechnology		1: 2000	1:500

1: Abbreviation of immunoprecipitation, 2: Abbreviation of immunofluorescence

### 2.4.2 Polyclonal antibodies

Antibody	Epitope	Reference / supplier	IP	blot	IF
3027	PS1 aa 263-407	(Walter et al., 1997)	1:250	1: 1000	
3711	PS2 aa 297-356	(Walter et al., 1998)	1:250		
N1660	NCT aa 693-709	Sigma		1: 5000	
434G	APH-1aL aa 245-265	(Prokop et al., 2004)		1 $\mu$ g/ml	
1638	PEN-2 aa 4-15	(Steiner et al., 2002)		1 $\mu$ g/ml	
8177	SPE-4 aa 206-389		1:250	1:1000	
5313	APP aa 444-592	(Steiner et al., 1999b)		1: 2000	
6687	APP last 20 aa	(Steiner et al., 2000)			
3552	A $\beta$ aa 1-40		1: 300		
Cleaved Notch-1	NICD aa V1744	Cell Signaling Technology		1: 1000	

### 2.4.3 Secondary antibodies

Antibody	Epitope	Reference / supplier	IP	blot	IF
anti-rabbit-HRP	Rabbit IgG	Promega		1:10000	
anti-mouse-HRP	Mouse IgG	Promega		1:5000	
anti-mouse-AP	Mouse IgG	Promega		1:5000	
Alexa Fluor 488	Mouse IgG	Molecular Probes			1:500

## 2.5 Protein analysis

### 2.5.1 Total cell lysate

#### 2.5.1.1 Materials

**PBS:**

See 2.3.1

**STEN-lysis buffer:**

50 mM Tris pH7.6, 150 mM NaCl, 2 mM EDTA, 1% NP-40 in dH<sub>2</sub>O

**Co-IP buffer:**

1% CHAPSO, 150 mM NaCitrate pH6.4 in dH<sub>2</sub>O

**BSA solution:**

2 mg/ml albmine from bovine serum in dH<sub>2</sub>O

Protease inhibitor cocktail P8340

Sigma

BIO-RAD protein assay

BIO-RAD

#### 2.5.1.2 Cell lysate preparation

Confluent cells were washed once with PBS buffer (see 2.3.1) and collected into eppendorf tubes by centrifugation for 5 min at 1000xg. Cell pellet was lysed with 500 µl of STEN-lysis buffer with protease inhibitor cocktail (see 2.5.1.1) per 10 cm dish for 20 min on ice, and the lysate was ultracentrifuged for 30 min at 100,000xg. Supernatant fraction was

## Materials and Methods

transferred into a new tube and an aliquot with drawn to measure the protein concentration by the Bradford protein assay from BIO-RAD (See 2.5.1.3).

### 2.5.1.3 Protein quantitation

The protein concentration of the total cell lysate was measured by the Bradford assay. 1-2  $\mu$ l of total cell lysate was mixed with 1 ml of BIO-RAD protein assay solution, diluted with dH<sub>2</sub>O (1:5), incubated 5 min at room temperature, and was measured by photometer at OD595. 2  $\mu$ l of 2 mg/ml BSA was included as standard in every measurement.

## 2.5.2 Membrane lysate

### 2.5.2.1 Materials

**PBS:**

See 2.3.1

**Hypotonic buffer:**

10 mM MOPS, 10 mM KCL in dH<sub>2</sub>O, pH 7.0

**10% lubrol:**

10% lubrol in dH<sub>2</sub>O

**10% n-Dodecyl- $\beta$ -D-maltoside (DDM):**

10% DDM in dH<sub>2</sub>O

**BSA solution:**

See 2.5.1.1

Glycerol

Surfact-Amps 35, 10% Brig-35 solution

Pierce

### 2.5.2.2 Preparation and solubilization of membrane

The cell pellet was resuspended in 500  $\mu$ l of hypotonic buffer (see 2.5.2.1) and incubated for 20 min on ice. The suspension was rapidly frozen in liquid nitrogen to break the cells. 10% lubrol and 10% Brig-35 solution (see 2.5.2.1) were added to the gently thawed



## Materials and Methods

cell lysate, either in co-IP buffer (see 2.5.1) or in 1% Triton X-100 buffer (see 2.5.3.1), from one 10 cm dish. After 2 h at 4°C incubation by rotating, anti-FLAG M2 agarose was collected by centrifugation for 5 min at 3000xg, and washed 4 times with 1 ml co-IP buffer. After the last wash, the supernatant was carefully removed as much as possible, and 40 µl of urea SDS-SB (see 2.5.6.1) was added.

### **2.5.3.3 Immunoprecipitation from conditioned medium**

Secreted A $\beta$  and F-N $\beta$  were analyzed from conditioned medium by combined immunoprecipitation/ immunoblotting. The conditioned media from transiently transfected PS1/2<sup>-/-</sup> MEF cells (see 2.3.4.3) were collected into falcontube and cleared by centrifugation for 10 min at 3000xg. For A $\beta$ , 4 ml of conditioned medium were pre-cleared with 30 µl of PAS (see 2.5.3.1) for 30 min at 4°C. After centrifugation for 5 min at 3000xg, the pre-cleared medium was transferred to a fresh tube, containing 30 µl of PAS and 3552 anti-A $\beta$  antibody (see 2.4.2). The proteins were immunoprecipitated overnight at 4°C by shaking. The immunoprecipitates were washed 10-15 min each with 1 ml of STEN-NaCl, STEN-SDS and STEN buffer (see 2.5.3.1).

For F-N $\beta$ , the conditioned medium was directly carried to immunoprecipitation without a pre-clear step. The same procedure as described for immunoprecipitation of A $\beta$  was performed using 30 µl anti-FLAG M2 agarose (see 2.5.3.1) for 4ml medium. Both A $\beta$  and F-N $\beta$  were eluted with urea SDS-SB (see 2.5.6.1).

To analyze A $\beta$ 40/42 ratio, HEK293/sw cell line stably expressing His-PS1 wt, His-PS1 D385A, and the respective his-tagged chimeric proteins, were cultured in 10 cm dish. The cells were conditioned for 4-6 h with 4.5 ml fresh medium. Secreted A $\beta$  species were immunoprecipitated as described above, eluted with urea SDS-SB or Wilgfang-SB (see 2.5.6.1) and subjected to SDS-PAGE (see 2.5.7).

## 2.5.4 Cell-free AICD assay

### 2.5.4.1 Materials

**PBS:**

See 2.3.1

**Hypotonic buffer:**

See 2.5.2.1

**Na-Citrate buffer:**

150 mM Na-Citrate pH6.4 in dH<sub>2</sub>O

**STEN-lysis buffer:**

See 2.5.1.1

Complete Mini, Protease inhibitor cocktail tablets

Roche

### 2.5.4.2 Membrane preparation

Stable HEK293/sw cells stably transfected respective PS constructs were used to analyze the *de novo* AICD generation. The cells were collected from confluent 10 cm dishes of each cell line after rinsing once with PBS (see 2.3.1), centrifuged for 5 min at 1000xg at 4°C, and the pellet was resuspended in 500 ml hypotonic buffer (see 2.5.4.1) containing 1x complete mini protease inhibitor cocktail (see 2.5.4.1). After the incubation for 20 min on ice, cell suspension was homogenized by passing through a 23G needle with 10 strokes. Homogenized suspension was centrifuged for 15 min at 1000xg at 4°C. The supernatant fraction was transferred into a fresh tube, and further centrifuged for 45 min at 16,000xg at 4°C to collect the membrane fraction. The Membrane pellet was resuspended in 50 µl Na-Citrate buffer containing complete mini (see 2.5.4.1). A 5 µl aliquot of the membrane suspension was lysed in 20 µl STEN-lysis buffer (see 2.5.1.1) as described above (see 0), and 10 µl of lysate was used for measuring the protein concentration by the Bradford assay (see 2.5.1.3). The volume membrane suspensions of the different cell lines to be used for assay were adjusted depending on the protein concentration.

### 2.5.4.3 AICD assay

40  $\mu$ l of the membrane suspension was incubated for 30 min at 37°C. Because of good efficiency of this assay, the incubation time was reduced from the original 2 h protocol (McLendon et al., 2000; Pinnix et al., 2001; Sastre et al., 2001; Moehlmann et al., 2002) to 30 min to avoid saturation of AICD production due to the remaining amount of the endogenous PSs. After 30 min of incubation, the membrane suspension was subjected ultracentrifugation for 30 min at 100,000xg at 4°C. The supernatant fraction containing AICD was collected into a fresh tube, and urea SDS-SB (see 2.5.6.1) was added.

## 2.5.5 In vitro $\gamma$ -secretase assay with C100

### 2.5.5.1 Materials

**Na-Citrate buffer:**

See 2.5.4.1

**1% CHAPSO:**

1% CHAPSO in dH<sub>2</sub>O

Purified recombinant C100 (Tian et al., 2002)

Phosphatidylcholine

DTT

BSA

**Reaction mix:**

150 mM Na-Citrate, pH6.4, 0.25% CHAPSO, 0.5 mg/ml Phosphatidylcholine, 10 mM DTT, 0.1 mg/ml BSA and 1x Complete Mini

Complete Mini, Protease inhibitor cocktail tablets

Roche

### 2.5.5.2 In vitro $\gamma$ -secretase assay

Membrane fraction was prepared from cells as described above (see 2.5.4.2) and solubilized with 1% CHAPSO. After 30 min centrifugation at 100,000xg at 4°C, the lysate was pre-cleared with PAS (see 2.5.3.1) for 30 min. The pre-cleared lysate was co-immunoprecipitated with either antibody against PS, 3027, or antibody against SPE-4,

8177, as described above (see 2.4 and 2.5.3.2). After 4 times washes with 0.5% CHAPSO in 150 mM Na-Citrate buffer, 20  $\mu$ l of reaction mix (see 2.5.5.1) was added on the beads and incubated with 1  $\mu$ l of C100 for over night either at 37°C or at 4°C.

## 2.5.6 Sample preparation for SDS-PAGE

### 2.5.6.1 Materials

#### **Urea SDS-sample buffer (SB):**

62.5 mM Tris pH6.8, 2% SDS, 10% Glycerol, 2.5%  $\beta$ -Mercaptoethanol, 2 M Urea, Bromophenolblue in dH<sub>2</sub>O

#### **SB for modified Tris-Bicine urea gel**

0.72 M Bis-Tris, 0.32 M Bicine, 2% SDS, 5%  $\beta$ -Mercaptoethanol, 30% Sucrose, Bromophenolblue in dH<sub>2</sub>O

Prestained protein standard; See Blue Plus2

Invitrogen

### 2.5.6.2 Sample preparation

To detect PS1 NTF/CTF, NCT, APH-1, PEN-2, APPsw-6myc, APP-CTFs AICD, F-NEXT and NICD, total cell lysates were analyzed by immunoblotting. Prior to SDS-PAGE, proteins were denatured by adding urea SDS-SB (see 2.5.6.1) and boiling for 10 min at 65°C before applying on the gel. 25  $\mu$ g proteins were separated by SDS-PAGE (see 2.5.7). 12% urea Tris-Glycine gels (see 2.5.7.1) for analyzing PS1 NTF/CTF, and 7% Tris-Glycine gels (see 2.5.7.1) for NCT, F-NEXT and NICD separation were used. 10-20% Tris-Tricine gels (see 2.5.7.2) were used to APPsw-6myc. 50  $\mu$ g of proteins were loaded for detecting NICD by “Cleaved Notch-1” anti-NICD specific antibody.

To detect AICD from cell-free AICD assay, urea SDS-SB was added to the supernatant fraction containing AICD and was boiled for 10 min at 95°C. 50% of the AICD fraction was separated on 10-20% Tricine gel (see 2.5.7.2).

To detect sAPP, urea SDS-SB was added directly to aliquot of the 5  $\mu$ l condition medium, and boiled for 10 min at 95°C before applying on 7% Tris-Glycine gel.

## Materials and Methods

Immunoprecipitated A $\beta$  and F-N $\beta$  from transiently transfected MEF cells on PAS or anti-FLAG M2 agarose were released and denatured by adding urea SDS-SB or SB for the modified Tris-Bicine urea gels (see 2.5.6.1), and boiling for 10 min at 95°C. Total A $\beta$  and F-N $\beta$  were separated on 10-20% Tris-Tricine gels. Modified Tris-Bicine urea gels (see 2.5.7.3) were used to separate A $\beta$ 40/42 species.

To detect  $\gamma$ -secretase complex components co-immunoprecipitated with F-NEXT, immunoprecipitates were boiled for 10 min at 65°C in urea SDS-SB. F-NEXT was separated in 7% Tris-Glycine gel, and the co-immunoprecipitated  $\gamma$ -secretase components were separated in 12% urea Tris-Glycine gel. 10% of immunoprecipitated fraction was applied for F-NEXT, and 50% was applied for  $\gamma$ -secretase components analysis.

Prestained protein standard was mixed with the corresponding SB for each gel system, and always applied in parallel.

### 2.5.7 SDS-Polyacrylamide gel electrophoresis (PAGE)

#### 2.5.7.1 Tris-Glycine gel

##### 2.5.7.1.1 Materials

**Lower Tris (4X):**

1.5 M Tris pH8.8, 0.4% SDS in dH<sub>2</sub>O

**Upper Tris (4X):**

0.5 M Tris pH6.8, 0.4% SDS in dH<sub>2</sub>O

**Acrylamide (SERVA):**

40% (w/v) Acrylamide / BIS-Acrylamid 37,5 :1 in dH<sub>2</sub>O

**8M Urea solution:**

8 M Urea in dH<sub>2</sub>O

**APS:**

10% (w/v) Ammonium Persulfat in dH<sub>2</sub>O

**Tris-Glycin gel running buffer:**

25 mM Tris, 200 mM Glycine, 0.1% SDS in dH<sub>2</sub>O

N,N,N',N'-tetramethylethylenediamine (TEMED)

Merck

### 2.5.7.1.2 Gel preparation

For one thick (1.5mm) mini gel:

	7% separating gel	Stacking gel	12% urea separating gel	Urea stacking gel
8 M Urea	-	-	2.625 ml	2.5 ml
40% Acrylamide	1.31 ml	487.5 $\mu$ l	2.25 ml	487.5 $\mu$ l
4x Lower Tris	1.875 ml	-	1.875 ml	-
4x Upper Tris	-	1.25 ml	-	1.25 ml
dH <sub>2</sub> O	4.315 ml	3.4 ml	0.75 ml	3.4 ml
APS	15 $\mu$ l	15 $\mu$ l	15 $\mu$ l	15 $\mu$ l
TEMED	15 $\mu$ l	15 $\mu$ l	15 $\mu$ l	15 $\mu$ l

### 2.5.7.1.3 Electrophoresis

Gels were set in Mini-PROTEAN 3 electrophoresis cell chamber (see 2.1.4), filled with Tris-Glycine gel running buffer. The power supply was (see 2.1.4) first set to constant voltage at 60 volt until all samples migrated into stacking gel then the voltage was raised to 120 volt.

### 2.5.7.2 Tris-Tricine gel

#### 2.5.7.2.1 Materials

**Tris-Tricine gel running buffer:**

100 mM Tris, 100 mM Tricine, 0.1% SDS in dH<sub>2</sub>O

10-20% Tris-Tricine gel

Invitrogen

#### 2.5.7.2.2 Electrophoresis

Pre-cast Tris-Tricine Gel was put into X Cell Sure Lock™ Mini Cell chamber (see 2.1.4). The gel chamber was filled with Tris-Tricine gel running buffer, and the Gel was run at constant voltage as described above (see 2.5.7.1.3).

### 2.5.7.3 Modified Tris-Bicine urea gel

#### 2.5.7.3.1 Materials

**Separating gel buffer:**

1.6 M Tris, 0.4 M H<sub>2</sub>SO<sub>4</sub> in dH<sub>2</sub>O

**Spacer gel buffer:**

0.8 M Bis-Tris, 0.2 M H<sub>2</sub>SO<sub>4</sub> in dH<sub>2</sub>O

**Stacking gel buffer:**

0.72 M Bis-Tris, 0.32 M Bicine in dH<sub>2</sub>O

**Acrylamide (BIO-RAD):**

40 % (w/v) Acrylamide / BIS-Acrylamid 19:1 in dH<sub>2</sub>O

**APS:**

See 2.5.7.1.1

**20% SDS solution:**

20% SDS in dH<sub>2</sub>O

Urea

TEMED (See 2.5.7.1.1)

**Cathode buffer:**

0.2 M Bicine, 0.25% SDS, 0.1 M NaOH in dH<sub>2</sub>O

**Anode buffer:**

0.2 M Tris, 50 mM H<sub>2</sub>SO<sub>4</sub> in dH<sub>2</sub>O

#### 2.5.7.3.2 Gel preparation

For one thick (1.5 mm) mini gel:

	Separating gel	Spacer gel	Stacking gel
Urea	4.8 g	-	-
40% Acrylamide	2.5 ml	300 µl	675 µl
Separation gel buffer	2.5 ml	-	-
Spacer gel buffer	-	1 ml	-
Stacking gel buffer	-	-	1.5 ml
20% SDS	50 µl	10 µl	10 µl
dH <sub>2</sub> O	1.25 ml	680 µl	740 µl
APS	40 µl	8 µl	18 µl
TEMED	5 µl	2 µl	6 µl

Spacer gel and stacking gel length were approximately 5 mm for each.

### 2.5.7.3.3 Electrophoresis

Modified Tris-Bicine urea gels were run as described above (see 2.5.7.1.3).

## 2.5.8 Western blotting

### 2.5.8.1 Materials

**Blotting buffer:**

25 mM Tris, 200 mM Glycine in dH<sub>2</sub>O

**Blocking buffer:**

0.2% I-Block (TROPIX, see 2.5.8.1), 0.1% Tween-20 in PBS (see 2.3.1)

**TBST:**

10 mM Tris pH7.4, 150 mM NaCl, 0.1% Tween-20 in dH<sub>2</sub>O

**Sodium azide solution:**

5% Sodium azide in dH<sub>2</sub>O

Filterpaper	Schleicher&Schuell
Immobilon-P (PVDF transfer membrane)	Millipore
Protran (Nitrocellulose transfer membrane)	Schleicher&Schuell
ECL, Western blotting detection reagent	Amersham Biosciences
ECL plus, Western blotting detection reagent	Amersham Biosciences
Western-Star, protein detection kit	Tropix
Super RX, Fuji Medical X-ray Film	Fujifilm

### 2.5.8.2 Blot

The PVDF transfer membrane (see 2.5.8.1) was soaked in isopropanol, washed with dH<sub>2</sub>O, and put in blotting buffer (see 2.5.8.1). For A $\beta$  and F-N $\beta$  analysis, Nitrocellulose transfer membrane (see 2.5.8.1) soaked directly in blotting buffer was used. Gel plates were opened and gels were carefully removed from the plates. The transfer membrane was placed on the gel between blotting buffer two filter papers (see 2.5.8.1) soaked with blotting buffer, and one sponge on both sides. They were put in the Mini Trans-Blot transfer cell transfer chamber (see 2.1.4) filled with blotting buffer together with ice cube block and the protein transfer was performed for 1 h at 400 mA.

### **2.5.8.3 Blocking procedure**

After blotting, transfer membrane was removed, and blocked for 1 h at room temperature in I-Block (see 2.5.8.1). Nitrocellulose membranes for A $\beta$  and F-N $\beta$  were boiled for 5 min in PBS (see 2.3.1) before blocking to increase the signal.

### **2.5.8.4 Primary antibody incubation**

Each primary antibody was diluted as described in 2.4 in I-Block (See 2.5.8.1) containing 0.05% sodium azide (see 2.5.8.1). Transfer membranes were incubated with the respective primary antibody overnight at 4°C with shaking.

### **2.5.8.5 Secondary antibody incubation**

After overnight primary antibody incubation, transfer membranes were washed 4 times for 15 min in TBST (see 2.5.8.1). After washing, transfer membranes were incubated with the appropriate horseradish peroxidase (HRP) conjugated secondary antibody at the optimal concentration (see 2.4.3) in TBST, for 1 h at room temperature. For A $\beta$  and F-N $\beta$ , Nitrocellulose transfer membrane was incubated in alkaline phosphatase (AP)-conjugated anti-mouse IgG secondary antibody, which was diluted in I-Block (See 2.5.8.1). After incubation, transfer membranes were washed in TBST.

### **2.5.8.6 Detection**

Proteins were visualized by chemiluminescence. ECL plus reagent (see 2.5.8.1) was used, following the protocol from the manufacture, for detecting APH-1 and PEN-2. A $\beta$  and F-N $\beta$  were detected by the Western-Star kit (see 2.5.8.1). All other proteins were detected by ECL (see 2.5.8.1). The signals were exposed on X-ray films for an appropriate time, and the films were developed using developer machine (see 2.1.4).

## 2.6 Immunofluorescence microscopy

### 2.6.1 Cell preparation and transient cotransfection

One tenth of PS1/2<sup>-/-</sup> MEF cells from confluent 10 cm culture dish was cultured on coverslips layed in 10 cm dish. The coverslips were transferred into 24 well plate with 1 ml culture medium without antibiotics next day, and the cells were transiently transfected with F-NEXT alone or cotransfected together with respective cDNAs as described above using in total 1 µg cDNAs (0.5 µg/cDNA) and 2 µl of lipofectamine 2000 in 50 µl OptiMEM per well (see 2.3.4.2).

### 2.6.2 Slide preparation

#### 2.6.2.1 Materials

**PBS:**

See 2.3.1

**Fixation buffer:**

4% paraformaldehyde/4% sucrose in PBS

**Quenching buffer:**

50 mM NH<sub>4</sub>Cl in PBS

**Permealisation buffer:**

0.2% Triton X-100 in PBS

**Blocking buffer:**

0.2% gelatin in PBS

Mowiol

CALBIOCHEM

#### 2.6.2.2 Cell fixation and permeabilisation

Cell fixation and permeabilisation were performed as described (Wacker et al., 1997). 48 h after transfection, the cells were rinsed once in 1 ml PBS (see 2.3.1), and fixed for 20 min in fixation buffer (see 2.6.2.1). After fixation, cells were rinsed three times in PBS, and quenched for 10 min in quenching buffer (see 2.6.2.1). After rinsing three times in PBS,

## Materials and Methods

permeabilisation was achieved in permeabilisation buffer (see 2.6.2.1) for 5 min. The cells were rinsed twice in PBS, and incubated for 10 min in blocking buffer (see 2.6.2.1).

### **2.6.2.3 Antibody incubation and mounting**

The cells were incubated with a mixture of primary antibody diluted 1:500, 9E10 (see 2.4.1) against the myc epitope to detect F-NEXT, in blocking buffer (see 2.6.2.1) for 20 min. After rinsing twice in PBS (see 2.3.1), coverslips were incubated with a mixture of secondary antibodies diluted 1:500, Alexa 488-labeled polyclonal antibody (see 2.4.3) in blocking buffer for 20 min for detection. After rinsing in PBS, coverslips were mounted in a drop of Mowiol (see 2.6.2.1).

### **2.6.2.4 Microscopic analysis**

Fixed cells were analyzed on a Zeiss Axioskop2 microscope equipped with a 63x/1.25 objective and standard FITC and TRITC fluorescence filter sets using an Axiocam HRm Camera and AxioVision software. Images were assembled and processed using Adobe Photoshop (see 2.1.5).

## **2.7 Transgenic lines of *C. elegans* and rescue assays**

The cDNAs were subcloned under the control of *sel-12* promoter in pBY895 vector (Wittenburg et al., 2000) to allow the expression of the constructs in *C. elegans*. The transgenic lines were established by microinjection of the constructs into *sel-12(ar171)* mutant hermaphrodites together with the co-injection marker pBY1153 (*sel-12::gfp*) at a concentration of 20 ng/μl, each. At least three independent transgenic lines from the progeny of F1 or F2 generation animals were established. The number of eggs laid by 50 individual transgenic animals was counted and grouped into four categories: "Egl+++",

robust egg laying, more than 50 eggs laid (wt phenotype); "Egl<sup>++</sup>," 15-50 eggs laid; "Egl<sup>+</sup>," 5-15 eggs laid; "Egl<sup>-</sup>," no eggs laid. These experiments were done by Dr. Stefan Eimer and Agata Smialowska in the laboratory of Prof. Dr. Ralf Baumeister.

### 3. Results

#### 3.1 Functional characterization of SPE-4

##### 3.1.1 SPE-4 is the most distant PS homologue

The *C. elegans* sperm protein, SPE-4 (L'Hernault and Arduengo, 1992) is the most distant PS homologue. SPE-4 amino acid sequence shows approximately 23% homology to that of PS1 according to BLAST searches (Table 3).

	<i>identity/similarity (%)</i> *			
	human PS1	SEL-12	HOP-1	SPE-4
human PS1	100	51/69	30/50	23/42
SEL-12		100	30/49	22/42
HOP-1			100	23/42
SPE-4				100

**Table 3: Sequence conservation of the *C. elegans* PSs**

\* The Blast2 program available at the NCBI site (<http://www.ncbi.nlm.nih.gov/BLAST/>) was used to calculate the percentage of amino acid identity and similarity.

Sequence alignment of PS1 and the three *C. elegans* PS homologues, SEL-12, HOP-1 and SPE-4, revealed that SPE-4 has a very short N- and C-terminus and a much longer cytoplasmic loop between TMD 6 and 7 compared to PS1. On the other hand, despite of this low homology, the two functional aspartates within TMDs 6 and 7, including the GxGD active site motif, and the PALP motif, which are characteristic for the PS-type protease family, are well conserved in SPE-4. This conservation of the functionally important motives and a known SPE-4 mutant with a mutation of the PALP motif of SPE-4 (Arduengo et al., 1998) indicates that this protein has a proteolytic function like PS.

```

PS1      MTELPAPLSYFQNAQMSEDNHLSEN*TVRSQNDNRERQEHNDRRSLGHPEPLSN*GRPOGNSRQVVEQDEEED*EELTL
SEL-12  M-----PSTRRQ*QEGGGADAETH*TVYGTN*LITNRNS-----QEDENVVEEAEL
HOP-1   -----M*PRTKR-----V-----
SPE-4   M-----D*TLRS-*ISSEL-----V-----

PS1      KYGAKHVIMLFV*PTLCMVV*VVATIKS-VSFYTRKDG*QLI*YTPF--TEDTE*TVG*ORAL*HSILNAAIMIS*VIVVM
SEL-12  KYGASHVIHLFV*PSLCMAL*VVFMNTITFYSONGRH*LYTPFVRETDSIVEKGLMSL---GNALV*MLCVV*VLM
HOP-1   -YSGK*TITGVL*YPVA*ICMLF*VAIN*VKIL-SQPE*QEQSKVV*GLF--HSYD*TADS*GTITL-----Y*LIG*FI*LIT
SPE-4   -RSSQLRWT*LF*SVIAN*MSL*TLS*W*IGV-YNM*EV*NSELSKT*FLD--PSFEQ*TGN*LLLD-GF*ING*VGT*L*VL*GCV

PS1      TILLV*VLYKYRCYK*VIHAWLI*SSLL*LFFFS*PIYLGEVFKT---YNVA*VD*IT*VAL*L*INW---F*GVV*GMIS*IH
SEL-12  TVLL*VVYKYK*FYKLI*HGWLI*VSSFL*LFL*FTI*YVOEVLKS---FDVS*PSALL*V*L*FGLGN---Y*GVL*GMCI*H
HOP-1   TSL*GVFCYQMK*FYKAI*KVYVLANS*IGILL*VYSV*FHFORIAEA---QSIP*V*SVPT*FFFL*L*LQ---F*GGL*GI*TCLH
SPE-4   SFIM*LAFV*LFDR*RIVKAWL*TLS*CLL*LIL*FGVSAQ*TLHDM*FSQV*FDQDD*NNQ*Y*YMTI*VLI*VVPT*VVY*G*FG*GI*YAFF

PS1      WKGP*LR*LQ*QAYL*IMISALMAL*VFKYL*PEWT*AWLI*LAVIS*Y*DL*VAVL*CPK*GPI*RMLV*ETA*OERN*ETL*F*PAL*IYS
SEL-12  WKGP*LR*LQ*QAYL*IMISALMAL*VFKYL*PEWT*VWV*LV*FVIS*VWDL*VAVL*TPK*GPI*RYLV*ETA*OERN*EPI*F*PAL*IYS
HOP-1   WKSH*RRL*HQ*FYLI*MLAGL*TAL*FILN*ILP*DW*VW*MAL*TAIS*FW*DI*VAVL*TPC*GPI*KMLV*ETAN*RRG*DDK*F*PAL*IYN
SPE-4   SNS*SI*LH*QIF*VV*TNC*SL*ISV*FYLR*VFP*SK*T*W*VL*WIV*LF*WDL*FAVL*AP*MG*PI*KKV*QEK*AS*DYSK*CVL*NL*IM*FS

PS1      STMVW---LV---NMAEGDPEAQR*RVSKNS*KYN-----AESTERESQDTVA
SEL-12  SGVI*YPV*LV---TAVENT*TDPREPT*SSDS*NTSTAF*PG*ASCS-----SETPK*R*PK*V*KRIP
HOP-1   SS-----SYVNEVD-----SPDT*TR*SN*ST*PLT
SPE-4   ANEK*R---L*TAGS*N*Q*E*TNEGEEST*IR*RTV*Q*T---IE*YYTK*REA*QDDEF*Y*Q*KIR*ORRA*AIN*PD*SV*PT*EH*S*PLV

PS1      END---D-----GGFSEEW*E*AQRD*SH*L*GFHR
SEL-12  QKV---Q-----IESNTAST*TQNS*G*V*RVER
HOP-1   EFN---N-----SSSR*LES---D*SL*LRPP-
SPE-4   EAEP*SP*IELKEKN*STEELS*DD*ESDT*SETSS*SSNL*SSSD*STTV*STSD*ISTAE*ECD*Q*KEW*DDL*V*S---NS*L*FN*ND-

PS1      STPE*SRAAVQELSS*ILAGED*PE*ERG*VK*LGL*GDF*IFYS*V*LV*GKASATAS*GDWNT*T*IAC*FVA*L*I*GL*CL*TL*LLAI
SEL-12  ELAA*ERPT*VODAN---FHRHE*EE*ERG*VK*LGL*GDF*IFYS*V*LV*GKASSYF--DWNT*T*IAC*FVA*L*I*GL*CL*TL*VLLAV
HOP-1   VIF*RQ---IREVR*VE*GTIR*LGM*GDF*VFYS*LM*LGNT*VQTC--PLPT*VVAC*FV*SN*LV*GL*TI*TL*PIV*TL
SPE-4   KRPA*T---AADAL*NDGEV*LR*LGF*GDF*VFYS*LL*I*GL*QFA*ASG--CPFAV*I*SAAL*GL*IF*GL*VV*TL*TVF*ST

PS1      FKR*AL*PAL*PIS*IT*FGL*V*F*Y*F*ADYL*VOP*FM*DQ*LAF*HQ*FY*I
SEL-12  FKR*AL*PAL*PIS*IT*FSL*IF*Y*F*CTR*WII*TP*FVT*Q*VSQ*KCL*LY
HOP-1   SQTAL*PAL*PF*PLA*IAA*IF*Y*FS*SHIAL*TP*FT*DL*CTS*QL*ILI
SPE-4   EEST*T*PAL*PL*PVIC*GT*FC*Y*FS*SM*FFWE*QLYG-----

```

**Figure 9: Sequence alignment of PS1 with its *C. elegans* homologues**

The amino acid sequence alignment of PS1 with SEL-12, HOP-1, and SPE-4. The sequence alignment was generated with T-Coffee and processed with BOXSHADE. Identical amino acid residues are displayed on black or red (identical in all PSs) background and similar ones on gray background. Putative TMDs 6 and 7 comprising the active site domain are underlined. Asterisks indicate the active site aspartate residues.

### 3.1.2 SPE-4 wt is not incorporated to the $\gamma$ -secretase complex

To test the possibility whether SPE-4 has a proteolytic function like PS, mammalian cells were employed because it is difficult to analyze SPE-4 in *C. elegans* due to its limited expression pattern. SPE-4 wt was therefore stably expressed in HEK293/sw cells (Citron et al., 1992). These cells stably express APP<sup>sw</sup> mutant to increase the amount of A $\beta$  production and to enhance amyloidogenic pathway. As shown in Figure 10A, SPE-4 wt was expressed. However, surprisingly, in contrast to exogenously expressed PS1 wt, SPE-4

## Results

wt failed to replace endogenous PSs despite of its robust expression (Figure 10B). When PS is stably expressed in the cells, it competes with endogenous PSs for interaction with the other  $\gamma$ -secretase complex components. This competition results in the replacement of the endogenous PSs by the exogenous one due to its overexpression. Therefore, the replacement of the endogenous PSs by the exogenous one due to its overexpression. Therefore, the replacement of the endogenous PSs is indication of  $\gamma$ -secretase complex formation of the exogenously expressed PS of interest. Thus, this result indicates that SPE-4 wt is not incorporated to the  $\gamma$ -secretase complex in HEK293/sw cells.

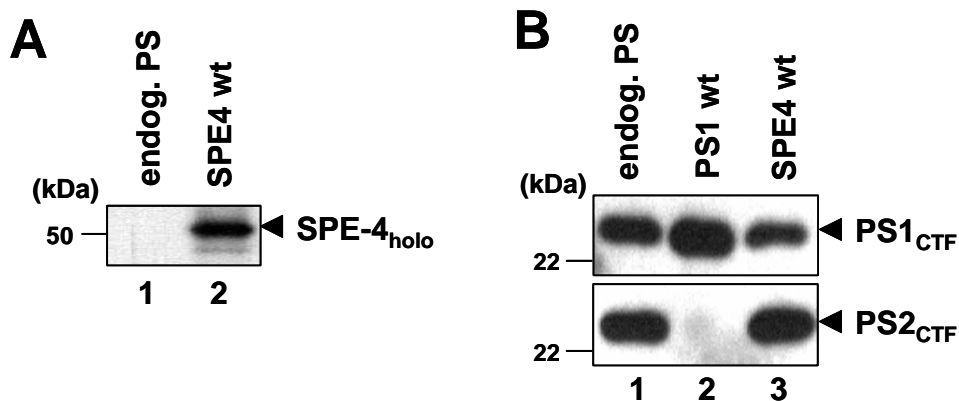


**Figure 10: SPE-4 does not replace endogenous PSs**

HEK293/sw cells stably expressing SPE-4 wt were analyzed for the SPE-4 wt expression and the endogenous PSs replacement. A: SPE-4 wt expression was analyzed by immunoprecipitation of the lysate from metabolically labeled cells using anti-SPE-4 loop antibody, 8177. Immunoprecipitated protein was separated by SDS-PAGE on a 10% Tris-glycine-urea gel. B: Total cell lysates from indicated cell lines were analyzed for PS1 and PS2 by combined immunoprecipitation/immunoblotting with polyclonal and monoclonal anti-PS1 loop antibodies, 3027/3D7, or polyclonal and monoclonal anti-PS2 loop antibodies, 3711/HF5C. Note that endogenous PSs are not replaced despite of its strong expression of SPE-4 wt.

### 3.1.3 SPE-4 does not process an APP-based substrate *in vitro*

The above result showed that SPE-4 wt is not incorporated into the  $\gamma$ -secretase complex in the cells. The reason may be that SPE-4 is unable to interact with human complex components because of its very distant sequence from PS. In addition, this result, however, also suggests the possibility that, unlike the other PSs, SPE-4 has a proteolytic function by its own without the need of other complex components. In order to analyze the possibility that SPE-4 may function as a protease without the requirement of other  $\gamma$ -secretase complex components, an *in vitro*  $\gamma$ -secretase assay was performed (Figure 11). SPE-4 wt was isolated from HEK293/sw cells stably expressing SPE-4 wt by immunoprecipitation. Endogenous  $\gamma$ -secretase complex, which was isolated from the same cell line by immunoprecipitation with an antibody against PS1, was included as a positive control. The endogenous  $\gamma$ -secretase complex generated AICD and A $\beta$  from the recombinant APP substrate, C100 in temperature dependent manner (Figure 11). In contrast, SPE-4 wt failed to generate neither AICD nor A $\beta$  (Figure 11, lane 3 and 4). This shows that SPE-4 does not function by itself as a protease at least in APP processing.

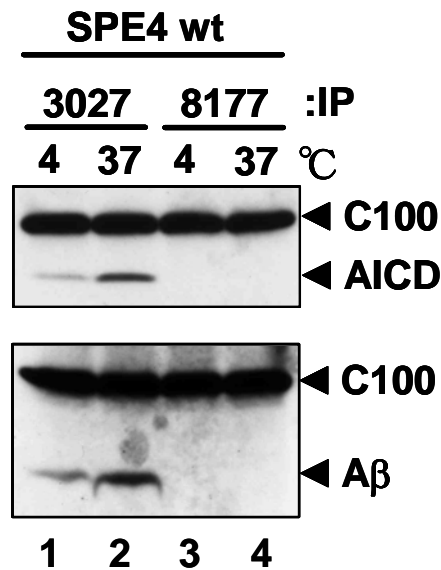


**Figure 11: SPE-4 wt does not process a recombinant APP substrate *in vitro***

*In vitro*  $\gamma$ -secretase assay was performed. SPE-4 wt and the PS1, which are an endogenous  $\gamma$ -secretase complex, were isolated by immunoprecipitation with either anti-SPE-4 loop antibody, 8177, or anti-PS1 loop antibody, 3027. The immunoprecipitates were used for *in vitro*  $\gamma$ -secretase assay. AICD and A $\beta$  generated from C100 were separated on a 10-20% Tris-tricine gel and were detected by immunoblotting with monoclonal Penta-His antibody, for AICD (upper panel), or monoclonal 6E10 antibody raised against amino acid 1-17 of A $\beta$ , for A $\beta$  (lower panel).

### 3.1.4 The C-terminus of PS1 is required for $\gamma$ -secretase complex assembly

#### 3.1.4.1 SPE-4 can undergo a partial $\gamma$ -secretase complex assembly by exchanging its C-terminus with that of PS1

Because SPE-4 wt did not undergo complex formation in HEK293 cells, it was next tried to forced it assemble into a  $\gamma$ -secretase complex with the aim of further examining the putative proteolytic function of this protein. To allow SPE-4 wt to be incorporated in the  $\gamma$ -secretase complex, a construct encoding SPE-4/PS1c, in which the C-terminus of SPE-4 after its PALP motif was exchanged with that of PS1, was generated (Figure 12). The C-terminal region of PS1 including the PALP motif is known to play a important role in  $\gamma$ -

secretase complex assembly (Tomita et al., 1999; Bergman et al., 2004; Kaether et al., 2004; Wang et al., 2006).

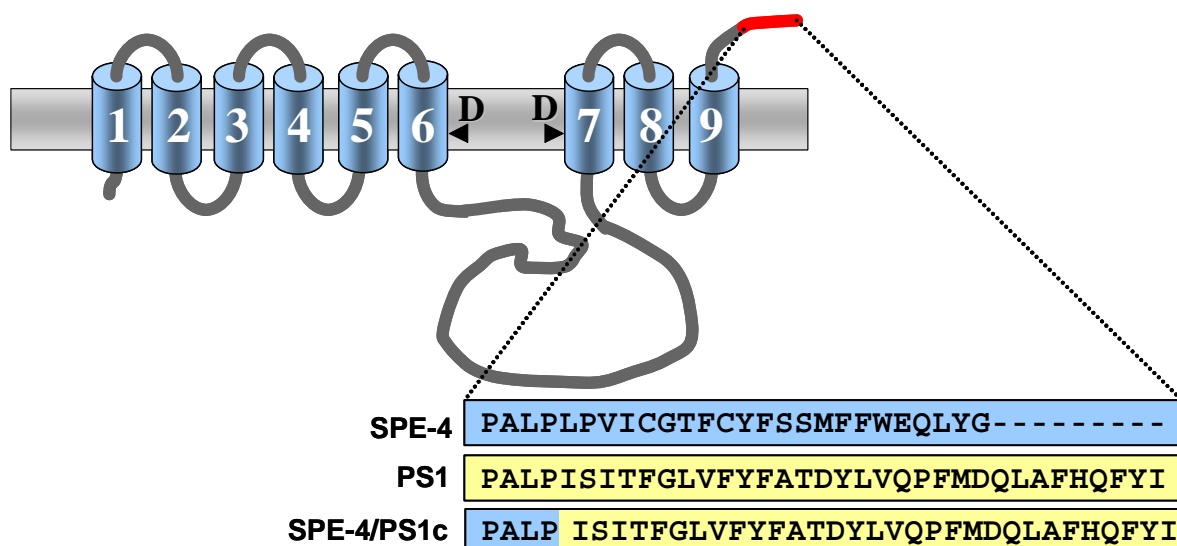


**Figure 12: Schematic model of SPE-4/PS1c**

Schematic representation of the SPE4-PS1c fusion protein. The C-terminus of SPE-4 (blue background), after the PALP motif, was replaced with that of PS1 (yellow background).

SPE-4/PS1c was stably expressed in HEK293/sw cells and it was analyzed as above (Figure 10). Immunoprecipitation of cell lysate from metabolically labeled SPE-4/PS1c expressing cells showed robust expression of the chimeric protein (Figure 13A). Compared to SPE-4 wt, SPE-4/PS1c successfully replaced endogenous PS1 and PS2 (Figure 13B). This result suggests that the PS1 C-terminus is indeed required to allow the SPE-4 molecule to enter the  $\gamma$ -secretase complex.

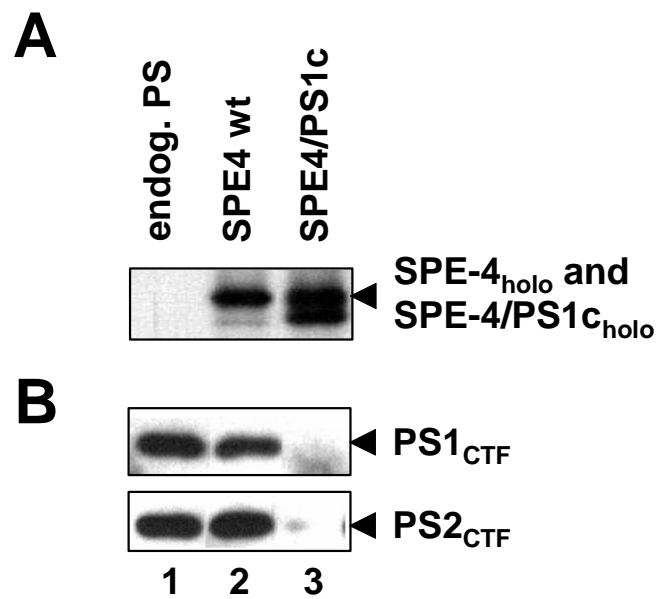


**Figure 13: SPE-4/PS1c replaces endogenous PSs in HEK293 cells**

HEK293/sw cells were stably transfected with the indicated cDNAs. A: SPE4-wt and SPE4-PS1c were analyzed by immunoprecipitation of cell lysates prepared from metabolically labeled cells with antibody 8177 as in Figure 10. B: Cell lysates were analyzed for PS1 and PS2 by combined immunoprecipitation/immunoblotting with antibodies 3027/3D7 or 3711/HF5c. Note that in contrast to SPE4-wt, SPE4-PS1c almost completely replaces endogenous PSs.

### 3.1.4.2 SPE-4/PS1c does not support $\gamma$ -secretase activity

Next, the influence of SPE-4/PS1c on  $\gamma$ -secretase activity was investigated by analyzing the levels of APP-CTFs in the cells. When  $\gamma$ -secretase is active, APP-CTFs are immediately processed to AICD, p3 and A $\beta$  (see Figure 4 in introduction). In contrary, when  $\gamma$ -secretase is inactive, APP-CTFs accumulate in the cells. Therefore, analyzing the levels of APP-CTFs accumulation was used as readout for  $\gamma$ -secretase activity. Cell lines stably expressing PS1 wt and PS1 D385N, a proteolytically inactive mutant (Steiner et al., 1998), were included as positive and negative controls. It is known that this proteolytically inactive aspartate mutant is incorporated into the  $\gamma$ -secretase complex. However, it does not undergo endoproteolysis unlike PS1 wt (Wolfe et al., 1999a). As shown in Figure 14, no accumulation of APP-CTFs was observed in the parental cells and PS1 wt expressing cells

due to normal  $\gamma$ -secretase activity (lane 1 and 2). In the cell line stably expressing SPE-4 wt, which does not undergo  $\gamma$ -secretase complex formation, no accumulation of APP-CTFs was observed (lane 4). Unexpectedly, APP-CTFs accumulated in SPE-4/PS1c expressing cells (lane 5) similar as in PS1 D385N expressing cells (lane 3). This result shows that although it successfully replaced endogenous PSs, SPE-4/PS1c does not support the  $\gamma$ -secretase activity.

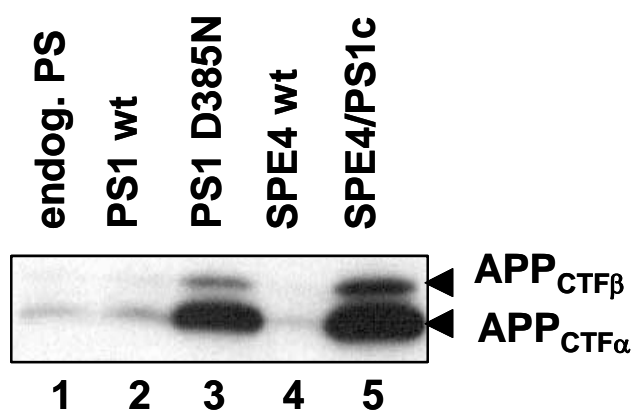


**Figure 14: Accumulation of APP-CTFs in SPE-4/PS1c expressing cells**

Total cell lysates from the indicated cell lines were analyzed for APP-CTFs by immunoblotting with antibody 6687 that is raised against the C-terminus of APP. The lysates were separated by SDS-PAGE on a 10-20% Tris-tricine gel.

### 3.1.4.3 Cells expressing SPE-4/PS1c are deficient in NCT maturation

In order to investigate whether or not the  $\gamma$ -secretase complex was properly formed in the SPE-4/PS1c expressing cells, the maturation of NCT, one of the  $\gamma$ -secretase complex components, was analyzed. Following proper  $\gamma$ -secretase complex assembly the complex traffics through the secretory pathway and NCT becomes complex-glycosylated (Edbauer et al., 2002; Kimberly et al., 2002; Tomita et al., 2002; Yang et al., 2002). Thus, the analysis of NCT maturation can be used as a readout for correct  $\gamma$ -secretase complex

## Results

formation. Total cell lysates from the indicated cell lines were immunoblotted with an anti-NCT antibody, N1660 (Figure 15A). Normal maturation of NCT consistent with the correct  $\gamma$ -secretase complex assembly was observed in the parental HEK293/sw cells, the SPE-4 wt expressing cells, and the PS1 wt or PS1 D385N expressing cells (Figure 15A, lane 1-4). In contrast, NCT remained immature in the SPE-4/PS1c expressing cells indicating incomplete  $\gamma$ -secretase complex formation (Figure 15A, lane 5). This result gives a plausible explanation for the  $\gamma$ -secretase deficiency of SPE-4/PS1c expressing cells. SPE-4/PS1c is able to replace endogenous PSs by forming a subcomplex with NCT, but is not able to bind to other complex components, therefore the complex cannot exit the ER. To further analyze this possibility, co-immunoprecipitation analysis was performed (Figure 15B). Membranes were solubilized with CHAPS, a detergent which preserves the  $\gamma$ -secretase complex and its activity (Li et al., 2000b) CHAPS-solubilized membrane lysates from the indicated cell lines were immunoprecipitated with an anti-PS1 loop antibody, 3027, or with an anti-SPE-4 loop antibody, 8177, and immunoblotted for NCT. Both mature and immature NCT were co-immunoprecipitated with PS1 in cells expressing endogenous PS1 or exogenous PS1 wt and PS1 D385N (Figure 15B, upper panel, lane 1-4). Interestingly, immature NCT was co-immunoprecipitated with an antibody 8177 in the SPE-4/PS1c expressing cells (Figure 15B, lower panel, lane 5). The absence of co-immunoprecipitated NCT in the lane of SPE-4 wt expressing cells indicates that the interaction between NCT and SPE-4/PS1c is specific (Figure 15B, lower panel, lane 4). These data thus suggest that SPE-4/PS1c is capable to form a complex, at least with NCT. However, this complex remains apparently immature.

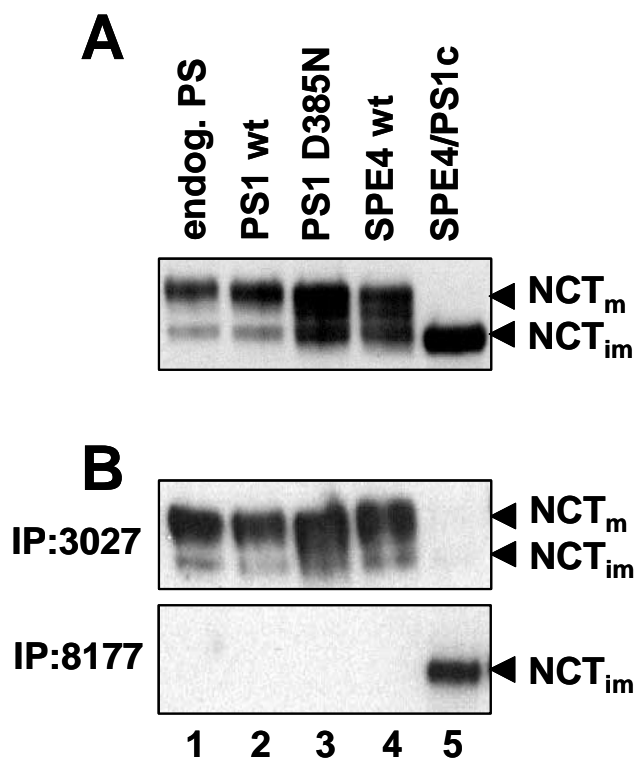


**Figure 15: NCT fails to mature in SPE-4/PS1c expressing cells**

A: NCT maturation was analyzed by immunoblotting. Cell lysates were separated by SDS-PAGE on a 7% Tris-glycine gel and immunoblotted with anti-NCT antibody N1660. Note that only immature NCT is detected in SPE4-PS1c expressing cells. B: Co-immunoprecipitation analysis. CHAPS-solubilized membrane extracts were immunoprecipitated with 3027 or 8177 antibodies, which are against the PS1 or SPE-4 loop region, respectively. The immunoprecipitates were analyzed by immunoblotting with N1660 antibody.

#### 3.1.4.4 Cells expressing SPE-4/PS1c show strongly decreased PEN-2 levels

To further analyze the reason for failure of NCT maturation of SPE-4/PS1c, the other  $\gamma$ -secretase complex components were analyzed. At this stage, to obtain more experimental flexibility, hexahistidine-Xpress-tagged (His)-proteins were constructed, because if necessary, these constructs allow distinguishing exogenously expressed  $\gamma$ -secretase activity from the endogenous one by using antibodies against the His-tag. In contrast to tagging the C-terminus of PS1, that disturbs the  $\gamma$ -secretase activity (Tomita et al., 1999), tagging the N-terminus allows  $\gamma$ -secretase complex formation (Steiner et al., 2002). In addition,

## Results

presence of the N-terminal His-tag did not disturb  $\gamma$ -secretase activity (see following results). The membrane lysate from HEK293/sw cells stably expressing His-proteins were immunoblotted with each corresponding antibodies. As shown in Figure 16A, all constructs were successfully expressed and, consistent with the above described results, replacement of endogenous PSs occurred in all cell lines except SPE-4 wt expressing cells. Notably, consistent with previous results (Wolfe et al., 1999a; Steiner et al., 2000), PS1 D385A did not undergo endoproteolysis, in contrast to PS1 wt. Like in Figure 15, SPE-4/PS1c expressing cell failed to mature NCT (Figure 16B, upper panel, lane 5). Interestingly, compared to the substantial levels of APH-1 expression, a strongly decreased level of PEN-2 was observed in this cell line (Figure 16B, middle and lower panels, lane 5). This result shows that the incompleteness of the  $\gamma$ -secretase complex formation in the SPE-4/PS1c expressing cells is caused by the absence of PEN-2, which is probably degraded because of the lack of a stabilizing interaction with SPE-4/PS1c. This observation indicates the requirement of other PS domains for the formation of an active  $\gamma$ -secretase complex in addition to its C-terminus. The above results revealed the importance of the PS1 C-terminus to initiate assembly of the  $\gamma$ -secretase complex. However, because SPE-4/PS1c underwent only partial  $\gamma$ -secretase complex assembly and thus did not support  $\gamma$ -secretase activity, the question whether SPE-4 has a protease activity remained unclear.

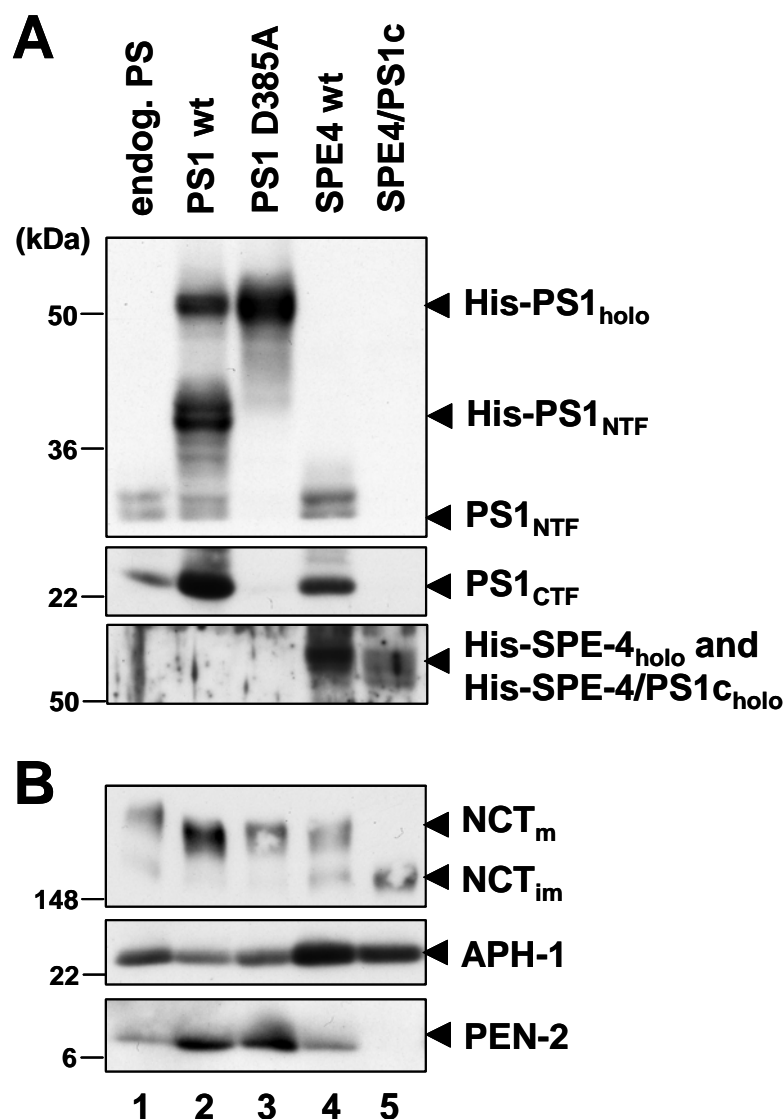


**Figure 16: Cells expressing SPE-4/PS1c are strongly deficient in PEN-2**

The effect of SPE-4/PS1c expression on the levels of the other  $\gamma$ -secretase complex components was analyzed. The membrane fractions from the indicated cells were solubilized with DDM and the lysates were analyzed by immunoblotting. 10% Tris-glycine urea gel for PS1 and SPE-4/PS1c (A), 7% Tris-glycine gel for NCT, and 10-20% Tris-tricine gel for APH-1 and PEN-2 (B) were used. A: The expression of each protein and the replacement of endogenous PS were analyzed by immunoblotting with antibodies PS1N, 3027 (upper and middle panels) or 8177 (lower panel). B: The other  $\gamma$ -secretase complex components were analyzed by immunoblotting with antibodies N1660 for NCT, 434G for APH-1, and 1638 for PEN-2.

### 3.1.5 The putative active site domain of SPE-4 may have proteolytic activity

#### 3.1.5.1 Construction of an active site chimeric protein

To study the open question whether SPE-4 has a proteolytic function, the putative SPE-4 active site domain was directly analyzed. Therefore, a chimeric protein, PS1/SPE-4<sub>6/7</sub>, in which TMDs 6 and 7 of PS1 are replaced with those of SPE-4 (Figure 17), was constructed. In addition, PS1/SPE-4<sub>6/7</sub> D394A in which the active site aspartate of TMD7 was changed to alanine, was constructed as a potential negative control like PS1 D385A.

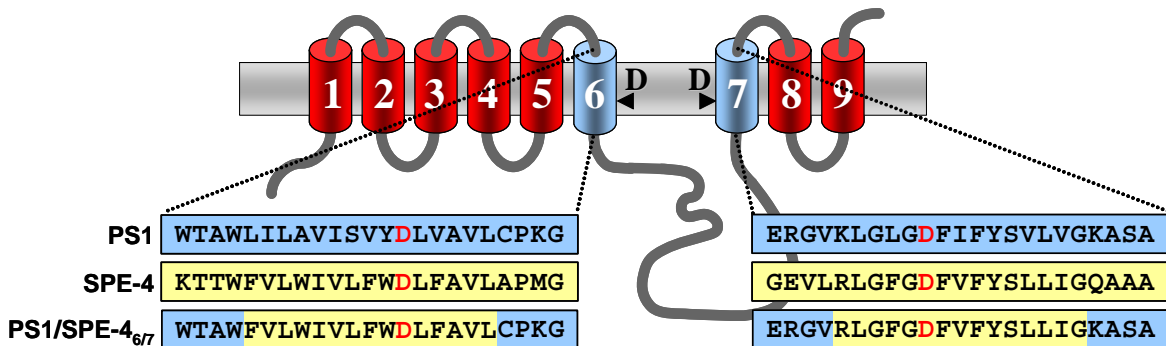


**Figure 17: Schematic model of PS1/SPE-4<sub>6/7</sub>**

A schematic model of PS1/SPE-4<sub>6/7</sub> is shown. The TMDs of PS1 are indicated in red and of SPE-4 in blue. The sequences of the swapped TMD domains are shown in detail.

#### 3.1.5.2 PS1/SPE-4<sub>6/7</sub> forms a $\gamma$ -secretase complex in PS1/2<sup>-/-</sup> MEF cells

All experiments described above were performed using HEK293 cells. However, there is the possibility that the observed effect on  $\gamma$ -secretase activity may not be fully reflecting the exogenously expressed PS due to incomplete replacement of the endogenous PSs. Therefore, PS1/2<sup>-/-</sup> mouse embryonic fibroblast (MEF) cells derived from mice deficient for PS1 and PS2 (Herreman et al., 1999) were employed to confirm the biological activity of the constructs described above in an endogenous PS-free background to avoid potential

interference of endogenous PSs in  $\gamma$ -secretase activity. Each cDNA was transiently cotransfected into PS1/2<sup>-/-</sup> MEF cells with cDNA encoding APP<sup>sw</sup>-6myc (Figure 18), a Swedish mutant of APP C-terminally tagged with six myc-epitopes (Hecimovic et al., 2004). Total cell lysates were analyzed by immunoblotting. Expression of PS1 wt, PS1 D385A, that were included as positive and negative controls, and the chimeric proteins was confirmed by immunoblotting with PS1N (to the PS1 NTF) or 3027 (to the PS1 CTF) antibodies. All four proteins were robustly expressed. As expected, PS1 D385A did not undergo endoproteolysis and remained as holoprotein, in contrast to PS1 wt (Figure 19A, lane 2 and 3). Likewise, PS1/SPE-4<sub>6/7</sub> was efficiently endoproteolyzed, whereas PS1/SPE-4<sub>6/7</sub> D394A like PS1 D385A failed to undergo endoproteolysis (Figure 19A, lane 3 and 4). Due to the lack of PSs, there is no maturation of the  $\gamma$ -secretase complex in PS1/2<sup>-/-</sup> MEF cells thus resulting in the accumulation of immature NCT. As expected, the vector-expressing cells showed no NCT maturation (Figure 19B, lane1). In contrast, all other cell lines expressing either PS wt, the D385A mutant, or PS chimeric proteins allowed a substantial recovery of NCT maturation demonstrating that these proteins are active in  $\gamma$ -secretase complex formation (Figure 19B, lane2-5).

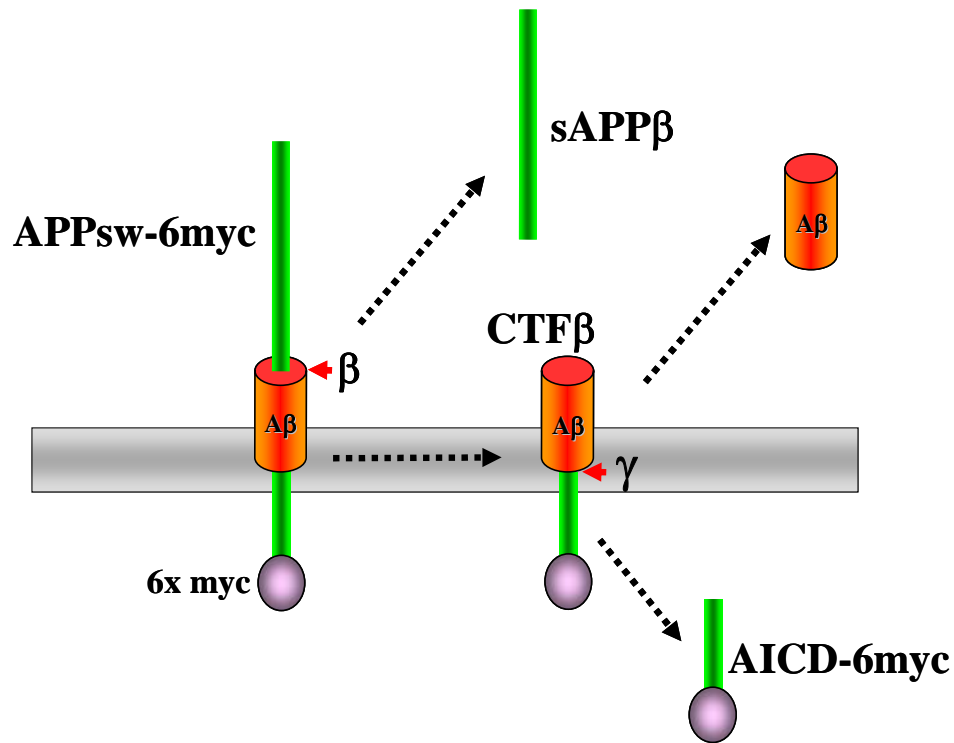


**Figure 18: Schematic representation of APPsw-6myc and its processing pathway**

The Swedish FAD mutant APP (2.3.3 and Figure 3) is tagged with 6xmyc tag at the C-terminus. The full-length molecule, APP-CTF $\beta$  and AICD fragments are detectable with an anti-myc antibody.

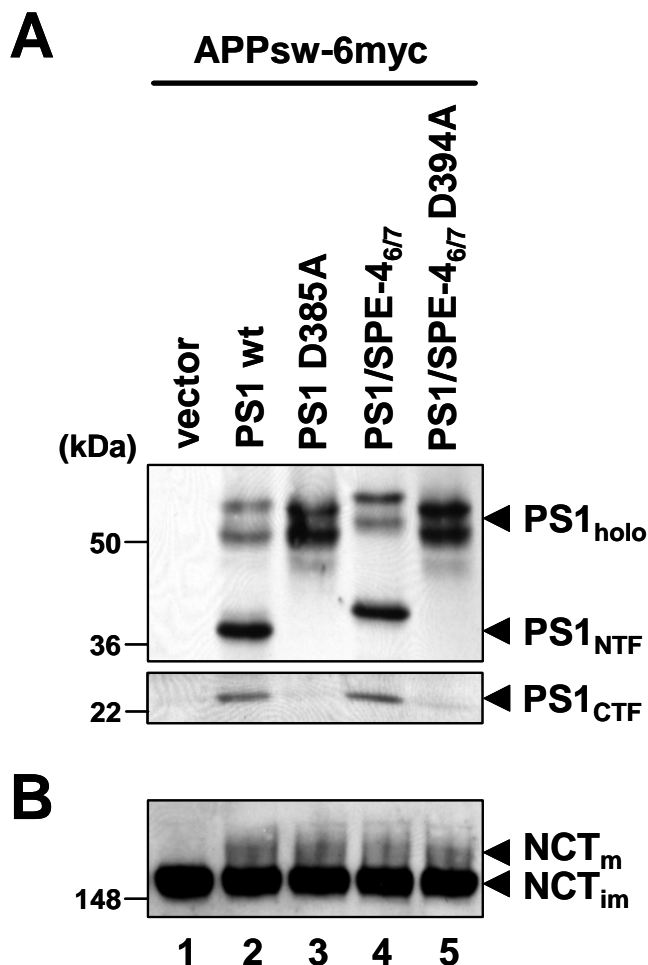


**Figure 19: PS1/SPE-4 chimeric proteins undergo  $\gamma$ -secretase complex formation**

Total cell lysates prepared from PS1/2<sup>-/-</sup> MEF cells, which were transiently cotransfected with the indicated cDNA constructs, were analyzed by immunoblotting. A: Total cell lysates were separated on 12% Tris-glycine urea gel and the expression of each protein was analyzed by immunoblotting with monoclonal anti-PS1 N-terminus antibody, PS1N (upper panel), or polyclonal anti-PS1 loop antibody, 3027 (lower panel). Antibody PS1N detected holoproteins and His-NTF, when the protein underwent endoproteolysis. Antibody 3027 detected CTF. B: NCT was separated on a 7% Tris-glycine gel, and detected by immunoblotting with polyclonal antibody N1660 that is raised against NCT C-terminus. NCT maturation was observed in every lane except the vector expressing cell line.

### 3.1.5.3 PS1/SPE-4<sub>6/7</sub> supports $\gamma$ -secretase-mediated APP processing

The above result demonstrated that PS1/SPE-4<sub>6/7</sub> is incorporated into a  $\gamma$ -secretase complex. To investigate its activity, processing of APPsw-6myc, which was co-expressed with either vector, PS1 wt, PS1 D385A, PS1/SPE-4<sub>6/7</sub> or PS1/SPE-4<sub>6/7</sub> D394A, was analyzed. The advantage of using APPsw-6myc is that 6myc-tagged AICD is rather stable as compared to non-tagged AICD, which is degraded rapidly in the cells. Despite robust expression level of substrate protein in every cell line (Figure 20A, upper panel), due to the lack of PSs, APP-CTFs accumulated and no AICD generation was observed in the vector expressing cells (Figure 20A, lower panel, lane 1) as expected. Moreover, combined immunoprecipitation/immunoblotting with antibodies 3552/6E10 did not detect any secreted A $\beta$  (~4 kDa) in this cell line (Figure 20C, lane 1). This defect of  $\gamma$ -secretase activity was rescued by co-expression of PS1 wt but not by proteolytically inactive PS1 D385A (Figure 20, lane 2 and 3). Like PS1 wt, PS1/SPE-4<sub>6/7</sub> was able to process APPsw-6myc as judged from the robust rescue of APP CTF accumulation and the substantial generation of AICD and A $\beta$ , whereas PS1/SPE-4<sub>6/7</sub> D394A like PS1 D385A failed to rescue the  $\gamma$ -secretase activity (Figure 20, lane 4 and 5). The secretion of APP itself of these cell lines was normal as judged from the secreted sAPP in the medium, which was detected by western blotting from conditioned medium using antibody 5313 (Figure 20B). These results suggest that the putative active site domain of SPE-4 is proteolytically active at least in APP processing.

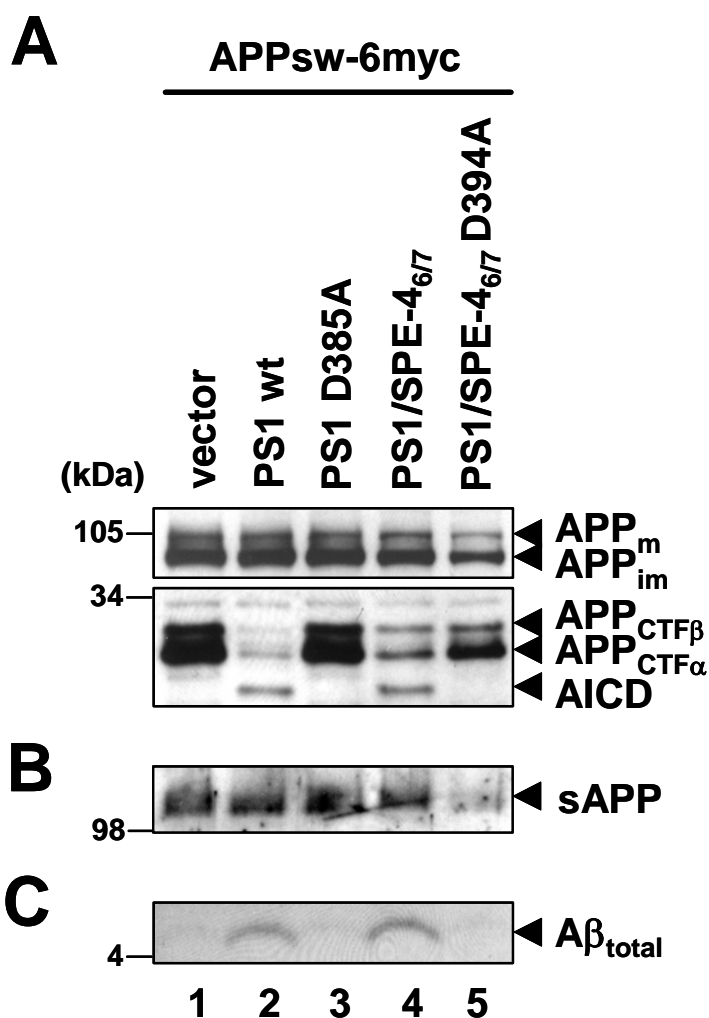


**Figure 20: PS1/SPE-4<sub>6/7</sub> supports APP processing**

The influence of each protein on APP processing was analyzed. A: Total cell lysates were separated on a 10-20% Tris-tricine gel and immunoblotted with a monoclonal anti-myc antibody 9E10. Robust amounts of APPsw-6myc were expressed in every cell line (upper panel). In contrast to cell lines which are expressing PS1 wt or PS1/SPE-4<sub>6/7</sub>, in vector, PS1 D385A, and PS1/SPE-4<sub>6/7</sub> D394A expressing cell lines, APP-CTFs accumulated and AICD generation was not observed (lower panel). B: Secreted sAPP was detected by immunoblotting from conditioned medium. Conditioned medium were applied on a 7% Tris-glycine gel and immunoblotted with polyclonal anti-APP antibody, 5313, that was raised against APP amino acid 444-592. C: Secreted total Aβ in conditioned medium was analyzed by combined immunoprecipitation/immunoblotting using polyclonal and monoclonal anti-Aβ antibodies 3552/6E10. Immunoprecipitates were separated on a 10-20% Tris-tricine gel. Aβ secretion was observed only in PS1 wt or PS1/SPE-4<sub>6/7</sub> expressing cells.

## **3.2 Identification of sequence requirements of PS for the $\gamma$ -secretase substrate selectivity**

### **3.2.1 PS1/SPE-4<sub>6/7</sub> does not support Notch processing in PS1/2<sup>-/-</sup> MEF cells**

Although the active site of SPE-4 supported the processing of APP, PS1/SPE-4<sub>6/7</sub> might influence the cleavage of other  $\gamma$ -secretase substrates due to sequence differences of TMDs 6 and 7 from those of PS1. If this was the case, PS1/SPE-4<sub>6/7</sub> could be used to identify putative sequence requirements of PS, in particular at the active site domain, for the  $\gamma$ -secretase substrate cleavage. Therefore, PS1/SPE-4<sub>6/7</sub> was probed for its  $\gamma$ -secretase activity in the processing of Notch, the most important physiological  $\gamma$ -secretase substrate. PS1/2<sup>-/-</sup> MEF cells were transiently cotransfected with cDNA encoding F-NEXT, an extracellular truncated Notch derivative with a FLAG-epitope tag at the N-terminus and six myc-epitope tags at the C-terminus ((Okochi et al., 2002) and Figure 21), and PS1/SPE-4<sub>6/7</sub>. PS1 wt and PS1 D385A were also transfected as positive and negative controls. Total cell lysate from each cell line was analyzed as described above. All cDNAs were successfully expressed, and PS1 wt and PS1/SPE-4<sub>6/7</sub> underwent endoproteolysis as expected (Figure 22A). As shown in Figure 22B lane 1, the cells expressing the vector control, which have no  $\gamma$ -secretase complex, accumulated F-NEXT and the generation of NICD was not observed. F-N $\beta$ , the secreted A $\beta$  analogue of Notch, was also not generated (Figure 22C, lane 1). Like in the case for the APP<sup>sw</sup>-6myc substrate, this deficiency of Notch processing was rescued by expressing PS1 wt, but not by PS1 D385A (Figure 22B and C, lane 2 and 3). Thus, strikingly, despite its capability in APP processing, PS1/SPE-4<sub>6/7</sub> showed a strong impairment in both NICD and F-N $\beta$  generation (Figure 22B and C, lane 4).

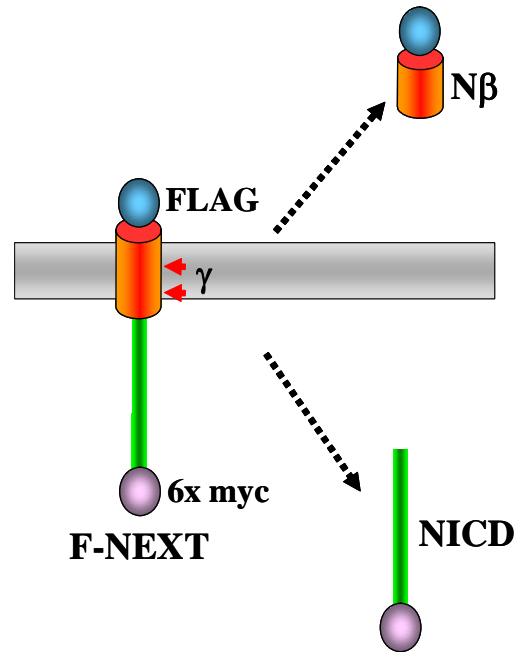


**Figure 21: Schematic model of F-NEXT protein and its processing pathway**

The extracellular truncated Notch (Figure 6) is tagged with a FLAG tag at the N-terminus and a 6x myc tag at the C-terminus. The anti-FLAG antibody facilitates the detecting of the full length molecule and the secreted Nβ peptide, and the anti-myc antibody facilitates the detecting of the full length molecule and the NICD fragment.

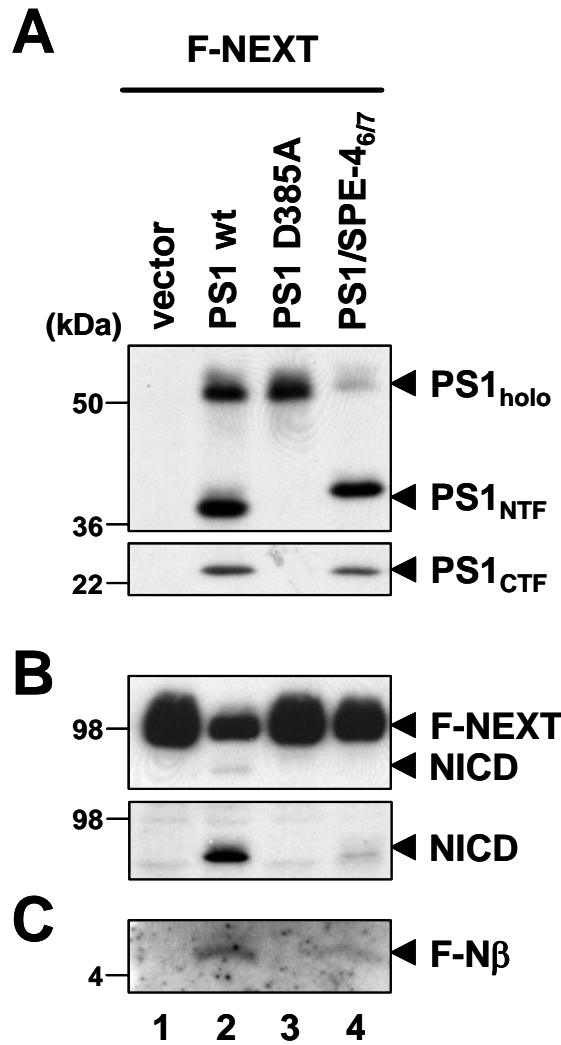


**Figure 22: F-NEXT is not processed in PS1/SPE-4<sub>6/7</sub> expressing cells**

The  $\gamma$ -secretase activity of PS1/SPE-4<sub>6/7</sub> on F-NEXT processing was analyzed. A: The expression level of each protein was analyzed as described in Figure 19. B: F-NEXT and NICD were separated on a 7% Tris-glycine gel. Total cell lysates were analyzed by immunoblotting with monoclonal anti-myc antibody 9E10 for F-NEXT and NICD or with an anti-NICD specific antibody, cleaved Notch-1, for NICD detection. F-NEXT accumulation and dramatically reduced NICD generation was observed in PS1/SPE-4<sub>6/7</sub> expressing cells. C: Secreted F-N $\beta$  in conditioned medium were analyzed by combined immunoprecipitation/immunoblotting with the anti-FLAG antibody. The immunoprecipitates were separated on a 10-20% Tris-tricine gel. Consistent with the deficient NICD generation shown in panel B, F-N $\beta$  secretion was strongly reduced in PS1/SPE-4<sub>6/7</sub> expressing cells.

To further confirm the observation that PS1/SPE-4<sub>6/7</sub> is deficient in processing of Notch, an immunocytochemical analysis was performed. PS1/2<sup>-/-</sup> MEF cells were transiently cotransfected with F-NEXT and cDNAs encoding PS1 wt, PS1 D385A or PS1/SPE-4<sub>6/7</sub>. 48 h after transfection, the cells were washed and fixed. For the detection of F-NEXT and NICD, the 9E10 anti-myc antibody as primary and anti-mouse Alexa Fluor 488 as secondary antibody was used. The cells expressing F-NEXT alone showed only plasma membrane staining indicating that F-NEXT accumulated on the cell surface (Figure 23A) due to the lack of  $\gamma$ -secretase activity of PS1/2<sup>-/-</sup> MEF cells. The same result was obtained in the cells coexpressing PS1 D385A (Figure 23C). In contrast, strong nuclear staining was observed in the F-NEXT/PS1 wt coexpressing cells demonstrating that F-NEXT was processed and that NICD was released and translocated into nucleus (Figure 23B). Consistent with the previous data (Figure 22), the PS1/SPE-4<sub>6/7</sub> expressing cells showed strongly reduced nuclear NICD staining (Figure 23D). Occasionally, some cells showed weak nuclear staining, which is consistent with the residual minor NICD formation in Figure 22. These data show that although SPE-4 contains a functional protease active site, which is able to process APP, it is deficient in processing Notch as substrate.

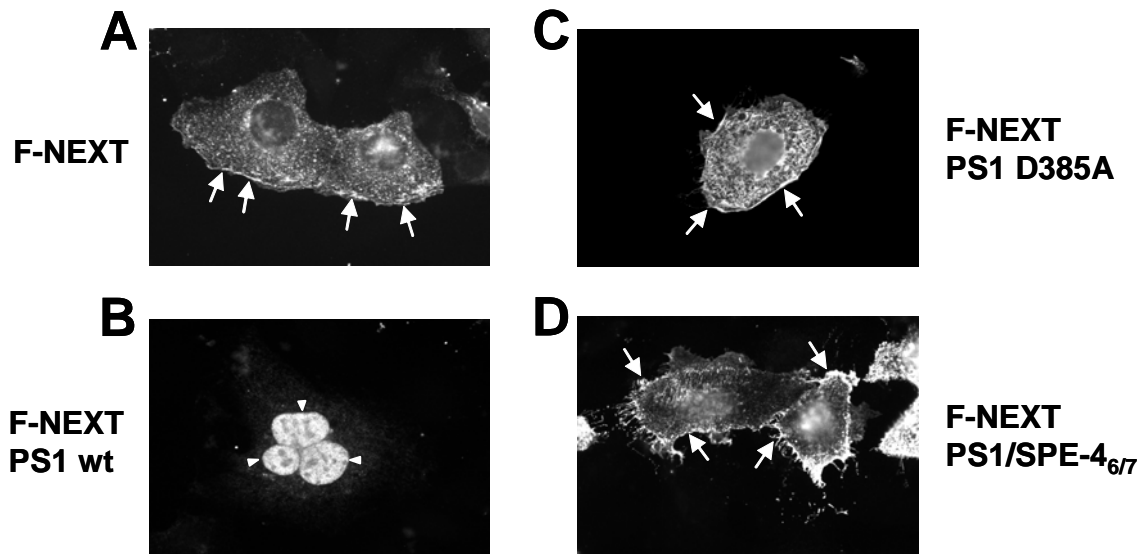


**Figure 23: NICD does not translocate into the nucleus in PS1/SPE-4<sub>6/7</sub> expressing cells**

PS1/2<sup>-/-</sup> MEF cells were transiently transfected with F-NEXT either only or together with cDNA encoding PS1 wt, PS1 D385A or PS1/SPE-4<sub>6/7</sub>. After fixation, F-NEXT or its cleavage product NICD, was visualized using monoclonal anti-myc antibody 9E10 and polyclonal Alexa-488 antibody raised against mouse IgG. A: F-NEXT expressing cells. Only plasma membrane staining was observed. B: F-NEXT/PS1 wt coexpressing cells. Strong nuclear staining was observed. C: F-NEXT/PS1 D385A coexpressing cells. Only plasma membrane staining was observed in this cell line. D: F-NEXT/PS1/SPE-4<sub>6/7</sub> coexpressing cells. Mainly plasma membrane staining was observed. Representative cell images are shown.

### 3.2.2 TMD7 is the responsible domain for the Notch cleavage deficiency of PS1/SPE-4<sub>6/7</sub>

#### 3.2.2.1 Construction of PS1/SPE-4<sub>6</sub> and PS1/SPE-4<sub>7</sub>

Next, the molecular basis of the apparent APP/Notch substrate discrimination by PS1/SPE-4<sub>6/7</sub> was investigated. To map which one of the two TMD in PS1/SPE-4<sub>6/7</sub> is responsible for the Notch processing deficiency, two additional constructs, in which only one TMD of PS1 is exchanged with the corresponding TMD of SPE-4, PS1/SPE-4<sub>6</sub> and PS1/SPE-4<sub>7</sub> (Figure 24), were generated.

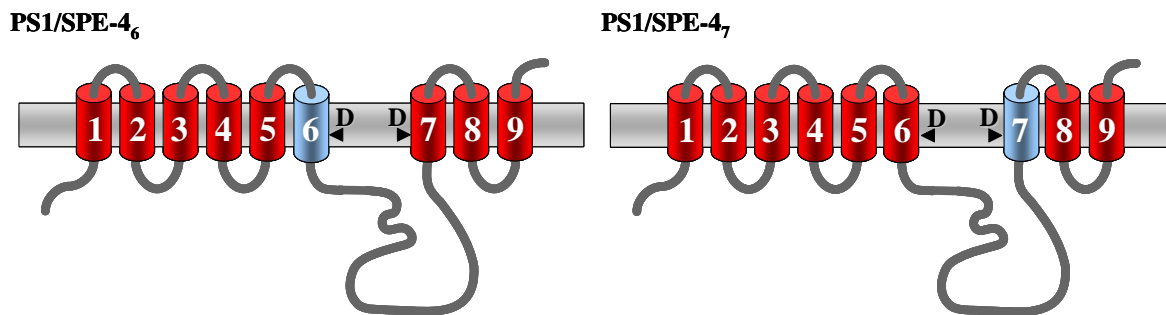


**Figure 24: Schematic model of PS1/SPE-4<sub>6</sub> and PS1/SPE-4<sub>7</sub>**

The TMDs of PS are indicated in red and those of SPE-4 in blue.

### 3.2.2.2 PS1/SPE-4<sub>6</sub> and PS1/SPE-4<sub>7</sub> support processing of APP

PS1<sup>2<sup>-/-</sup></sup> MEF cells were transiently cotransfected with cDNA constructs encoding APPsw-6myc and PS1/SPE-4<sub>6</sub> or PS1/SPE-4<sub>7</sub>. The expression level, their biochemical behavior, and the  $\gamma$ -secretase activity on APP processing of these hybrid active site proteins were analyzed as described above (see 3.1.5.2 and 3.1.5.3). The PS1/SPE-4<sub>6/7</sub> construct was included for comparison. PS1 wt and PS1 D385A were included as positive and negative controls like above. All constructs were expressed (Figure 25A) and both PS1/SPE-4<sub>6</sub> and PS1/SPE-4<sub>7</sub> underwent endoproteolysis (Figure 25A, lane 5 and 6) like PS1/SPE-4<sub>6/7</sub> demonstrating that they formed a  $\gamma$ -secretase complex, which could additionally be confirmed by the maturation of NCT (Figure 25B). Note that NTF and holoprotein of PS1/SPE-4<sub>6/7</sub> migrated higher than the calculated molecular size of these fragments, which are supposed to be the same as those of PS1/SPE-4<sub>6</sub>, for unknown reasons.

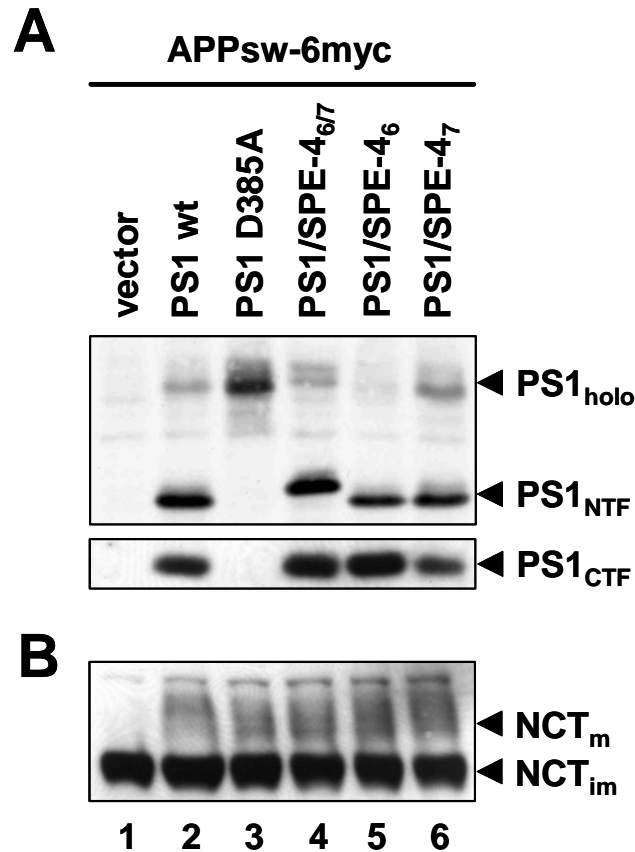


**Figure 25: PS1/SPE-4<sub>6</sub> and PS1/SPE-4<sub>7</sub> form a  $\gamma$ -secretase complex**

PS1/2<sup>-/-</sup> MEF cells were transiently cotransfected with PS1/SPE-4<sub>6</sub> and PS1/SPE-4<sub>7</sub> together with APPsw-6myc. Total cell lysates were analyzed as Figure 19. A: Expression of each protein was detected by immunoblotting with monoclonal anti-PS1 N-terminus antibody PS1N (upper panel) and polyclonal anti-PS1 loop antibody 3027 (lower panel). B: NCT maturation was analyzed using anti-NCT antibody N1660. Note that both PS1/SPE-4<sub>6</sub> and PS1/SPE-4<sub>7</sub> underwent endoproteolysis and allowed NCT maturation.

As shown in Figure 26A, similar amounts of APPsw-6myc were expressed in each cell line (upper panel). Compared to the PS1 D385A expressing cells, APP-CTFs accumulation was dramatically reduced in the PS1/SPE-4<sub>6</sub> or PS1/SPE-4<sub>7</sub> expressing cells (Figure 26A, lower panel). Moreover, substantial generation of AICD (Figure 26A, lower panel) and secretion of A $\beta$  (Figure 26C) were also observed in these cells. In addition, although there was some variation in the levels of secreted sAPP observed in this experiment, Figure 26B indicates the capability of secretion in each cell line. Notably, the cells expressing PS1/SPE-4<sub>7</sub>

(Figure 26B and C, lane 6) showed substantial A $\beta$  secretion despite its lower sAPP level compared to the other cell lines. Therefore, the level of secreted A $\beta$  reflects the  $\gamma$ -secretase activity of each cell line. These results suggest that like PS1/SPE-4<sub>6/7</sub>, both PS1/SPE-4<sub>6</sub> and PS1/SPE-4<sub>7</sub> were capable to process APP.

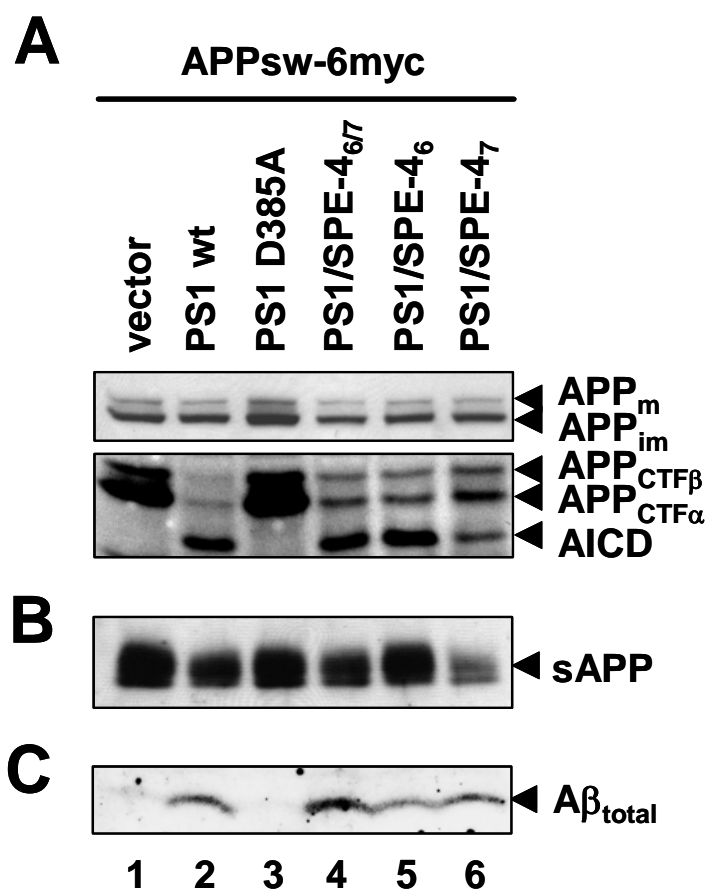


**Figure 26: PS1/SPE-4<sub>6</sub> and PS1/SPE-4<sub>7</sub> support APP processing**

APP processing was analyzed as in Figure 20. A: APPsw-6myc expression level (upper panel), APP-CTF accumulation and AICD generation (lower panel) were analyzed from total cell lysates by immunoblotting using monoclonal anti-myc antibody 9E10. B: Secretion of sAPP in conditioned medium were analyzed by immunoblotting with polyclonal anti-APP antibody 5313. C: A $\beta$  secretion was analyzed from conditioned medium by combined immunoprecipitation/immunoblotting with polyclonal and monoclonal anti-A $\beta$  antibodies 3552/6E10. Note that both PS1/SPE-4<sub>6</sub> and PS1/SPE-4<sub>7</sub> were capable to process APPsw-6myc.

### 3.2.2.3 PS1/SPE-4<sub>7</sub> is inactive in Notch processing

To analyze the capability of PS1/SPE-4<sub>6</sub> and PS1/SPE-4<sub>7</sub> on Notch processing, these constructs were transiently coexpressed in PS1/2<sup>-/-</sup> MEF cells with F-NEXT as described above (see 3.2.1), including the control constructs. All the constructs were successfully expressed and underwent endoproteolysis except PS1 D385A, as expected (Figure 27A). Interestingly, in contrast to PS1/SPE-4<sub>6</sub>, expression of PS1/SPE-4<sub>7</sub> strongly impaired the generation of NICD (Figure 27B, lane 5 and 6) and the secretion of F-N $\beta$  (Figure 27C, lane 5 and 6) from F-NEXT. These results demonstrate that TMD7 of PS1/SPE-4<sub>6/7</sub> is responsible for the deficiency of the chimeric protein in Notch processing.

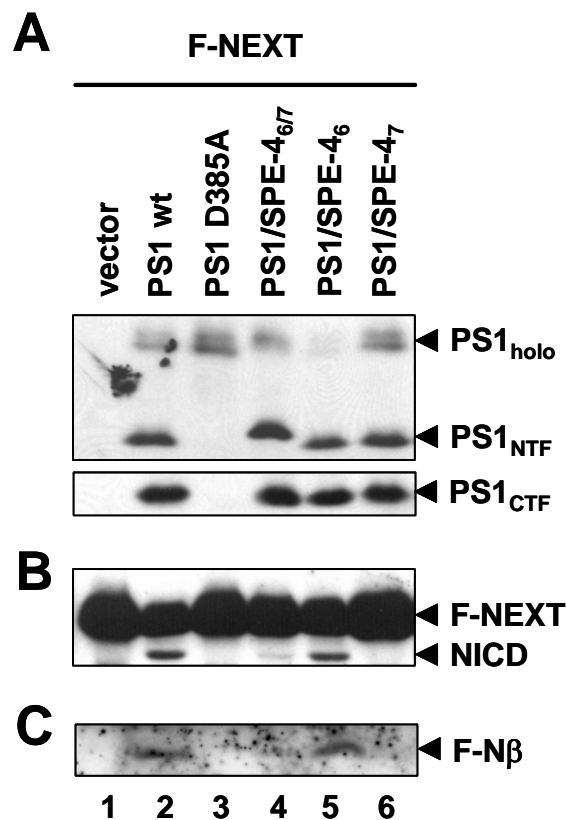


**Figure 27: Cells expressing PS1/SPE-4<sub>7</sub> are deficient in Notch processing**

Influence of PS1/SPE-4<sub>6</sub> and PS1/SPE-4<sub>7</sub> on Notch processing was analyzed as in Figure 22. A: Total cell lysates were analyzed by immunoblotting with monoclonal anti-PS1 N-terminus antibody PS1N (upper panel) and polyclonal anti-PS1 loop antibody 3027 (lower panel). B: F-NEXT accumulation and NICD generation were analyzed by immunoblotting with monoclonal anti-myc antibody 9E10. C: Levels of secreted F-N $\beta$  in conditioned medium were analyzed by combined immunoprecipitation/immunoblotting with monoclonal anti-FLAG antibody M2. Note that unlike PS1/SPE-4<sub>6</sub>, PS1/SPE-4<sub>7</sub> failed to process Notch.

### 3.2.3 A single amino acid at position x of the G<sub>x</sub>GD motif contributes to the Notch processing deficiency of PS1/SPE-4<sub>7</sub>

#### 3.2.3.1 The G<sub>x</sub>GD active site motif of SPE-4 contains a phenylalanine residue at position x instead of leucine

To further map the responsible sequence within the TMD7 of PS1/SPE-4<sub>6/7</sub>, the amino acid sequence of TMD7 including the other *C. elegans* PS homologues was compared (Figure 28). Interestingly, among the non-conserved amino acids, there was a more drastic amino acid change of the residue at the position x of the G<sub>x</sub>GD motif within the TMD7 in SPE-4 from PS1. This residue of PS1 (L383) is rather conserved SEL-12 (L362) and in HOP-1 (M276). However, it is drastically changed to an aromatic amino acid, phenylalanine, in SPE-4 (F392). To address the functional significance of this amino acid change, the phenylalanine residue of the GFGD motif in PS1/SPE-4<sub>7</sub> was mutagenized to L to restore the PS1 or SEL-12 GLGD motif (PS1/SPE-4<sub>7</sub>F392L) or to M to restore the GMGD motif of HOP-1 (PS1/SPE-4<sub>7</sub>F392M).

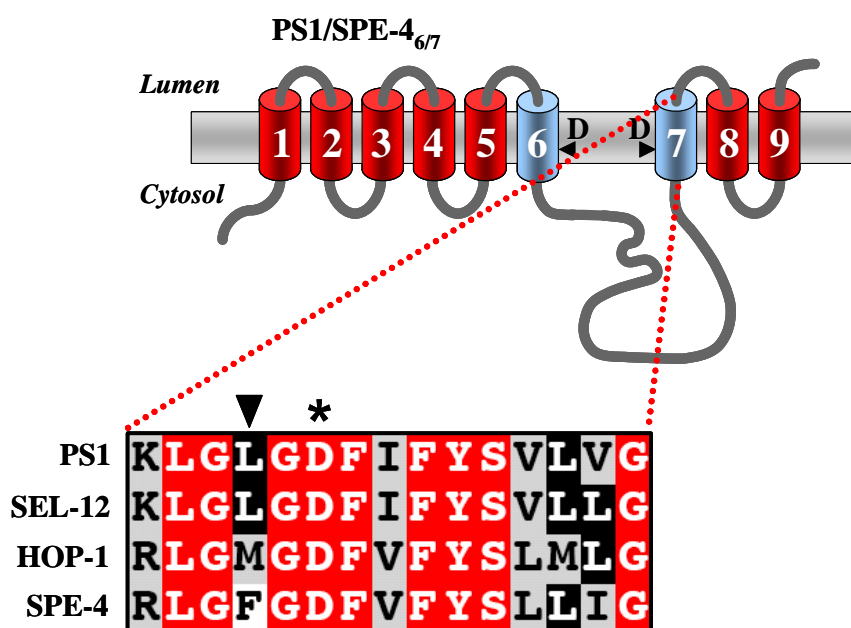


**Figure 28: Sequence comparison of TMD7**

The amino acid sequence alignment of TMD7 of PS1, SEL-12, HOP-1, and SPE-4. Identical amino acid residues are displayed on black or red (identical in all PSs) background and similar ones on gray background. Arrowhead indicates the residues at position x of the G<sub>x</sub>GD motif. Asterisks indicate the active site aspartate residues.

### **3.2.3.2 PS1/SPE-4<sub>7</sub> F392L and PS1/SPE-4<sub>7</sub> F392M support APP processing**

The activity of the two new constructs on APP and Notch processing was then analyzed as described above. As shown in Figure 29A, both PS1/SPE-4<sub>7</sub> F392L and PS1/SPE-4<sub>7</sub> F392M underwent endoproteolysis (upper and middle panels), and allowed NCT maturation (lower panel) demonstrating  $\gamma$ -secretase complex formation of these constructs. They were also capable to process APP<sup>sw-6myc</sup> (Figure 29B) as judged from the substantial amount of AICD and A $\beta$  generated and from the rescue of APP-CTF accumulation (Figure 29B and C). The expression of APP<sup>sw-6myc</sup> (Figure 29B, upper panel) and sAPP secretion (Figure 29C, upper panel) were controlled as above.

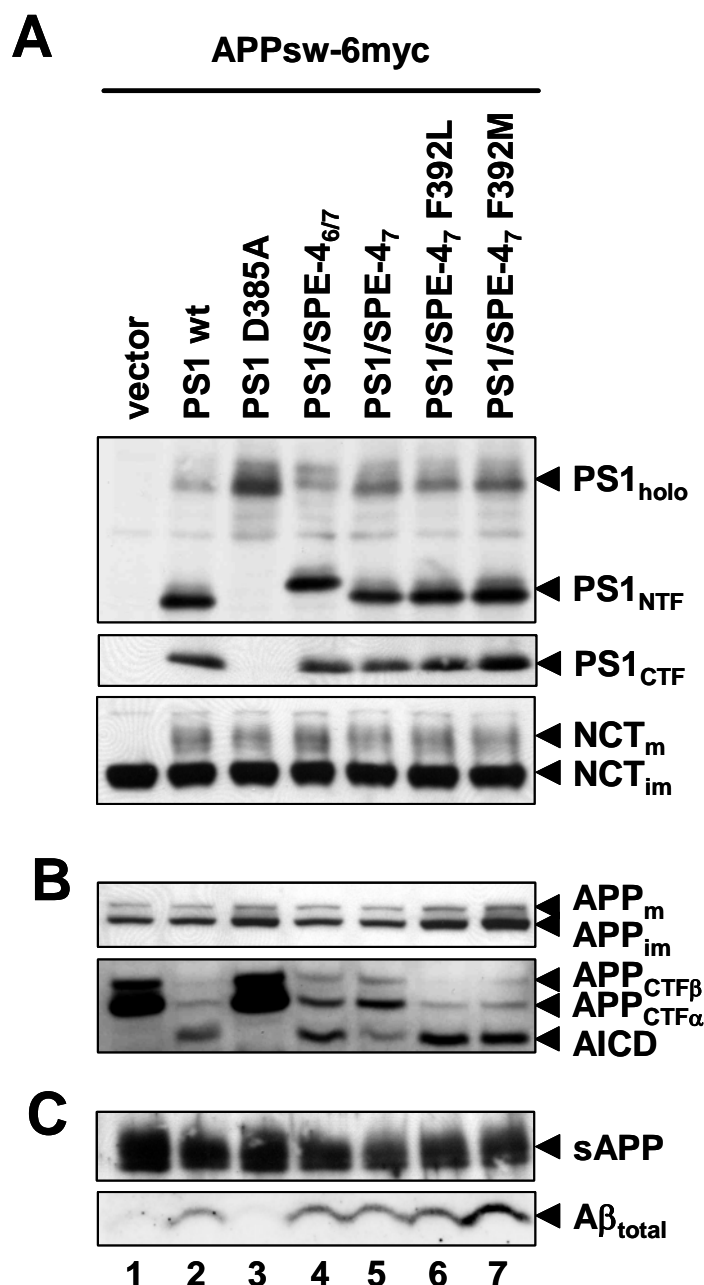


**Figure 29: PS1/SPE-4<sub>7</sub> F392L and PS1/SPE-4<sub>7</sub> F392M are active in APP processing**

PS1<sup>2<sup>-/-</sup></sup> MEF cells were transiently cotransfected with the indicated constructs and APPsw-6myc and analyzed as in Figure 26. A: The expression of each construct was analyzed by immunoblotting with monoclonal anti-PS1 N-terminus antibody PS1N (upper panel) or polyclonal anti-PS1 loop antibody 3027 (middle panel). NCT maturation was analyzed by immunoblotting using antibody N1660 (lower panel). B: Total cell lysates were analyzed by immunoblotting with monoclonal anti-myc antibody 9E10 to detect the expression (upper panel) and the processing (lower panel) of APPsw-6myc. C: Secretion of sAPP was analyzed by immunoblotting with polyclonal anti-APP antibody 5313 (upper panel) and secretion of Aβ was analyzed by combined immunoprecipitation/immunoblotting with polyclonal and monoclonal anti-Aβ antibodies 3552/6E10 (lower panel) from conditioned medium.

### 3.2.3.3 PS1/SPE-4<sub>7</sub> F392L and PS1/SPE-4<sub>7</sub> F392M support Notch processing

Next, processing of Notch was analyzed. All constructs were expressed and underwent  $\gamma$ -secretase complex formation (Figure 30A). Strikingly, both PS1/SPE-4<sub>7</sub> F392L and PS1/SPE-4<sub>7</sub> F392M allowed the generation of NICD and F-N $\beta$  as shown in Figure 30B (lane 6 and 7). These results suggest that phenylalanine at position x within the GxGD motif is indeed important for Notch processing.

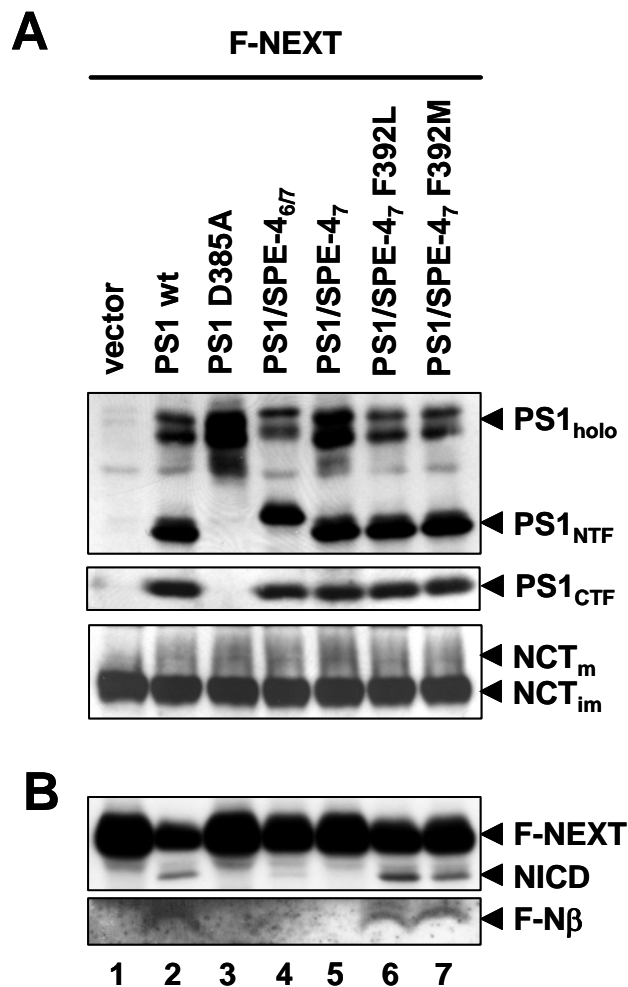


**Figure 30: PS1/SPE-4<sub>7</sub> F392L and PS1/SPE-4<sub>7</sub> F392M are active in Notch processing**

Notch processing was analyzed in transiently cotransfected PS1/2<sup>-/-</sup> MEF cells as in Figure 27. A: Total cell lysates were analyzed by immunoblotting using monoclonal anti-PS1 N-terminus antibody PS1N (upper panel), polyclonal anti-PS1 loop antibody 3027 (middle panel) or polyclonal anti-NCT antibody N1660 (lower panel). B: Levels of F-NEXT expression and NICD generation were analyzed from total cell lysates by immunoblotting with monoclonal anti-myc antibody 9E10 (upper panel). Combined immunoprecipitation/immunoblotting with monoclonal anti-FLAG antibody M2 was performed from conditioned medium to analyze secreted F-N $\beta$  (lower panel).

### **3.2.4 Leucine at the position x of the GxGD motif is important for Notch processing in PS1**

The above results suggest that the residue at the position x within the GxGD motif determines the efficiency of Notch processing. However, this effect might only occur in the context of the PS1/SPE-4<sub>7</sub> and PS1/SPE-4<sub>6/7</sub> chimeric proteins. To exclude this possibility and to obtain further evidence for an importance of this residue within the GxGD motif, L383 was mutated to F directly in PS1. The consequence of PS1 L383F on  $\gamma$ -secretase activity was then analyzed as above.

PS1/2<sup>-/-</sup> MEF cells were transiently cotransfected with PS1 L383F and APPsw-6myc (Figure 31) or F-NEXT (Figure 32). PS1 L383F was capable of  $\gamma$ -secretase complex formation as judged from the generation of PS1 NTF (Figure 31A and Figure 32A, upper panels) and CTF (Figure 31A and Figure 32A, middle panels), and the maturation of NCT (Figure 31A and Figure 32A, lower panels). PS1 L383F was also able to process APPsw-6myc, which showed substantial AICD (Figure 31B, lower panel) and A $\beta$  (Figure 31C, lower panel) generation.

In contrast, when PS1 L383F was expressed together with F-NEXT, an accumulation of F-NEXT (Figure 32B, upper panel) was observed concomitant with dramatically reduced NICD (Figure 32B, upper panel) and F-N $\beta$  (Figure 32B, lower panel) generation. These data indicate that the L383 residue is required in PS1 itself for efficient Notch processing.

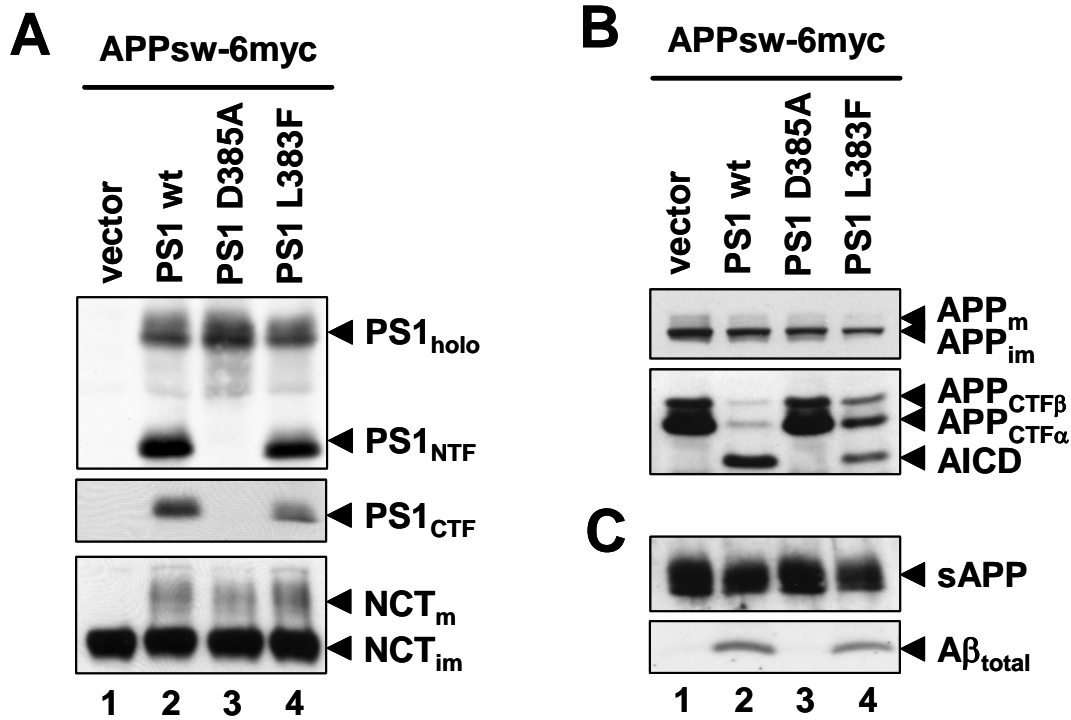


**Figure 31: PS1 L383F is active in APP processing**

PS1 L383F was transiently coexpressed together with APPsw-6myc in PS1<sup>2-/-</sup> MEF cells and analyzed as in Figure 29. A: The expression of each construct was analyzed by immunoblotting with monoclonal anti-PS1 N-terminus antibody PS1N (upper panel) or polyclonal anti-PS1 loop antibody 3027 (middle panel). NCT maturation was analyzed by immunoblotting using polyclonal anti-NCT antibody N1660 (lower panel). B: Total cell lysates were analyzed by immunoblotting with monoclonal anti-myc antibody 9E10 to detect the level of expression (upper panel) and the processing (lower panel) of APPsw-6myc. C: The secreted sAPP and Aβ were analyzed either by immunoblotting with polyclonal anti-APP antibody 5313 (upper panel) or combined immunoprecipitation/immunoblotting with polyclonal and monoclonal anti-Aβ antibodies 3552/6E10 (lower panel) from conditioned medium.

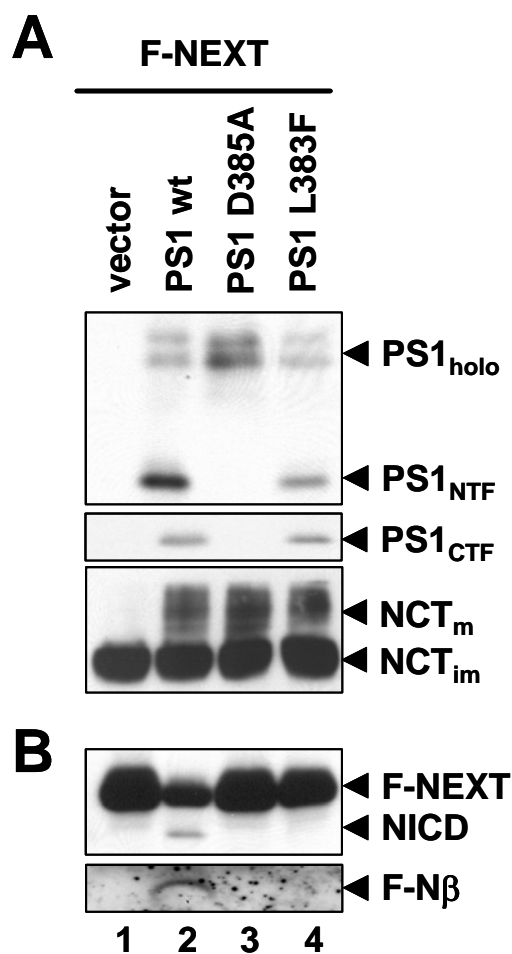


**Figure 32: PS1 L383F is deficient in Notch processing**

PS1 L383F activity in Notch processing was analyzed as in Figure 30. A: Total cell lysates were analyzed by immunoblotting using monoclonal anti-PS1 N-terminus antibody PS1N (upper panel), polyclonal anti-PS1 loop antibody 3027 (middle panel) or polyclonal anti-NCT antibody N1660 (lower panel). B: The levels of F-NEXT expression and NICD generation were analyzed from total cell lysates by immunoblotting with monoclonal anti-myc antibody 9E10 (upper panel). Combined immunoprecipitation/immunoblotting with monoclonal anti-FLAG antibody M2 was performed from conditioned medium for analyzing secreted F-N $\beta$  (lower panel).

## 4. Discussion

### 4.1 A proteolytic function of SPE-4

#### 4.1.1 SPE-4 does not undergo $\gamma$ -secretase complex formation

SPE-4 was identified as the most distant PS homologue with approximately 23% of homology to PS1 based on the BLAST search. Despite of its low homology, the two catalytic aspartates within TMD6 and 7, including the GxGD active site motif, and the C-terminal PALP motif, which are characteristic for the PS protease family, are well conserved in SPE-4. The PALP motif is required for PS activity in humans and *Drosophila*. Mutation of the first proline in *Drosophila* presenilin eliminated its function in Notch signaling (Guo et al., 1999). Furthermore, as shown in human cells, this mutation eliminated both endoproteolysis of PS and  $\gamma$ -secretase activity even though they were incorporated into a high molecular weight complex (Tomita et al., 2001; Takasugi et al., 2002; Kaether et al., 2004; Wang et al., 2004). These observations suggest that the PALP motif is crucial for  $\gamma$ -secretase activity. In case of SPE-4, a mutation of the first proline within the PALP motif results in arrests of spermatogenesis at an unusual cellular stage in a similar manner to a null phenotype (Arduengo et al., 1998). The conservation of the functional aspartates and motifs in SPE-4 suggests the conservation of a PS-type proteolytic function of SPE-4. Because it is difficult to analyze SPE-4 function directly in *C. elegans* due to its temporally and spatially limited expression, mammalian cells were employed to address to analyze this question.

When PS is stably overexpressed in HEK293 cells, the exogenous PS replaces the endogenous PSs as a result of competition for the interaction with the other  $\gamma$ -secretase complex components. This replacement could be an indicator of  $\gamma$ -secretase complex formation of the exogenously expressed PS. Interestingly, despite its robust expression, SPE-4 wt was not able to replace endogenous PS1 and PS2 in HEK293/sw cells (Figure 10), which indicates that at least in this situation this molecule is unable to assemble into the  $\gamma$ -secretase complex. It may be that SPE-4 is not able to interact with human complex components, because of its very distant sequence from PS. In addition, one could also speculate on the possibility that SPE-4 functions alone without forming a complex with other components. These possibilities will be discussed below.

To further investigate the putative proteolytic activity of SPE-4, it was forced to replace endogenous PSs by exchanging its C-terminus after the PALP motif with the corresponding region of PS1 which had been suggested to be required for  $\gamma$ -secretase complex formation (Tomita et al., 1999; Bergman et al., 2004; Kaether et al., 2004; Wang et al., 2006) (Figure 12). This construct, SPE-4/PS1c, with successfully replaced endogenous PSs shows this chimeric protein incorporated into  $\gamma$ -secretase complex (Figure 13). However, surprisingly, the SPE-4/PS1c expressing cells showed an impairment of  $\gamma$ -secretase activity, which was caused by the failure of NCT maturation (Figure 14 and Figure 15) and by the lack of PEN-2 interaction (Figure 16). Co-immunoprecipitation experiments revealed an interaction between NCT and SPE-4/PS1c (Figure 15). The absence of NCT binding to SPE-4 wt indicates that NCT binds specifically to SPE-4/PS1c via the exchanged PS1 C-terminal region. This observation is consistent with previous reports (Tomita et al., 2002; Bergman et al., 2004; Kaether et al., 2004) that showed the deletion or the mutation of the last amino acids of PS1 result in the inhibition of PS1 endoproteolysis and the  $\gamma$ -secretase activity due to the lack of NCT binding. These observations could also explain why SPE-4 wt failed to form a  $\gamma$ -secretase complex, either because of its shorter C-terminus compared to the PS1 or by the difference in sequence in human cells at the C-terminus (Figure 9). Despite the fact that SPE-4/PS1c was able to bind NCT,  $\gamma$ -secretase complex formation remained incomplete. The analysis of the other  $\gamma$ -secretase components revealed the absence of PEN-2 in this cell line (Figure 16). This result suggested that the complex formed by SPE-4/PS1c, NCT and APH-1 failed to stabilize PEN-2, which is rapidly degraded in the cells when it is not incorporated into the complex (Bergman et al., 2004; Crystal et al., 2004). This observation accords to recent findings that suggest a direct interaction of PEN-2 with the PS1 NTF occurring via the PS1 TMD4 (Kim and Sisodia, 2005; Watanabe et al., 2005), which is different in SPE-4/PS1c. Interestingly, the sequence of TMD4 that is suggested to be required for PEN2 binding is not very well conserved in *C. elegans* PS homologues. The result above thus also supports the notion that *C. elegans* PS/PEN-2 interactions might be different from that in mammals or insects (Watanabe et al., 2005). Moreover, it also suggests that  $\gamma$ -secretase complex assembly occurs stepwise as follows: i) subcomplex formation by APH-1 and NCT interaction, ii) stable high molecular weight complex formation together with PS holoprotein and iii) final maturation step of active  $\gamma$ -secretase complex by joining of PEN-2, which elicits endoproteolysis of PS (Figure 7) (Takasugi et al., 2003). Taken together,

## Discussion

the above results indicate that it is most likely that APH-1/NCT subcomplex formation and subsequent SPE-4/PS1c binding of this subcomplex occurred via the PS1 C-terminus. Also noteworthy, the interaction between NCT and SPE-4/PS1c was confirmed by co-immunoprecipitation. In contrast, PEN-2 was degraded most likely due to the absence of a functional binding site on SPE-4/PS1c. Thus, a PS domain(s) other than its C-terminus is required for functional  $\gamma$ -secretase complex formation.

### **4.1.2 The active site domain of SPE-4 supports APP processing**

Although the importance of the PS1 C-terminus in initiating  $\gamma$ -secretase complex formation was shown, the question whether or not SPE-4 has a proteolytic function remained unclear because of its incomplete  $\gamma$ -secretase complex formation in the mammalian cells. To investigate this area further, the capability of a proteolytic function of the putative active site domain of SPE-4 was directly tested separated from its sequence using the active site chimera PS1/SPE-4<sub>6/7</sub> (Figure 17).

PS1/SPE-4<sub>6/7</sub> was able to assemble a complete  $\gamma$ -secretase complex in PS1/2<sup>-/-</sup> MEF cells, as judged from the NTF and CTF generated by PS endoproteolysis and the rescue of NCT maturation (Figure 19). This result supports the above observation that SPE-4/PS1c lacks an important domain required to form a mature  $\gamma$ -secretase complex. Moreover, PS1/SPE-4<sub>6/7</sub> showed substantial activity in APP processing (Figure 20). Unlike the aspartate mutant variant of this chimeric protein, PS1/SPE-4<sub>6/7</sub> D394A, it rescued APP-CTF accumulation of the PS1/2<sup>-/-</sup> MEF cells caused by the lack of  $\gamma$ -secretase activity and allowed AICD and A $\beta$  formation. The similar amount of APPsw-6myc expression and sAPP secretion suggest that the  $\gamma$ -secretase inactivity in the PS1/SPE-4<sub>6/7</sub> D394A expressing cell is due to the mutation of the catalytically active aspartate residue. The fact that both endoproteolysis and APP processing were dependent on an active site aspartate is a strong indication of the functional conservation of the putative SPE-4 active site domain. Notably, this is the first demonstration that  $\gamma$ -secretase can function with a related but not identical active site domain in its catalytic subunit PS.

## **4.2 Identification of sequence requirements of PS for $\gamma$ -secretase substrate cleavage**

### **4.2.1 The active site of SPE-4 discriminates APP and Notch substrates**

The conservation of the proteolytic activity of SPE-4 active site domain provided an opportunity to investigate the putative sequence requirements of PS for the  $\gamma$ -secretase activity. It was reasoned that despite its substantial activity on APP processing a  $\gamma$ -secretase complex containing PS1/SPE-4<sub>6/7</sub> might have an influence on the cleavage of the other  $\gamma$ -secretase substrates due to its sequence difference of TMDs 6 and 7 from PS. Therefore, the influence of PS1/SPE-4<sub>6/7</sub> on processing of Notch was analyzed. Surprisingly, despite of its substantial  $\gamma$ -secretase activity on APP processing, PS1/SPE-4<sub>6/7</sub> did not support Notch processing. The generation of NICD and F-N $\beta$  was impaired in transiently cotransfected PS1/2<sup>-/-</sup> MEF cells (Figure 22). This observation was confirmed by immunocytochemical analysis. Consistent with the biochemical data, PS1/SPE-4<sub>6/7</sub> failed to process F-NEXT and mainly plasma membrane staining was observed (Figure 23). These data indicate that the TMDs 6 and 7 of SPE-4 including the active site domain could discriminate two substrates APP and Notch, at least in the context of this chimeric protein.

### **4.2.2 Identification of a critical amino acid within TMD7 at position x of the GxGD motif**

Mapping of the responsible sequence determinant(s) for APP/Notch substrate selectivity revealed that a single amino acid at the position x of the GxGD motif within TMD7 plays a crucial role. The amino acid sequence comparison of PS1, SEL-12, HOP-1 and SPE-4 showed one significant amino acid change in SPE-4 from the other PSs. Among the PS protease family, the residue x is typically an aliphatic amino acid leucine, with the exceptions of the *C. elegans* homologues HOP-1 and SPE-4 (Figure 9 and Figure 17). Compared to the change from leucine to methionine as in HOP-1, the change to an aromatic amino acid, phenylalanine, as in SPE-4 seems rather drastic. In fact, the Notch processing deficiency was rescued in mammalian cells by changing the phenylalanine residue to either leucine or methionine to restore the PS and SEL-12 GLGD motif or the HOP-1 GMGD motif within PS1/SPE-4<sub>7</sub> chimeric protein (Figure 30). This result suggests

## Discussion

the significance of the phenylalanine residue at the position x of the GxGD motif on APP/Notch substrate selectivity. However, it could have been possible that these results were obtained only in the context of PS1/SPE-4<sub>7</sub>. To eliminate this possibility, PS1 L383F mutant, in which the corresponding leucine residue was mutated to phenylalanine in PS1, was further analyzed. The PS1 L383F mutant allowed substantial APP processing but showed strong impairment in Notch processing (Figure 32). This observation strongly suggests the importance of phenylalanine at the position x of the GxGD motif for PS.

All above results were obtained in cultured cells. These observations were also confirmed *in vivo* in a collaboration with Dr. Stefan Eimer and Prof. Dr. Ralf Baumeister. It has been shown that *sel-12* loss of function mutants in *C. elegans* exhibit an egg-laying defect (Egl) phenotype due to an abnormal vulva muscle development, which is caused by a defect of Notch signaling (Levitan and Greenwald, 1995). This Egl defect phenotype can be rescued by SEL-12, HOP-1 and human PS1 and 2 (Levitan et al., 1996; Baumeister et al., 1997; Li and Greenwald, 1997; Steiner et al., 1999b). cDNAs encoding the PS1/SPE-4 species and PS1 L383F, which were subcloned under the *sel-12* promoter, were injected to *sel-12(ar171)* mutant hermaphroditic worms and the Egl behavior was scored. The cDNAs encoding PS1, SEL-12 and HOP-1 SPE-4 wt were also injected in parallel. As shown in Table 4, Egl phenotype was rescued by PS1, SEL-12, HOP-1 as expected. SPE-4 itself, which is normally only expressed in the spermatheca (L'Hernault and Arduengo, 1992; Arduengo et al., 1998), was also analyzed to see if it could replace SEL-12 function under the control of the *sel-12* promoter. Interestingly, SPE-4, unlike PS1, SEL-12 and HOP-1, was not able to rescue the Egl defect phenotype. However, consistent with the above results, PS1/SPE-4<sub>6/7</sub>, PS1/SPE-4<sub>7</sub> and PS1 L383F that are deficient in Notch processing *in vitro* failed to rescue the Egl defect phenotype. In contrast, PS1/SPE-4<sub>6</sub> was able to rescue the phenotype. PS1/SPE-4<sub>7</sub> F392L and PS1/SPE-4<sub>7</sub> F392M mutants showed lesser but still considerable rescuing activity. This data confirmed the importance of the amino acid residue at position x of the GxGD (i.e. a leucine) motif in Notch signaling also *in vivo*.

Strain	Transgene#	Genotype	egg-laying behavior*			
			+++	++	+	-
N2	-	wild type	50	0	0	0
BR1129	-	<i>sel-12(ar171)</i>	0	0	0	50
BR1964	PS1	<i>sel-12(ar171)</i>	45	3	1	0
BR2364	<i>sel-12</i>	<i>sel-12(ar171)</i>	48	2	0	0
BR2993	<i>hop-1</i>	<i>sel-12(ar171)</i>	50	0	0	1
§	<i>spe-4</i>	<i>sel-12(ar171)</i>	0	0	0	34
§	<i>spe-4</i>	<i>sel-12(ar171)</i>	0	0	0	27
§	<i>spe-4</i>	<i>sel-12(ar171)</i>	0	0	0	16
BR3209	PS1/SPE-4 <sub>6/7</sub>	<i>sel-12(ar171)</i>	3	2	1	44
BR3210	PS1/SPE-4 <sub>6/7</sub>	<i>sel-12(ar171)</i>	0	0	2	48
	His-PS1 wt	<i>sel-12(ar171)</i>	48	1	1	0
	His-PS1/SPE-4 <sub>6</sub>	<i>sel-12(ar171)</i>	46	2	2	0
	His-PS1/SPE-4 <sub>6</sub>	<i>sel-12(ar171)</i>	48	0	2	0
	His-PS1/SPE-4 <sub>7</sub>	<i>sel-12(ar171)</i>	0	0	3	47
	His-PS1/SPE-4 <sub>7</sub>	<i>sel-12(ar171)</i>	0	1	1	48
	His-PS1/SPE-4 <sub>7</sub> F392L	<i>sel-12(ar171)</i>	14	10	21	13
	His-PS1/SPE-4 <sub>7</sub> F392L	<i>sel-12(ar171)</i>	11	19	15	5
	His-PS1/SPE-4 <sub>7</sub> F392M	<i>sel-12(ar171)</i>	10	8	25	7
	His-PS1/SPE-4 <sub>7</sub> F392M	<i>sel-12(ar171)</i>	17	14	10	9
	His-PS1 L383F	<i>sel-12(ar171)</i>	0	1	4	45
	His-PS1 L383F	<i>sel-12(ar171)</i>	0	0	2	48

**Table 4: Rescuing activity of the *sel-12* Egl defect of different PSs expressed in *C. elegans*.**

\* For each transgenic animal the number of eggs laid were counted and were grouped into the following categories: +++, over 50 eggs progeny laid by an individual animal; ++, 15-50 eggs laid; +, 5-15 eggs laid; -, 0-5 eggs laid.

# For all constructs at least three independent lines were tested, only two representative lines are shown.

§ Stable lines could not be maintained due to progressive sterility.

### 4.2.3 Putative molecular basis of substrate discrimination by the GxGD motif

What could be the mechanism of the apparent substrate discrimination by the GFGD active site motif? The presence of an aromatic amino acid residue, phenylalanine, at position x of the GxGD motif may cause subtle differences in the conformation of TMD6 and 7. During this study, the presence of two substrate-binding steps in the  $\gamma$ -secretase complex before the cleavage occurs at the active site was reported. The ectodomain-shedded substrate is first recognized by NCT via its length (Shah et al., 2005). Then, the substrate is further transferred to the other binding site, termed docking site, before it reaches the active site to be cleaved (Esler et al., 2002; Tian et al., 2002; Beher et al., 2003; Tian et al., 2003). The docking site was mapped very close to the active site within a distance of three amino acids (Kornilova et al., 2005). Considering the estimated distance of the docking site from the active site, it could be that changing leucine to phenylalanine at the position x of GxGD motif, which is just two amino acids away from the active site aspartate, caused some effect on the docking event or on a post-docking event due to a slight structural alteration. These observations suggest two possible scenarios that are i) Notch is not able to bind on the docking site of the complex or ii) Notch is able to bind on the docking site but is not cleaved. There is also a possibility that NCT in a GFGD-type  $\gamma$ -secretase complex cannot recognize F-NEXT because the overall structure of the complex might be influenced by the alteration of the active site motif due to the phenylalanine residue. However, this can be ruled out because of substantial APP processing mediated by the GFGD active site motif. Furthermore, NCT recognizes a free amino terminus of the short ectodomain-shedded substrate (Shah et al., 2005) arguing against this possibility. This is because F-NEXT is a short Notch extracellular truncated substrate that mimics the direct substrate of  $\gamma$ -secretase. In addition, preliminary co-immunoprecipitation experiments indicate an interaction of F-NEXT and the GFGD-type  $\gamma$ -secretase. There was comparable F-NEXT binding between GLGD-type (as present in PS1 wt) and GFGD-type  $\gamma$ -secretase complex (as present in PS1 L383F). This result demonstrates that Notch can bind to a GFGD-type  $\gamma$ -secretase complex, but is not processed. Thus, the structural alteration caused by the phenylalanine residue rather affects a limited region around the GxGD active site motif including the docking site instead of the overall structure of  $\gamma$ -secretase.

Interestingly, compared to Notch processing, this structural alteration apparently had only a little influence on APP processing (see below). This observation may suggest that APP and Notch may have different docking sites on the  $\gamma$ -secretase complex. It may be that

phenylalanine residue at position x of the GxGD motif altered the docking site for Notch whereas the docking site for APP is not affected by this residue. The other possibility would be that, no matter whether APP and Notch share the same docking site, the docking site plays a role as a gate to the catalytic center. For example, it could be that after the initial recognition by NCT, Notch will be transferred to the docking site, but it is not able to enter the catalytic center to be processed because of the bulky aromatic amino acid phenylalanine, whereas APP is still able to pass through. Interestingly, a comparison of the TMD sequences of APP and Notch shows that there are four aromatic amino acids within the Notch TMD and none in the APP TMD (Figure 33). The combination of the bulky aromatic phenylalanine at the protease active site and the bulky residues in Notch TMD may account for the Notch processing deficiency. Interestingly, leucine/isoleucine–phenylalanine variations at position x in the GxGD motif are also found in and/or between the SPP/SPPL (SPP-like protease) protease families (Figure 34)(Weihofen et al., 2002). As in PSs, these differences may have an impact on substrate identification. Future studies will be needed to answer these questions.

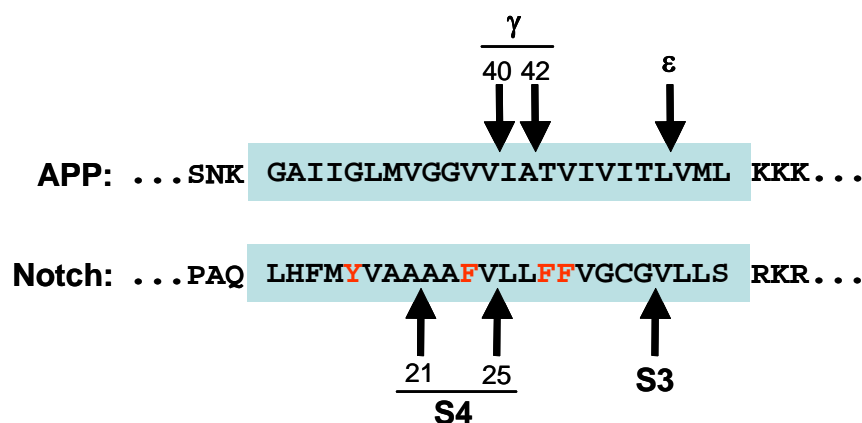


**Figure 33: Comparison of the APP and Notch TMDs**

The amino acid sequence of the TMDs of APP and Notch are shown. TMDs are indicated with blue background. Aromatic amino acid residues are indicated with red letters.

	<i>Homo sapience</i> : <b>GLGD</b>
	<i>Mus musculus</i> : <b>GLGD</b>
<b>SPP</b>	<i>Drosophila melanogaster</i> : <b>GLGD</b>
	<i>Caenorhabditis elegans</i> : <b>GLGD</b>
	<i>Arabidopsis thaliana</i> : <b>GLGD</b>
<b>SPPL1</b>	<i>Saccharomyces pombe</i> : <b>GLGD</b>
	<i>Homo sapience</i> : <b>GFGD</b>
	<i>Mus musculus</i> : <b>GFGD</b>
<b>SPPL2</b>	<i>Caenorhabditis elegans</i> : <b>GLGD</b>
	<i>Arabidopsis thaliana</i> : <b>GFGD</b>
	<i>Homo sapience</i> : <b>GIGD</b>
	<i>Mus musculus</i> : <b>GIGD</b>
<b>SPPL3</b>	<i>Drosophila melanogaster</i> : <b>GLGD</b>
<b>SPPL4</b>	<i>Saccharomyces cerevisiae</i> : <b>GLGD</b>

**Figure 34: Sequence comparison of the GxGD motif of the SPP family**

The GxGD motifs of SPP family from different species are shown. Aromatic amino acid residues are indicated in red letters. (Excerpt from Weihofen et al., 2002)

When a single amino acid residue at position x of the GxGD motif has such a strong influence on the processing of Notch, it might also have an effect on APP cleavage specificity as well. Considering that FAD single point mutations cause a shift in APP cleavage site, APP cleavage specificity at the A $\beta$ 40 and 42 site might be also slightly affected by the GFGD active site motif even though it is processed. Indeed, preliminary data showed an altered A $\beta$ 40/42 ratio in cells expressing the GFGD-type  $\gamma$ -secretase complex. Interestingly, cells expressing PS1 with the GMGD active site motif, as present in HOP-1, showed an alteration of the A $\beta$ 40/42 ratio. Although these are preliminary data, it seems the precise APP processing is mediated only by the GLGD active site motif, as

present in PS and SEL-12. As discussed above, a slight structural change of active site domain region might be caused by a single amino acid at position x of the GxGD active site motif. The difference of the effects caused by the structural alteration is probably dependent on the amino acid residue present at position x of the GxGD active site motif, i.e. the alteration by methionine only changes the specificity of APP processing whereas the alteration by phenylalanine not only changes APP processing but also blocks Notch cleavage. Taken together, it may be that a residue at position x of the GxGD active site motif is not only contributing to substrate identification but also is required for the accurate processing of the substrate.

### **4.3 Putative function of SPE-4 in *C. elegans***

The result in this study strongly suggested the conservation of proteolytic function in SPE-4. However, its physiological role in *C. elegans* is remained to be investigated. Interestingly, SPE-4 wt failed to rescue the Notch signaling-dependent Egl phenotype in the mutant worms (Table 4). This observation together with the finding of the contribution of the phenylalanine residue within the GxGD motif raises some ideas about the function of SPE-4 in *C. elegans*. Since SPE-4 failed to replace SEL-12 function, even though it was forced to be expressed under the control of *sel-12* promoter, it can be speculated that SPE-4 has more specific function as a protease in the worm during the spermatogenesis at L4 stage. It may have its own substrate(s) that should be discriminated from Notch using its GFGD active site motif. On the other hand, the failure in rescue of the Egl defect phenotype in the mutant worms could be because of the absence of  $\gamma$ -secretase complex formation ability of SPE-4 (Figure 10 and Figure 13). In this case, one may also speculate that SPE-4 functions alone like the SPP family. To analyze the possibility that SPE-4 functions independent of other proteins, an *in vitro*  $\gamma$ -secretase assay was performed (Figure 11). SPE-4 wt isolated from HEK293/sw cells stably expressing SPE-4 wt failed to generate AICD or A $\beta$  from recombinant APP-based substrate, C100. This result indicates that either APP is not the right substrate for SPE-4 or SPE-4 does not function alone at least in this context. However, with this result, the possibility cannot be ignored that SPE-4 forms a complex in *C. elegans*. SPE-4 might only not be able to interact with human NCT,

## Discussion

APH-1 and PEN-2 because their sequences are different from those homologues found in *C. elegans*. If this was the case, the inability of SPE-4 to replace the SEL-12 function in *C. elegans* might be due to its phenylalanine residue at the position x of the GxGD motif. Moreover, it is also possible that SPE-4 forms a complex with its own partner(s).

## 4.4 Outlook

The experiments using SPE-4/PS1c expressing cells demonstrated the importance of the PS1 C-terminus region for complex formation. To further map domains in PS that are required for an active  $\gamma$ -secretase complex formation, various SPE-4/PS1 swapping mutations can now be constructed and analyzed. For example, it would be interesting to analyze a construct, in which TMD4 of SPE-4 is exchanged with that of PS1 in the context of SPE-4/PS1c, to see whether or not PEN-2 would be stabilized by interaction with this construct (Kim and Sisodia, 2005; Watanabe et al., 2005).

In this study, it was also demonstrated that a single amino acid residue, phenylalanine, at position x of the GxGD motif plays a critical role in APP/Notch substrate selectivity. The precise mechanism of this selectivity is still unclear. However, two possible explanations for the observed substrate discrimination were discussed above based on this study. i) APP and Notch have different docking sites, and the phenylalanine residue at position x of the GxGD motif only affects the Notch docking site. ii) The docking site plays a role as a gate to the active site and the combination of bulky aromatic amino acids within GxGD active site motif and the TMD of the substrate results in a blockage of the gate. When a bulky aromatic amino acid residue, phenylalanine, is present at the position x of the GxGD motif, Notch is not able to reach the active site whereas APP is. This may potentially be because the TMD of Notch contains more aromatic amino acids than APP. Apart from further obtaining the co-immunoprecipitation data described above, cross-linking experiments would be helpful to investigate the interaction between the substrate and the  $\gamma$ -secretase complex. Moreover, to explore the second possibility, other  $\gamma$ -secretase substrates or an APP TMD that is mutated to contain more aromatic amino acids can be examined to see whether a GFGD-type  $\gamma$ -secretase complex processes them. For example, it is known that

all four Notch homologues (Notch1-4) in mouse undergo  $\gamma$ -secretase dependent proteolysis (Saxena et al., 2001). Interestingly, each Notch homologue has a different number of aromatic amino acids within its TMD, Notch1; four, Notch2; three, Notch3; two, and Notch4; one (Figure 35). It will be very interesting to analyze the activity of a GFGD-type  $\gamma$ -secretase on these four homologues to compare the efficiency of the proteolysis to see whether there is any correlation between the efficiency and the number of the aromatic amino acids. Moreover, the constructs containing various point mutations at position x of the GxGD active site motif can be also tested. For example, one could insert other aromatic amino acids, tyrosine or tryptophan, at position x of the GxGD motif to generate GYGD or GWGD active site motifs for analyzing whether they discriminate APP and Notch like the GFGD active site motif does.

**Notch1:** . . . PSQLHLMYVAAAAFVLLFFVGCGLLSRKR . . .  
**Notch2:** . . . NAQLLYLLAVAVVIILFFILLGVIMAKRK . . .  
**Notch3:** . . . QSVPLLPLLVAGAVFLLIIFILGVMVARRKR . . .  
**Notch4:** . . . ANQLPWPILCSPVVGVLALLGALLVLQLIRRR . . .

**Figure 35: The TMD amino acid sequence comparison of the mouse Notch homologues**

The amino acid sequences around TMDs of mouse Notch homologues are shown. TMDs are indicated with blue background. Aromatic amino acid residues are indicated with red letters.

Finally, the physiological function of SPE-4 in *C. elegans* is remained to be investigated. As shown in this study, not only the functional motifs are conserved in SPE-4, but also the active site of SPE-4 has a proteolytic function in APP processing at least in the context of PS1/SPE-4<sub>6/7</sub>. These observations strongly suggest the conservation of a proteolytic function in SPE-4. However, as discussed above, whether SPE-4 functions without its partner proteins or has its own distinct substrate(s) is unclear. It will be very helpful to

## Discussion

analyze endogenous SPE-4 to study these open questions. Unfortunately, because it is exclusively expressed during the L4 stage in the spermatheca in *C. elegans* during spermatogenesis, it has been difficult to analyze the endogenous SPE-4 so far. Therefore, establishing a sensitive antibody against SPE-4 that can detect endogenous SPE-4 in *C. elegans* or an efficient method that can isolate endogenous SPE-4 from *C. elegans* is required. Once it becomes possible to analyze endogenous SPE-4, it will be very interesting to examine the molecular weight of isolated SPE-4 under native conditions to find out whether SPE-4 forms a complex. Moreover, identification of endogenous SPE-4 substrate(s) using methods such as co-immunoprecipitation would be also very important to understand the function of SPE-4 in *C. elegans*. These future studies will be also very helpful for the further characterization of the intramembrane proteolytic activity by PS family.

## 5. Summary

The *C. elegans* transmembrane sperm protein SPE-4 is the most distant homologue of presenilin (PS), which represents the catalytic subunit of  $\gamma$ -secretase, an intramembrane-cleaving aspartyl protease complex. Besides PS,  $\gamma$ -secretase consists of three other components, nicastrin (NCT), APH-1 and PEN-2.  $\gamma$ -Secretase catalyzes the intramembrane cleavage of Alzheimer's disease-associated APP and many other type I transmembrane proteins including Notch, a major physiological  $\gamma$ -secretase substrate, which is required for cell differentiation during development and in adulthood. PS contains two functional aspartates within its transmembrane domains (TMDs) 6 and 7. The active site motif residing in TMD 7 of PS is an unusual GxGD motif, which presents a novel signature motif of a number of intramembrane cleaving aspartyl proteases. Despite its low homology to PS, the two functional aspartates including the GxGD active site motif are conserved in SPE-4 indicating a proteolytic function of this *C. elegans* PS homologue. In this study, the putative proteolytic activity of SPE-4 was examined. Because it was difficult to analyze the endogenous SPE-4 in *C. elegans* due to its temporally and spatially limited expression pattern, mammalian cells were chosen as experimental system. Surprisingly, when SPE-4 was expressed in mammalian cells, it did not support  $\gamma$ -secretase complex formation suggesting that SPE-4 cannot interact with human  $\gamma$ -secretase complex components. Consistent with this observation, SPE-4 did not process a recombinant APP-based  $\gamma$ -secretase substrate *in vitro*. These results indicated that SPE-4 cannot function as a protease alone and/or might have its own partner protein(s) and/or own substrate(s) in *C. elegans*. SPE-4 was incorporated into a  $\gamma$ -secretase complex only when its C-terminal region had been exchanged with the corresponding region of PS1, which is known to be required for  $\gamma$ -secretase complex assembly. Although the chimeric protein SPE-4/PS1c showed an interaction with NCT, it failed to support APP processing. This was due to the failure of an efficient interaction with PEN-2 thus resulting in incomplete  $\gamma$ -secretase complex formation. This result suggested a requirement of other PS domains for assembly of an active  $\gamma$ -secretase complex in addition to its C-terminus. Because SPE-4/PS1c failed to be incorporated into a functional  $\gamma$ -secretase complex, the proteolytic function of the putative SPE-4 active site domain was subsequently directly assessed by an active site domain exchange approach with PS. To this end, an active site chimeric protein PS1/SPE-4<sub>6/7</sub>, in which TMDs 6 and 7 of PS1 had been replaced by those of SPE-4, was constructed.

## Summary

This chimeric protein PS1/SPE-4<sub>6/7</sub> underwent normal  $\gamma$ -secretase complex formation and was able to process APP, demonstrating that the putative active site of SPE-4 has a proteolytic function.

Surprisingly, despite its substantial activity in APP processing, PS1/SPE-4<sub>6/7</sub> did not support Notch processing. Mapping the residue responsible for the Notch processing defect revealed that a single amino acid at position x of the GxGD active site motif in TMD 7 of PS affects Notch processing.

During the progress of this study, the presence of two substrate-binding sites in the  $\gamma$ -secretase complex was reported. One site is provided by NCT, which mediates the initial substrate recognition by recognizing the length of the ectodomain-shedded substrates. The other binding site, termed docking site, was mapped very close to the active site within a distance of three amino acids. The results of this study identifying a single amino acid critical for APP/Notch substrate selectivity, which is only two amino acids away from the active site aspartate supports the concept of a substrate-docking site close to the active site, and suggests that the GxGD active site motif region may be a part of it.

Taken together, the findings in this thesis suggest a proteolytic function of SPE-4 in *C. elegans* and indicate an important role of the GxGD active site motif of PS in substrate identification in addition to its role in the catalytic function of  $\gamma$ -secretase.

## 6. References

- Alzheimer A (1907) Über eine eigenartige Erkrankung der Hirnrinde. *Allg Z Psychiatrie Psychisch-Gerichtl Med* 64:146-148.
- Alzheimer A, Stelzmann RA, Schnitzlein HN, Murtagh FR (1995) An English translation of Alzheimer's 1907 paper, "Über eine eigenartige Erkrankung der Hirnrinde". *Clin Anat* 8:429-431.
- Arduengo PM, Appleberry OK, Chuang P, L'Hernault SW (1998) The presenilin protein family member SPE-4 localizes to an ER/Golgi derived organelle and is required for proper cytoplasmic partitioning during *Caenorhabditis elegans* spermatogenesis. *J Cell Sci* 111:3645-3654.
- Baki L, Marambaud P, Efthimiopoulos S, Georgakopoulos A, Wen P, Cui W, Shioi J, Koo E, Ozawa M, Friedrich VL, Jr., Robakis NK (2001) Presenilin-1 binds cytoplasmic epithelial cadherin, inhibits cadherin/p120 association, and regulates stability and function of the cadherin/catenin adhesion complex. *Proc Natl Acad Sci U S A* 98:2381-2386.
- Baumeister R, Leimer U, Zweckbronner I, Jakubek C, Grunberg J, Haass C (1997) Human presenilin-1, but not familial Alzheimer's disease (FAD) mutants, facilitate *Caenorhabditis elegans* Notch signalling independently of proteolytic processing. *Genes Funct* 1:149-159.
- Behr D, Fricker M, Nadin A, Clarke EE, Wrigley JD, Li YM, Culvenor JG, Masters CL, Harrison T, Shearman MS (2003) In vitro characterization of the presenilin-dependent  $\gamma$ -secretase complex using a novel affinity ligand. *Biochemistry* 42:8133-8142.
- Berezovska O, Frosch M, McLean P, Knowles R, Koo E, Kang D, Shen J, Lu FM, Lux SE, Tonegawa S, Hyman BT (1999) The Alzheimer-related gene presenilin 1 facilitates notch 1 in primary mammalian neurons. *Brain Res Mol Brain Res* 69:273-280.
- Bergman A, Hansson EM, Pursglove SE, Farmery MR, Lannfelt L, Lendahl U, Lundkvist J, Naslund J (2004) Pen-2 is sequestered in the endoplasmic reticulum and subjected to ubiquitylation and proteasome-mediated degradation in the absence of presenilin. *J Biol Chem* 279:16744-16753.
- Bray SJ (2006) Notch signalling: a simple pathway becomes complex. *Nat Rev Mol Cell Biol* 7:678-689.
- Buxbaum JD, Liu KN, Luo Y, Slack JL, Stocking KL, Peschon JJ, Johnson RS, Castner BJ, Cerretti DP, Black RA (1998) Evidence that tumor necrosis factor  $\alpha$  converting enzyme is involved in regulated  $\alpha$ -secretase cleavage of the Alzheimer amyloid protein precursor. *J Biol Chem* 273:27765-27767.
- Cai H, Wang Y, McCarthy D, Wen H, Borchelt DR, Price DL, Wong PC (2001) BACE1 is the major beta-secretase for generation of A $\beta$  peptides by neurons. *Nat Neurosci* 4:233-234.
- Capell A, Behr D, Prokop S, Steiner H, Kaether C, Shearman MS, Haass C (2005) Gamma-secretase complex assembly within the early secretory pathway. *J Biol Chem* 280:6471-6478.
- Capell A, Grunberg J, Pesold B, Diehlmann A, Citron M, Nixon R, Beyreuther K, Selkoe DJ, Haass C (1998) The proteolytic fragments of the Alzheimer's disease-associated presenilin-1 form heterodimers and occur as a 100-150-kDa molecular mass complex. *J Biol Chem* 273:3205-3211.
- Capell A, Saffrich R, Olivo JC, Meyn L, Walter J, Grunberg J, Mathews P, Nixon R, Dotti C, Haass C (1997) Cellular expression and proteolytic processing of presenilin

## References

- proteins is developmentally regulated during neuronal differentiation. *J Neurochem* 69:2432-2440.
- Chen F, Yu G, Arawaka S, Nishimura M, Kawarai T, Yu H, Tandon A, Supala A, Song YQ, Rogaeva E, Milman P, Sato C, Yu C, Janus C, Lee J, Song L, Zhang L, Fraser PE, St George-Hyslop PH (2001) Nicastrin binds to membrane-tethered Notch. *Nat Cell Biol* 3:751-754.
- Citron M, Oltersdorf T, Haass C, McConlogue L, Hung AY, Seubert P, Vigo-Pelfrey C, Lieberburg I, Selkoe DJ (1992) Mutation of the  $\beta$ -amyloid precursor protein in familial Alzheimer's disease increases  $\beta$ -protein production. *Nature* 360:672-674.
- Corder EH, Saunders AM, Strittmatter WJ, Schmechel DE, Gaskell PC, Small GW, Roses AD, Haines JL, Pericak-Vance MA (1993) Gene dose of apolipoprotein E type 4 allele and the risk of Alzheimer's disease in late onset families. *Science* 261:921-923.
- Crystal AS, Morais VA, Fortna RR, Carlin D, Pierson TC, Wilson CA, Lee VM, Doms RW (2004) Presenilin modulates Pen-2 levels posttranslationally by protecting it from proteasomal degradation. *Biochemistry* 43:3555-3563.
- Davis JA, Naruse S, Chen H, Eckman C, Younkin S, Price DL, Borchelt DR, Sisodia SS, Wong PC (1998) An Alzheimer's disease-linked PS1 variant rescues the developmental abnormalities of PS1-deficient embryos. *Neuron* 20:603-609.
- De Strooper B, Saftig P, Craessaerts K, Vanderstichele H, Guhde G, Annaert W, Von Figura K, Van Leuven F (1998) Deficiency of presenilin-1 inhibits the normal cleavage of amyloid precursor protein. *Nature* 391:387-390.
- De Strooper B, Annaert W, Cupers P, Saftig P, Craessaerts K, Mumm JS, Schroeter EH, Schrijvers V, Wolfe MS, Ray WJ, Goate A, Kopan R (1999) A presenilin-1-dependent  $\gamma$ -secretase-like protease mediates release of Notch intracellular domain. *Nature* 398:518-522.
- Donoviel DB, Hadjantonakis AK, Ikeda M, Zheng H, Hyslop PS, Bernstein A (1999) Mice lacking both presenilin genes exhibit early embryonic patterning defects. *Genes Dev* 13:2801-2810.
- Edbauer D, Winkler E, Haass C, Steiner H (2002) Presenilin and nicastrin regulate each other and determine amyloid  $\beta$ -peptide production via complex formation. *Proc Natl Acad Sci USA* 99:8666-8671.
- Edbauer D, Winkler E, Regula JT, Pesold B, Steiner H, Haass C (2003) Reconstitution of  $\gamma$ -secretase activity. *Nat Cell Biol* 5:486-488.
- Esler WP, Kimberly WT, Ostaszewski BL, Ye W, Diehl TS, Selkoe DJ, Wolfe MS (2002) Activity-dependent isolation of the presenilin- $\gamma$ -secretase complex reveals nicastrin and a  $\gamma$  substrate. *Proc Natl Acad Sci USA* 99:2720-2725.
- Esler WP, Kimberly WT, Ostaszewski BL, Diehl TS, Moore CL, Tsai J-Y, Rahmati T, Xia W, Selkoe DJ, Wolfe MS (2000) Transition-state analogue inhibitors of  $\gamma$ -secretase bind directly to presenilin-1. *Nat Cell Biol* 2:428-433.
- Fluhrer R, Grammer G, Israel L, Condrón MM, Haffner C, Friedmann E, Bohland C, Imhof A, Martoglio B, Teplow DB, Haass C (2006) A gamma-secretase-like intramembrane cleavage of TNF $\alpha$  by the GxGD aspartyl protease SPPL2b. *Nat Cell Biol* 8:894-896.
- Fortna RR, Crystal AS, Morais VA, Pijak DS, Lee VM, Doms RW (2004) Membrane topology and nicastrin-enhanced endoproteolysis of APH-1, a component of the  $\gamma$ -secretase complex. *J Biol Chem* 279:3685-3693.
- Francis R, McGrath G, Zhang J, Ruddy DA, Sym M, Apfeld J, Nicoll M, Maxwell M, Hai B, Ellis MC, Parks AL, Xu W, Li J, Gurney M, Myers RL, Himes CS, Hiesch RD, Ruble C, Nye JS, Curtis D (2002) aph-1 and pen-2 are required for Notch pathway

- signaling,  $\gamma$ -secretase cleavage of  $\beta$ APP, and presenilin protein accumulation. *Dev Cell* 3:85-97.
- Friedmann E, Lemberg MK, Weihofen A, Dev KK, Dengler U, Rovelli G, Martoglio B (2004) Consensus analysis of signal peptide peptidase and homologous human aspartic proteases reveals opposite topology of catalytic domains compared with presenilins. *J Biol Chem* 279:50790-50798.
- Friedmann E, Hauben E, Maylandt K, Schleegeer S, Vreugde S, Lichtenthaler SF, Kuhn PH, Stauffer D, Rovelli G, Martoglio B (2006) SPPL2a and SPPL2b promote intramembrane proteolysis of TNF $\alpha$  in activated dendritic cells to trigger IL-12 production. *Nat Cell Biol* 8:843-848.
- Georgakopoulos A, Marambaud P, Efthimiopoulos S, Shioi J, Cui W, Li HC, Schutte M, Gordon R, Holstein GR, Martinelli G, Mehta P, Friedrich VL, Jr., Robakis NK (1999) Presenilin-1 forms complexes with the cadherin/catenin cell-cell adhesion system and is recruited to intercellular and synaptic contacts. *Mol Cell* 4:893-902.
- Glenner GG, Wong CW (1984) Alzheimer's disease: initial report of the purification and characterization of a novel cerebrovascular amyloid protein. *Biochem Biophys Res Commun* 120:885-890.
- Goate A, Chartier-Harlin MC, Mullan M, Brown J, Crawford F, Fidani L, Giuffra L, Haynes A, Irving N, James L, et al. (1991) Segregation of a missense mutation in the amyloid precursor protein gene with familial Alzheimer's disease. *Nature* 349:704-706.
- Goedert M, Spillantini MG, Cairns NJ, Crowther RA (1992) Tau proteins of Alzheimer paired helical filaments: abnormal phosphorylation of all six brain isoforms. *Neuron* 8:159-168.
- Goutte C, Hepler W, Mickey KM, Priess JR (2000) aph-2 encodes a novel extracellular protein required for GLP-1-mediated signaling. *Development* 127:2481-2492.
- Goutte C, Tsunozaki M, Hale VA, Priess JR (2002) APH-1 is a multipass membrane protein essential for the Notch signaling pathway in *Caenorhabditis elegans* embryos. *Proc Natl Acad Sci USA* 99:775-779.
- Grundke-Iqbal I, Iqbal K, Tung YC, Quinlan M, Wisniewski HM, Binder LI (1986) Abnormal phosphorylation of the microtubule-associated protein tau ( $\tau$ ) in Alzheimer cytoskeletal pathology. *Proc Natl Acad Sci U S A* 83:4913-4917.
- Guo Y, Livne-Bar I, Zhou L, Boulianne GL (1999) Drosophila presenilin is required for neuronal differentiation and affects notch subcellular localization and signaling. *J Neurosci* 19:8435-8442.
- Haass C, Hung AY, Selkoe DJ (1991) Processing of beta-amyloid precursor protein in microglia and astrocytes favors an internal localization over constitutive secretion. *J Neurosci* 11:3783-3793.
- Hasegawa H, Sanjo N, Chen F, Gu YJ, Shier C, Petit A, Kawarai T, Katayama T, Schmidt SD, Mathews PM, Schmitt-Ulms G, Fraser PE, St George-Hyslop P (2004) Both the sequence and length of the C terminus of PEN-2 are critical for intermolecular interactions and function of presenilin complexes. *J Biol Chem* 279:46455-46463.
- Head E, Lott IT (2004) Down syndrome and beta-amyloid deposition. *Curr Opin Neurol* 17:95-100.
- Hebert SS, Serneels L, Dejaegere T, Horre K, Dabrowski M, Baert V, Annaert W, Hartmann D, De Strooper B (2004) Coordinated and widespread expression of gamma-secretase in vivo: evidence for size and molecular heterogeneity. *Neurobiol Dis* 17:260-272.

## References

- Hecimovic S, Wang J, Dolios G, Martinez M, Wang R, Goate AM (2004) Mutations in APP have independent effects on Abeta and CTFgamma generation. *Neurobiol Dis* 17:205-218.
- Henricson A, Kall L, Sonnhammer EL (2005) A novel transmembrane topology of presenilin based on reconciling experimental and computational evidence. *Febs J* 272:2727-2733.
- Herreman A, Serneels L, Annaert W, Collen D, Schoonjans L, De Strooper B (2000) Total inactivation of  $\gamma$ -secretase activity in presenilin-deficient embryonic stem cells. *Nat Cell Biol* 2:461-462.
- Herreman A, Hartmann D, Annaert W, Saftig P, Craessaerts K, Serneels L, Umans L, Schrijvers V, Checler F, Vanderstichele H, Baekelandt V, Dressel R, Cupers P, Huylebroeck D, Zwijsen A, Van Leuven F, De Strooper B (1999) Presenilin 2 deficiency causes a mild pulmonary phenotype and no changes in amyloid precursor protein processing but enhances the embryonic lethal phenotype of presenilin 1 deficiency. *Proc Natl Acad Sci USA* 96:11872-11877.
- Holsinger RM, McLean CA, Beyreuther K, Masters CL, Evin G (2002) Increased expression of the amyloid precursor beta-secretase in Alzheimer's disease. *Ann Neurol* 51:783-786.
- Hussain I, Powell D, Howlett DR, Tew DG, Meek TD, Chapman C, Gloger IS, Murphy KE, Southan CD, Ryan DM, Smith TS, Simmons DL, Walsh FS, Dingwall C, Christie G (1999) Identification of a novel aspartic protease (Asp 2) as  $\beta$ -secretase. *Mol Cell Neurosci* 14:419-427.
- Ikeuchi T, Sisodia SS (2003) The Notch ligands, Delta1 and Jagged2, are substrates for presenilin-dependent "gamma-secretase" cleavage. *J Biol Chem* 278:7751-7754.
- Jarrett JT, Berger EP, Lansbury PT, Jr. (1993) The carboxy terminus of the  $\beta$ -amyloid protein is critical for the seeding of amyloid formation: implications for the pathogenesis of Alzheimer's disease. *Biochemistry* 32:4693-4697.
- Jarriault S, Brou C, Logeat F, Schroeter EH, Kopan R, Israel A (1995) Signalling downstream of activated mammalian Notch. *Nature* 377:355-358.
- Kaether C, Capell A, Edbauer D, Winkler E, Novak B, Steiner H, Haass C (2004) The presenilin C-terminus is required for ER-retention, nicastrin-binding and gamma-secretase activity. *Embo J* 23:4738-4748.
- Kaether C, Lammich S, Edbauer D, Ertl M, Rietdorf J, Capell A, Steiner H, Haass C (2002) A presenilin-1/nicastrin complex is targeted to the plasma membrane and affects trafficking and processing of the  $\beta$ -amyloid precursor protein. *J Cell Biol* in press.
- Kakuda N, Funamoto S, Yagishita S, Takami M, Osawa S, Dohmae N, Ihara Y (2006) Equimolar production of amyloid beta-protein and amyloid precursor protein intracellular domain from beta-carboxyl-terminal fragment by gamma-secretase. *J Biol Chem* 281:14776-14786.
- Kim SH, Sisodia SS (2005) Evidence that the "NF" motif in transmembrane domain 4 of presenilin 1 is critical for binding with PEN-2. *J Biol Chem* 280:41953-41966.
- Kimberly WT, LaVoie MJ, Ostaszewski BL, Ye W, Wolfe MS, Selkoe DJ (2002) Complex N-linked glycosylated nicastrin associates with active  $\gamma$ -secretase and undergoes tight cellular regulation. *J Biol Chem* 277:35113-35117.
- Kimberly WT, LaVoie MJ, Ostaszewski BL, Ye W, Wolfe MS, Selkoe DJ (2003)  $\gamma$ -Secretase is a membrane protein complex comprised of presenilin, nicastrin, Aph-1, and Pen-2. *Proc Natl Acad Sci USA* 100:6382-6387.
- Koike H, Tomioka S, Sorimachi H, Saido TC, Maruyama K, Okuyama A, Fujisawa-Sehara A, Ohno S, Suzuki K, Ishiura S (1999) Membrane-anchored metalloprotease

- MDC9 has an  $\alpha$ -secretase activity responsible for processing the amyloid precursor protein. *Biochem J* 343:371-375.
- Kopan R, Schroeter EH, Weintraub H, Nye JS (1996) Signal transduction by activated mNotch: importance of proteolytic processing and its regulation by the extracellular domain. *Proc Natl Acad Sci U S A* 93:1683-1688.
- Kornilova AY, Bihel F, Das C, Wolfe MS (2005) The initial substrate-binding site of gamma-secretase is located on presenilin near the active site. *Proc Natl Acad Sci U S A* 102:3230-3235.
- LaFerla FM, Oddo S (2005) Alzheimer's disease: Abeta, tau and synaptic dysfunction. *Trends Mol Med* 11:170-176.
- Lammich S, Kojro E, Postina R, Gilbert S, Pfeiffer R, Jasionowski M, Haass C, Fahrenholz F (1999) Constitutive and regulated  $\alpha$ -secretase cleavage of Alzheimer's amyloid precursor protein by a disintegrin metalloprotease. *Proc Natl Acad Sci USA* 96:3922-3927.
- Lammich S, Okochi M, Takeda M, Kaether C, Capell A, Zimmer A-K, Edbauer D, Walter J, Steiner H, Haass C (2002) Presenilin-dependent intramembrane proteolysis of CD44 leads to the liberation of its intracellular domain and the secretion of an A $\beta$ -like peptide. *J Biol Chem* in press.
- LaPointe CF, Taylor RK (2000) The type 4 prepilin peptidases comprise a novel family of aspartic acid proteases. *J Biol Chem* 275:1502-1510.
- Laudon H, Hansson EM, Melen K, Bergman A, Farmery MR, Winblad B, Lendahl U, von Heijne G, Naslund J (2005) A nine-transmembrane domain topology for presenilin 1. *J Biol Chem* 280:35352-35360.
- LaVoie MJ, Selkoe DJ (2003) The Notch ligands, Jagged and Delta, are sequentially processed by alpha-secretase and presenilin/ $\gamma$ -secretase and release signaling fragments. *J Biol Chem* 278:34427-34437.
- LaVoie MJ, Fraering PC, Ostaszewski BL, Ye W, Kimberly WT, Wolfe MS, Selkoe DJ (2003) Assembly of the  $\gamma$ -secretase complex involves early formation of an intermediate subcomplex of Aph-1 and nicastrin. *J Biol Chem* 278:37213-37222.
- Lee SF, Shah S, Li H, Yu C, Han W, Yu G (2002) Mammalian APH-1 interacts with presenilin and nicastrin and is required for intramembrane proteolysis of amyloid- $\beta$  precursor protein and Notch. *J Biol Chem* 277:45013-45019.
- Leem JY, Vijayan S, Han P, Cai D, Machura M, Lopes KO, Veselits ML, Xu H, Thinakaran G (2002) Presenilin 1 is required for maturation and cell surface accumulation of nicastrin. *J Biol Chem* 277:19236-19240.
- Levitan D, Greenwald I (1995) Facilitation of lin-12-mediated signalling by sel-12, a *Caenorhabditis elegans* S182 Alzheimer's disease gene. *Nature* 377:351-354.
- Levitan D, Greenwald I (1998) Effects of SEL-12 presenilin on LIN-12 localization and function in *Caenorhabditis elegans*. *Development* 125:3599-3606.
- Levitan D, Yu G, St George Hyslop P, Goutte C (2001) Aph-2/nicastrin functions in lin-12/Notch signaling in the *Caenorhabditis elegans* somatic gonad. *Dev Biol* 240:654-661.
- Levitan D, Doyle TG, Brousseau D, Lee MK, Thinakaran G, Slunt HH, Sisodia SS, Greenwald I (1996) Assessment of normal and mutant human presenilin function in *Caenorhabditis elegans*. *Proc Natl Acad Sci USA* 93:14940-14944.
- Levy-Lahad E, Wasco W, Poorkaj P, Romano DM, Oshima J, Pettingell WH, Yu CE, Jondro PD, Schmidt SD, Wang K, et al. (1995) Candidate gene for the chromosome 1 familial Alzheimer's disease locus. *Science* 269:973-977.

## References

- L'Hernault SW, Arduengo PM (1992) Mutation of a putative sperm membrane protein in *Caenorhabditis elegans* prevents sperm differentiation but not its associated meiotic divisions. *J Cell Biol* 119:55-68.
- Li X, Greenwald I (1997) HOP-1, a *Caenorhabditis elegans* presenilin, appears to be functionally redundant with SEL-12 presenilin and to facilitate LIN-12 and GLP-1 signaling. *Proc Natl Acad Sci USA* 94:12204-12209.
- Li YM, Lai MT, Xu M, Huang Q, DiMuzio-Mower J, Sardana MK, Shi XP, Yin KC, Shafer JA, Gardell SJ (2000a) Presenilin 1 is linked with  $\gamma$ -secretase activity in the detergent solubilized state. *Proc Natl Acad Sci USA* 97:6138-6143.
- Li YM, Xu M, Lai MT, Huang Q, Castro JL, DiMuzio-Mower J, Harrison T, Lellis C, Nadin A, Neduvelli JG, Register RB, Sardana MK, Shearman MS, Smith AL, Shi XP, Yin KC, Shafer JA, Gardell SJ (2000b) Photoactivated  $\gamma$ -secretase inhibitors directed to the active site covalently label presenilin 1. *Nature* 405:689-694.
- Lin X, Koelsch G, Wu S, Downs D, Dashti A, Tang J (2000) Human aspartic protease memapsin 2 cleaves the  $\beta$ -secretase site of  $\beta$ -amyloid precursor protein. *Proc Natl Acad Sci USA* 97:1456-1460.
- Luo WJ, Wang H, Li H, Kim BS, Shah S, Lee HJ, Thinakaran G, Kim TW, Yu G, Xu H (2003) PEN-2 and APH-1 coordinately regulate proteolytic processing of presenilin 1. *J Biol Chem* 278:7850-7854.
- Luo Y, Bolon B, Kahn S, Bennett BD, Babu-Khan S, Denis P, Fan W, Kha H, Zhang J, Gong Y, Martin L, Louis JC, Yan Q, Richards WG, Citron M, Vassar R (2001) Mice deficient in BACE1, the Alzheimer's beta-secretase, have normal phenotype and abolished beta-amyloid generation. *Nat Neurosci* 4:231-232.
- Ma G, Li T, Price DL, Wong PC (2005) APH-1a is the principal mammalian APH-1 isoform present in gamma-secretase complexes during embryonic development. *J Neurosci* 25:192-198.
- Marambaud P, Shioi J, Serban G, Georgakopoulos A, Sarner S, Nagy V, Baki L, Wen P, Efthimiopoulos S, Shao Z, Wisniewski T, Robakis NK (2002) A presenilin-1/ $\gamma$ -secretase cleavage releases the E-cadherin intracellular domain and regulates disassembly of adherens junctions. *Embo J* 21:1948-1956.
- McLendon C, Xin T, Ziani-Cherif C, Murphy MP, Findlay KA, Lewis PA, Pinnix I, Sambamurti K, Wang R, Fauq A, Golde TE (2000) Cell-free assays for  $\gamma$ -secretase activity. *Faseb J* 14:2383-2386.
- Moehlmann T, Winkler E, Xia X, Edbauer D, Murrell J, Capell A, Kaether C, Zheng H, Ghetti B, Haass C, Steiner H (2002) Presenilin-1 mutations of leucine 166 equally affect the generation of the Notch and APP intracellular domains independent of their effect on A $\beta$  42 production. *Proc Natl Acad Sci USA* 99:8025-8030.
- Morais VA, Crystal AS, Pijak DS, Carlin D, Costa J, Lee VM, Doms RW (2003) The transmembrane domain region of nicastrin mediates direct interactions with APH-1 and the  $\gamma$ -secretase complex. *J Biol Chem* 278:43284-43291.
- Nakajima M, Shimizu T, Shirasawa T (2000) Notch-1 activation by familial Alzheimer's disease (FAD)-linked mutant forms of presenilin-1. *J Neurosci Res* 62:311-317.
- Ni CY, Murphy MP, Golde TE, Carpenter G (2001)  $\gamma$ -Secretase cleavage and nuclear localization of ErbB-4 receptor tyrosine kinase. *Science* 294:2179-2181.
- Nyabi O, Bentahir M, Horre K, Herreman A, Gottardi-Littell N, Van Broeckhoven C, Merchiers P, Spittaels K, Annaert W, De Strooper B (2003) Presenilins mutated at Asp257 or Asp385 restore Pen-2 expression and Nicastrin glycosylation but remain catalytically inactive in the absence of wild type Presenilin. *J Biol Chem* 278:43430-43436.

- Oh YS, Turner RJ (2005) Topology of the C-terminal fragment of human presenilin 1. *Biochemistry* 44:11821-11828.
- Okochi M, Fukumori A, Jiang J, Itoh N, Kimura R, Steiner H, Haass C, Tagami S, Takeda M (2006) Secretion of the Notch-1 Abeta-like peptide during Notch signaling. *J Biol Chem* 281:7890-7898.
- Okochi M, Steiner H, Fukumori A, Tanii H, Tomita T, Tanaka T, Iwatsubo T, Kudo T, Takeda M, Haass C (2002) Presenilins mediate a dual intramembraneous  $\gamma$ -secretase cleavage of Notch, which is required for signaling and removal of the transmembrane domain. *EMBO J* in press.
- Parks AL, Klueg KM, Stout JR, Muskavitch MA (2000) Ligand endocytosis drives receptor dissociation and activation in the Notch pathway. *Development* 127:1373-1385.
- Pinnix I, Musunuru U, Tun H, Sridharan A, Golde T, Eckman C, Ziani-Cherif C, Onstead L, Sambamurti K (2001) A novel  $\gamma$ -secretase assay based on detection of the putative C-terminal fragment- $\gamma$  of amyloid  $\beta$  protein precursor. *J Biol Chem* 276:481-487.
- Prokop S, Shirotani K, Edbauer D, Haass C, Steiner H (2004) Requirement of PEN-2 for stabilization of the presenilin NTF/CTF heterodimer within the  $\gamma$ -secretase complex. *J Biol Chem* 279:23255-23261.
- Qian S, Jiang P, Guan XM, Singh G, Trumbauer ME, Yu H, Chen HY, Van de Ploeg LH, Zheng H (1998) Mutant human presenilin 1 protects presenilin 1 null mouse against embryonic lethality and elevates A $\beta$ 1-42/43 expression. *Neuron* 20:611-617.
- Qi-Takahara Y, Morishima-Kawashima M, Tanimura Y, Dolios G, Hirotani N, Horikoshi Y, Kametani F, Maeda M, Saido TC, Wang R, Ihara Y (2005) Longer forms of amyloid beta protein: implications for the mechanism of intramembrane cleavage by gamma-secretase. *J Neurosci* 25:436-445.
- Ratovitski T, Slunt HH, Thinakaran G, Price DL, Sisodia SS, Borchelt DR (1997) Endoproteolytic processing and stabilization of wild-type and mutant presenilin. *J Biol Chem* 272:24536-24541.
- Ray WJ, Yao M, Nowotny P, Mumm J, Zhang W, Wu JY, Kopan R, Goate AM (1999) Evidence for a physical interaction between presenilin and Notch. *Proc Natl Acad Sci U S A* 96:3263-3268.
- Rogaev EI, Sherrington R, Rogaeva EA, Levesque G, Ikeda M, Liang Y, Chi H, Lin C, Holman K, Tsuda T, et al. (1995) Familial Alzheimer's disease in kindreds with missense mutations in a gene on chromosome 1 related to the Alzheimer's disease type 3 gene. *Nature* 376:775-778.
- Sastre M, Steiner H, Fuchs K, Capell A, Multhaup G, Condron MM, Teplow DB, Haass C (2001) Presenilin-dependent  $\gamma$ -secretase processing of  $\beta$ -amyloid precursor protein at a site corresponding to the S3 cleavage of Notch. *EMBO Rep* 2:835-841.
- Saura CA, Tomita T, Davenport F, Harris CL, Iwatsubo T, Thinakaran G (1999) Evidence that intramolecular associations between presenilin domains are obligatory for endoproteolytic processing. *J Biol Chem* 274:13818-13823.
- Saxena MT, Schroeter EH, Mumm JS, Kopan R (2001) Murine Notch homologs (N1-4) undergo presenilin-dependent proteolysis. *J Biol Chem* 276:40268-40273.
- Scheinfeld MH, Ghersi E, Laky K, Fowlkes BJ, D'Adamio L (2002) Processing of beta-amyloid precursor-like protein-1 and -2 by gamma-secretase regulates transcription. *J Biol Chem* 277:44195-44201.
- Schroeter EH, Kisslinger JA, Kopan R (1998) Notch-1 signalling requires ligand-induced proteolytic release of intracellular domain. *Nature* 393:382-386.

## References

- Selkoe DJ (2001) Alzheimer's disease: genes, proteins, and therapy. *Physiol Rev* 81:741-766.
- Serneels L, DeJaegere T, Craessaerts K, Horre K, Jorissen E, Tousseyn T, Hebert S, Coolen M, Martens G, Zwijsen A, Annaert W, Hartmann D, De Strooper B (2005) Differential contribution of the three Aph1 genes to gamma-secretase activity in vivo. *Proc Natl Acad Sci U S A* 102:1719-1724.
- Shah S, Lee SF, Tabuchi K, Hao YH, Yu C, LaPlant Q, Ball H, Dann CE, 3rd, Sudhof T, Yu G (2005) Nicastrin functions as a gamma-secretase-substrate receptor. *Cell* 122:435-447.
- Shen J, Bronson RT, Chen DF, Xia W, Selkoe DJ, Tonegawa S (1997) Skeletal and CNS defects in Presenilin-1-deficient mice. *Cell* 89:629-639.
- Sherrington R, Rogaev EI, Liang Y, Rogaeva EA, Levesque G, Ikeda M, Chi H, Lin C, Li G, Holman K, et al. (1995) Cloning of a gene bearing missense mutations in early-onset familial Alzheimer's disease. *Nature* 375:754-760.
- Shirotani K, Edbauer D, Kostka M, Steiner H, Haass C (2004a) Immature nicastrin stabilizes APH-1 independent of PEN-2 and presenilin - identification of nicastrin mutants which selectively interact with APH-1. *J Neurochem* in press.
- Shirotani K, Edbauer D, Prokop S, Haass C, Steiner H (2004b) Identification of distinct gamma-secretase complexes with different APH-1 variants. *J Biol Chem*.
- Sinha S, Anderson JP, Barbour R, Basi GS, Caccavello R, Davis D, Doan M, Dovey HF, Frigon N, Hong J, Jacobson-Croak K, Jewett N, Keim P, Knops J, Lieberburg I, Power M, Tan H, Tatsuno G, Tung J, Schenk D, Seubert P, Suomensaaari SM, Wang S, Walker D, John V, et al. (1999) Purification and cloning of amyloid precursor protein  $\beta$ -secretase from human brain. *Nature* 402:537-540.
- Sisodia SS, St George-Hyslop PH (2002) gamma-Secretase, Notch, Abeta and Alzheimer's disease: where do the presenilins fit in? *Nat Rev Neurosci* 3:281-290.
- Song W, Nadeau P, Yuan M, Yang X, Shen J, Yankner BA (1999) Proteolytic release and nuclear translocation of Notch-1 are induced by presenilin-1 and impaired by pathogenic presenilin-1 mutations. *Proc Natl Acad Sci USA* 96:6959-6963.
- St George-Hyslop P, Haines J, Rogaev E, Mortilla M, Vaula G, Pericak-Vance M, Foncin JF, Montesi M, Bruni A, Sorbi S, et al. (1992) Genetic evidence for a novel familial Alzheimer's disease locus on chromosome 14. *Nat Genet* 2:330-334.
- Steiner H, Romig H, Grim MG, Philipp U, Pesold B, Citron M, Baumeister R, Haass C (1999a) The biological and pathological function of the presenilin-1  $\Delta$ exon 9 mutation is independent of its defect to undergo proteolytic processing. *J Biol Chem* 274:7615-7618.
- Steiner H, Winkler E, Edbauer D, Prokop S, Basset G, Yamasaki A, Kostka M, Haass C (2002) PEN-2 is an integral component of the  $\gamma$ -secretase complex required for coordinated expression of presenilin and nicastrin. *J Biol Chem* 277:39062-39065.
- Steiner H, Capell A, Pesold B, Citron M, Kloetzel PM, Selkoe DJ, Romig H, Mendla K, Haass C (1998) Expression of Alzheimer's disease-associated presenilin-1 is controlled by proteolytic degradation and complex formation. *J Biol Chem* 273:32322-32331.
- Steiner H, Kostka M, Romig H, Basset G, Pesold B, Hardy J, Capell A, Meyn L, Grim MG, Baumeister R, Fichteler K, Haass C (2000) Glycine 384 is required for presenilin-1 function and is conserved in polytopic bacterial aspartyl proteases. *Nat Cell Biol* 2:848-851.
- Steiner H, Duff K, Capell A, Romig H, Grim MG, Lincoln S, Hardy J, Yu X, Picciano M, Fichteler K, Citron M, Kopan R, Pesold B, Keck S, Baader M, Tomita T, Iwatsubo T, Baumeister R, Haass C (1999b) A loss of function mutation of presenilin-2

- interferes with amyloid  $\beta$ -peptide production and Notch signaling. *J Biol Chem* 274:28669-28673.
- Struhl G, Adachi A (2000) Requirements for presenilin-dependent cleavage of Notch and other transmembrane proteins. *Mol Cell* 6:625-636.
- Struhl G, Greenwald I (2001) Presenilin-mediated transmembrane cleavage is required for Notch signal transduction in *Drosophila*. *Proc Natl Acad Sci U S A* 98:229-234.
- Takasugi N, Takahashi Y, Morohashi Y, Tomita T, Iwatsubo T (2002) The mechanism of gamma-secretase activities through high molecular weight complex formation of presenilins is conserved in *Drosophila melanogaster* and mammals. *J Biol Chem* 277:50198-50205.
- Takasugi N, Tomita T, Hayashi I, Tsuruoka M, Niimura M, Takahashi Y, Thinakaran G, Iwatsubo T (2003) The role of presenilin cofactors in the  $\gamma$ -secretase complex. *Nature* 422:438-441.
- Thal DR, Rub U, Orantes M, Braak H (2002) Phases of A beta-deposition in the human brain and its relevance for the development of AD. *Neurology* 58:1791-1800.
- Thinakaran G, Harris CL, Ratovitski T, Davenport F, Slunt HH, Price DL, Borchelt DR, Sisodia SS (1997) Evidence that levels of presenilins (PS1 and PS2) are coordinately regulated by competition for limiting cellular factors. *J Biol Chem* 272:28415-28422.
- Thinakaran G, Borchelt DR, Lee MK, Slunt HH, Spitzer L, Kim G, Ratovitsky T, Davenport F, Nordstedt C, Seeger M, Hardy J, Levey AI, Gandy SE, Jenkins NA, Copeland NG, Price DL, Sisodia SS (1996) Endoproteolysis of presenilin 1 and accumulation of processed derivatives in vivo. *Neuron* 17:181-190.
- Tian G, Ghanekar SV, Aharony D, Shenvi AB, Jacobs RT, Liu X, Greenberg BD (2003) The mechanism of gamma-secretase: multiple inhibitor binding sites for transition state analogs and small molecule inhibitors. *J Biol Chem* 278:28968-28975.
- Tian G, Sobotka-Briner CD, Zysk J, Liu X, Birr C, Sylvester MA, Edwards PD, Scott CD, Greenberg BD (2002) Linear non-competitive inhibition of solubilized human  $\gamma$ -secretase by pepstatin A methylester, L685458, sulfonamides, and benzodiazepines. *J Biol Chem* 277:31499-31505.
- Tomita T, Katayama R, Takikawa R, Iwatsubo T (2002) Complex N-glycosylated form of nicastrin is stabilized and selectively bound to presenilin fragments. *FEBS Lett* 520:117-121.
- Tomita T, Watabiki T, Takikawa R, Morohashi Y, Takasugi N, Kopan R (2001) The first proline of PALP motif at the C terminus of presenilins is obligatory for stabilization, complex formation and  $\gamma$ -secretase activities of presenilins. *J Biol Chem* 276:33273-33281.
- Tomita T, Takikawa R, Koyama A, Morohashi Y, Takasugi N, Saido TC, Maruyama K, Iwatsubo T (1999) C terminus of presenilin is required for overproduction of amyloidogenic A $\beta$ 42 through stabilization and endoproteolysis of presenilin. *J Neurosci* 19:10627-10634.
- Vassar R, Bennett BD, Babu-Khan S, Kahn S, Mendiaz EA, Denis P, Teplow DB, Ross S, Amarante P, Loeloff R, Luo Y, Fisher S, Fuller J, Edenson S, Lile J, Jarosinski MA, Biere AL, Curran E, Burgess T, Louis JC, Collins F, Treanor J, Rogers G, Citron M (1999) Beta-secretase cleavage of Alzheimer's amyloid precursor protein by the transmembrane aspartic protease BACE [see comments]. *Science* 286:735-741.
- Walter J, Grunberg J, Schindzielorz A, Haass C (1998) Proteolytic fragments of the Alzheimer's disease associated presenilins- 1 and -2 are phosphorylated in vivo by distinct cellular mechanisms. *Biochemistry* 37:5961-5967.

## References

- Walter J, Grunberg J, Capell A, Pesold B, Schindzielorz A, Citron M, Mendla K, George-Hyslop PS, Multhaup G, Selkoe DJ, Haass C (1997) Proteolytic processing of the Alzheimer disease-associated presenilin-1 generates an in vivo substrate for protein kinase C. *Proc Natl Acad Sci USA* 94:5349-5354.
- Wang J, Brunkan AL, Hecimovic S, Walker E, Goate A (2004) Conserved "PAL" sequence in presenilins is essential for gamma-secretase activity, but not required for formation or stabilization of gamma-secretase complexes. *Neurobiol Dis* 15:654-666.
- Wang J, Beher D, Nyborg AC, Shearman MS, Golde TE, Goate A (2006) C-terminal PAL motif of presenilin and presenilin homologues required for normal active site conformation. *J Neurochem* 96:218-227.
- Watanabe N, Tomita T, Sato C, Kitamura T, Morohashi Y, Iwatsubo T (2005) Pen-2 is incorporated into the gamma-secretase complex through binding to transmembrane domain 4 of presenilin 1. *J Biol Chem* 280:41967-41975.
- Weidemann A, Eggert S, Reinhard FB, Vogel M, Paliga K, Baier G, Masters CL, Beyreuther K, Evin G (2002) A novel  $\epsilon$ -cleavage within the transmembrane domain of the Alzheimer amyloid precursor protein demonstrates homology with Notch processing. *Biochemistry* 41:2825-2835.
- Weihofen A, Martoglio B (2003) Intramembrane-cleaving proteases: controlled liberation of functional proteins and peptides from membranes. *Trends Cell Biol* 13:71-78.
- Weihofen A, Binns K, Lemberg MK, Ashman K, Martoglio B (2002) Identification of signal peptide peptidase, a presenilin-type aspartic protease. *Science* 296:2215-2218.
- Westlund B, Parry D, Clover R, Basson M, Johnson CD (1999) Reverse genetic analysis of *Caenorhabditis elegans* presenilins reveals redundant but unequal roles for sel-12 and hop-1 in Notch-pathway signaling. *Proc Natl Acad Sci USA* 96:2497-2502.
- Wittenburg N, Eimer S, Lakowski B, Rohrig S, Rudolph C, Baumeister R (2000) Presenilin is required for proper morphology and function of neurons in *C. elegans*. *Nature* 406:306-309.
- Wolfe MS, Xia W, Ostaszewski BL, Diehl TS, Kimberly WT, Selkoe DJ (1999a) Two transmembrane aspartates in presenilin-1 required for presenilin endoproteolysis and  $\gamma$ -secretase activity. *Nature* 398:513-517.
- Wolfe MS, Xia W, Moore CL, Leatherwood DD, Ostaszewski B, Rahmati T, Donkor IO, Selkoe DJ (1999b) Peptidomimetic probes and molecular modeling suggest that Alzheimer's  $\gamma$ -secretase is an intramembrane-cleaving aspartyl protease. *Biochemistry* 38:4720-4727.
- Wong PC, Zheng H, Chen H, Becher MW, Sirinathsinghji DJ, Trumbauer ME, Chen HY, Price DL, Van der Ploeg LH, Sisodia SS (1997) Presenilin 1 is required for Notch1 and Dll1 expression in the paraxial mesoderm. *Nature* 387:288-292.
- Yan R, Bienkowski MJ, Shuck ME, Miao H, Tory MC, Pauley AM, Brashier JR, Stratman NC, Mathews WR, Buhl AE, Carter DB, Tomasselli AG, Parodi LA, Heinrichson RL, Gurney ME (1999) Membrane-anchored aspartyl protease with Alzheimer's disease  $\beta$ -secretase activity. *Nature* 402:533-537.
- Yang DS, Tandon A, Chen F, Yu G, Yu H, Arawaka S, Hasegawa H, Duthie M, Schmidt SD, Ramabhadran TV, Nixon RA, Mathews PM, Gandy SE, Mount HT, George-Hyslop P, Fraser PE (2002) Mature glycosylation and trafficking of nicastrin modulate its binding to presenilins. *J Biol Chem* 277:28135-28142.
- Yang LB, Lindholm K, Yan R, Citron M, Xia W, Yang XL, Beach T, Sue L, Wong P, Price D, Li R, Shen Y (2003) Elevated beta-secretase expression and enzymatic activity detected in sporadic Alzheimer disease. *Nat Med* 9:3-4.

- Yasojima K, McGeer EG, McGeer PL (2001) Relationship between beta amyloid peptide generating molecules and neprilysin in Alzheimer disease and normal brain. *Brain Res* 919:115-121.
- Yu G, Chen F, Levesque G, Nishimura M, Zhang DM, Levesque L, Rogaeva E, Xu D, Liang Y, Duthie M, St George-Hyslop PH, Fraser PE (1998) The presenilin 1 protein is a component of a high molecular weight intracellular complex that contains  $\beta$ -catenin. *J Biol Chem* 273:16470-16475.
- Yu G, Nishimura M, Arawaka S, Levitan D, Zhang L, Tandon A, Song YQ, Rogaeva E, Chen F, Kawarai T, Supala A, Levesque L, Yu H, Yang DS, Holmes E, Milman P, Liang Y, Zhang DM, Xu DH, Sato C, Rogaev E, Smith M, Janus C, Zhang Y, Aebersold R, Farrer LS, Sorbi S, Bruni A, Fraser P, St George-Hyslop P (2000) Nicastrin modulates presenilin-mediated notch/glp-1 signal transduction and  $\beta$ APP processing. *Nature* 407:48-54.
- Zhang Z, Nadeau P, Song W, Donoviel D, Yuan M, Bernstein A, Yankner BA (2000) Presenilins are required for  $\gamma$ -secretase cleavage of  $\beta$ APP and transmembrane cleavage of Notch-1. *Nat Cell Biol* 2:463-465.
- Zhao G, Mao G, Tan J, Dong Y, Cui MZ, Kim SH, Xu X (2004) Identification of a new presenilin-dependent zeta-cleavage site within the transmembrane domain of amyloid precursor protein. *J Biol Chem* 279:50647-50650.
- Zhao G, Cui MZ, Mao G, Dong Y, Tan J, Sun L, Xu X (2005) gamma -cleavage is dependent on zeta -cleavage during the proteolytic processing of amyloid precursor protein within its transmembrane domain. *J Biol Chem*.

## Acknowledgements

I would like to thank Prof. Dr. Christian Haass for providing me the opportunity to join his laboratory to work on this interesting theme and also for the important suggestions to my work and this dissertation.

I would also like to thank Prof. Dr. Ralf-Peter Jansen, who kindly became my supervisor and made it possible that this dissertation was accepted at the Faculty of Chemistry and Pharmacy.

This study would not have been possible without the guidance of my group leader Dr. Harald Steiner, who always provided me with generous suggestions. I would like to express to him my deepest gratitude for his support over the years.

I appreciate the great collaboration with Agata Smialowska, Dr. Stefan Eimer and Prof. Dr. Ralf Baumeister. Their *in vivo* data contributed a strong back up of my results.

It was my honor to be a member of the Elitenetzwerk Bayern. It provided me a great opportunity to meet students from the other fields and to learn important skills outside the laboratory work such as organizing science meetings or finances.

Anja, Ayako, Blanca, Bozo, Christoph (Haffner), Edith, Gabi, Keiro, Masanori, Michael, Regina, Sven, and all other colleagues made the laboratory life really easy and fun. Without their friendship I could not have enjoyed my work that much. Their scientific suggestions were also very important for me. I would also like to thank Dr. Masayasu Okochi, Christoph (Kaether), Eddie, Tobias, Stefan and all other former colleagues for their scientific assistance as well as for the non-scientific discussions we had.

Friends from outside the laboratory, especially Ilse, Joseph and Akemi, always encouraged me and my work.

Finally, I thank Tobi, Kai and my parents for all their different kinds of support and for always being there for me.

## Curriculum vitae

### **Personal data:**

Name: Aya Yamasaki-Meythaler  
Sex: Female  
Address: Posener Str. 4, 81929 München  
e-mail: Aya.Yamasaki@med.uni-muenchen.de  
Date of birth: 29.08.1975  
Place of birth: Tokyo, Japan  
Nationality: Japan  
Marital status: Married

### **Education:**

#### ***Dissertation***

2000 – 2006 Ludwig-Maximilians-University Munich, Adolf-Butenandt Institute, Prof. Dr. C. Haass

#### ***MSc in medical science***

March 2000 Yokohama City University, Graduate School of Medical Science, Master's Program, Department of Psychiatry, Prof. Dr. med. K. Kosaka, Kanagawa, Japan

#### ***BSc in Bioscience***

March 1998 Kitasato University, School of Science, Department of Bioscience, Kanagawa, Japan

#### ***High school***

March 1994: Seisen High School, Kanagawa, Japan

### **Presentations/Conferences**

July 2002: poster presentation at the 8<sup>th</sup> International Conference on Alzheimer's Disease and Related Disorders, Stockholm, Sweden

October 2002: poster presentation at the 21<sup>st</sup> Conference of Dementia Japan, Osaka, Japan

July 2004: poster presentation at the 9<sup>th</sup> International Conference on Alzheimer's Disease and Related Disorders, Philadelphia, Pennsylvania, U.S.A.

November 2005: presentation at SFB meeting, "Meeting of the Alzheimer's Disease Research Focus, Third Progress Report", Adolf-Butenandt Institute

**Publications**

**Membrane topology of Alzheimer's disease-related presenilin 1. Evidence for the existence of a molecular species with a seven membrane-spanning and one membrane-embedded structure.**

Nakai T, Yamasaki A, Sakaguchi M, Kosaka K, Mihara K, Amaya Y, Miura S  
*J Biol Chem.* 1999 Aug 13;274(33):23647-58.

**PEN-2 is an integral component of the gamma-secretase complex required for coordinated expression of presenilin and nicastrin.**

Steiner H, Winkler E, Edbauer D, Prokop S, Basset G, Yamasaki A, Kostka M, and Haass C  
*J Biol Chem.* 2002 Oct 18;277(42):39062-5

**The GxGD Motif of Presenilin Contributes to Catalytic Function and Substrate Identification of  $\gamma$ -Secretase**

Yamasaki A, Eimer S, Okochi M, Smialowska A, Kaether C, Baumeister R, Haass C, and Steiner H  
*The Journal of Neuroscience*, April 5, 2006 • 26(14):3821–3828 • 3821

## **Appendix: Publications**

# Membrane Topology of Alzheimer's Disease-related Presenilin 1

EVIDENCE FOR THE EXISTENCE OF A MOLECULAR SPECIES WITH A SEVEN MEMBRANE-SPANNING AND ONE MEMBRANE-EMBEDDED STRUCTURE\*

(Received for publication, December 21, 1998, and in revised form, April 12, 1999)

Toshiki Nakai‡, Aya Yamasaki‡§, Masao Sakaguchi¶, Kenji Kosaka§, Katsuyoshi Mihara¶, Yoshihiro Amaya||\*\*, and Satoshi Miura‡ ‡‡

From the ‡Radioisotope Research Center, §Department of Psychiatry, ¶Department of Biochemistry, Yokohama City University School of Medicine, 3-9 Fukuura, Kanazawa-ku, Yokohama 236-0004 and the ||Department of Molecular Biology, Graduate School of Medical Science, Kyushu University, 3-1-1 Maidashi, Higashi-ku, Fukuoka 812-8582, Japan

**A significant member of early-onset familial type of Alzheimer's disease cases has been shown to be caused by dominant mutations in either of the two genes encoding presenilin 1 (PS1) and presenilin 2 (PS2). These two proteins are highly homologous to each other and have been reported to be mainly localized to the membranes of intracellular compartments such as the endoplasmic reticulum. Information about the membrane topological structures of these proteins is indispensable for understanding their physiological and pathological roles. Although several models have been proposed previously, their precise membrane topologies remain unknown. In this study, we examined this issue in detail by expressing a series of C-terminally deleted PS1 mutants fused to the hydrophilic portion of *Escherichia coli* leader peptidase *in vitro* using a reticulocyte lysate in the presence of microsomal membranes. Our results predict that PS1 exists mainly in a seven membrane-spanning structure with its C-terminal end exposed to the luminal space. This was also confirmed by expressing these fusion proteins in cultured cells. We further showed that a ninth hydrophobic segment is tightly bound to the membrane without spanning it. Based on the above observations, we propose a novel "seven membrane-spanning and one membrane-embedded" topological model for presenilins.**

A significant portion of inheritable familial Alzheimer's disease (FAD)<sup>1</sup> is caused and transmitted in a dominant manner through mutations in either of the two highly homologous genes encoding presenilin 1 (PS1) and presenilin 2 (PS2) on

\* This work was supported in part by grants in Support of the Promotion of Research at Yokohama City University, a grant-in-aid for Scientific Research (C) from the Ministry of Education, Science, Sports and Culture of Japan, and research grants from the Mitsui Life Social Welfare Foundation, Chiyoda Mutual Life Foundation, and Sasakawa Health Science Foundation. The costs of publication of this article were defrayed in part by the payment of page charges. This article must therefore be hereby marked "advertisement" in accordance with 18 U.S.C. Section 1734 solely to indicate this fact.

\*\* Present address: Dept. of Biochemistry, School of Dentistry, Niigata University, 2-5274, Gakkocho, Niigata 951-8514, Japan.

‡‡ To whom correspondence should be addressed: Radioisotope Research Center, Yokohama City University School of Medicine, 3-9, Fukuura, Kanazawa-ku, Yokohama 236-0004, Japan. Tel.: 81-45-787-2760; Fax: 81-45-782-1251; E-mail: smiura@med.yokohama-cu.ac.jp.

<sup>1</sup> The abbreviations used are: FAD, familial Alzheimer's disease; A $\beta$ , amyloid beta protein; CTF, C-terminal fragment; ER, endoplasmic reticulum; ERGIC, ER-Golgi-intermediate compartment; GH, growth hormone; HR, hydrophobic region; LPase, *E. coli* leader peptidase; MS, dog pancreas microsomal membranes; PS1, presenilin 1; PS2, presenilin 2; PAGE, polyacrylamide gel electrophoresis; aa, amino acid; PCR, polymerase chain reaction; PBS, phosphate-buffered saline; CHO, Chinese hamster ovary.

chromosomes 14 and 1, respectively (1–5). These proteins have been shown to be mainly localized to the endoplasmic reticulum (ER), the Golgi apparatus, and the ER-Golgi-intermediate compartment (ERGIC) (6–8), although their localization to other compartments such as the plasma membrane has also been suggested (9, 10). One of the physiological roles of presenilins has been suggested through genetic analysis of *Caenorhabditis elegans* SEL-12, which codes for a protein highly homologous to mammalian presenilins (11), and through analysis of PS1-knockout mice (12, 13). These studies have suggested that presenilins are involved in the Notch signaling pathway, which is known to be involved in many different aspects of the regulation of cell differentiation in *C. elegans* and higher eukaryotes. Several roles of presenilins in the pathogenesis of FAD have also been suggested. First, in the cerebrospinal fluid of FAD patients or in the medium of cultured cells expressing FAD-linked mutant presenilins, elevation of the level of amyloid  $\beta$  protein consisting of 42 amino acid residues (A $\beta$ 42), which is thought to play a key role in the pathological progression of Alzheimer's disease, especially for senile plaque formation, has been observed (14–17). This suggests that FAD-associated mutations cause the disease by elevating the production of A $\beta$ 42 either intracellularly or extracellularly. Furthermore, analysis of neuronal cell primary cultures derived from PS1 knockout mouse embryos implied that PS1 is required for  $\gamma$ -secretase cleavage of A $\beta$  from amyloid precursor protein (18). Second, several works have shown that wild-type or mutant presenilins are involved in the regulation of the cellular apoptotic pathway (19–22), implying the possibility that they may be related to the neural cell loss or degeneration commonly observed in this disease. However, the mechanisms underlying both the physiological and pathogenic functions of presenilins at the molecular level remain to be elucidated.

To understand the function(s) of presenilins at the molecular level, conformational information on these proteins in membranes is indispensable. Several previous reports have suggested different models for the membrane topologies of these or related proteins differing in the number of membrane-spanning segments (six to eight), but in all of them the C terminus is exposed to the cytosolic space (23–27). In this study, we re-examined this issue using a series of fusion proteins consisting of C-terminally deleted PS1 and a reporter sequence, with special emphasis on the C-terminal half region, where significant discordance still exists. Although two previous studies involved similar strategies (25, 26), in our study special attention was paid when choosing the reporter fragment to be fused because we consider it possible that the relatively hydrophobic nature of the extreme C-terminal region of PS1 would affect the results if the N-terminal portion of the reporter is also hydro-

TABLE I  
PCR primers used for PS1 subcloning

Amino acid residue		Primer
1–156	Sense	GGCGAATTC <b>TCACC</b> ATGACAGAGTTACCTGCACCG <sup>a</sup>
	Antisense	CGGATCGATATTTATACAGAACCCAGG <sup>b</sup>
157–269	Sense	GGCATCGATGCTATAAGGTCATCCATGCC <sup>b</sup>
	Antisense	CAACCAGCATGCGAAGTGGACCTTTCCGGACA <sup>b</sup>
270–401	Sense	CACTTCGCATGCTGGTTGAAACAGCTCA <sup>b</sup>
	Antisense	CAGTCTCCGGAGGCTGTTGCTGAGGCTTTC <sup>b</sup>
402–467	Sense	CAGCCTCCGGAGACTGGAACACACACCAT <sup>b</sup>
	Antisense	CCGCTCGAGCTAGATATAAAATTGATGGA <sup>c</sup>

<sup>a</sup> An *Eco*RI restriction site (underlined) and a Kozak sequence (boldface) were introduced just before the initiation codon (double underlined).

<sup>b</sup> *Cla*I, *Sph*I, and *Bsp*EI restriction sites (underlined) were introduced at the junctions on adjoining sites, respectively, without changing the encoded amino acids for convenience for further construction.

<sup>c</sup> An *Xho*I restriction site (underlined) was introduced just after the stop codon.

phobic. The results we obtained using a series of such fusion proteins confirmed the notion that the N-terminal and the large hydrophobic loop regions of PS1 face the cytosol, as suggested by several previous studies. However, by using a reporter sequence that does not include hydrophobic residues in the vicinity of the N-terminal portion of the reporter region just after the fused point, we unexpectedly observed that a significant fraction of the molecules expressed *in vitro* or in cultured cells exposed their C-terminal ends to the luminal space on the ER membrane. In addition, we show here that the eighth and ninth hydrophobic segments do not span the membrane and that, despite this, the latter is tightly bound to the lipid bilayer from the cytosolic face. Based on the data presented in this study, we here propose a “seven membrane-spanning and one membrane-embedded” model for the topological structures of presenilins. Possible causes for the discrepancy between our results and the models proposed by several other groups are also discussed.

#### MATERIALS AND METHODS

**Cloning of the PS1 Gene and Plasmid Construction**—cDNAs for four contiguous parts spanning the whole coding region of human PS1 were amplified from a human fetal brain cDNA library (Stratagene) by PCR using four sets of oligonucleotides as primers (Table I). The four PCR products were digested with appropriate restriction enzymes, then subcloned into appropriate vectors, and finally recombined between the *Eco*RI and *Xho*I sites of the Bluescript II vector (Stratagene) to reconstitute the whole PS1 coding region. For the most N-terminal region, we subcloned the cDNAs for both of the two known variants in which VRSQ between the 26th and 29th amino acid residues is retained or deleted, respectively. Throughout this study, the VRSQ-deleted variant was used. However, the amino acid residue number of PS1 used in this study is based on that of the VRSQ-containing variant. The 1.4-kilobase pair *Eco*RI-*Xho*I fragment containing the whole PS1 coding region was excised and subcloned between the *Eco*RI-*Xho*I sites of the pcDNA3.1(+) vector (Invitrogen) to produce pcDNA-PS1.

A series of C-terminally deleted fragments of PS1 was amplified by PCR using appropriate N-terminal primers and the C-terminal primers listed in Table II. For fusion plasmid construction, C-terminal fragments of the *Escherichia coli* leader peptidase (LPase) coding region beginning from codons corresponding to 104 or 142 aa were amplified from pRD8 (28) as a template using the following primers: sense primer, GACGGATCCGAGAAGTTTGCTTATGGCATT or GACGGATCCGAT-TACATCAAGCGCGGGTTC, and antisense primer, GGCCTCGAGTT-AGGGCTAGTCGGGCACGTCGTAGGGGTAATGGATGCCGCCAA-TGCGACT. A *Bam*HI site (underlined) was added to the N-terminal end. A hemagglutinin tag sequence (boldface) was inserted before the stop codon, and an *Xho*I site (underlined) was introduced after the stop codon. To construct fusion plasmids expressing C-terminally deleted PS1 and LPase fusion proteins, the PCR products of PS1 deletion mutants digested with *Bam*HI and an appropriate restriction enzyme together with either of the two different *Bam*HI-*Xho*I fragments for LPase were substituted for the corresponding regions of pcDNA-PS1 except in the cases of ΔH3-C and ΔH9-C, in which a 0.9-kilobase pair *Cla*I-*Xho*I fragment and a 0.2-kilobase pair *Bsp*EI-*Xho*I fragment of pcDNA-PS1, respectively, were replaced with a *Bam*HI-*Xho*I LPase fragment together with adapters consisting of the following oligonucleotides: CGCTGCTATAAGG and GATCCCTTATAGCAG or CCGGC-

TABLE II  
PCR primers used for deletion mutant construction

Construct	Primer <sup>a</sup>
ΔH1-C	GGCGGATCCATGCTTGGCGCCATATTTCAA
ΔH2-C	GGCGGATCCTGAGTGCAGGGCTCTCTGGCC
ΔH4-C	GGCGGATCCGTCACAGCAACGTTATAGGT
ΔH5-C	GGCGGATCCTCGAAGTGGACCTTCCAGGTG
ΔH6-C	GGCGGATCCTTCAGGGAGGTACTTGATAAA
ΔH7-C	GGCGGATCCTTCATTTCTCTCTCTGAGC
ΔH8-C	GGCGGATCCTTTTACTCCCCTTTCTCTC
ΔH10-C	GGCGGATCCTTTCTTGAAAATGGCAAG
ΔC	GGCGGATCCATAATCTGTGGCAAAGTA
Full-C	GGCGGATCCGATATAAAATTGATGGAATGC

<sup>a</sup> A *Bam*HI restriction site (underlined) was introduced next to the C-terminal end of each deletion mutant.

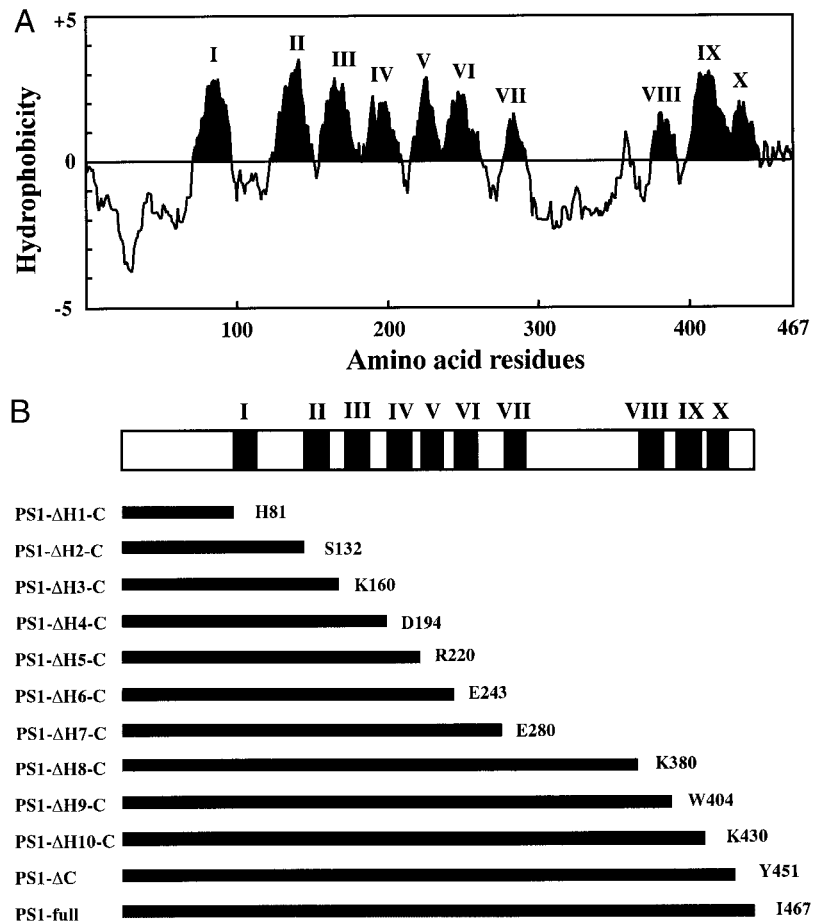
GACTGGG and GATCCCCAGTCG, respectively.

For PS1-newt growth hormone (GH) fusion construction, a portion of newt GH coding sequence spanning the region from the 3rd amino acid residue of the mature protein to the C terminus was amplified by PCR using its cDNA subcloned in a pBluescript II vector (Stratagene) as a template (29). Primers used for amplification were GGTGGATCCG-GCGTGTCCCTGACAAATCTC and CCGctcgagTCAATGATGATGATGATGATGATGAATGGTCAATTATTATCTA. A *Bam*HI site (underlined) was introduced to the N-terminal flanking region, and 6× His tag (boldface) was introduced to the C-terminal end, and *Xho*I restriction site (lowercase letters) was introduced to the C-terminal flanking region. Amplified PCR fragment digested with *Bam*HI and *Xho*I was used for the construction of PS1-GH as in the case of the PS1-LPase fusion construction described above.

**Antibodies and Immunological Procedures**—Anti-LPase polyclonal antibody LP-1 was raised against N-terminally 6× His-tagged LPase spanning amino acids 104–323, which was expressed in *E. coli* using pET16b (Novagen). Polyclonal antibody LOOP1 against the mouse PS1 loop region (332–371 aa) was raised by injecting a rabbit with glutathione S-transferase fusion protein containing this region expressed in *E. coli* using pGEX-5X-1 (Amersham Pharmacia Biotech) and was used after purification using an Affi-Gel matrix (Bio-Rad) to which a fusion protein consisting of maltose-binding protein and 263–407 aa of human PS1 expressed using pMAL-c2 (New England Biolabs) was attached. This antibody cross-reacts with the corresponding region of human PS1. For immunoprecipitation, samples were diluted with immunoprecipitation buffer (10 mM Tris-HCl, pH 7.4, 0.1% SDS, 0.1% Triton X-100, 2 mM EDTA) and then incubated with the antibody for 1 h at room temperature and further for 1 h in the presence of Pansorbion cell, fixed *Staphylococcus aureus* cells (Calbiochem). After centrifugation, the pellets were washed four times with immunoprecipitation buffer, and proteins were extracted with 2× SDS-PAGE sample buffer (30) for 30 min at room temperature. Western blotting was performed after the proteins had been separated by SDS-PAGE and transferred to polyvinylidene difluoride membranes (Bio-Rad). Proteins were detected using an ECL chemiluminescence detection kit (Amersham Pharmacia Biotech) according to the manufacturer's instructions.

**In Vitro Transcription and Translation**—Linearized plasmids were transcribed *in vitro* from the T7 promoter located upstream of the multicloning site of pcDNA3.1(+) using T7 RNA polymerase (Stratagene) according to the manufacturer's instructions. The transcribed mRNAs were used for translation *in vitro* using a rabbit reticulocyte lysate (31) in the presence or absence of dog pancreas microsomal membranes (MS) prepared as described previously (32).

**FIG. 1. Hydrophathy of human PS1 and construction of deletion mutants.** A, the hydrophathy of human PS1 was plotted using the published algorithm (51). A window size of 12 was used. Ten detected hydrophobic segments (HR1 to HR10) are indicated by *roman numerals*. B, *top*, 10 hydrophobic segments are schematically presented. Each segment spans the region between the following amino acid residues: HR1, Val<sup>82</sup>-Ile<sup>100</sup>; HR2, Ile<sup>133</sup>-Tyr<sup>154</sup>; HR3, His<sup>164</sup>-Gly<sup>183</sup>; HR4, Tyr<sup>195</sup>-Ile<sup>213</sup>; HR5, Leu<sup>221</sup>-Ile<sup>238</sup>; HR6, Trp<sup>240</sup>-Leu<sup>262</sup>; HR7, Leu<sup>282</sup>-Ala<sup>299</sup>; HR8, Leu<sup>381</sup>-Gly<sup>394</sup>; HR9, Ile<sup>408</sup>-he<sup>428</sup>; and HR10, Ala<sup>431</sup>-Ala<sup>448</sup>. *Bottom*, the constructs of deletion mutants for PS1 used in this study are indicated by *horizontal bars*. To the *right of each bar* is shown the amino acid residue to which each deletion mutant spans. PS1- $\Delta$ H1-C means that the region from HR1 to the C terminus of PS1 was deleted, the same holds for PS1- $\Delta$ H2-C to PS1- $\Delta$ H10-C. PS1- $\Delta$ C lacks the C-terminal region beginning just after HR10, and PS1-full contains the full-length PS1. Each deletion mutant was fused in frame to *E. coli* LPase to produce fusion genes PS1- $\Delta$ H1-C-LP to PS1- $\Delta$ H10-C-LP, PS1- $\Delta$ C-LP, and PS1-full-LP through the *Bam*HI restriction site which inserts additional glycine and serine residues between the PS1 region and LPase.



**Human Placenta Homogenate Preparation and Na<sub>2</sub>CO<sub>3</sub> Extraction**—Human placenta tissue was homogenized in PBS(-) (0.2 g/liter KH<sub>2</sub>PO<sub>4</sub>, 2.16 g/liter Na<sub>2</sub>HPO<sub>4</sub>, 7H<sub>2</sub>O, 8 g/liter NaCl, 0.2 g/liter KCl) in the presence of 1 mM phenylmethylsulfonyl fluoride and then centrifuged at 1,500 × *g* for 10 min. The supernatant was further centrifuged at 100,000 × *g* for 1 h. The pelleted membrane fraction was resuspended in 0.1 M Na<sub>2</sub>CO<sub>3</sub> and then incubated on ice for 30 min. One-half of it was further centrifuged at 100,000 × *g* for 1 h, and then the supernatant and pellet fractions were analyzed, together with the uncentrifuged half, for the presence of C-terminal fragment (CTF) by SDS-PAGE and Western blotting.

**Cell Culture and Plasmid Transfection**—COS-1 and CHO-K1 cells were cultured in Dulbecco's modified Eagle's medium/high glucose medium and F12 medium, respectively, both of which were supplemented with 10% fetal bovine serum, penicillin, and streptomycin. Cells were transfected with the indicated plasmids using LipofectAMINE (Life Technologies, Inc.) according to the manufacturer's instructions.

**Cell Labeling**—Cells cultured on 35-mm dishes were washed once with PBS(-) and then preincubated for 2 h in Dulbecco's modified Eagle's medium/high glucose without cysteine and methionine but supplemented with dialyzed 10% fetal bovine serum at 37 °C under a 5% CO<sub>2</sub> atmosphere. Labeling was started by the addition of 100  $\mu$ Ci of Met-<sup>35</sup>S-label (mixture of L-[<sup>35</sup>S]methionine and L-[<sup>35</sup>S]cysteine, >37 TBq/mmol; American Radiolabeled Chemicals, Inc.) to the culture. After 5 h labeling, the cells were washed three times with PBS(-), and then the proteins were extracted with extraction buffer (PBS(-) supplemented with 0.5% Nonidet P-40, 0.1% SDS, 1 mM phenylmethylsulfonyl fluoride, 10  $\mu$ M antipain, 10  $\mu$ M leupeptin, 10  $\mu$ M chymostatin, and 10  $\mu$ M pepstatin) and processed for immunoprecipitation.

## RESULTS

**Strategies for Membrane Topology Analysis**—Hydrophathy analysis of the predicted primary structure of PS1 revealed 10 distinct hydrophobic regions (HR1 to HR10) that are candidate membrane-spanning segments (Fig. 1A). In order to determine which of these regions actually span the membrane, we adopted a deletion strategy based on the assumption that poly-

topic membrane proteins are inserted into the membrane sequentially from the N terminus without the requirement of a more distal C-terminal region (33). According to this assumption, when a series of C-terminally deleted mutants for a polytopic membrane protein is expressed in the presence of ER membrane, localization of the C-terminal end of each deletion mutant should reflect the topology of the corresponding point when the full-length protein is expressed. Thus, when a reporter protein is fused to the C terminus of such a deletion mutant, the localization of the reporter protein according to the membrane should reflect that of the fusion point in the wild-type protein if the reporter region is neutral as to membrane translocation. As a reporter protein, we used the C-terminal hydrophilic region of *E. coli* leader peptidase (LPase). In *E. coli*, LPase is expressed as an inner membrane protein, the C-terminal region of which contains an active site located in the periplasmic space (34). Thus, this portion should not interfere with its translocation across the membrane. Moreover, it is known that, when expressed *in vitro* in a eukaryotic system in the presence of dog pancreas microsomes, this protein retains the same topogenic ability as in *E. coli*, and the C-terminal hydrophilic region localized in the luminal space undergoes *N*-glycosylation efficiently (35). The latter property also enabled us to determine whether or not this portion is localized in the luminal space.

**Construction of C-terminally Deleted PS1 Fusion Genes**—For the analysis of PS1 topogenicity, based on the results of hydrophathy analysis, a series of C-terminally deleted PS1 mutant cDNAs truncated at the points just prior to the hydrophobic regions (PS1- $\Delta$ H1-C to PS1- $\Delta$ H10-C, Fig. 1B) and just after HR10, the most C-terminal hydrophobic segment (PS1- $\Delta$ C), were constructed, and they, together with the whole PS1 coding

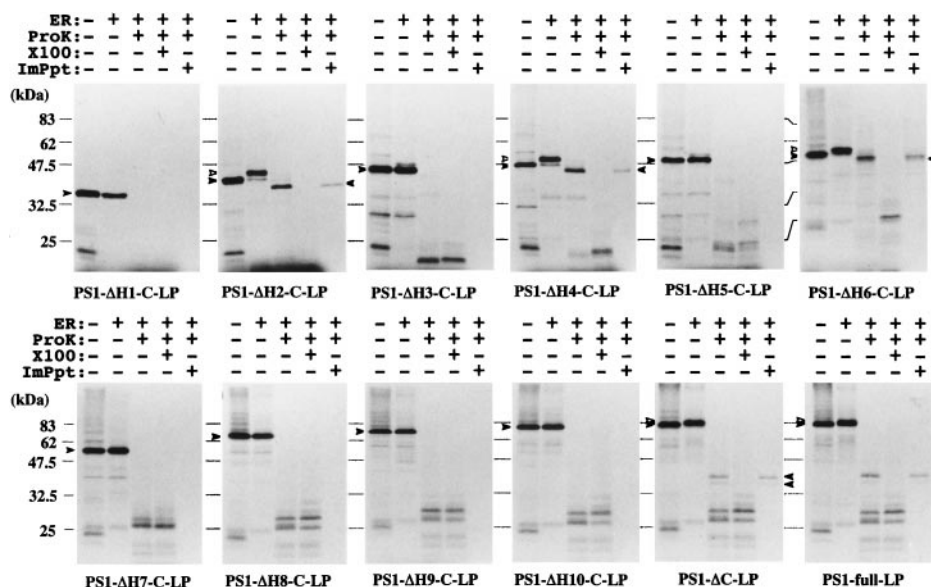


**FIG. 2. *In vitro* translation of the fusion genes in a rabbit reticulocyte lysate and proteinase K protection assaying of the translation products.** The plasmids indicated *below* each panel were linearized with *Xba*I, and mRNA was synthesized using T7 RNA polymerase. Transcripts were translated in a rabbit reticulocyte lysate in the presence of [<sup>35</sup>S]methionine and the presence (*ER*+, lanes 2–5 in each panel) or absence (*ER*–, lane 1 in each panel) of dog pancreas microsomal membrane. The translation products obtained in the presence of the membrane were divided into four parts, three of which were treated with proteinase K (20 μg/ml) in the presence (*X100*+, lane 4 in each panel) or absence (*X100*–, lanes 3 and 5 in each panel) of 1% Triton X-100. A part of the latter was further immunoprecipitated with anti-LPase polyclonal antibody, LP-1 (*ImPpt*+, lane 5 of each panel). The proteins in all samples were separated by 10% SDS-polyacrylamide gel electrophoresis, and isotopically labeled proteins were detected by fluorography. The positions for the bands of unglycosylated or glycosylated proteins are indicated by closed or open arrowheads, respectively, on the left of each panel. The bands for proteinase K-protected fragments containing the LPase region are indicated by closed arrowheads on the right of the panels for PS1-ΔH2-C-LP, PS1-ΔH4-C-LP, PS1-ΔH6-C-LP, PS1-ΔC-LP, and PS1-full-LP. The positions of prestained marker proteins (New England Biolabs) are indicated on the left of the fluorograms.

region (*PS1-full*), were fused in frame to the sequence encoding the C-terminal region of LPase corresponding to 104–323 amino acid residues. When choosing a reporter, especially for the construction of a fusion protein with full-length PS1, the hydrophilic property of the N terminus of the reporter fragment is important to prevent fortuitous production of a hydrophobic segment at the junction, because the extreme C-terminal portion of PS1 is relatively rich in hydrophobic residues. The N terminus of the above LPase region is hydrophilic enough to prevent the creation of such hydrophobic segments together with the C terminus of PS1, as judged by hydropathy analysis (data not shown). These fusion constructs were transcribed *in vitro*, and the synthesized mRNAs were translated in an *in vitro* translation system using a rabbit reticulocyte lysate in the presence of [<sup>35</sup>S]methionine and in the presence or absence of MS. The translation products were analyzed by fluorography.

***PS1 Spans the Membrane Seven Times***—We assessed the membrane orientation of the reporter portion of each fusion protein expressed *in vitro* in the presence of MS using two distinct criteria as follows: 1) susceptibility of the reporter portion to proteinase K added via the cytosolic space; and 2) *N*-linked glycosylation, specific for the luminal space of ER, of the consensus sequence present in the reporter portion. Fig. 2 shows a fluorogram of the *in vitro* translation product for each fusion construct. These data indicate first that, in the presence of MS, translation products with slightly reduced electrophoretic mobility, as compared with those in the absence of the membrane, were predominant for PS1-ΔH2-C-LP, PS1-ΔH4-C-LP, PS1-ΔH6-C-LP, PS1-ΔC-LP, and PS1-full-LP (lanes 1 and 2 for each set in Fig. 2); however, in the cases of PS1-ΔH1-C-LP, PS1-ΔH3-C-LP, PS1-ΔH5-C-LP, PS1-ΔH7-C-LP, PS1-ΔH8-C-LP, PS1-ΔH9-C-LP, and PS1-ΔH10-C-LP (lanes 1 and 2 for each set in Fig. 2), no such mobility shift was observed. These results suggest that, for the former constructs, an *N*-linked glycosyl chain was attached to the reporter portion as a result

of its translocation through the membrane and subsequent exposure to *N*-glycosyltransferase, whose active site resides in the luminal face of ER. This was confirmed by endoglycosidase H treatment, which is known to remove *N*-linked glycosyl chains from a polypeptide. Such treatment effectively restored the mobility to the extent that was observed for the translation products in the absence of microsomal membranes for all of the five constructs above (Fig. 3).

Second, when proteinase K is added via the cytosolic space to the translation products inserted into MS, the reporter portion located in the luminal space is expected to be protected from digestion because the protease cannot go into the luminal space due to the lipid bilayer of the microsomal vesicles. As shown in Fig. 2, only when a shift of the electrophoretic mobility was observed in the presence of MS (PS1-ΔH2-C-LP, PS1-ΔH4-C-LP, PS1-ΔH6-C-LP, PS1-ΔC-LP and PS1-full-LP) were protected fragments also observed (lane 3), which can be immunoprecipitated with LP-1 specific for LPase (lane 5). These fragments were abolished when proteinase K was added in the presence of Triton X-100, which disrupts the membrane (lane 4). These results, together with the presence of *N*-linked glycosylation, indicate that the reporter LPase portion of these products derived from PS1-ΔH2-C-LP, PS1-ΔH4-C-LP, PS1-ΔH6-C-LP, PS1-ΔC-LP, and PS1-full-LP is sequestered on the luminal side of microsomal vesicles, whereas that in the fusion proteins expressed by other constructs (PS1-ΔH1-C-LP, PS1-ΔH3-C-LP, PS1-ΔH5-C-LP, PS1-ΔH7-C-LP, PS1-ΔH8-C-LP, PS1-ΔH9-C-LP, and PS1-ΔH10-C-LP) is located on the cytosolic face.

To confirm the above results, we further examined two additional distinct series of constructs. On the one hand, in order to determine whether or not the above results hold true when another reporter protein, especially with a different N-terminal sequence, is used, a series of distinct fusion constructs corresponding to PS1-ΔH6-C, PS1-ΔH10-C, and PS1-ΔC were constructed using a shorter region of LPase (142–323 aa) having a

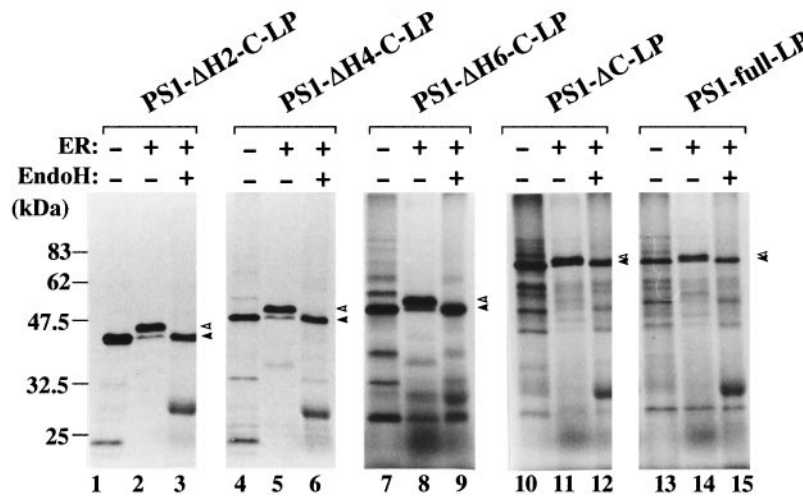


**FIG. 3. The mobility shift is due to *N*-glycosylation.** The *in vitro* translation products obtained in the presence of MS from the plasmids exhibiting a mobility shift (PS1- $\Delta$ H2-C-LP, lanes 1–3; PS1- $\Delta$ H4-C-LP, lanes 4–6; PS1- $\Delta$ H6-C-LP, lanes 7–9; PS1- $\Delta$ C-LP, lanes 10–12; PS1-full-LP, lanes 13–15) were treated with endoglycosidase H (*EndoH*<sup>+</sup>, lanes 3, 6, 9, 12, and 15) and then electrophoresed side by side with the products obtained in the absence of MS (*ER*<sup>–</sup>, lanes 1, 4, 7, 10, and 13) and those in the presence of MS without endoglycosidase H treatment (*ER*<sup>+</sup> and *EndoH*<sup>–</sup>, lanes 2, 5, 8, 11, and 14). The positions for unglycosylated or glycosylated bands are indicated by closed or open arrowheads, respectively, on the right of each panel. The positions of prestained marker proteins (New England Biolabs) are indicated on the left of the fluorograms.

different N-terminal sequence as a reporter. Experiments involving these constructs gave results consistent with those described above (data not shown). On the other hand, when an extra membrane-spanning segment corresponding to TM2 of LPase (58–76 aa), which spans the ER membrane from the cytosol to the lumen when full-length LPase is expressed in a eukaryotic system (34), was inserted between the presenilin region and the reporter region, a complementary pattern of *N*-linked glycosylation was observed (Fig. 4). For constructs derived from PS1- $\Delta$ H7-C to PS1- $\Delta$ H10-C, the translation products were mainly *N*-glycosylated, whereas for those from PS1- $\Delta$ H6-C, PS1- $\Delta$ C, and PS1-full, the translation products were predominantly unglycosylated, although minor glycosylated products were observed for the last two of the latter. The existence of glycosylated species for PS1- $\Delta$ C-TM-LP and PS1-full-TM-LP may be due to incompleteness of the translocation efficiency of HR10. In such minor molecular species with cytosolic HR10, the extra membrane-spanning segment could span the membrane from the cytosol to the lumen and hence result in the translocation of the reporter portion to the luminal space.

The consistent results obtained with the above three series of constructs strongly suggest that PS1 spans the membrane seven times with the portions of the PS1 molecule just proximal to HR2, HR4, and HR6, the region just distal to HR10, and the C terminus exposed to the luminal space, and the portions just proximal to HR1, HR3, HR5, HR7, HR8, HR9, and HR10 exposed to the cytosolic space.

We also examined a series of PS1-GH fusion constructs (Fig. 5). When GH was fused just prior to HR10 (PS1- $\Delta$ H10-C-GH), or just after HR10 (PS1- $\Delta$ C-GH), results were consistent with those in the case when LPase was used as a reporter, although *N*-glycosylation and protection against proteinase K in PS1- $\Delta$ C-GH were less efficient than those in PS1- $\Delta$ C-LP. When GH was fused after the C terminus of PS1 (PS1-full-GH), the results were contradictory. *N*-Glycosylation and protection against proteinase K were very inefficient as compared with the case with the corresponding LPase fusion construct. As the C-terminal portion of PS1 and the N-terminal portion of the GH region fused to PS1 are intermediately hydrophobic, we think the results of PS1-full-GH as an artifact of synthetic hydrophobicity of the region around the fusion point (see “Discussion”).

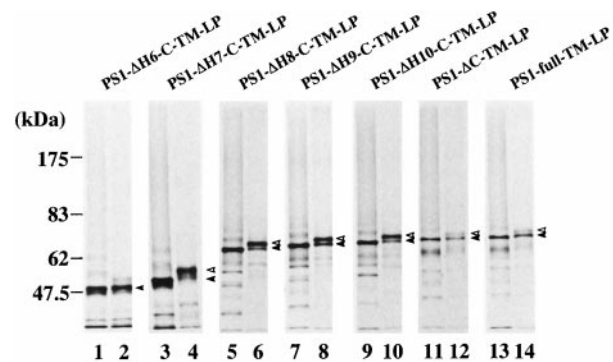


**FIG. 4. *N*-Glycosylation of the fusion proteins with an additional membrane-spanning segment.** A series of PS1-LPase fusion constructs in which an extra membrane-spanning segment was inserted at the fusion point (PS1- $\Delta$ H6-C-TM-LP, lanes 1 and 2; PS1- $\Delta$ H7-C-TM-LP, lanes 3 and 4; PS1- $\Delta$ H8-C-TM-LP, lanes 5 and 6; PS1- $\Delta$ H9-C-TM-LP, lanes 7 and 8; PS1- $\Delta$ H10-C-TM-LP, lanes 9 and 10; PS1- $\Delta$ C-TM-LP, lanes 11 and 12; and PS1-full-TM-LP, lanes 13 and 14) were constructed, and the presence of *N*-glycosylation was assessed by comparing the mobilities of the translation products *in vitro* in the absence (lanes 1, 3, 5, 7, 9, 11, and 13) and presence (lanes 2, 4, 6, 8, 10, 12, and 14) of MS as described in Fig. 3. The positions of *N*-glycosylated or glycosylated proteins are indicated by closed or open arrowheads on the right of each panel, respectively. The positions of prestained marker proteins (New England Biolabs) are indicated on the left of the fluorograms.

**Topological analysis of PS1 in Cultured Cells**—To confirm the results obtained with the *in vitro* experimental system, we transiently expressed PS1- $\Delta$ H6-C-LP to PS1- $\Delta$ H10-C-LP, PS1- $\Delta$ C-LP, and PS1-full-LP in COS-1 cells in the presence of a mixture of [<sup>35</sup>S]methionine and [<sup>35</sup>S]cysteine to label newly synthesized proteins isotopically. As shown in Fig. 6, the electrophoretic mobilities of the major translation products for PS1- $\Delta$ H6-C-LP, PS1- $\Delta$ C-LP, and PS1-full-LP decreased when the cell extracts were treated with endoglycosidase H prior to immunoprecipitation, indicating that in the majority of the fusion proteins expressed in living cells, the reporter regions underwent *N*-linked glycosylation and were therefore translocated to the luminal space. Note that significant portions of them were unglycosylated, implying the existence of PS1 molecules with the C terminus exposed to the cytosol in living cells. This may explain the discrepancy between our results and

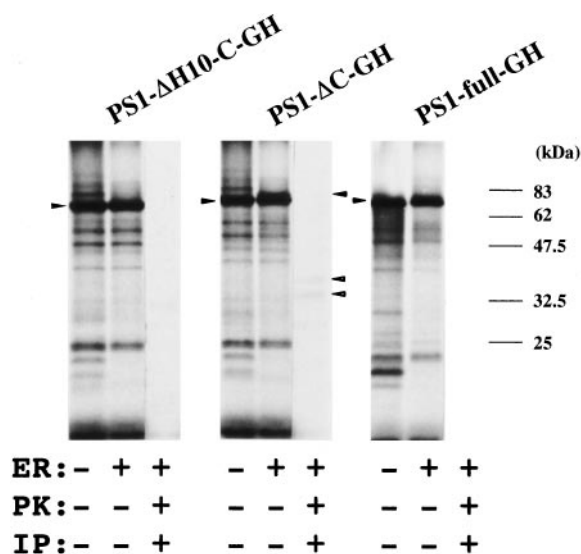


**FIG. 5. Inefficiency of the membrane translocation of the C terminus of PS1 when fused with growth hormone.** The plasmids encoding three different PS1-GH fusion proteins (PS1-ΔH10-C-GH, PS1-ΔC-GH, and PS1-full-GH) were transcribed and translated in the presence (ER+) or absence (ER-) of microsomal membrane as described in Fig. 2. A portion of each was further proteinase K-treated and immunoprecipitated with the polyclonal antibody GH-1 specific for new growth hormone (PK+ and IP+). Radiolabeled proteins were separated by SDS-PAGE and detected fluorographically. Positions for unglycosylated or glycosylated proteins are indicated by closed arrowheads on the left or right of each panel, respectively. Positions for proteinase K-protected fragments in PS1-ΔC-GH are shown by open arrowheads on the right of the panel. The positions of prestained marker proteins (New England Biolabs) are indicated on the right of the fluorogram.

those from other groups (see "Discussion"). The mobility of PS1-ΔH7-C-LP to PS1-ΔH10-C-LP was not changed by the endoglycosidase H treatment. Expression of these proteins in CHO-K1 cells showed similar results (data not shown). The above results suggest strongly that the membrane topology of PS1 predicted from the *in vitro* experimental system faithfully reflects that in the living cell.

**CTF Expressed Separately Can Be Assembled into the Membrane in the Same Topology as in the case of Full-length PS1 Molecule**—It has been reported that PS1 and PS2 undergo processing into two fragments (N-terminal fragment and CTF) *in vivo* (36, 37). In order to determine the specific function of each of the two fragments, the separate expression of each fragment will be a powerful approach. However, when the results of such experiments are interpreted, especially in the case of CTF, it is important to know whether or not this portion expressed separately can be assembled into the membrane in the same topological structure as in the case of the full-length PS1 molecule. Moreover, the C-terminal portion of PS2 expressed alone has been shown to have the biological ability to suppress apoptosis in several experimental contexts (21, 22). So, we investigated this subject using a similar strategy to that adopted above for full-length PS1. We constructed a series of fusion genes in which the PS1 coding sequence starting at the 289th methionine, around which processing has been shown to occur (38), and ending at either of the points corresponding to PS1-ΔH8-C to PS1-ΔH10-C, PS1-ΔC, and PS1-full, was fused to LPase (PS1-CTF-ΔH8-C-LP to PS1-CTF-ΔH10-C-LP, PS1-CTF-ΔC-LP, and PS1-CTF-full-LP). These constructs were transcribed and translated *in vitro* in the presence of MS, and the translation products were examined for protection against proteinase K and for *N*-linked glycosylation. The results unambiguously showed that only for the translation products of

PS1-CTF-ΔC-LP and PS1-CTF-full-LP were the reporter portions proteinase K-resistant and *N*-glycosylated (Fig. 7, A and B). These results are in accord with those obtained in the experiments involving the constructs starting at the authentic initiation codon and indicate that CTF expressed alone can be assembled into the membrane in the same membrane topology as the corresponding portion of the full-length PS1 molecule.

**The Ninth Hydrophobic Segment of PS1 Is Embedded in the Membrane without Spanning It**—Although the above *in vitro* and *in vivo* experiments suggested that HR8 and HR9 do not span the membrane and are located on the cytosolic face of the membrane, whether or not they interact with the membrane remains unclear. The above results indicating that the CTF portion can be assembled into the ER membrane in the same topological structure as in the case of the full-length PS1 encouraged us to examine this issue in detail, because analysis of the interaction of these segments with the membrane would be much simpler in the absence of HR1 to HR7.

First, we examined the interaction of the CTF of PS1 with the membrane *in vivo* using a homogenate of human placenta by testing the extractability with sodium carbonate, which is known to deplete the membrane of peripherally bound proteins but not integral ones (39). The supernatant and pellet fractions of the human placenta homogenate after sodium carbonate treatment were analyzed by Western blotting for CTF using LOOP1, which recognizes the loop region between HR7 and HR8 of mouse and human PS1. This antibody detected three polypeptides with apparent molecular masses of about 21, 24, and 51 kDa, respectively. The dominant 21-kDa band and the fainter 24-kDa band correspond to CTF, and the 51-kDa band corresponds to the full-length molecule. The 21- and 24-kDa bands may represent unphosphorylated and phosphorylated molecular species, respectively, as described recently (40, 41). These CTF polypeptides were not extracted with 0.1 M sodium carbonate, suggesting that some portion(s) of CTF is inserted into the lipid bilayer of the membrane *in vivo* (Fig. 8A), consistent with the idea that HR10 spans the membrane.

Next, in order to investigate the interaction of HR8 and HR9 with the membrane, we analyzed the extractability of the *in vitro* translation products for a series of CTF fusion constructs expressed in the presence of MS with either a neutral buffer (20 mM HEPES, pH 7.6, 0.25 M sucrose, 1 M NaCl), in the presence or absence of 1% Triton X-100, or 0.1 M sodium carbonate. In order to assess the interaction between HR8 and the membrane, PS1-CTF-ΔH9-C-LP containing only HR8 as a hydrophobic segment was examined. As shown in Fig. 8B (left panel), this translation product was extracted with either the neutral buffer (lanes 2 and 3) or sodium carbonate (lanes 4 and 5) mainly into the soluble fraction, indicating that there is little, if any, interaction between them. This result enabled us to assess the interaction between HR9 and the membrane by examining PS1-CTF-ΔH10-C-LP. Because the product of this construct contains HR8 and HR9 as hydrophobic regions and, as shown above, HR8 does not interact with the membrane, the results for this construct should reflect the interaction between HR9 and the membrane. As shown in Fig. 8B (middle panel), the product derived from this construct could not be extracted with either the neutral buffer in the absence of Triton X-100 (lanes 2 and 3) or sodium carbonate (lanes 4 and 5), suggesting strongly that HR9 interacts tightly with the membrane and is most likely embedded in the lipid bilayer. The product of PS1-CTF-ΔC-LP was partitioned into the pellet fraction either with the neutral buffer in the absence of Triton X-100 (lanes 2 and 3) or with sodium carbonate (lanes 4 and 5), consistent with the prediction that HR9 is embedded in the membrane and HR10 spans it. As an internal control, mRNA for PS1-ΔH6-C-LP

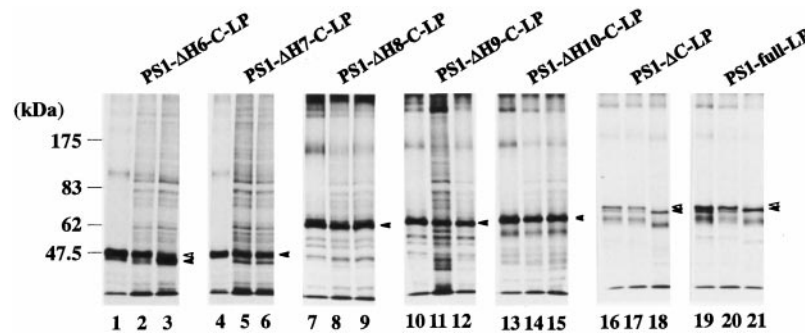


**FIG. 6. Fusion proteins expressed in cultured cells are capable of being assembled into the membrane with the same topology as those translated *in vitro*.** COS-1 cells were transfected with the indicated plasmids, and the newly synthesized proteins were isotopically labeled in the presence of [<sup>35</sup>S]methionine and [<sup>35</sup>S]cysteine for 4 h. After the cells have been washed twice with PBS(-), the proteins were extracted. The extract from each lot of transfected cells was divided into three parts. One of them was treated with endoglycosidase H and another one was treated with the enzyme reaction buffer only. These two samples together with the untreated sample were immunoprecipitated with LP-1 and then separated by SDS-PAGE on 7.5% gels. The <sup>35</sup>S-labeled proteins were detected by fluorography. All samples were exposed for 24 h except for PS1-ΔC-LP and PS1-full-LP, which were exposed for 4 days because the labeling efficiency was very low for these constructs. Lanes 1–3, PS1-ΔH6-C-LP; lanes 4–6, PS1-ΔH7-C-LP; lanes 7–9, PS1-ΔH8-C-LP; lanes 10–12, PS1-ΔH9-C-LP; lanes 13–15, PS1-ΔH10-C-LP; lanes 16–18, PS1-ΔC-LP; lanes 19–21, PS1-full-LP. Lanes 1, 4, 7, 10, 13, 16, and 19, untreated; lanes 2, 5, 8, 11, 14, 17, and 20, buffer-treated; lanes 3, 6, 9, 12, 15, 18, and 21, endoglycosidase H-treated. The positions of unglycosylated or glycosylated proteins are indicated by closed or open arrowheads on the right of each panel, respectively. The positions of prestained marker proteins (New England Biolabs) are indicated on the left of the fluorogram.

having five membrane-spanning hydrophobic segments was co-translated with each of the constructs used. As expected, the product of PS1-ΔH6-C-LP was partitioned mainly into the insoluble fraction with both sodium carbonate and the neutral buffer in the absence of the detergent. Taken together, these results suggest strongly that HR9 is embedded in the membrane with both of its flanking regions exposed to the cytosolic space (see Fig. 9 for our model).

#### DISCUSSION

Detailed knowledge of the membrane topological structures of presenilins is crucial for understanding their molecular functions in normal cells and in the pathogenesis of Alzheimer's disease. Earlier, based only on the information derived from the primary structures of presenilins, a seven membrane-spanning model, in which HR1 to HR6 and HR9 span the membrane, was proposed (5). Since then, based on at least some experimental results, several groups have proposed distinct topological models for these proteins (23–26, 40), although significant disagreement exists among these models, especially with regard to the C-terminal half portion. In this study, we addressed this controversial subject in detail using a series of fusion proteins in which C-terminally deleted PS1 is fused to a reporter protein. We expressed such fusion proteins either *in vitro* in the presence of the microsomal membrane (MS) or *in vivo* using cultured cells, and we determined the localization of the reporter portion by examining the N-glycosylation of this portion and its susceptibility to cytosolically added proteinase K. Based on the results of such experiments, together with several lines of evidence also described in this study, we here propose a novel model for the membrane topology of presenilins with a seven membrane-spanning and one membrane-embedded structure, as illustrated in Fig. 9A. According to this model, (a) the N-terminal region is located in the cytosolic space and the first six (HR1 to HR6) hydrophobic regions span the membrane in alternating directions; (b) HR7, HR8, and the large hydrophilic region between them are exposed to the cytosolic space; (c) HR9 does not span the membrane, but it is tightly associated with, most probably being embedded in, the lipid bilayer; and (d) HR10 spans the membrane and the C-terminal portion after this region is located in the luminal space.

The topology of the N-terminal half portion up to HR6 in our model is consistent with most of the others (24–26, 40), further confirming that the N terminus and the large hydrophilic loop

region between HR7 and HR8 are exposed to the cytosol and that HR1 to HR6 span the membrane. Although our results demonstrate that HR7 does not span the membrane and is localized on the cytosolic face, it is still unclear from our results whether or not a part of this portion is associated with the membrane, as in one of the models proposed by Doan *et al.* (24). Based on the accessibility of region-specific antibodies to presenilin molecules expressed on the surface of unfixed living DAMI cells, one group proposed that the N termini of cell surface presenilins are extracellular and that HR1 to HR6 span the membrane in opposite directions as compared with other models including ours (23). The reason for this discrepancy is unclear at present. Although it might be that presenilin molecules expressed on the cell surface show a distinct membrane topological structure from those retained on ER or ERGIC, it is also possible that some misassembled PS1 molecules with a non-physiologically inverted membrane topology caused by overexpression leak out onto the cell surface because their retention signal(s) to ER, ERGIC, or the Golgi apparatus cannot function correctly in this membrane topology.

Meanwhile, regarding the topological structure of the portion from HR8 to the C terminus of PS1 or its homolog, SEL-12, several different models have been proposed (24–26). First, according to our model, HR10 spans the membrane in the direction from the cytosol to the lumen, and the C terminus is exposed to the luminal space, whereas in all other models it is exposed to the cytosolic space. In some models (24, 26), HR10 is exposed to the cytosol, and in others (24), it spans the membrane in the opposite direction to that in our model. Although we cannot completely exclude the possibility that the LPase sequence we used as a reporter artificially enhanced the insertion of a naturally cytosolic HR10 segment into the membrane, or that it interferes with the stop transfer activity of HR10 non-physiologically, we think this is unlikely for the following reasons. First, in our fusion constructs LPase does not abolish the stop transfer ability of HR2, HR4, and HR6 when fused after them. Second, our three different reporter sequences, long and short versions of LPase with different N-terminal sequences and LPase with an extra membrane-spanning segment at the N-terminal end, gave consistent results. Third, when the N-glycosylation consensus sequence and hemagglutinin tag sequence were introduced into the extreme C-terminal region of

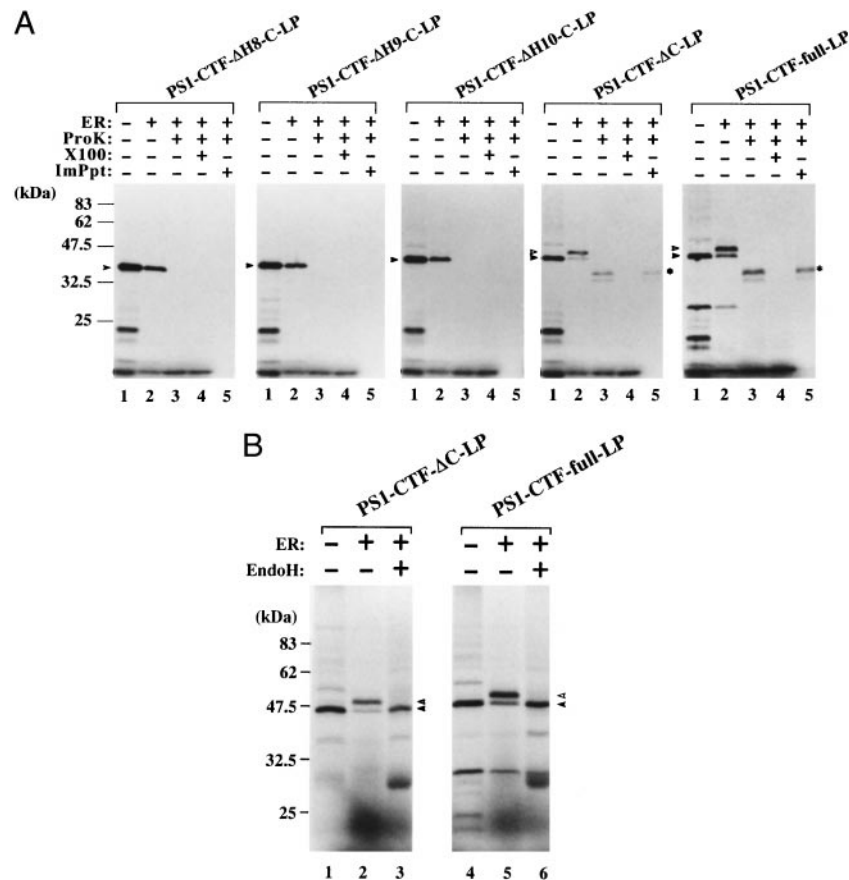


**FIG. 7. CTF separately expressed is assembled in the same membrane topology as in the case of full-length PS1.** *A*, plasmids encoding a series of fusion proteins starting from the 298th methionine of PS1 indicated on the top were transcribed and translated *in vitro* in the absence (lane 1 in each panel) or presence (lanes 2–5 in each panel) of MS. The translation products obtained in the presence of MS were treated with proteinase K in the absence (lanes 3 and 5 in each panel) or presence (lane 4 in each panel) of Triton X-100 (X100). A portion of the translation products in the absence of Triton X-100 was further immunoprecipitated with LP-1 to identify fragments containing the LPase region (lane 5 in each panel). Isotopically labeled proteins were detected as in Fig. 2. The positions of unglycosylated or glycosylated proteins are indicated by closed or open arrowheads on the left of each panel, respectively. Proteinase K-protected fragments containing the LPase region in PS1-CTF-ΔC-LP and PS1-CTF-full-LP are indicated by an asterisk on the right of each panel. The positions of prestained marker proteins (New England Biolabs) are indicated on the left of the fluorograms. *B*, the mobility of the translation products of PS1-CTF-ΔC-LP and PS1-CTF-full-LP observed in the presence of MS was due to *N*-type glycosylation: lanes 1 and 4, in the absence of MS; lanes 2 and 5, in the presence of MS; lanes 3 and 6, in the presence of MS with endoglycosidase H treatment. *In vitro* translation, endoglycosidase H treatment and detection of the translation products were carried out as in Fig. 4. The positions of unglycosylated or glycosylated proteins are indicated by closed or open arrowheads on the right of each panel, respectively. The positions of prestained marker proteins (New England Biolabs) are indicated on the left of the fluorograms.

PS1, such a protein still underwent *N*-glycosylation,<sup>2</sup> indicating that the luminal localization of the C-terminal portion of PS1 is not specific for the LPase fusion constructs we employed. Fourth, no previous study has demonstrated that a hydrophilic region interferes with the stop transfer activity or enhances the membrane anchoring ability of a preceding hydrophobic segment.

Some of the cytosolic C-terminal models are based on results obtained in experiments involving fusion proteins, as in this study. On the one hand, Lehmann *et al.* (25) constructed a series of fusion proteins in which C-terminally deleted PS1 is fused to a portion of prolactin with several artificial *N*-glycosylation consensus sequences at the C terminus, and the fusion proteins were expressed either in an *in vitro* translation system in the presence of the microsomal membrane or in cultured cells. Based on their observation that neither *N*-glycosylation in the reporter region nor protection of this region against cytosolically added proteinase K was detected when a chimera protein containing full-length PS1 was examined, they con-

cluded that the C terminus of PS1 is located in the cytosolic space. On the other hand, Li and Greenwald (26) expressed in *C. elegans* a series of C-terminally deleted SEL-12, the counterpart of presenilins in the worm, fused to  $\beta$ -galactosidase, and they examined  $\beta$ -galactosidase activity using 5-bromo-4-chloro-3-indoyl- $\beta$ -D-galactoside (X-Gal) staining *in situ*. They observed that the activity was observed when  $\beta$ -galactosidase was fused to the C-terminal portion of full-length SEL-12 and that it was lost when an additional artificial hydrophobic segment was inserted between SEL-12 and  $\beta$ -galactosidase. As it is empirically known that  $\beta$ -galactosidase activity is lost when it is translocated to the luminal face of the ER membrane, they concluded that the C terminus end of SEL-12 is exposed to the cytosolic space.

So, what is the cause for such discrepancies between our results and others? We think that the relatively hydrophobic nature of the C-terminal region of PS1 or SEL-12 could lead to artificial results unless care is taken when choosing the reporter protein to be fused. In fact, nine or eight out of 16 amino acid residues of the C-terminal region after HR10 of human PS1 or SEL-12, respectively, are hydrophobic. Although this

<sup>2</sup> T. Nakai and S. Miura, unpublished results.

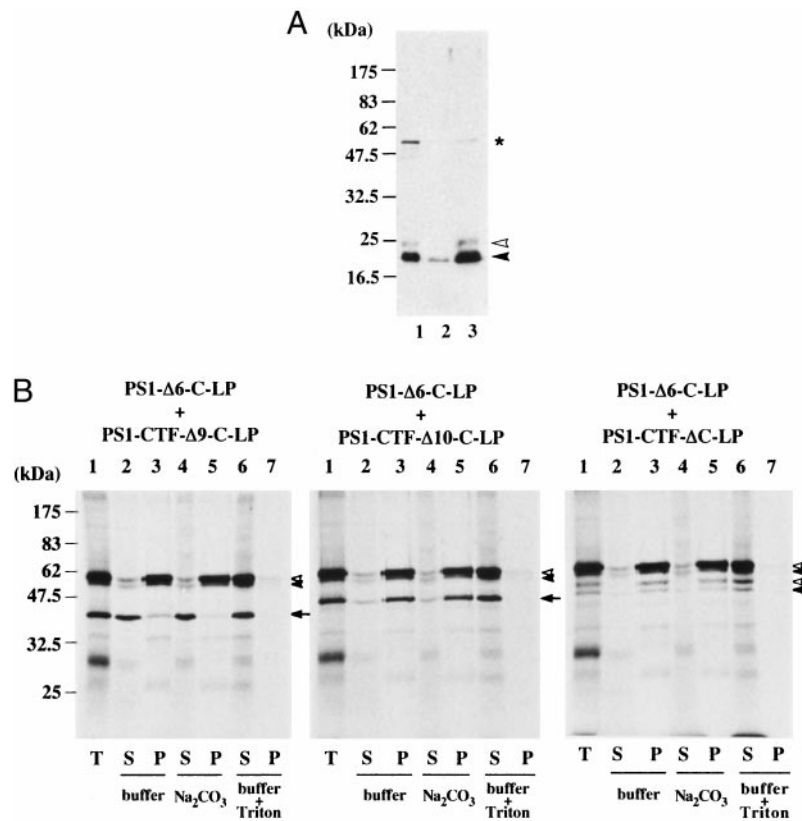


**FIG. 8. Interaction of HR8 and HR9 with the membrane.** *A*, a 100,000  $\times g$  membrane fraction of the human placenta homogenate was prepared and suspended in 0.1 M sodium carbonate as described under "Materials and Methods." A portion was fractionated by centrifugation at 100,000  $\times g$ . Each fraction was analyzed for the presence of PS1-CTF by SDS-PAGE and Western blotting with a polyclonal antibody; PS1-LOOP: *lane 1*, total membrane fraction before sodium carbonate extraction; *lanes 2 and 3*, supernatant and pellet fractions, respectively, obtained on 100,000  $\times g$  centrifugation after sodium carbonate extraction. The positions of CTF are indicated by *closed or open arrowhead* on the right of the panel. The *upper bands (open arrowhead)* may represent a phosphorylated molecular species. The full-length form is indicated by an *asterisk* on the right of the panel. The positions of prestained marker proteins (New England Biolabs) are indicated on the left of the fluorograms. *B*, PS1-CTF- $\Delta$ H9-C-LP, PS1-CTF- $\Delta$ H10-C-LP, and PS1-CTF- $\Delta$ C-LP were transcribed and translated *in vitro* as in Fig. 3 together with PS1- $\Delta$ H6-C-LP as an internal control in the presence of MS. Each sample was divided into four parts, three of which were extracted with solutions containing the following reagents: *lanes 2 and 3*, 20 mM HEPES, pH 7.6, 0.25 M sucrose, 1 M NaCl (buffer); *lanes 4 and 5*, 0.1 M  $\text{Na}_2\text{CO}_3$  ( $\text{Na}_2\text{CO}_3$ ); *lanes 6 and 7*, 20 mM HEPES, pH 7.6, 0.25 M sucrose, 1% Triton X-100 (buffer + Triton), for each panel, respectively. After centrifugation at 100,000  $\times g$  for 1 h, the supernatants (*S*, *lanes 2, 4, and 6*) and pellets (*P*, *lanes 3, 5, and 7*) were separated by SDS-PAGE together with total unextracted samples (*T*, *lane 1*), and labeled proteins were detected by fluorography. The positions of glycosylated or unglycosylated translation products for PS1-CTF- $\Delta$ H9-C-LP, PS1-CTF- $\Delta$ H10-C-LP, and PS1-CTF- $\Delta$ C-LP (*open or closed arrows*, respectively) as well as the doublet bands for glycosylated and unglycosylated translation products of PS1- $\Delta$ H6-C-LP (*open and closed arrowheads*, respectively) are indicated. The positions of prestained marker proteins (New England Biolabs) are indicated on the left of the fluorograms.

region is not hydrophobic enough to constitute solely a membrane-spanning stop-transfer segment, it could create a new additional artificial membrane-spanning segment when it is fused to a protein with a short hydrophobic region at its N-terminal end, which is not hydrophobic enough to have membrane-spanning ability itself. In such a case, the reporter region would be exposed to the cytosolic space despite the luminal localization of the free C-terminal end of these proteins. To prevent this, care was especially taken not to use a reporter sequence with an N terminus of a hydrophobic nature. Indeed, hydropathy analysis of the amino acid sequence around the junction point of the PS1-prolactin fusion protein expected from the construction in the literature (25) revealed an additional hydrophobic segment which could span the membrane (data not shown), although we could not examine the case of SEL-12 because of a lack of precise sequence information regarding the fusion constructs in their report. Such a possibility will be tested by examining constructs in which the reporter portion is fused to PS1 or SEL-12 just after HR10, like in our PS1- $\Delta$ C-LP. If our prediction is correct, such experiments should provide results consistent with the translocation of the reporter portion to the luminal space for such constructs because the C-terminal hydrophobic portion after HR10 is eliminated in this case.

Supporting this view, we actually observed that *N*-glycosylation of the reporter portion or protection against proteinase K was very inefficient when the whole PS1 was fused to a portion of newt GH, whose N terminus is relatively hydrophobic (Fig. 5, *right*). In contrast, when a fusion construct of PS1- $\Delta$ C, in which the C-terminal portion of PS1 after HR10 was lacking, and GH were used, the two indices for membrane translocation were clearly positive (Fig. 5, *middle*). These results suggest that the extreme C-terminal portion of PS1 after HR10 became an additional eighth membrane-spanning segment when fused to GH. In the case of SEL-12, an alternative possibility that its C-terminal membrane topological structure is different from those of mammalian presenilins cannot be excluded.

Another line of experimental evidence for the cytosolic localization of the C terminus is the accessibility of antibodies specific to the C-terminal region of PS1 from the cytosolic space in cultured cells. Doan *et al.* (24) observed positive staining of intracellular structures when CHO cells or N2a cells overexpressing PS1 were probed with anti-C-terminal-specific polyclonal antibodies after treatment with streptolysin O, which is known to permeabilize specifically the plasma membrane without disrupting the membranes of intracellular organelles. Under such conditions, extracellularly added antibody molecules

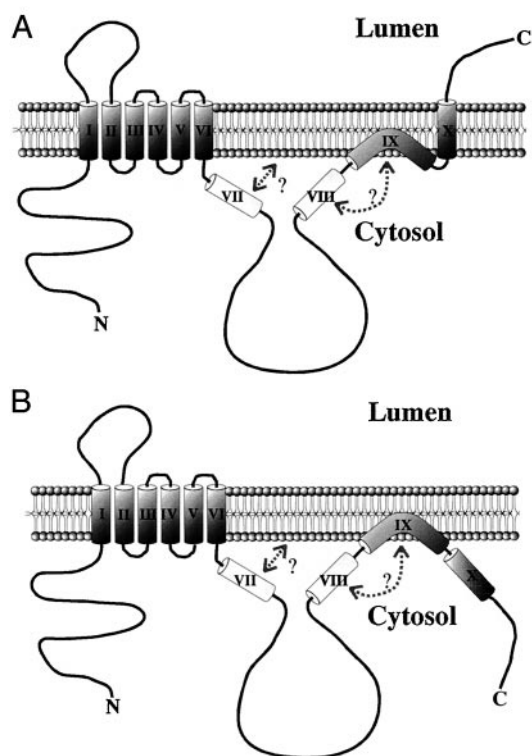


**FIG. 9. Seven spanning and one embedded model for the membrane topology of PS1.** *A*, a schematic drawing of the seven membrane-spanning and one membrane-embedded structure for the PS1 topology is depicted. This model has several novel features as follows. (*a*) The N-terminal end is localized in the cytosolic space. (*b*) Hydrophobic segments HR1 to HR6 span the membrane in alternative directions, respectively. (*c*) HR7, HR8, and large hydrophilic loop between them are located in the cytosolic space. (*d*) HR9 is tightly bound to the membrane, most likely being embedded in the lipid bilayer, without spanning it. (*e*) HR10 spans the membrane from the cytosol to the lumen. (*f*) The C-terminal portion after HR10 is exposed to the luminal space. Our results suggest that interaction between HR8 and the membrane is very weak, if any. It is possible that HR8 interacts with HR9 for the formation of the membrane topological structure of the latter segment as indicated (see the text). HR7 can interact with the lipid bilayer as depicted in the drawing, although we have no experimental evidence for this at present. *B*, it is also possible that a molecular species in which HR10 and a more C-terminal region is localized in the cytosolic space co-exists physiologically together with the species with the novel structure as indicated in *A*, although our data imply that the latter species with the seven membrane-spanning and one membrane-embedded structure is predominant. Furthermore, the intriguing possibility exists that the two species are interchangeable post-translationally in response to some physiological signals (see the text).

can diffuse into the cytosol through the plasma membrane but are not expected to go into the luminal space of intracellular organelles. Based on these observations, they concluded that the C terminus is exposed to the cytosolic space. However, in our view, although these data show the existence of PS1 molecules with the C terminus exposed to the cytosol in PS1-overexpressing cultured cells, they do not logically exclude the possibility of the existence of a molecular species whose C terminus is topologically exposed to the luminal space. So, we think it is highly possible that two topologically distinct molecular species co-exist in these cells. Supporting this possibility, when the PS1-LPase fusion protein was expressed transiently in COS-1 cells, we occasionally observed, in addition to a predominant band corresponding to the *N*-glycosylated form, a minor band corresponding to the unglycosylated form (for example, see Fig. 6, lanes 16–21). The latter may represent those that failed to translocate the C-terminal end of PS1, together with the reporter portion, to the luminal space and may corre-

spond to the molecular species that Doan *et al.* (24) observed.

The molecular species of PS1 with the C-terminal region facing the cytosol might be an artifact of overexpression. In fact, although Doan *et al.* (24) also examined stably transfected cell lines, these lines may still overexpress PS1 when compared with cells expressing endogenous PS1. An alternative interpretation would be that both topological species exist physiologically. They might have distinct functions, as suggested for several other proteins (42–45). For example, the C-terminal region might interact with distinct cellular factors in the cytosol and luminal space of ER. Alternatively, cells might regulate the ratio of these two forms dynamically in a post-translational manner by actively translocating the C-terminal region to and fro across the membrane in response to some signals. For example, upon processing or interaction with other factor(s), one of the forms will be converted to the other. In fact, a protein exhibiting a change in its topology post-translationally has been recently reported (46). In this regard, it will be important to determine whether or not presenilins with the C terminus exposed to the cytosol can also be observed in cells physiologically without overexpressing them and to search for cytosolic or luminal factors interacting with the C terminus of PS1.

It is also an arguable point as to whether or not HR9 spans the membrane. Our results suggest strongly that this segment does not span the membrane, which is consistent with the results of Lehman *et al.* (25). Consistent results obtained with two different fusion strategies reinforce this idea and make it unlikely that this is caused by an unusual property of the reporter protein fused after this segment. Furthermore, we also showed that, at least when the C-terminal half region of PS1 from the 298th methionine is expressed separately, HR9 interacts with the membrane tightly. The *N*-glycosylation and proteinase K protection patterns of the fusion proteins starting from two different residues, the 1st and 298th methionines, suggest strongly that, in the full-length PS1, HR9 is also inserted into the lipid bilayer without spanning the membrane. Previously, similar structures have been implicated to exist in several polytopic membrane proteins such as subunits of several ion channels including glutamate receptors (47–49). Additionally, a glycine residue (Gly-417) is present at approximately the center of HR9. As a glycine residue is known to tend to form a turn in the secondary structure of a polypeptide (50), it is possible that HR9 forms a bending structure in the lipid bilayer which prevents it from spanning the membrane and facilitates the embedded topological structure, as illustrated in Fig. 9.

On the contrary, the experimental evidence in the literature supporting the membrane spanning of HR9 seems to be weak. On the one hand, Li and Greenwald (26) examined the activity of  $\beta$ -galactosidase as a reporter protein, which was fused after HR9 of SEL-12, and detected such activity, implying that the C-terminal flanking region of HR9 is exposed to the cytosol. In order to determine the location of the region between HR8 and HR9, they examined the activity of  $\beta$ -galactosidase when this enzyme was fused after HR8 or after an artificial extra membrane-spanning segment which was placed just after HR8, but no activity was detected for either of the fusion proteins. So, they further examined similar chimera proteins in which HR8 was deleted and detected such activity only in the presence of the artificial membrane-spanning segment. From this result, they argued that HR9 spans the membrane. However, although this result implies that HR9 could span the membrane from the cytosol to the lumen of ER in some situations, it does not necessarily prove that HR9 spans the membrane from the lumen to the cytosol as in their model. Their result implies that

HR9 spans the membrane from the cytosol to the luminal space, which apparently contradicts our model. One interpretation explaining this would be that some of the missing sequence in their HR8-deleted construct is required for the correct topogenesis of HR9. For example, the whole HR8 region or a part of it might be needed for such an embedded structure of HR9 through its direct interaction with HR9. Another possibility would be that the newly exposed flanking sequence before HR9 in the HR8-deleted construct perturbed the topogenesis of HR9. We are now examining such possibilities. On the other hand, Doan *et al.* (24) proposed two possible models in which both HR9 and HR10 span the membrane. However, no description of the experimental evidence for such a topological structure of these segments could be found in their report.

As to HR8, our results suggest that it does not span the membrane. With PS1-ΔH9-C-LP as well as with PS1-CTF-ΔH9-C-LP, in which the reporter LPase was fused just after HR8, neither *N*-glycosylated nor proteinase K-protected LPase was observed in contrast to the case of PS1-ΔH9-C-TM-LP, where the two criteria for the translocation were clearly positive. Moreover, the results of sodium carbonate extraction experiments with PS1-CTF-ΔH9-C-LP strongly suggested that there is no physical interaction between HR8 and the membrane. On the contrary, Li and Greenwald (27) claimed that HR8 spans the membrane based on the observation that deletion of this segment of PS1 or SEL-12 (26) changes the localization of β-galactosidase fused after HR9 from the cytosol to the lumen. However, as discussed above, these results can also be explained by our model assuming that the N-terminal flanking region of HR9 affects its topology. More recently, in experiments involving an altered HR8 made more hydrophobic by the addition of some hydrophobic amino acid residues, the same group obtained results suggesting that this altered HR8 spans the membrane from the cytosol to the lumen (27). However, based on our results, we consider it highly likely that their results are artifacts caused by the alteration of HR8. Although they also showed that SEL-12 with this altered HR8 exhibits complementing ability as to the egg-laying defect of the SEL-12 mutant worm, it is also possible that whether or not HR8 spans the membrane is not important for the complementing activity of SEL-12.

To summarize, in this study, we obtained evidence for the existence of PS1 molecules with a seven membrane-spanning and one membrane-embedded topology, in which tight binding of HR9 to the membrane without spanning it, membrane spanning of HR10 from the cytosolic to the luminal face, and luminal localization of the C terminus are novel features. Further study is necessary to elucidate the biological meaning of these structural aspects. For example, exposure of the C terminus to the luminal space might be essential for this protein to undergo proper processing, which is known to occur normally in the cell, or for a specific interaction of this protein with an unknown cellular factor localized to the lumen of ER or the Golgi apparatus. Experiments are underway to assess these possibilities.

**Acknowledgments**—We thank Prof. S. Kikuyama (Waseda University) for the generous gift of newt GH cDNA and Dr. K. Kamijo (Shinsyu University) and Dr. T. Tsukamoto (Himeji Institute of Technology) for kindly providing COS-1 cells and CHO-K1 cells, respectively. We also thank Nicholas J. Halewood for assistance with preparation of the manuscript.

## REFERENCES

- Levy-Lahad, E., Wasco, W., Poorkaj, P., Romano, D. M., Oshima, J., Pettingell, W. H., Yu, C., Jondro, P. D., Schmidt, S. D., Wang, K., Crowley, A. C., Fu, Y.-H., Guenette, S. Y., Galas, D., Nemens, E., Wijsman, E. M., Bird, T. D., Schellenberg, G. D., and Tanzi, R. E. (1995) *Science* **269**, 973–977
- Levy-Lahad, E., Wijsman, E. M., Nemens, E., Anderson, L., Goddard, K. A., Weber, J. L., Bird, T. D., and Schellenberg, G. D. (1995) *Science* **269**, 970–973
- Rogaev, E. I., Sherrington, R., Rogaeva, E. A., Levesque, G., Ikeda, M., Liang, Y., Chi, H., Lin, C., Holman, K., Tsuda, T., Mar, L., Sorbi, S., Nacmias, B., Piacentini, S., Amaducci, L., Chumakov, I., Cohen, D., Lannfelt, L., Fraser, P. E., Rommens, J. M., and St. George-Hyslop, P. H. (1995) *Nature* **376**, 775–778
- Li, J., Ma, J., and Potter, H. (1995) *Proc. Natl. Acad. Sci. U. S. A.* **92**, 12180–12184
- Sherrington, R., Rogaev, E. I., Liang, Y., Rogaeva, E. A., Levesque, G., Ikeda, M., Chi, H., Lin, C., Li, G., Holman, K., Tsuda, T., Mar, L., Foncin, J.-F., Bruni, A. C., Montesi, M. P., Sorbi, S., Rainero, I., Pinessi, L., Nee, L., Chumakov, I., Pollen, D., Brookes, A., Sanseau, P., Polinsky, R. J., Wasco, W., Da Silva, H. A., Haines, J. L., Pericak-Vance, M. A., Tanzi, R. E., Roses, A. D., Fraser, P. E., Rommens, J. M., and St. George-Hyslop, P. H. (1995) *Nature* **375**, 754–760
- Culvenor, J. G., Maher, F., Evin, G., Malchiodi-Albedi, F., Cappai, R., Underwood, J. R., Davis, J. B., Karran, E. H., Roberts, G. W., Beyreuther, K., and Masters, C. L. (1997) *J. Neurosci. Res.* **49**, 719–731
- Kovacs, D. M., Fausett, H. J., Page, K. J., Kim, T.-W., Moir, R. D., Merriam, D. E., Hollister, R. D., Hallmark, O. G., Mancini, R., Felsenstein, K. M., Hyman, B. T., Tanzi, R. E., and Wasco, W. (1996) *Nat. Med.* **2**, 224–229
- Lah, J. J., Heilman, C. J., Nash, N. R., Rees, H. D., Yi, H., Counts, S. E., and Levey, A. I. (1997) *J. Neurosci.* **17**, 1971–1980
- Takashima, A., Sato, M., Mercken, M., Tanaka, S., Kondo, S., Honda, T., Sato, K., Murayama, M., Noguchi, K., Nakazato, Y., and Takahashi, H. (1996) *Biochem. Biophys. Res. Commun.* **227**, 423–426
- Dewji, N. N., and Singer, S. J. (1997) *Proc. Natl. Acad. Sci. U. S. A.* **94**, 9926–9931
- Levitan, D., and Greenwald, I. (1995) *Nature* **377**, 351–354
- Shen, J., Bronson, R. T., Chen, D. F., Xia, W., Selkoe, D. J., and Tonegawa, S. (1997) *Cell* **89**, 629–639
- Wong, P. C., Zheng, H., Chen, H., Becher, M. W., Sirinathsinghji, D. J., Trumbauer, M. E., Chen, H. Y., Price, D. L., Van der Ploeg, L. H., and Sisodia, S. S. (1997) *Nature* **387**, 288–292
- Borchelt, D. R., Thinakaran, G., Eckman, C. B., Lee, M. K., Davenport, F., Ratovitsky, T., Prada, C. M., Kim, G., Seekins, S., Yager, D., Slunt, H. H., Wang, R., Seeger, M., Levey, A. I., Gandy, S. E., Copeland, N. G., Jenkins, N. A., Price, D. L., Younkin, S. G., and Sisodia, S. S. (1996) *Neuron* **17**, 1005–1013
- Citron, M., Westaway, D., Xia, W., Carlson, G., Diehl, T., Levesque, G., Johnson-Wood, K., Lee, M., Seubert, P., Davis, A., Kholodenko, D., Motter, R., Sherrington, R., Perry, B., Yao, H., Strome, R., Lieberburg, I., Rommens, J., Kim, S., Schenk, D., Fraser, P., St. George-Hyslop, P., and Selkoe, D. J. (1997) *Nat. Med.* **3**, 67–72
- Scheuner, D., Eckman, C., Jensen, M., Song, X., Citron, M., Suzuki, N., Bird, T. D., Hardy, J., Hutton, M., Kukull, W., Larson, E., Levy-Lahad, E., Viitanen, M., Peskind, E., Poorkaj, P., Schellenberg, G., Tanzi, R., Wasco, W., Lannfelt, L., Selkoe, D., and Younkin, S. (1996) *Nat. Med.* **2**, 864–870
- Xia, W., Zhang, J., Kholodenko, D., Citron, M., Podlisny, M. B., Teplow, D. B., Haass, C., Seubert, P., Koo, E. H., and Selkoe, D. J. (1997) *J. Biol. Chem.* **272**, 7977–7982
- De Strooper, B., Saftig, P., Craessaerts, K., Vanderstichele, H., Gahde, G., Annaert, W., Von Figura, K., and Van Leuven, F. (1998) *Neuron* **39**, 387–390
- Guo, Q., Furukawa, K., Sopher, B. L., Pham, D. G., Xie, J., Robinson, N., Martin, G. M., and Mattson, M. P. (1996) *Neuroreport* **8**, 379–383
- Janicki, S., and Monteiro, M. J. (1997) *J. Cell Biol.* **139**, 485–495
- Vito, P., Lacana, E., and D'Adamo, L. (1996) *Science* **271**, 521–525
- Wolozin, B., Iwasaki, K., Vito, P., Ganjei, J. K., Lacana, E., Sunderland, T., Zhao, B., Kusiak, J. W., Wasco, W., and D'Adamo, L. (1996) *Science* **274**, 1710–1713
- Dewji, N. N., and Singer, S. J. (1997b) *Proc. Natl. Acad. Sci. U. S. A.* **94**, 14025–14030
- Doan, A., Thinakaran, G., Borchelt, D. R., Slunt, H. H., Ratovitsky, T., Podlisny, M., Selkoe, D. J., Seeger, M., Gandy, S. E., Price, D. L., and Sisodia, S. S. (1996) *Neuron* **17**, 1023–1030
- Lehmann, S., Chiesa, R., and Harris, D. A. (1997) *J. Biol. Chem.* **272**, 12047–12051
- Li, X., and Greenwald, I. (1996) *Neuron* **17**, 1015–1021
- Li, X., and Greenwald, I. (1998) *Proc. Natl. Acad. Sci. U. S. A.* **95**, 7109–7114
- Dalbey, R. E., and Wickner, W. (1985) *J. Biol. Chem.* **260**, 15925–15931
- Yamamoto, K., Takahashi, N., Shioda, A., Kobayashi, T., Nakai, T., Miura, S., Kouki, T., and Kikuyama, S. (1997) *Adv. Comp. Endocrinol.* **2**, 921–925
- Laemmli, U. K. (1970) *Nature* **227**, 680–685
- Mori, M., Miura, S., Tatibana, M., and Cohen, P. P. (1980) *J. Biochem. (Tokyo)* **88**, 1829–1836
- Walter, P., Ibrahim, I., and Blobel, G. (1981) *J. Cell Biol.* **91**, 545–550
- Wessels, H. P., and Spiess, M. (1988) *Cell* **55**, 61–70
- Moore, K. E., and Miura, S. (1987) *J. Biol. Chem.* **262**, 8806–8813
- Johansson, M., Nilsson, I., and von Heijne, G. (1993) *Mol. Gen. Genet.* **239**, 251–256
- Mercken, M., Takahashi, H., Honda, T., Sato, K., Murayama, M., Nakazato, Y., Noguchi, K., Imahori, K., and Takahashi, A. (1996) *FEBS Lett.* **389**, 297–303
- Thinakaran, G., Borchelt, D. R., Lee, M. K., Slunt, H. H., Spitzer, L., Kim, G., Ratovitsky, T., Davenport, F., Nordstedt, C., Seeger, M., Hardy, J., Levey, A. I., Gandy, S. E., Jenkins, N. A., Copeland, N. G., Price, D. L., and Sisodia, S. S. (1996) *Neuron* **17**, 181–190
- Podlisny, M. B., Citron, M., Amarante, P., Sherrington, R., Xia, W., Zhang, J., Diehl, T., Levesque, G., Fraser, P., Haass, C., Koo, E. H., Seubert, P., St. George-Hyslop, P., Teplow, D. B., and Selkoe, D. J. (1997) *Neurobiol. Dis.* **3**, 325–337
- Fujiki, Y., Hubbard, A. L., Fowler, S., and Lazarow, P. B. (1982) *J. Cell Biol.*

- 93, 97–102
40. De Strooper, B., Beullens, M., Contreras, B., Levesque, L., Craessaerts, K., Cordell, B., Moechars, D., Bollen, M., Fraser, P., St. George-Hyslop, P. H., and Van Leuven, F. (1997) *J. Biol. Chem.* **272**, 3590–3598
41. Walter, J., Grunberg, J., Capell, A., Pesold, B., Schindzielorz, A., Citron, M., Menda, K., St. George-Hyslop, P., Multhaup, G., Selkoe, D. J., and Haass, C. (1997) *Proc. Natl. Acad. Sci. U. S. A.* **94**, 5349–5354
42. Dunlop, J., Jones, P. C., and Finbow, M. E. (1995) *EMBO J.* **14**, 3609–3616
43. Finbow, M. E., Goodwin, S. F., Meagher, L., Lane, N. J., Keen, J., Findlay, J. B., and Kaiser, K. (1994) *J. Cell Sci.* **107**, 1817–1824
44. Lopez, C. D., Yost, C. S., Prusiner, S. B., Myers, R. M., and Lingappa, V. R. (1990) *Science* **248**, 226–229
45. Yost, C. S., Lopez, C. D., Prusiner, S. B., Myers, R. M., and Lingappa, V. R. (1990) *Nature* **343**, 669–672
46. Nishiyama, K., Suzuki, T., and Tokuda, H. (1996) *Cell* **85**, 71–81
47. MacKinnon, R. (1995) *Neuron* **14**, 889–892
48. Hallmann M., Maron, C., and Heinemann, S. (1994) *Neuron* **13**, 1331–1343
49. Bennett, J. A., and Dingleline, R. (1995) *Neuron* **14**, 373–384
50. Venkatachalam, C. M. (1968) *Biopolymers* **6**, 1425–1436
51. Kyte, J., and Doolittle, R. F. (1982) *J. Mol. Biol.* **157**, 105–132

## PEN-2 Is an Integral Component of the $\gamma$ -Secretase Complex Required for Coordinated Expression of Presenilin and Nicastrin\*

Received for publication, August 19, 2002,  
and in revised form, August 26, 2002  
Published, JBC Papers in Press, August 26, 2002,  
DOI 10.1074/jbc.C200469200

Harald Steiner<sup>‡§</sup>, Edith Winkler<sup>‡</sup>,  
Dieter Edbauer<sup>‡</sup>, Stefan Prokop<sup>‡</sup>,  
Gabriele Basset<sup>‡</sup>, Aya Yamasaki<sup>‡</sup>,  
Marcus Kostka<sup>¶</sup>, and Christian Haass<sup>‡||</sup>

From the <sup>‡</sup>Adolf-Butenandt-Institute, Department of Biochemistry, Laboratory for Alzheimer's and Parkinson's Disease Research, Schillerstrasse 44, Ludwig-Maximilians-University, 80336 Munich, Germany and <sup>¶</sup>Boehringer Ingelheim Pharma KG, Department of CNS Research, Birkendorferstrasse 65, 88397 Biberach/Riss, Germany

**The Alzheimer disease-associated presenilin (PS) proteins apparently provide the active site of  $\gamma$ -secretase, an unusual intramembrane-cleaving aspartyl protease. PSs principally occur as high molecular weight protein complexes that contain nicastrin (Nct) and additional so far unidentified components. Recently, PEN-2 has been implicated in  $\gamma$ -secretase function. Here we identify PEN-2 as a critical component of PS1/ $\gamma$ -secretase and PS2/ $\gamma$ -secretase complexes. Strikingly, in the absence of PS1 and PS1/PS2, PEN-2 levels are strongly reduced. Similarly, PEN-2 levels are reduced upon RNA interference-mediated down-regulation of Nct. On the other side, down-regulation of PEN-2 by RNA interference is associated with reduced PS levels, impaired Nct maturation, and deficient  $\gamma$ -secretase complex formation. We conclude that PEN-2 is an integral  $\gamma$ -secretase complex component and that  $\gamma$ -secretase complex components are expressed in a coordinated manner.**

The Alzheimer disease-associated polytopic membrane proteins presenilin 1 (PS1)<sup>1</sup> and presenilin 2 (PS2) are required for the intramembraneous  $\gamma$ -secretase cleavage of the  $\beta$ -amyloid precursor protein (APP) (1). Following an initial cleavage by  $\beta$ -secretase within the APP ectodomain,  $\gamma$ -secretase cleavage

releases the 40–42-amino acid amyloid  $\beta$ -peptide (A $\beta$ ) from the membrane (1). The majority of familial Alzheimer disease cases are associated with mutations in the PS1 gene (1). Apparently all PS1 mutations investigated cause an increased generation of the highly amyloidogenic A $\beta$ 42 (1). Absence of PS1 reduces  $\gamma$ -secretase activity (2, 3) and absence of PS1/PS2 eliminates  $\gamma$ -secretase function completely (4, 5). Mounting evidence suggests that PSs are unusual aspartyl proteases with  $\gamma$ -secretase activity (6). All PSs contain two aspartates within transmembrane domains 6 and 7 that are critically required for  $\gamma$ -secretase activity (7, 8). Moreover,  $\gamma$ -secretase inhibitors designed to mimic the transition state of the catalytic mechanism of aspartyl proteases can be covalently cross-linked to PSs (9, 10). Finally, PSs are apparently members of a group of polytopic membrane-bound aspartyl proteases that are all characterized by a GXGD (X = variable amino acid) signature motif in which the C-terminal active site aspartate is embedded (11). Besides the PSs, the bacterial type 4 prepilin peptidases (11, 12) and signal peptide peptidase and its related proteins carry this signature motif (13, 14).

The PSs reside in high molecular weight complexes (15–18). An integral component of these high molecular weight complexes is the membrane glycoprotein nicastrin (Nct) (18–20). Down-regulation of Nct in cultured mammalian or *Drosophila* cells inhibits  $\gamma$ -secretase cleavage of APP (18, 21) and site 3 (S3) cleavage of Notch (21) and reduces PS levels (18, 21, 22). On the other side, absence of PS1 and PS1/PS2 causes a strong inhibition of Nct maturation (18, 23).

PSs are not only required for the  $\gamma$ -secretase-mediated processing of APP but also for intramembrane proteolysis of several other type I transmembrane proteins including the Notch cell surface receptors that are critically required for cell fate decisions (24). Notch signaling depends on the PS-dependent S3 cleavage of Notch that leads to the liberation of the Notch intracellular domain (NICD) from the membrane (24). NICD translocates to the nucleus where it is involved in the transcription of target genes (24). Genetic screening in *Caenorhabditis elegans* led to the identification of novel components, APH-1 and PEN-2, that are required for  $\gamma$ -secretase activity in APP and Notch S3 cleavage (21, 25). The function of APH-1 and PEN-2 is currently unclear. Apparently, APH-1 and PEN-2 could either be transiently required for the assembly of the  $\gamma$ -secretase complex or may even be novel *bona fide* complex components required for  $\gamma$ -secretase activity (21). Here we investigated whether PEN-2 is an integral  $\gamma$ -secretase complex component.

### EXPERIMENTAL PROCEDURES

**Antibodies**—The polyclonal antibody 1638 was raised to the N terminus (residues 4–15) of human PEN-2 (21). The polyclonal and monoclonal antibodies against the PS1 C terminus (3027 and BI.3D7) (26) and N terminus (2953) (27) and against the PS2 C terminus (3711 and BI.HF5c) (26) and N terminus (2972) (28) were described. The polyclonal antibody N1660 against the C terminus (residues 693–709) of Nct was obtained from Sigma. The anti-Xpress antibody was obtained from Invitrogen.

**cDNA Constructs and Transfections**—N-terminally hexahistidine-Xpress (H<sub>6</sub>X)-epitope-tagged PS1, PS1  $\Delta$ exon9, and PS2 variants were generated by cloning the respective cDNAs into pcDNA4/HisC expression vector (Invitrogen) and stably transfected into human embryonic kidney 293 (HEK 293) stably expressing Swedish mutant APP (swAPP) (29).

\* This work was supported by the Deutsche Forschungsgemeinschaft (Priority program "Cellular Mechanisms of Alzheimer's Disease") and the National Genome Research Network (NGFN). The costs of publication of this article were defrayed in part by the payment of page charges. This article must therefore be hereby marked "advertisement" in accordance with 18 U.S.C. Section 1734 solely to indicate this fact.

§ To whom correspondence may be addressed. Tel.: 49-89-5996-480; Fax: 49-89-5996-415; E-mail: hsteiner@pbm.med.uni-muenchen.de.

|| To whom correspondence may be addressed. Tel.: 49-89-5996-471/472; Fax: 49-89-5996-415; E-mail: chaass@pbm.med.uni-muenchen.de.

<sup>1</sup> The abbreviations used are: PS, presenilin; A $\beta$ , amyloid  $\beta$ -peptide; APP,  $\beta$ -amyloid precursor protein; swAPP, Swedish mutant APP; RNAi, RNA interference; Nct, nicastrin; NICD, Notch intracellular domain; PEN-2, presenilin enhancer 2; DDM, *n*-dodecyl  $\beta$ -D-maltoside; siRNA, small interfering RNA.

**Cell Culture, Cell Lines, RNA Interference (RNAi), and Protein Analysis**—HEK 293 stably expressing swAPP and mouse embryonic fibroblast cells derived from PS knock-out or littermate control mice (30) were cultured as described (18). To inhibit expression of PEN-2 and Nct by RNAi, HEK 293 cells were transiently transfected with siRNA duplexes PEN-2-160 (directed to the target sequence 5'-AAAGGCTATGTCTGGCGCTCA-3') and Nct-1045 as described (18). Cell lysates of HEK 293 cells were analyzed for PEN-2 by combined immunoprecipitation/immunoblotting with antibody 1638, for PSs by combined immunoprecipitation/immunoblotting as described (26), and for Nct by direct immunoblotting with antibody N1660. Immunoprecipitations of PEN-2 were carried out in the presence of 0.1% SDS. To analyze PEN-2, PS, and Nct expression levels in mouse embryonic fibroblast cells, cell homogenates were subjected to ultracentrifugation, and the pellet fraction was solubilized in the presence of 1% SDS as described (31). The SDS extracts were diluted 10-fold and analyzed for PEN-2, PSs, and Nct by combined immunoprecipitation/immunoblotting or immunoblotting as described above.

**Isolation and Analysis of PS Complexes**—PS complexes were isolated by detergent solubilization of membrane preparations with *n*-dodecyl  $\beta$ -D-maltoside (DDM) (18). Homogenates of HEK 293 cells were extracted with 1% Brij-35, 1% Lubrol WX, and membranes were isolated by ultracentrifugation from the postnuclear supernatant fraction and solubilized in DDM-lysis buffer (0.7% DDM, 50 mM sodium citrate, pH 6.4, 1 mM EDTA, 5% glycerol, protease inhibitors (Sigma)). Following a clarifying spin by ultracentrifugation, DDM-solubilized membrane fractions were subjected to co-immunoprecipitation analysis or analyzed for the PS1 complex by blue native PAGE as described (18, 32). Co-immunoprecipitation analysis was performed with the indicated antibodies for 1–4 h at 4 °C followed by two washes in DDM-wash buffer (0.5% DDM, 50 mM sodium citrate, pH 6.4, 1 mM EDTA, 5% glycerol, protease inhibitors). Immunoprecipitates were analyzed on 10–20% Tris-Tricine gels (Invitrogen).

#### RESULTS AND DISCUSSION

To identify endogenous PEN-2, we raised antibody 1638 to the N terminus of human PEN-2. To prove the specificity of this antibody, cell lysates of HEK 293 cells were subjected to immunoprecipitation with antibody 1638 or the corresponding preimmune serum. HEK 293 cells are known from numerous previous studies to express a  $\gamma$ -secretase activity, which has identical functional and biochemical properties as the  $\gamma$ -secretase activity in neuronal cells or brain tissue (see Ref. 33 and citations therein). As shown in Fig. 1A, robust amounts of the ~10-kDa PEN-2 were immunoprecipitated with antibody 1638 but not with preimmune serum.

To address the question whether PEN-2 is a *bona fide* component of PS1- and PS2/ $\gamma$ -secretase complexes we first performed co-immunoprecipitation analyses using HEK 293 cells stably transfected with N-terminal hexahistidine-Xpress ( $H_6X$ )-epitope-tagged PS1 or PS2.  $\gamma$ -Secretase complexes were isolated from DDM-solubilized membrane fractions by immunoprecipitation with an anti-Xpress antibody. As expected, PS1 and PS2 holoproteins and N-terminal fragments were immunoprecipitated, and the corresponding C-terminal fragments were co-immunoprecipitated (Fig. 1B). Under these conditions endogenous PEN-2 was found to co-immunoprecipitate with PS1 and PS2. In addition, Nct also co-immunoprecipitated (Fig. 1B). As shown in Fig. 1C, association of PEN-2 with the  $\gamma$ -secretase complex is independent of endoproteolysis of PS1. Upon stable expression of  $H_6X$ -PS1  $\Delta$ exon9, which does not undergo endoproteolysis due to the lack of the cleavage site for PS endoproteolysis (34), PEN-2 was still co-isolated with the PS1  $\Delta$ exon9 holoprotein and with Nct (Fig. 1C). These results suggest that PEN-2 is a component of individual PS1/ $\gamma$ -secretase and PS2/ $\gamma$ -secretase complexes. Under these conditions we could only immunoprecipitate very minor amounts of PEN-2 with antibody 1638 (data not shown), whereas mild denaturation with 0.1% SDS was sufficient to robustly immunoprecipitate PEN-2 (see Fig. 1A). This suggests that PEN-2 is tightly packed within the  $\gamma$ -secretase complex.

To confirm that PEN-2 is an integral component of the en-

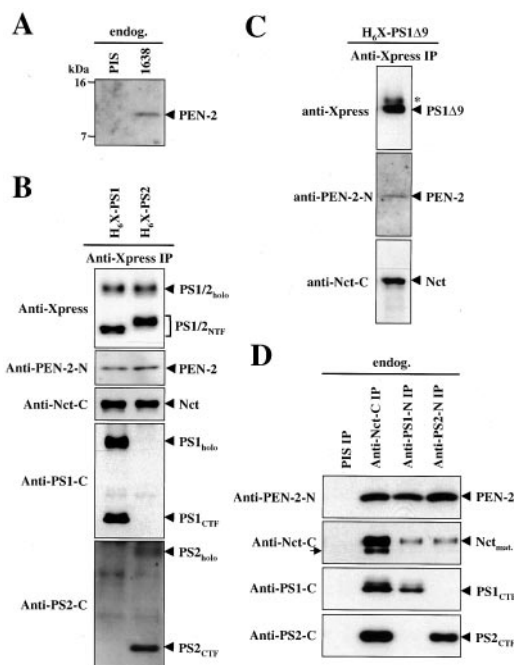


**FIG. 1. PEN-2 binds to Nct, PS1, and PS2.** A, identification of endogenous PEN-2. Cell lysates from HEK 293 cells expressing endogenous (*endog.*) PEN-2 were analyzed for PEN-2 by immunoprecipitation with antibody 1638 or with the corresponding preimmune serum (*PIS*) and analyzed by immunoblotting with antibody 1638. B, co-immunoprecipitation of endogenous PEN-2 with  $H_6X$ -PS1 and  $H_6X$ -PS2. DDM-solubilized membrane fractions from HEK 293 cells stably expressing  $H_6X$ -tagged PS1 or PS2 were subjected to immunoprecipitation with an anti-Xpress antibody (*anti-Xpress IP*) and analyzed for PEN-2, Nct, PS1, and PS2 by immunoblotting with an anti-Xpress antibody (*anti-Xpress*) and with antibodies 1638 (*anti-PEN-2-N*), N1660 (*anti-Nct-C*), 3027 (*anti-PS1-C*), and 3711 (*anti-PS2-C*). C, PEN-2 co-immunoprecipitates with uncleavable  $H_6X$ -PS1  $\Delta$ exon9. DDM-solubilized membrane fractions from HEK 293 cells stably expressing  $H_6X$ -tagged PS1  $\Delta$ exon9 (*PS1 $\Delta$ 9*) were immunoprecipitated with an anti-Xpress-antibody (*anti-Xpress IP*) and analyzed by immunoblotting with the indicated antibodies as in B. The asterisk denotes the IgG heavy chain. D, PEN-2 co-immunoprecipitates with endogenous Nct, PS1, and PS2. Membrane fractions of HEK 293 cells expressing endogenous (*endog.*)  $\gamma$ -secretase complex components were solubilized with DDM and analyzed for Nct/PEN-2, PS1/PEN-2, and PS2/PEN-2 interactions by immunoprecipitation with preimmune serum (*PIS IP*) and the antibodies N1660 (*anti-Nct-C IP*), 2953 (*anti-PS1-N IP*), and 2972 (*anti-PS2-N IP*) and immunoblotting with antibodies 1638 (*anti-PEN-2-N*), N1660 (*anti-Nct-C*), BI.3D7 (*anti-PS1-C*), and BI.HF5c (*anti-PS2-C*). The arrow indicates immature Nct.

dogenous  $\gamma$ -secretase complex co-immunoprecipitations were carried out with untransfected HEK 293 cells. DDM-solubilized membrane fractions were immunoprecipitated with antibodies to the C terminus of Nct and the N terminus of PS1 or PS2. Immunoblotting with anti-PEN-2 antibody 1638 revealed robust amounts of co-immunoprecipitated PEN-2 demonstrating that PEN-2 is a component of endogenous PS/ $\gamma$ -secretase complexes (Fig. 1D). As expected, antibodies to the N termini of PS1 or PS2 co-immunoprecipitated the corresponding PS1 and PS2 C-terminal fragments and mature Nct (Fig. 1D). Taken together, these experiments demonstrate that PEN-2 is an integral *bona fide*  $\gamma$ -secretase complex component.

Eliminating PS1 or PS1/PS2 causes reduced levels of the  $\gamma$ -secretase complex and inhibits Nct maturation (18, 23). Moreover inhibition of Nct expression also strongly reduced PS expression and inhibited  $\gamma$ -secretase complex formation (18). This suggested that expression of  $\gamma$ -secretase complex components might be coordinately regulated. We therefore analyzed PEN-2 expression in PS knock-out mice (2, 4, 30). As expected, robust levels of PEN-2 were observed in embryonic fibroblasts

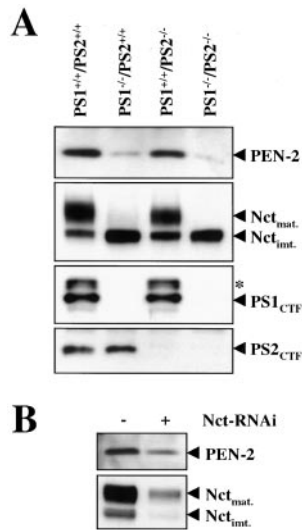


**FIG. 2. PS1, PS2, and Nct are required for the expression of PEN-2.** A, membrane lysates from mouse embryonic fibroblasts (PS1<sup>+/+</sup>/PS2<sup>+/+</sup>, PS1<sup>-/-</sup>/PS2<sup>+/+</sup>, PS1<sup>+/+</sup>/PS2<sup>-/-</sup>, PS1<sup>-/-</sup>/PS2<sup>-/-</sup>) were analyzed for levels of PEN-2, PS1, and PS2 by combined immunoprecipitation/immunoblotting with antibody 1638 (to PEN-2) and with antibodies 3027/BI.3D7 (to PS1) and 3711/BI.HF5c (to PS2). Nct was analyzed by immunoblotting with antibody N1660. Cells lacking PS1 and PS1/PS2 show significantly reduced levels of PEN-2. Note that Nct maturation is strongly reduced in the absence of PS1 and PS1/PS2. The asterisk denotes the phosphorylated form of the PS1 C-terminal fragment (27). B, HEK 293 cells were subjected to two consecutive transfections with siRNA duplex Nct-1045 as described (18). Cell lysates were analyzed for levels of PEN-2 by combined immunoprecipitation/immunoblotting with antibody 1638. Down-regulation of Nct was confirmed by immunoblotting with antibody N1660.

derived from littermate control mice (Fig. 2A). Ablation of PS1 caused a strong reduction of PEN-2 levels, and the absence of PS1/PS2 eliminated PEN-2 expression nearly completely. Compared with the PS1 ablation, ablation of PS2 still allowed significant PEN-2 expression (Fig. 2A). Similar effects of the PS ablations were found on Nct expression. Ablation of PS1 or PS1/PS2 dramatically reduced Nct maturation, whereas ablation of PS2 allowed Nct maturation (Fig. 2A). We next investigated whether PEN-2 expression is also dependent on the presence of Nct. HEK 293 cells were transfected with the siRNA duplex Nct-1045 to down-regulate Nct expression by RNAi (18). As shown in Fig. 2B, RNAi-mediated down-regulation of Nct caused a reduction of PEN-2 levels. Thus, expression of PEN-2 not only requires the presence of PSs (predominantly PS1) but that of Nct as well. To investigate whether lowering PEN-2 levels affects PS and Nct levels, we next transfected HEK 293 cells with the siRNA duplex PEN-2-160. PEN-2-RNAi reduced PEN-2 expression, which was accompanied by reduced levels of PS1 and PS2 (Fig. 3A). RNAi-mediated down-regulation of PEN-2 levels also impaired the maturation of Nct (Fig. 3A) as had been observed upon inhibition of PS1 or PS1/PS2 (Fig. 2A). As a consequence of reduced PS expression and impaired Nct maturation, inhibition of PEN-2 expression caused a deficiency in the PS1/ $\gamma$ -secretase complex (Fig. 3B) as revealed by blue native PAGE analysis (18).

Taken together our findings demonstrate that at least PS, Nct, and PEN-2 are integral components of the  $\gamma$ -secretase complex. Expression of these  $\gamma$ -secretase complex components is coordinately regulated. Removing any of these three components results in reduced amounts of the  $\gamma$ -secretase complex and consequently in a loss of  $\gamma$ -secretase activity (18, 21). We propose that any additional so far unknown  $\gamma$ -secretase complex component may affect PS, Nct, and PEN-2 expression. Obvious candidates for additional  $\gamma$ -secretase complex compo-

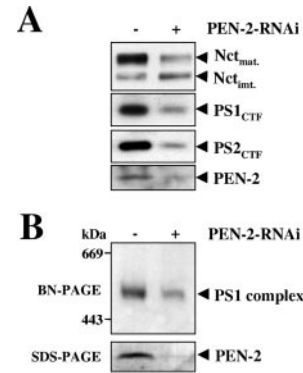


**FIG. 3. Down-regulation of PEN-2 by RNAi is associated with reduced PS levels, impaired Nct maturation, and PS1 complex deficiency.** A, HEK 293 cells were subjected to two consecutive transfections with siRNA duplex PEN-2-160 as described (18). PEN-2 and Nct were analyzed as in Fig. 2B, and PSs were analyzed by combined immunoprecipitation/immunoblotting with antibodies 3027/BI.3D7 (to PS1) and 3711/BI.HF5c (to PS2). Note the altered ratio of mature/immature Nct in cells subjected to PEN-2-RNAi compared with untreated control cells. B, HEK 293 cells were subjected to PEN-2-RNAi as in A. Membrane fractions were solubilized with DDM, subjected to blue native PAGE, and analyzed for the PS1 complex by immunoblotting with antibody 2953. Aliquots were subjected to SDS-PAGE to confirm down-regulation of PEN-2 by immunoblotting with antibody 1638.

nents are APH-1a and APH-1b, the two human homologues of *C. elegans* APH-1 (21). Both act directly at or upstream of  $\gamma$ -secretase activity and apparently affect APH-2 (the *C. elegans* homologue of Nct) transport to the cell surface (25). Moreover, like Nct and PEN-2, APH-1a and APH-1b are required for  $\gamma$ -secretase activity (21).

**Acknowledgments**—We thank Drs. Bart De Strooper and Paul Saftig for PS knock-out cells.

#### REFERENCES

- Steiner, H., and Haass, C. (2000) *Nat. Rev. Mol. Cell. Biol.* **1**, 217–224
- De Strooper, B., Saftig, P., Craessaerts, K., Vanderstichele, H., Guhde, G., Annaert, W., Von Figura, K., and Van Leuven, F. (1998) *Nature* **391**, 387–390
- Naruse, S., Thinakaran, G., Luo, J. J., Kusiak, J. W., Tomita, T., Iwatsubo, T., Qian, X., Ginty, D. D., Price, D. L., Borchelt, D. R., Wong, P. C., and Sisodia, S. S. (1998) *Neuron* **21**, 1213–1221
- Herreman, A., Serneels, L., Annaert, W., Collen, D., Schoonjans, L., and De Strooper, B. (2000) *Nat. Cell Biol.* **2**, 461–462
- Zhang, Z., Nadeau, P., Song, W., Donoviel, D., Yuan, M., Bernstein, A., and Yankner, B. A. (2000) *Nat. Cell Biol.* **2**, 463–465
- Wolfe, M. S., and Haass, C. (2001) *J. Biol. Chem.* **276**, 5413–5416
- Wolfe, M. S., Xia, W., Ostaszewski, B. L., Diehl, T. S., Kimberly, W. T., and Selkoe, D. J. (1999) *Nature* **398**, 513–517
- Steiner, H., Duff, K., Capell, A., Romig, H., Grim, M. G., Lincoln, S., Hardy, J., Yu, X., Picciano, M., Fichteler, K., Citron, M., Kopan, R., Pesold, B., Keck, S., Baader, M., Tomita, T., Iwatsubo, T., Baumeister, R., and Haass, C. (1999) *J. Biol. Chem.* **274**, 28669–28673
- Esler, W. P., Kimberly, W. T., Ostaszewski, B. L., Diehl, T. S., Moore, C. L., Tsai, J.-Y., Rahmati, T., Xia, W., Selkoe, D. J., and Wolfe, M. S. (2000) *Nat. Cell Biol.* **2**, 428–433
- Li, Y. M., Xu, M., Lai, M. T., Huang, Q., Castro, J. L., DiMuzio-Mower, J., Harrison, T., Lellis, C., Nadin, A., Neduvelli, J. G., Register, R. B., Sardana, M. K., Shearman, M. S., Smith, A. L., Shi, X. P., Yin, K. C., Shafer, J. A., and Gardell, S. J. (2000) *Nature* **405**, 689–694
- Steiner, H., Kostka, M., Romig, H., Basset, G., Pesold, B., Hardy, J., Capell, A., Meyn, L., Grim, M. G., Baumeister, R., Fichteler, K., and Haass, C. (2000) *Nat. Cell Biol.* **2**, 848–851
- LaPointe, C. F., and Taylor, R. K. (2000) *J. Biol. Chem.* **275**, 1502–1510
- Weihofen, A., Binns, K., Lemberg, M. K., Ashman, K., and Martoglio, B. (2002) *Science* **296**, 2215–2218
- Ponting, C. P., Hutton, M., Nyborg, A., Baker, M., Jansen, K., and Golde, T. E. (2002) *Hum. Mol. Genet.* **11**, 1037–1044
- Capell, A., Grunberg, J., Pesold, B., Diehlmann, A., Citron, M., Nixon, R., Beyreuther, K., Selkoe, D. J., and Haass, C. (1998) *J. Biol. Chem.* **273**, 3205–3211
- Yu, G., Chen, F., Levesque, G., Nishimura, M., Zhang, D. M., Levesque, L., Rogaeva, E., Xu, D., Liang, Y., Duthie, M., St. George-Hyslop, P. H., and Fraser, P. E. (1998) *J. Biol. Chem.* **273**, 16470–16475
- Li, Y. M., Lai, M. T., Xu, M., Huang, Q., DiMuzio-Mower, J., Sardana, M. K., Shi, X. P., Yin, K. C., Shafer, J. A., and Gardell, S. J. (2000) *Proc. Natl. Acad. Sci. U. S. A.* **97**, 6138–6143
- Edbauer, D., Winkler, E., Haass, C., and Steiner, H. (2002) *Proc. Natl. Acad. Sci. U. S. A.* **99**, 8666–8671

19. Yu, G., Nishimura, M., Arawaka, S., Levitan, D., Zhang, L., Tandon, A., Song, Y. Q., Rogaeva, E., Chen, F., Kawarai, T., Supala, A., Levesque, L., Yu, H., Yang, D. S., Holmes, E., Milman, P., Liang, Y., Zhang, D. M., Xu, D. H., Sato, C., Rogaev, E., Smith, M., Janus, C., Zhang, Y., Aebbersold, R., Farrer, L. S., Sorbi, S., Bruni, A., Fraser, P., and St. George-Hyslop, P. (2000) *Nature* **407**, 48–54
20. Esler, W. P., Kimberly, W. T., Ostaszewski, B. L., Ye, W., Diehl, T. S., Selkoe, D. J., and Wolfe, M. S. (2002) *Proc. Natl. Acad. Sci. U. S. A.* **99**, 2720–2725
21. Francis, R., McGrath, G., Zhang, J., Ruddy, D. A., Sym, M., Apfeld, J., Nicoll, M., Maxwell, M., Hai, B., Ellis, M. C., Parks, A. L., Xu, W., Li, J., Gurney, M., Myers, R. L., Himes, C. S., Hiebsch, R. D., Ruble, C., Nye, J. S., and Curtis, D. (2002) *Dev. Cell* **3**, 85–97
22. Hu, Y., Ye, Y., and Fortini, M. E. (2002) *Dev. Cell* **2**, 69–78
23. Leem, J. Y., Vijayan, S., Han, P., Cai, D., Machura, M., Lopes, K. O., Veselits, M. L., Xu, H., and Thinakaran, G. (2002) *J. Biol. Chem.* **277**, 19236–19240
24. Mumm, J. S., and Kopan, R. (2000) *Dev. Biol.* **228**, 151–165
25. Goutte, C., Tsunozaki, M., Hale, V. A., and Priess, J. R. (2002) *Proc. Natl. Acad. Sci. U. S. A.* **99**, 775–779
26. Steiner, H., Romig, H., Grim, M. G., Philipp, U., Pesold, B., Citron, M., Baumeister, R., and Haass, C. (1999) *J. Biol. Chem.* **274**, 7615–7618
27. Walter, J., Grunberg, J., Capell, A., Pesold, B., Schindzielorz, A., Citron, M., Mendla, K., St. George-Hyslop, P., Multhaupt, G., Selkoe, D. J., and Haass, C. (1997) *Proc. Natl. Acad. Sci. U. S. A.* **94**, 5349–5354
28. Walter, J., Grunberg, J., Schindzielorz, A., and Haass, C. (1998) *Biochemistry* **37**, 5961–5967
29. Citron, M., Oltersdorf, T., Haass, C., McConlogue, L., Hung, A. Y., Seubert, P., Vigo-Pelfrey, C., Lieberburg, I., and Selkoe, D. J. (1992) *Nature* **360**, 672–674
30. Herreman, A., Hartmann, D., Annaert, W., Saftig, P., Craessaerts, K., Serneels, L., Umans, L., Schrijvers, V., Checler, F., Vanderstichele, H., Baekelandt, V., Dressel, R., Cupers, P., Huylebroeck, D., Zwijsen, A., Van Leuven, F., and De Strooper, B. (1999) *Proc. Natl. Acad. Sci. U. S. A.* **96**, 11872–11877
31. Steiner, H., Capell, A., Pesold, B., Citron, M., Kloetzel, P. M., Selkoe, D. J., Romig, H., Mendla, K., and Haass, C. (1998) *J. Biol. Chem.* **273**, 32322–32331
32. Schagger, H., and von Jagow, G. (1991) *Anal. Biochem.* **199**, 223–231
33. Steiner, H., Romig, H., Pesold, B., Philipp, U., Baader, M., Citron, M., Loetscher, H., Jacobsen, H., and Haass, C. (1999) *Biochemistry* **38**, 14600–14605
34. Thinakaran, G., Borchelt, D. R., Lee, M. K., Slunt, H. H., Spitzer, L., Kim, G., Ratovitsky, T., Davenport, F., Nordstedt, C., Seeger, M., Hardy, J., Levey, A. I., Gandy, S. E., Jenkins, N. A., Copeland, N. G., Price, D. L., and Sisodia, S. S. (1996) *Neuron* **17**, 181–190

# The GxGD Motif of Presenilin Contributes to Catalytic Function and Substrate Identification of $\gamma$ -Secretase

Aya Yamasaki,<sup>1</sup> Stefan Eimer,<sup>2</sup> Masayasu Okochi,<sup>3</sup> Agata Smialowska,<sup>2,4</sup> Christoph Kaether,<sup>1</sup> Ralf Baumeister,<sup>2,4</sup> Christian Haass,<sup>1</sup> and Harald Steiner<sup>1</sup>

<sup>1</sup>Laboratory for Alzheimer's and Parkinson's Disease Research and <sup>2</sup>Laboratory of Molecular Neurogenetics, Department of Biochemistry, Adolf Butenandt Institute, Ludwig Maximilians University, 80336 Munich, Germany, <sup>3</sup>Department of Post-Genomics and Diseases, Division of Psychiatry and Behavioral Proteomics, Osaka University Graduate School of Medicine, Osaka 565-0871, Japan, and <sup>4</sup>Bio3/Bioinformatics and Molecular Genetics, Albert Ludwigs University, 79104 Freiburg, Germany

$\gamma$ -Secretase is a multisubunit aspartyl protease complex that catalyzes intramembrane cleavage of  $\beta$ -amyloid precursor protein (APP), a substrate key to Alzheimer's disease pathogenesis, and of Notch, a substrate crucial for cell differentiation. How  $\gamma$ -secretase recognizes and selects substrates is currently barely understood. Recent data suggest that its subunit nicastrin serves as an initial substrate receptor, which might subsequently forward substrates to the active site domain located in its catalytic subunit presenilin (PS), where an additional substrate binding site has been proposed. We now used an active site domain swapping approach of PS1 with its most distant homolog, spermatogenesis defective (SPE-4), to identify sequence determinants in this region. Strikingly, when the active site domain of PS1 was exchanged with that of SPE-4, the chimeric protein, PS1/SPE-4<sub>6/7</sub>, supported APP but not Notch processing. In addition, PS1/SPE-4<sub>6/7</sub> was strongly impaired in *Caenorhabditis elegans* Notch signaling *in vivo*. Mapping experiments identified a single amino acid at position x of the GxGD motif, which contains one of the two active site aspartates, to be responsible for the observed defect in Notch processing and signaling. Our data thus implicate a role of the GxGD motif in catalytic function and substrate identification of  $\gamma$ -secretase.

**Key words:** Alzheimer's disease; amyloid  $\beta$ -peptide;  $\gamma$ -secretase; Notch; presenilin; SPE-4

## Introduction

Presenilin (PS1, PS2) is the catalytic subunit of  $\gamma$ -secretase, an aspartyl protease complex, which mediates the regulated intramembrane cleavage of an increasing number of type I transmembrane proteins including the prototypic  $\beta$ -amyloid precursor protein (APP) implicated in Alzheimer's disease (AD) (De Strooper, 2003; Haass, 2004; Steiner, 2004).  $\gamma$ -Secretase cleavage is typically preceded by ectodomain shedding of the substrate, which removes the bulk of the extracellular domain. In the amyloidogenic pathway of APP, ectodomain cleavage by  $\beta$ -secretase generates a membrane-retained C-terminal fragment (CTF). The APP CTF is subsequently cleaved by  $\gamma$ -secretase to release the amyloid  $\beta$ -peptide (A $\beta$ ), which is deposited as senile plaques in the brains of patients affected with AD, and the intracellular domain (ICD) of APP (AICD) from the membrane (Haass, 2004; Steiner, 2004).  $\gamma$ -Secretase-dependent liberation of ICDs has

been shown for many other substrates (Kopan and Ilagan, 2004) including Notch-1, a major  $\gamma$ -secretase substrate (De Strooper et al., 1999). When released from the membrane, the Notch-1 ICD (NICD) translocates to the nucleus where it functions as a key transcriptional regulator required for cell differentiation during development and in adulthood (Lai, 2004).

The two active site aspartates of  $\gamma$ -secretase are located in transmembrane domains (TMDs) 6 and 7 (Wolfe et al., 1999) of the N-terminal fragment (NTF) and CTF of PS (Thinakaran et al., 1996), which are likely derived by autoproteolysis (Wolfe et al., 1999; Edbauer et al., 2003). PSs are founding members of polytopic GxGD-type aspartyl proteases (Haass and Steiner, 2002) that include the type 4 prepilin peptidases (LaPointe and Taylor, 2000), signal peptide peptidase (SPP) (Weihs et al., 2002), and its homologs (Krawitz et al., 2005). These protease families are characterized by a highly conserved GxGD sequence motif (Steiner et al., 2000), which includes the C-terminal active site aspartate. Homology outside this signature sequence is scarce, and the proteases carry out distinct biological functions (Haass, 2004; Steiner, 2004). Together with the catalytic subunit PS, three other integral membrane proteins, nicastrin (NCT), anterior pharynx defective (APH-1), and presenilin enhancer (PEN-2) have been identified, which are necessary and sufficient for  $\gamma$ -secretase complex formation and activity (Francis et al., 2002; Edbauer et al., 2003; Kimberly et al., 2003; Takasugi et al., 2003). In mammalian cells, PS1 and PS2 are the catalytic subunits of distinct  $\gamma$ -secretase complexes, which additionally differ in

Received Dec. 15, 2005; revised Feb. 15, 2006; accepted Feb. 16, 2006.

This work was supported by the priority program "Cellular Mechanisms of Alzheimer's Disease" (R.B., C.H., H.S.) and the SFB596 "Molecular Mechanisms of Neurodegeneration" (C.H., H.S.) of the Deutsche Forschungsgemeinschaft and the Fonds der Chemischen Industrie (R.B.). We thank Bart De Strooper for PS<sup>-/-</sup> MEF cells; Ralph Nixon for monoclonal antibody PS1N; Alison Goate for the APPsw-6myc construct; Steve L'Hernault for SPE-4 cDNA; Bob Barsted for the *C. elegans* mixed-stage cDNA library; Christine Baumeister, Alice Suelzen, and Roland Donhauser for excellent technical help; and Keiro Shirota for critically reading this manuscript.

Correspondence should be addressed to either Harald Steiner or Christian Haass, Department of Biochemistry, Adolf Butenandt Institute, Ludwig Maximilians University Munich, Schillerstrasse 44, 80336 Munich, Germany. E-mail: harald.steiner@med.uni-muenchen.de or christian.haass@med.uni-muenchen.de.

DOI:10.1523/JNEUROSCI.5354-05.2006

Copyright © 2006 Society for Neuroscience 0270-6474/06/263821-08\$15.00/0

their APH-1 subunits, suggesting that  $\gamma$ -secretase is a heterogeneous activity (Hebert et al., 2004; Shirovani et al., 2004).

Apart from the requirement for ectodomain shedding (Struhl and Adachi, 2000), little information is available about substrate selection by  $\gamma$ -secretase. The C-terminal stubs that are left in the membrane after ectodomain shedding need to be recognized subsequently by  $\gamma$ -secretase as substrate. NCT with its large ectodomain is a candidate subunit of the  $\gamma$ -secretase complex for this initial substrate recognition, and indeed it has recently been shown that it serves as a  $\gamma$ -secretase substrate receptor (Shah et al., 2005). In addition, previous work indicated that docking of  $\gamma$ -secretase substrates occurs at a site very close to but different from the active site (Tian et al., 2002, 2003), and more recently it was shown that such a docking site is located in PS (Kornilova et al., 2005).

Based on these studies, we reasoned that, after initial substrate recognition by NCT, the active site domain of PS in TMDs 6 and 7 might directly contribute to subsequent substrate docking and probably a final substrate selection before cleavage by  $\gamma$ -secretase. We thus sought to identify sequence requirements in TMDs 6 and 7 of PS potentially involved in this process. We now have mapped a single amino acid in TMD7 at position x of the GxGD active site motif that influences APP/Notch substrate selectivity of  $\gamma$ -secretase. These data implicate a role of the PS active site domain in  $\gamma$ -secretase substrate selectivity and support the concept of a substrate-docking site close to the active site of  $\gamma$ -secretase in PS.

## Materials and Methods

**Antibodies.** The monoclonal antibody against the N terminus of PS1 (PS1N) has been described (Capell et al., 1997), and the polyclonal antibody against the C terminus of NCT (N1660) was obtained from Sigma (St. Louis, MO). Polyclonal antibody 3552 was raised to A $\beta$ 1–40 and monoclonal antibody 6E10 against A $\beta$ 1–17 was obtained from Signet Laboratories (Dedham, MA). Monoclonal antibodies against FLAG and myc tags were from Sigma (anti-FLAG, M2) and Santa Cruz Biotechnology (Santa Cruz, CA) (anti-myc, 9E10). Cleaved Notch-1 (V1744) antibody against NICD was obtained from Cell Signaling Technology (Beverly, MA).

**cDNA constructs.** PS1 wild-type (wt) and mutant cDNAs were generated by PCR using appropriate primers and subcloned into the expression vector pcDNA4/HisC (Invitrogen, San Diego, CA). The suppressor/enhancer of *lin-12* (*sel-12*) cDNA (GenBank accession number AF171064) was amplified by PCR from a *Caenorhabditis elegans* mixed-stage cDNA library and subcloned as a *SmaI/NotI* fragment under the control of a 2.8 kb *sel-12* promoter fragment starting at the translational start ATG of *sel-12* to generate pBY895 (Wittenburg et al., 2000). PCR-amplified cDNAs encoding homolog of presenilin (HOP-1) (amplified from the *C. elegans* mixed-stage cDNA library), spermatogenesis defective (SPE-4), and PS1 were subcloned into pBY895 as *SmaI/NotI* fragments replacing the *sel-12* cDNA, thus placing them under the control of the *sel-12* promoter. cDNAs encoding H<sub>6</sub>X-tagged wt PS1, PS1 L383F, and PS1/SPE-4 chimera were placed under control of the *sel-12* promoter by subcloning them into pBY2019 as *NcoI/XhoI* fragments. All constructs were confirmed by sequencing.

**Cell culture, cell lines, and cDNA transfections.** Mouse embryonic fibroblast (MEF) cells derived from PS1/2<sup>-/-</sup> mice (Herreman et al., 1999) were cultured as described previously (Steiner et al., 2002) and transiently transfected with the indicated cDNA constructs using Lipofectamine 2000 (Invitrogen) according to the instructions of the manufacturer.

**Protein analysis.** PS and derivatives and NCT were analyzed by immunoblotting of cell lysates with PS1N or N1660 antibody, respectively. Processing of myc-tagged Swedish mutant APP (Wang et al., 2004) and myc-tagged F-NEXT (Okochi et al., 2002) was analyzed by immunoblotting of cell lysates with antibody 9E10. Where indicated, NICD was ad-

ditionally analyzed by immunoblotting of cell lysates with Cleaved Notch-1 (V1744) antibody. To analyze secreted A $\beta$  and F-N $\beta$ , the medium was replaced 24 h after transfection with fresh medium and conditioned for 16 h. A $\beta$  was analyzed from conditioned medium by combined immunoprecipitation/immunoblotting with antibodies 3552/6E10 and F-N $\beta$  by combined immunoprecipitation with anti-FLAG M2-agarose (Sigma) and immunoblotting with antibody M2.

**Immunofluorescence microscopy.** Immunofluorescence was performed as described (Wacker et al., 1997). Anti-myc antibody 9E10 was used as primary antibody and Alexa 488-labeled secondary antibody (Invitrogen, Leiden, The Netherlands) was used for detection. Fixed cells were analyzed on an Axioskop2 microscope (Zeiss, Oberkochen, Germany) equipped with a 63 $\times$ /1.25 objective and standard FITC and TRITC (tetramethylrhodamine isothiocyanate) fluorescence filter sets using an AxioCam HRm camera and AxioVision software. Images were assembled and processed using Adobe Photoshop.

**Transgenic lines of *C. elegans* and rescue assays.** To determine whether the PS constructs are able to rescue the egg-laying defect of *sel-12* mutant hermaphrodites, all constructs were injected into *sel-12(ar171)* mutant hermaphrodites together with the coinjection marker pBY1153 (*sel-12::gfp*) at a concentration of 20 ng/ $\mu$ l, each. The egg-laying behavior of the transgenic animals was scored at 20°C as described previously (Steiner et al., 1999).

## Results

### A PS1-based active site domain chimera supports

#### APP processing

To identify sequence determinants in TMDs 6 and 7 of PS potentially involved in substrate docking and/or selection, we sought to compare the active site domain of PS1 on  $\gamma$ -secretase activity with that of a distant PS by swapping TMDs 6 and 7. BLAST (basic local alignment search tool) searches identified the *C. elegans* sperm protein SPE-4 (L'Hernault and Arduengo, 1992) as the most distant PS homolog with a low amino acid identity of 23% to PS1. Sequence comparison of PS1 with SPE-4 including the functional *C. elegans* PS orthologs SEL-12 and HOP-1 (Levitan and Greenwald, 1995; Westlund et al., 1999) revealed conservation of key functional residues and sequence blocks, like the critical aspartates in TMDs 6 and 7 including the GxGD active site motif and the C-terminal PALP motif (Fig. 1A). The latter motif is required for SPE-4 function (Arduengo et al., 1998) and also for PS activity in humans and *Drosophila* (Tomita et al., 2001; Takasugi et al., 2002; Kaether et al., 2004; Wang et al., 2004) indicating that SPE-4 functionally belongs to the PS family. Compared with PS1, SPE-4 contains a very short N terminus, a much larger cytoplasmic loop between TMDs 6 and 7, and a shorter C terminus (Fig. 1A). We then asked whether  $\gamma$ -secretase is functional with the related but not identical active site domain of SPE-4 and constructed the N-terminally hexahistidine-Xpress (H<sub>6</sub>X)-tagged chimeric protein PS1/SPE-4<sub>6/7</sub>. In this construct, the putative TMDs 6 and 7 of PS1 are replaced with those of SPE-4 (Fig. 1B). In addition, we generated the PS1/SPE-4<sub>6/7</sub> D394A mutant in which the active site aspartate of TMD7 was changed to alanine. Constructs encoding H<sub>6</sub>X-tagged wt PS1 or inactive PS1 D385A were used as controls. We sought to assess the biological activity of these constructs in a PS-free background to avoid potential interference of endogenous wt PS in  $\gamma$ -secretase activity. We therefore transiently cotransfected MEF cells derived from mice deficient for PS1 and PS2 (PS<sup>-/-</sup>) (Herreman et al., 1999) with the above constructs and a construct encoding APPsw-6myc, a Swedish mutant of APP C-terminally tagged with six myc epitopes (Wang et al., 2004). As shown in Figure 2A, all four PS variants were robustly expressed. PS1/SPE-4<sub>6/7</sub> was efficiently endoproteolyzed similar to wt PS1 (Fig. 2A). In contrast, PS1/SPE-4<sub>6/7</sub> D394A, like PS1 D385A, failed to undergo endoproteolysis,

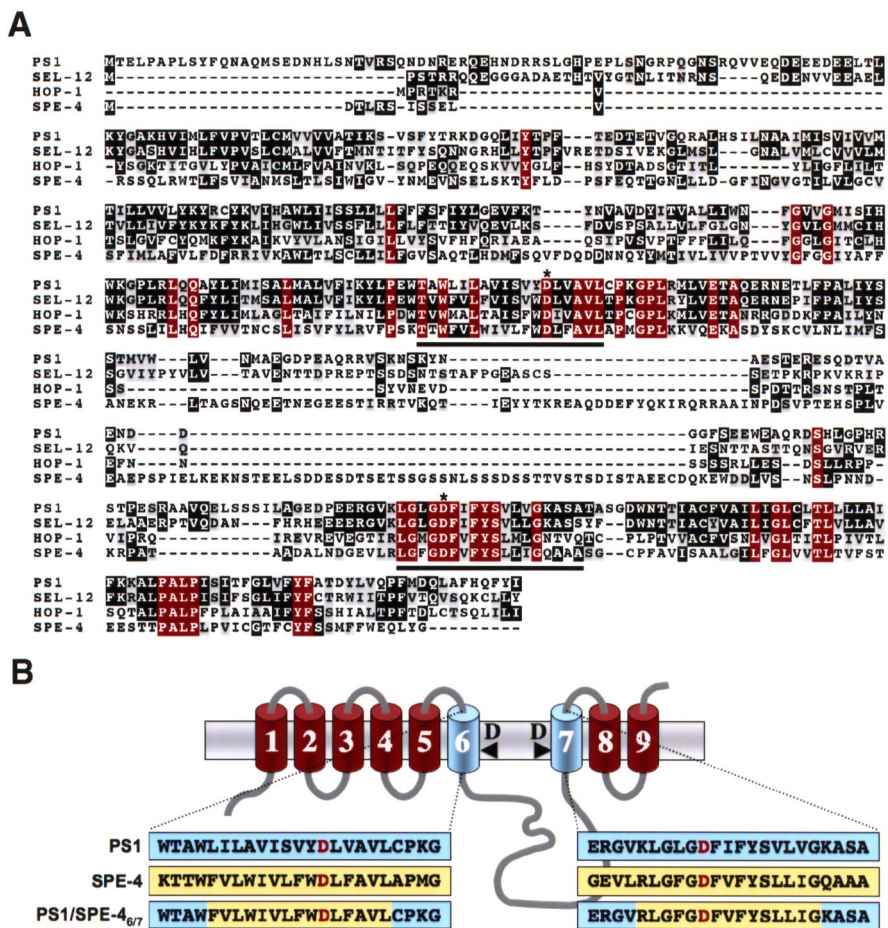


**Figure 1.** Sequence comparison of PS1 with its *C. elegans* homologs and schematic representation of the PS1/SPE-4<sub>6/7</sub> chimera. **A**, Sequence alignment of PS1 with SEL-12, HOP-1, and SPE-4 identifies the GxGD active site motif and the PALP motif as the most conserved regions between PS1 and SPE-4. The sequence alignment was generated with T-Coffee and processed with BOXSHADE. Identical amino acids residues are displayed on black or red (identical in all PSs) background and similar ones on gray background. Putative TMDs 6 and 7 comprising the active site domain are underlined. Asterisks indicate the active site aspartate residues. **B**, Schematic representation of PS1, SPE-4, and PS1/SPE-4<sub>6/7</sub>. The primary sequences representing the putative TMDs 6 and 7 of PS1, SPE-4, and the PS1/SPE-4<sub>6/7</sub> hybrid are highlighted in blue (PS1 sequences) or yellow (SPE-4 sequences). The active site aspartate residues are displayed in red. PS is depicted according to the recent nine TMD model (Henricson et al., 2005; Laudon et al., 2005; Oh and Turner, 2005).

indicating a functional conservation of the putative SPE-4 active site domain (Fig. 2A). Both wt PS1 and PS1/SPE-4<sub>6/7</sub> underwent  $\gamma$ -secretase complex formation, as evident from their capability to undergo PS endoproteolysis, which occurs as final step in  $\gamma$ -secretase complex assembly (Kim et al., 2003; Takasugi et al., 2003).  $\gamma$ -Secretase complex formation was further supported by the restoration of NCT maturation (Fig. 2B), which is deficient in the absence of PS (Edbauer et al., 2002; Leem et al., 2002) and which occurs subsequently to PS endoproteolysis (Kim et al., 2003; Kimberly et al., 2003). In agreement with previous results (Nyabi et al., 2003), the recovery of NCT maturation also suggested  $\gamma$ -secretase complex formation (Fig. 2B) of PS1 D385A and PS1/SPE-4<sub>6/7</sub> D394A, although they were not endoproteolyzed. We next investigated whether PS1/SPE-4<sub>6/7</sub> supports  $\gamma$ -secretase activity in APP processing using APPsw-6myc as substrate (Fig. 2C,D). Consistent with the absence of  $\gamma$ -secretase activity in PS<sup>-/-</sup> cells (Herreman et al., 2000; Zhang et al., 2000), APP C-terminal fragments accumulated and both AICD and A $\beta$  failed to be generated (Fig. 2C,D). As expected, the defect in  $\gamma$ -secretase activity was rescued by the coexpression of wt PS1 but not by proteolytically inactive PS1 D385A. PS1/SPE-4<sub>6/7</sub>, in con-

trast to PS1/SPE-4<sub>6/7</sub> D394A, was capable to process APPsw-6myc as judged from the robust reduction of APP CTF accumulation and the substantial generation of AICD and A $\beta$  (Fig. 2C,D). These data show that  $\gamma$ -secretase can be functional with a homologous but distant GxGD-type active site domain derived from SPE-4 and that this particular active site domain is capable of APP processing.

**PS1/SPE-4<sub>6/7</sub> does not process Notch**

We next investigated the capability of PS1/SPE-4<sub>6/7</sub> to process Notch, a major physiological substrate of  $\gamma$ -secretase. We transiently cotransfected the PS<sup>-/-</sup> MEF cells with the above-described wt PS1, PS1 D385A, and PS1/SPE-4<sub>6/7</sub> constructs and a cDNA construct encoding the Notch-1-based  $\gamma$ -secretase substrate F-NEXT (Okochi et al., 2002). F-NEXT is a derivative of Notch $\Delta$ E lacking the bulk of the ectodomain and carrying a FLAG-epitope tag at the N- and six myc-epitope tags at the C terminus (Okochi et al., 2002). Strikingly, processing of F-NEXT was strongly impaired in cells expressing PS1/SPE-4<sub>6/7</sub>. Compared with wt PS1-expressing cells, F-NEXT accumulated similarly as observed in PS1 D385A-expressing cells, whereas NICD generation was strongly reduced (Fig. 3B). Likewise, the generation of F-N $\beta$ , the secreted peptide of Notch analogous to A $\beta$  (Okochi et al., 2002), was strongly impaired (Fig. 3C). To further corroborate these findings, immunocytochemical analysis of PS<sup>-/-</sup> MEF cells transfected with F-NEXT alone or cotransfected with the PS constructs above was performed (Fig. 3D). When PS<sup>-/-</sup> MEF cells were transfected with F-NEXT, a strong Notch staining at the plasma membrane was observed, which is consistent with an accumulation of unprocessed F-NEXT (Fig. 3B) because of the  $\gamma$ -secretase deficiency of these cells. Cotransfection of F-NEXT with wt PS1 restored  $\gamma$ -secretase activity, resulting in Notch processing as evident from the nuclear Notch staining because of the recovery of NICD formation. In contrast, cotransfection of F-NEXT with proteolytically inactive PS1 D385A did not restore  $\gamma$ -secretase activity as suggested from the strong plasma membrane staining of Notch. Similarly, PS<sup>-/-</sup> MEF cells transiently cotransfected with PS1/SPE-4<sub>6/7</sub> and F-NEXT revealed Notch staining at the plasma membrane. Consistent with the residual minor NICD formation (Fig. 3B), occasionally some cells showed weak nuclear staining (data not shown). These data suggest that the SPE-4-derived active site of PS1/SPE-4<sub>6/7</sub>, which is able to process APP, is severely reduced in processing Notch as substrate.

**PS1/SPE-4<sub>6/7</sub> is deficient in Notch signaling**

The above results prompted us to also analyze Notch signaling in an *in vivo* setting. PS1/SPE-4<sub>6/7</sub> was therefore next tested for its activity to rescue the Notch signaling deficiency caused by loss of function mutations in *sel-12* (Levitani and Greenwald, 1995).

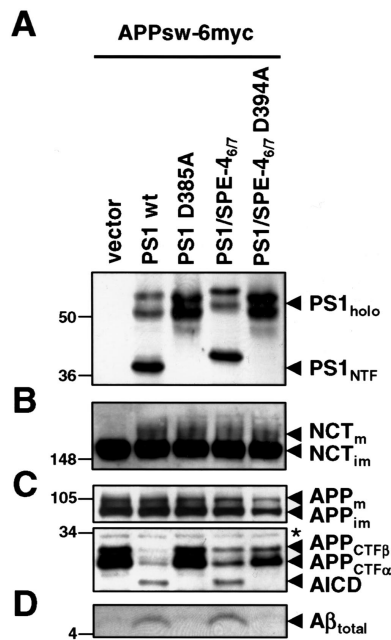


**Figure 2.** PS1/SPE-4<sub>6/7</sub> supports APP processing. **A**, Cell lysates of PS<sup>-/-</sup> MEF transiently cotransfected with the APPsw-6myc and the indicated H<sub>2</sub>X-tagged PS1 constructs were analyzed for PS1 expression and endoproteolysis by immunoblotting with antibody PS1N. Note that, for unknown reasons, both PS1/SPE-4<sub>6/7</sub> holoprotein and its NTF migrated slightly slower in SDS-PAGE. **B**, Maturation of NCT was analyzed by immunoblotting with antibody N1660. **C**, Full-length APP, APP CTFs, and AICD were analyzed by immunoblotting with anti-myc antibody 9E10. **D**, Secreted A $\beta$  was analyzed from conditioned media by combined immunoprecipitation/immunoblotting with antibodies 3552/6E10, respectively. In **A–D**, molecular mass markers are shown on the left in kilodaltons. The asterisk indicates a nonspecific band.

These mutations cause an egg-laying defect (Egl) that can be rescued by SEL-12, HOP-1, PS1, and PS2 (Levitani et al., 1996; Baumeister et al., 1997; Li and Greenwald, 1997; Steiner et al., 1999). In contrast to wt PS1, PS1/SPE-4<sub>6/7</sub> was not able to rescue the Egl defect of the *sel-12(ar171)* mutant hermaphrodites (Table 1), suggesting that PS1/SPE-4<sub>6/7</sub> unlike PS1 does not support Notch signaling, consistent with the above results. We also investigated whether SPE-4 itself might be able to replace SEL-12 function. Because *spe-4* expression is normally restricted to the spermatheca (L'Hernault and Arduengo, 1992; Arduengo et al., 1998), we expressed the *spe-4* gene under the control of the *sel-12* promoter in *sel-12(ar171)* mutant hermaphrodites and scored the Egl defect in the transgenic animals. Surprisingly, SPE-4, unlike PS1, SEL-12, and HOP-1, was not able to rescue the *sel-12* Egl defect when expressed under the *sel-12* promoter (Table 1). *sel-12* mutant hermaphrodites carrying a *sel-12::spe-4* extrachromosomal array never laid any eggs like the *sel-12* mutants alone (Table 1) demonstrating that SPE-4 is unexpectedly unable to replace SEL-12 function.

### Notch processing depends on the amino acid at position x of the GxGD active site motif

We next sought to define the molecular basis for the apparent substrate preference of PS1/SPE-4<sub>6/7</sub> for APP versus Notch. We first addressed the question which of the two SPE-4 TMDs was responsible for the deficiency in Notch processing and thus generated the PS1/SPE-4<sub>6</sub> and PS1/SPE-4<sub>7</sub> hybrid active site constructs in which only one TMD of PS1 is exchanged with the corresponding TMD of SPE-4. We then transiently cotransfected PS<sup>-/-</sup> MEF cells with cDNA constructs encoding the PS1/SPE-4<sub>6</sub> and PS1/SPE-4<sub>7</sub> and the APPsw-6myc or F-NEXT constructs.

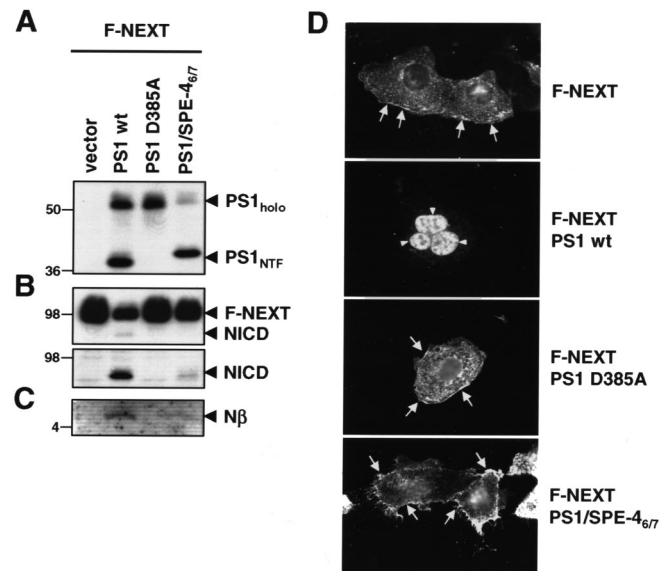


**Figure 3.** PS1/SPE-4<sub>6/7</sub> is defective in Notch processing. **A**, Cell lysates of PS<sup>-/-</sup> MEF transiently cotransfected with F-NEXT and the indicated H<sub>2</sub>X-tagged PS1 constructs were analyzed for PS expression and endoproteolysis as in Figure 2B. **B**, Expression and processing of F-NEXT was analyzed by immunoblotting with antibody 9E10 (top panel). NICD was additionally analyzed by immunoblotting with Cleaved Notch-1 antibody (bottom panel). **C**, F-N $\beta$  levels were analyzed from conditioned media by combined immunoprecipitation/immunoblotting with anti-FLAG-M2 antibody. **D**, PS<sup>-/-</sup> MEF were transiently transfected with F-NEXT and the indicated H<sub>2</sub>X-tagged PS1 constructs. Forty-eight hours after transfection, cells were fixed and analyzed for Notch processing by immunofluorescence microscopy with anti-myc antibody 9E10. Expression of wt PS1, but not of PS1/SPE-4<sub>6/7</sub> or PS1 D385A, restores  $\gamma$ -secretase activity as indicated by nuclear Notch staining (arrowheads). Similarly as the proteolytically inactive PS1 D385A mutant, PS1/SPE-4<sub>6/7</sub> causes reduced nuclear Notch staining (arrowheads) and increased cell surface staining (arrows). In **A–C**, molecular mass markers are shown on the left in kilodaltons.

**Table 1.** Activity of different PSs to rescue the *sel-12* Egl defect

Strain	Transgene <sup>a</sup>	Genotype	Egg-laying behavior <sup>b</sup>			
			+++	++	+	–
N2		Wild type	50	0	0	0
BR1129		<i>sel-12(ar171)</i>	0	0	0	50
BR1964	PS1	<i>sel-12(ar171)</i>	45	3	1	0
BR3536	PS1/SPE-4 <sub>6/7</sub>	<i>sel-12(ar171)</i>	0	0	1	49
BR3210	PS1/SPE-4 <sub>6/7</sub>	<i>sel-12(ar171)</i>	0	0	2	48
BR2364	<i>sel-12</i>	<i>sel-12(ar171)</i>	48	2	0	0
BR2993	<i>hop-1</i>	<i>sel-12(ar171)</i>	50	0	0	1
<sup>c</sup>	<i>spe-4</i>	<i>sel-12(ar171)</i>	0	0	0	34
<sup>c</sup>	<i>spe-4</i>	<i>sel-12(ar171)</i>	0	0	0	27
<sup>c</sup>	<i>spe-4</i>	<i>sel-12(ar171)</i>	0	0	0	16

<sup>a</sup>All constructs used were untagged.

<sup>b</sup>For each transgenic animal, the number of eggs laid were counted and were grouped into the following categories: +++, >50 eggs of progeny laid by an individual animal; ++, 15–50 eggs laid; +, 5–15 eggs laid; –, 0–5 eggs laid.

<sup>c</sup>Stable lines could not be maintained because of the sterility of *spe-4* transgenic animals. Instead, F<sub>1</sub> progeny from three independent transformation experiments was scored.

The PS1/SPE-4<sub>6/7</sub> construct was used for comparison in these settings. In addition, in these and the subsequent experiments, wt PS1 and PS1 D385A constructs were again included as positive and negative controls, respectively. Both PS1/SPE-4<sub>6</sub> and PS1/SPE-4<sub>7</sub> underwent  $\gamma$ -secretase complex formation as judged from their capability to undergo PS endoproteolysis (Fig. 4A, B) and from the NCT maturation (data not shown). Like PS1/SPE-4<sub>6/7</sub>, both PS1/SPE-4<sub>6</sub> and PS1/SPE-4<sub>7</sub> were capable to process APPsw-6myc as judged from the robust reduction of APP CTF accumulation and the substantial generation of AICD and A $\beta$

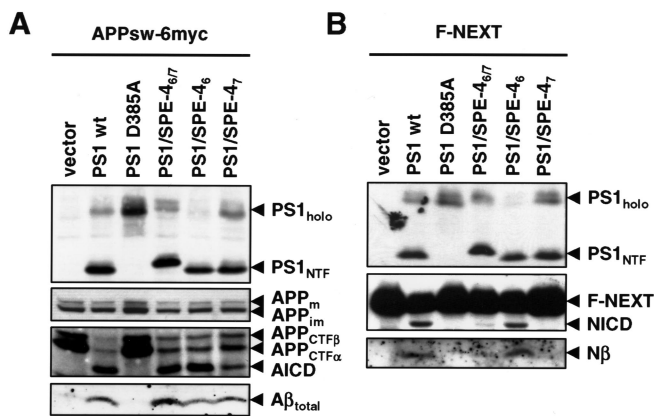


**Figure 4.** Mapping of the TMD in PS1/SPE-4<sub>6/7</sub> required for Notch processing. **A**, PS<sup>-/-</sup> MEF were transiently cotransfected with APPsw-6myc and the indicated H<sub>6</sub>X-tagged PS1 constructs. Cell lysates were analyzed for PS expression and processing as in Figure 2*A* and for full-length APP, APP CTFs, and AICD as in Figure 2*C*. Secreted A $\beta$  levels were analyzed from the conditioned media as in Figure 2*D*. **B**, PS<sup>-/-</sup> MEF were transiently cotransfected with F-NEXT and the indicated H<sub>6</sub>X-tagged PS1 constructs. Cell lysates were analyzed for PS expression and processing as in Figure 2*A* and for processing of F-NEXT by immunoblotting with 9E10 as in Figure 3*B*. F-N $\beta$  levels were analyzed from the conditioned media as in Figure 3*C*.

(Fig. 4*A*). However, in contrast to PS1/SPE-4<sub>6</sub>, expression of PS1/SPE-4<sub>7</sub> strongly impaired the generation of NICD and F-N $\beta$  from F-NEXT (Fig. 4*B*). Together, these results suggest that TMD7 of PS1/SPE-4<sub>6/7</sub> is responsible for the observed defect in Notch processing.

To further map the responsible sequence within the TMD7 of PS1/SPE-4<sub>6/7</sub>, we made advantage of our above finding that PS1, SEL-12, and HOP-1, but not PS1/SPE-4<sub>6/7</sub> and SPE-4 was able to rescue the Notch signaling-deficient phenotype of the *sel-12(ar171)* mutant worms (Table 1). We reasoned that there may be differences in the conservation of crucial amino acids, which may underlie the observed rescuing activity of PS1, SEL-12, HOP-1 compared with the nonrescuing activity of PS1/SPE-4<sub>6/7</sub> and SPE-4. We thus compared the sequences of TMD7 of PS1, SEL-12, HOP-1, and SPE-4. Interestingly, we found the only potentially significant difference within their GxGD active site motifs. Although the residue x position of PS1 (L383) is rather conserved in SEL-12 (L362) and HOP-1 (M276), it is more drastically changed to a phenylalanine residue (F392) in SPE-4 (Fig. 1*A,B*). To address the functional significance of this amino acid change, we mutated F392 of the GFGD motif in PS1/SPE-4<sub>7</sub> to L to restore the PS1 or SEL-12 GLGD motif or to M to restore the GMGD motif of HOP-1. We then analyzed the PS1/SPE-4<sub>7</sub> F392L and PS1/SPE-4<sub>7</sub> F392M mutants using the same experimental paradigms as above. As shown in Figure 5*A*, when assayed in the PS<sup>-/-</sup> background, the PS1/SPE-4<sub>7</sub> F392L and PS1/SPE-4<sub>7</sub> F392M mutants underwent endoproteolysis and allowed NCT maturation (data not shown) consistent with  $\gamma$ -secretase complex formation. They also allowed a robust reduction of APP CTF accumulation concomitant with a notable generation of APP CTF accumulation concomitant with a notable generation of AICD and A $\beta$ . Strikingly, both mutants allowed also the generation of substantial levels of NICD and F-N $\beta$ , suggesting that the presence of leucine or methionine at position x within the GxGD motif is indeed crucial for the capability of PS1/SPE-4<sub>7</sub> to process Notch (Fig. 5*B*).

The above data suggested that the presence or absence of a phenylalanine at position x of the GxGD motif determines whether Notch can be efficiently processed or not. To obtain additional evidence for the functional importance of this residue within the GxGD motif, we next mutated L383 to F directly in PS1. We then

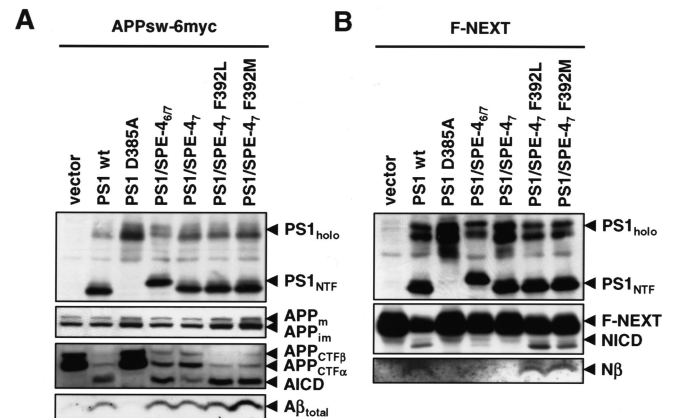


**Figure 5.** Identification of phenylalanine at position x in the GxGD motif of PS1/SPE-4<sub>6/7</sub> as a critical determinant for Notch processing. **A**, PS<sup>-/-</sup> MEF were transiently transfected with APPsw-6myc and the indicated H<sub>6</sub>X-tagged PS1 constructs. Cell lysates were analyzed for PS expression and processing as in Figure 4*A*. APP processing was analyzed from cell lysates and conditioned media as in Figure 4*A*. **B**, PS<sup>-/-</sup> MEF were transiently transfected with F-NEXT and the indicated H<sub>6</sub>X-tagged PS1 constructs. Cell lysates were analyzed for PS expression and endoproteolysis and for processing of F-NEXT as in Figure 4*B*.

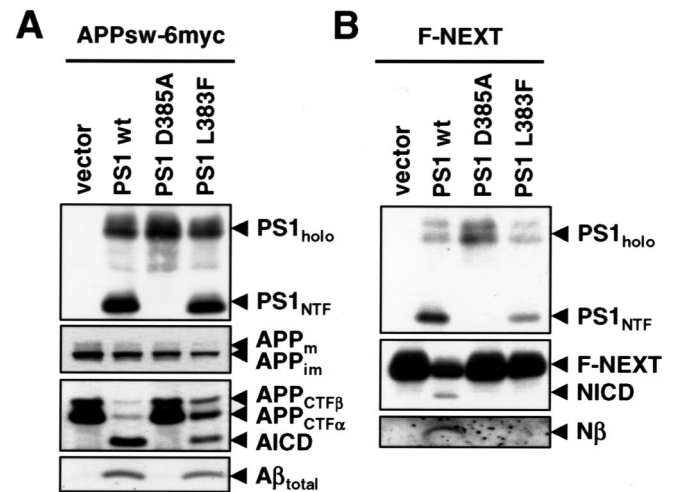


**Figure 6.** Leucine 383 of PS1 is critical for Notch processing. **A**, PS<sup>-/-</sup> MEFs were transiently transfected with APPsw-6myc and the H<sub>6</sub>X-tagged wt PS1, PS1 D385A, or PS1 L383F constructs. Cell lysates were analyzed for PS expression and processing as in Figure 4*A*. APP processing was analyzed from cell lysates and conditioned media as in Figure 4*A*. **B**, PS<sup>-/-</sup> MEF were transiently transfected with F-NEXT and the H<sub>6</sub>X-tagged wt PS1, PS1 D385A, or PS1 L383F constructs. Cell lysates were analyzed for PS expression and endoproteolysis and for F-NEXT processing as in Figure 4*B*.

analyzed the influence of the L383F mutation in PS1 on the processing of APP and Notch as above. The PS1 L383F mutant was endoproteolytically processed and allowed maturation of NCT (data not shown), suggesting  $\gamma$ -secretase complex formation. PS1 L383F also allowed robust rescue of APP CTF accumulation concomitant with a notable generation of AICD and A $\beta$  (Fig. 6*A*). In sharp contrast, the PS1 L383F mutant was defective in the processing of Notch as judged from the strong reduction in NICD and F-N $\beta$  formation (Fig. 6*B*). Thus, the L383 residue within the GxGD motif is also required in PS1 itself for efficient processing of Notch.

#### PS1 L383F is deficient in Notch signaling

To further substantiate the above findings, we examined the above constructs for their activity to rescue the *sel-12* mutant

**Table 2. Activity of the different PS1/SPE-4 hybrid proteins to rescue the *sel-12* Egl defect**

Strain	Transgene <sup>a</sup>	Genotype	Egg-laying behavior <sup>b</sup>			
			+++	++	+	–
N2		Wild type	50	0	0	0
BR1129		<i>sel-12(ar171)</i>	0	0	0	50
BR3537	PS1	<i>sel-12(ar171)</i>	48	1	1	0
BR3538	PS1/SPE-4 <sub>6</sub>	<i>sel-12(ar171)</i>	46	2	2	0
BR3539	PS1/SPE-4 <sub>6</sub>	<i>sel-12(ar171)</i>	48	0	2	0
BR3540	PS1/SPE-4 <sub>7</sub>	<i>sel-12(ar171)</i>	0	0	3	47
BR3541	PS1/SPE-4 <sub>7</sub>	<i>sel-12(ar171)</i>	0	1	1	48
BR3552	PS1/SPE-4 <sub>7</sub> F392L	<i>sel-12(ar171)</i>	10	10	19	11
BR3544	PS1/SPE-4 <sub>7</sub> F392L	<i>sel-12(ar171)</i>	11	19	15	5
BR3546	PS1/SPE-4 <sub>7</sub> F392M	<i>sel-12(ar171)</i>	10	8	25	7
BR3547	PS1/SPE-4 <sub>7</sub> F392M	<i>sel-12(ar171)</i>	17	14	10	9
BR3549	PS1 L383F	<i>sel-12(ar171)</i>	0	1	4	45
BR3550	PS1 L383F	<i>sel-12(ar171)</i>	0	0	2	48

<sup>a</sup>All constructs used were H<sub>6</sub>X-tagged at their N termini. For all constructs, at least three independent lines were tested; only two representative lines are shown.

<sup>b</sup>For each transgenic animal, the number of eggs laid were counted and were grouped into the following categories: ++++, >50 eggs of progeny laid by an individual animal; +++, 15–50 eggs laid; ++, 5–15 eggs laid; +, 0–5 eggs laid.

deficiency in Notch signaling *in vivo*. The PS1/SPE-4<sub>6</sub>, PS1/SPE-4<sub>7</sub>, PS1/SPE-4<sub>7</sub> F392L, and PS1/SPE-4<sub>7</sub> F392M mutants and PS1 L383F were expressed under the control of the *sel-12* promoter in the transgenic animals was scored (Table 2). As expected from the above results, PS1/SPE-4<sub>6</sub> rescued the Egl phenotype, whereas, consistent with its defect in Notch processing, PS1/SPE-4<sub>7</sub> did not. The PS1/SPE-4<sub>7</sub> F392L and PS1/SPE-4<sub>7</sub> F392M mutants, which comprise the GLGD motif of PS1 or SEL-12 or the GMGD motif of HOP-1, respectively, showed lesser but still considerable rescuing activity. PS1 L383F, restoring the GFGD motif of SPE-4, was not able to rescue the *sel-12* mutant phenotype. Thus, these data confirm *in vivo* that the presence of a phenylalanine residue at position x of the GxGD motif strongly impairs Notch signaling.

## Discussion

In this study, using an active site domain swapping approach of PS1 with its most distant homolog SPE-4, we obtained evidence that the PS active site domain is implicated in APP/Notch substrate selectivity of  $\gamma$ -secretase. The active site chimera PS1/SPE-4<sub>6/7</sub> that we generated was active in  $\gamma$ -secretase complex formation, underwent endoproteolysis, and displayed robust  $\gamma$ -secretase activity in APP processing. Both endoproteolysis and  $\gamma$ -secretase activity were dependent on an active site aspartate. This is the first demonstration that  $\gamma$ -secretase can function with a related but not identical active site domain in its catalytic subunit PS. Interestingly, despite its  $\gamma$ -secretase activity in APP processing, PS1/SPE-4<sub>6/7</sub> was deficient in processing of Notch. In agreement with this finding, we found that, in contrast to wt PS1, PS1/SPE-4<sub>6/7</sub> failed to rescue the Notch signaling-deficient *C. elegans sel-12(ar171)* mutant. These data indicated that the active site domain of SPE-4 in TMDs 6 and 7 could discriminate substrates such that processing of one substrate (APP) remains possible, whereas that of another substrate (Notch) is greatly impaired. Mapping of the molecular basis for the underlying substrate discrimination between APP and Notch revealed a single amino acid difference in TMD7 as responsible site. This difference was identified as a phenylalanine at position x of the conserved GxGD motif. In the PS family of proteases, x is typically the aliphatic amino acid leucine, with the exceptions of the *C. elegans* homologs HOP-1 and SPE-4. Whereas a methionine is

found instead of leucine in HOP-1, a rather strong amino acid exchange is present in SPE-4 with the aromatic phenylalanine. The phenylalanine is conserved in the SPE-4 homologs of the related nematodes *Caenorhabditis remanei* (data not shown) and *Caenorhabditis briggsae*, suggesting that it is an essential residue of the GxGD motif of SPE-4. We found that changing the phenylalanine to leucine or methionine to restore the GLGD or GMGD active site motifs of PS1, PS2, and SEL-12 or HOP-1, respectively, allowed recovery of Notch processing and significant activity in Notch signaling *in vivo*. The significance of the amino acid change could be further corroborated when we mutated the corresponding leucine in PS1 to phenylalanine. The PS1 L383F mutant allowed substantial APP processing but was strongly impaired in Notch processing and Notch signaling *in vivo*. This observation suggests that the residue at position x of the GxGD motif is not only of critical relevance for Notch processing in the PS1/SPE-4<sub>6/7</sub> hybrid but of general importance for Notch processing in all PSs.

The activity of PS1/SPE-4<sub>6/7</sub> in PS endoproteolysis and  $\gamma$ -secretase activity on APP processing also implies that SPE-4 itself has a proteolytic function. Because SPE-4 cannot functionally replace SEL-12, one may speculate that SPE-4 is a more specialized *C. elegans* PS protease, which may not be able to use the *C. elegans* Notch receptors as substrates because of the presence of the phenylalanine at position x in the GxGD motif. However, at present, we cannot exclude the possibility that the failure of SPE-4 to substitute for SEL-12 function may be attributable to a potential incapability of SPE-4 to undergo  $\gamma$ -secretase complex formation (as observed in mammalian cells) (data not shown). Interestingly, leucine/isoleucine–phenylalanine variations at position x in the GxGD motif are also found in and/or between the SPP/SPPL (SPP-like protease) protease families (Weihs et al., 2002). As in PSs, these differences may have an impact on substrate selectivity. Future studies will be needed to answer these questions.

Mechanistically, the presence of a phenylalanine at position x in the GxGD motif may cause subtle differences in the conformation of TMDs 6 and 7. Although such a conformational alteration has apparently little influence on APP processing, it may affect sufficient Notch binding. Alternatively, the bulky phenylalanine may interfere with the transfer of the Notch substrate from the docking site (Esler et al., 2002), a substrate-binding site outside the active site, to the active site. The existence of a substrate binding site different from the active site had been suggested previously (Annaert et al., 2001), and strong evidence for such an exosite in  $\gamma$ -secretase was obtained by coisolation of APP CTFs with  $\gamma$ -secretase using immobilized active site-directed inhibitors (Esler et al., 2002; Behr et al., 2003). The concept of a docking site has been further supported by the noncompetitive inhibition of  $\gamma$ -secretase by transition-state analog inhibitors (Tian et al., 2002, 2003). The docking site was recently shown to be located in PS in very close proximity to the active site (Kornilova et al., 2005). Interestingly, the distance between the two sites has been estimated to be less than three amino acid residues in length (Kornilova et al., 2005). Our identification of a critical amino acid involved in APP/Notch substrate selection just two residues away of an active site aspartate may thus indicate that residues of the GxGD motif, in particular L383, preceding the active site aspartate in TMD7 of PS contribute to the substrate docking site of  $\gamma$ -secretase.

Precisely how  $\gamma$ -secretase recognizes and selects substrates following the obligatory step of ectodomain shedding and recognition by NCT (Shah et al., 2005) are intriguing and challenging questions. Additional studies on these questions will not only be

of particular interest for targeting PS as the catalytic subunit of  $\gamma$ -secretase for AD treatment but should also further our understanding of intramembrane proteolysis in general.

## References

- Annaert WG, Esselens C, Baert V, Boeve C, Snellings G, Cupers P, Craessaerts K, De Strooper B (2001) Interaction with telencephalin and the amyloid precursor protein predicts a ring structure for presenilins. *Neuron* 32:579–589.
- Arduengo PM, Appleberry OK, Chuang P, L'Hernault SW (1998) The presenilin protein family member SPE-4 localizes to an ER/Golgi derived organelle and is required for proper cytoplasmic partitioning during *Caenorhabditis elegans* spermatogenesis. *J Cell Sci* 111:3645–3654.
- Baumeister R, Leimer U, Zweckbronner I, Jakubek C, Grunberg J, Haass C (1997) Human presenilin-1, but not familial Alzheimer's disease (FAD) mutants, facilitate *Caenorhabditis elegans* Notch signalling independently of proteolytic processing. *Genes Funct* 1:149–159.
- Behr D, Fricker M, Nadin A, Clarke EE, Wrigley JD, Li YM, Culvenor JG, Masters CL, Harrison T, Shearman MS (2003) *In vitro* characterization of the presenilin-dependent  $\gamma$ -secretase complex using a novel affinity ligand. *Biochemistry* 42:8133–8142.
- Capell A, Saffrich R, Olivo JC, Meyn L, Walter J, Grunberg J, Mathews P, Nixon R, Dotti C, Haass C (1997) Cellular expression and proteolytic processing of presenilin proteins is developmentally regulated during neuronal differentiation. *J Neurochem* 69:2432–2440.
- De Strooper B (2003) Aph-1, pen-2, and nicastrin with presenilin generate an active  $\gamma$ -secretase complex. *Neuron* 38:9–12.
- De Strooper B, Annaert W, Cupers P, Saftig P, Craessaerts K, Mumm JS, Schroeter EH, Schrijvers V, Wolfe MS, Ray WJ, Goate A, Kopan R (1999) A presenilin-1-dependent  $\gamma$ -secretase-like protease mediates release of Notch intracellular domain. *Nature* 398:518–522.
- Edbauer D, Winkler E, Haass C, Steiner H (2002) Presenilin and nicastrin regulate each other and determine amyloid  $\beta$ -peptide production via complex formation. *Proc Natl Acad Sci USA* 99:8666–8671.
- Edbauer D, Winkler E, Regula JT, Pesold B, Steiner H, Haass C (2003) Reconstitution of  $\gamma$ -secretase activity. *Nat Cell Biol* 5:486–488.
- Esler WP, Kimberly WT, Ostaszewski BL, Ye W, Diehl TS, Selkoe DJ, Wolfe MS (2002) Activity-dependent isolation of the presenilin- $\gamma$ -secretase complex reveals nicastrin and a  $\gamma$  substrate. *Proc Natl Acad Sci USA* 99:2720–2725.
- Francis R, McGrath G, Zhang J, Ruddy DA, Sym M, Apfeld J, Nicoll M, Maxwell M, Hai B, Ellis MC, Parks AL, Xu W, Li J, Gurney M, Myers RL, Himes CS, Hiesch RD, Ruble C, Nye JS, Curtis D (2002) aph-1 and pen-2 are required for Notch pathway signaling,  $\gamma$ -secretase cleavage of  $\beta$ APP, and presenilin protein accumulation. *Dev Cell* 3:85–97.
- Haass C (2004) Take five-BACE and the  $\gamma$ -secretase quartet conduct Alzheimer's amyloid  $\beta$ -peptide generation. *EMBO J* 23:483–488.
- Haass C, Steiner H (2002) Alzheimer disease  $\gamma$ -secretase: a complex story of GxGD-type presenilin proteases. *Trends Cell Biol* 12:556–562.
- Hebert SS, Serneels L, Dejaegere T, Horre K, Dabrowski M, Baert V, Annaert W, Hartmann D, De Strooper B (2004) Coordinated and widespread expression of  $\gamma$ -secretase in vivo: evidence for size and molecular heterogeneity. *Neurobiol Dis* 17:260–272.
- Henricson A, Kall L, Sonnhammer EL (2005) A novel transmembrane topology of presenilin based on reconciling experimental and computational evidence. *FEBS J* 272:2727–2733.
- Herreman A, Hartmann D, Annaert W, Saftig P, Craessaerts K, Serneels L, Umans L, Schrijvers V, Checler F, Vanderstichele H, Baekelandt V, Dressel R, Cupers P, Huylebroeck D, Zwijsen A, Van Leuven F, De Strooper B (1999) Presenilin 2 deficiency causes a mild pulmonary phenotype and no changes in amyloid precursor protein processing but enhances the embryonic lethal phenotype of presenilin 1 deficiency. *Proc Natl Acad Sci USA* 96:11872–11877.
- Herreman A, Serneels L, Annaert W, Collen D, Schoonjans L, De Strooper B (2000) Total inactivation of  $\gamma$ -secretase activity in presenilin-deficient embryonic stem cells. *Nat Cell Biol* 2:461–462.
- Kaether C, Capell A, Edbauer D, Winkler E, Novak B, Steiner H, Haass C (2004) The presenilin C-terminus is required for ER-retention, nicastrin-binding and  $\gamma$ -secretase activity. *EMBO J* 23:4738–4748.
- Kim SH, Ikeuchi T, Yu C, Sisodia SS (2003) Regulated hyperaccumulation of presenilin-1 and the " $\gamma$ -secretase" complex. Evidence for differential intramembraneous processing of transmembrane substrates. *J Biol Chem* 278:33992–34002.
- Kimberly WT, LaVoie MJ, Ostaszewski BL, Ye W, Wolfe MS, Selkoe DJ (2003)  $\gamma$ -Secretase is a membrane protein complex comprised of presenilin, nicastrin, Aph-1, and Pen-2. *Proc Natl Acad Sci USA* 100:6382–6387.
- Kopan R, Ilgan MX (2004)  $\gamma$ -Secretase: proteasome of the membrane? *Nat Rev Mol Cell Biol* 5:499–504.
- Kornilova AY, Bihel F, Das C, Wolfe MS (2005) The initial substrate-binding site of  $\gamma$ -secretase is located on presenilin near the active site. *Proc Natl Acad Sci USA* 102:3230–3235.
- Krawitz P, Haffner C, Fluhrer R, Steiner H, Schmid B, Haass C (2005) Differential localization and identification of a critical aspartate suggest non-redundant proteolytic functions of the presenilin homologues SPPL2b and SPPL3. *J Biol Chem* 280:39515–39523.
- Lai EC (2004) Notch signaling: control of cell communication and cell fate. *Development* 131:965–973.
- LaPointe CF, Taylor RK (2000) The type 4 prepilin peptidases comprise a novel family of aspartic acid proteases. *J Biol Chem* 275:1502–1510.
- Laudon H, Hansson EM, Melen K, Bergman A, Farmery MR, Winblad B, Lendahl U, von Heijne G, Naslund J (2005) A nine-transmembrane domain topology for presenilin 1. *J Biol Chem* 280:35352–35360.
- Leem JY, Vijayan S, Han P, Cai D, Machura M, Lopes KO, Veselits ML, Xu H, Thinakaran G (2002) Presenilin 1 is required for maturation and cell surface accumulation of nicastrin. *J Biol Chem* 277:19236–19240.
- Leviton D, Greenwald I (1995) Facilitation of lin-12-mediated signalling by sel-12, a *Caenorhabditis elegans* S182 Alzheimer's disease gene. *Nature* 377:351–354.
- Leviton D, Doyle TG, Brousseau D, Lee MK, Thinakaran G, Slunt HH, Sisodia SS, Greenwald I (1996) Assessment of normal and mutant human presenilin function in *Caenorhabditis elegans*. *Proc Natl Acad Sci USA* 93:14940–14944.
- L'Hernault SW, Arduengo PM (1992) Mutation of a putative sperm membrane protein in *Caenorhabditis elegans* prevents sperm differentiation but not its associated meiotic divisions. *J Cell Biol* 119:55–68.
- Li X, Greenwald I (1997) HOP-1, a *Caenorhabditis elegans* presenilin, appears to be functionally redundant with SEL-12 presenilin and to facilitate LIN-12 and GLP-1 signaling. *Proc Natl Acad Sci USA* 94:12204–12209.
- Nyabi O, Bentahir M, Horre K, Herreman A, Gottardi-Littell N, Van Broeckhoven C, Merchiers P, Spittaels K, Annaert W, De Strooper B (2003) Presenilins mutated at Asp257 or Asp385 restore Pen-2 expression and Nicastrin glycosylation but remain catalytically inactive in the absence of wild type Presenilin. *J Biol Chem* 278:43430–43436.
- Oh YS, Turner RJ (2005) Evidence that the COOH terminus of human presenilin 1 is located in extracytoplasmic space. *Am J Physiol* 289:C576–C581.
- Okochi M, Steiner H, Fukumori A, Tani H, Tomita T, Tanaka T, Iwatsubo T, Kudo T, Takeda M, Haass C (2002) Presenilins mediate a dual intramembraneous  $\gamma$ -secretase cleavage of Notch, which is required for signaling and removal of the transmembrane domain. *EMBO J* 21:5408–5416.
- Shah S, Lee SF, Tabuchi K, Hao YH, Yu C, Laplant Q, Ball H, Dann III CE, Sudhof T, Yu G (2005) Nicastrin functions as a  $\gamma$ -secretase-substrate receptor. *Cell* 122:435–447.
- Shirotani K, Edbauer D, Prokop S, Haass C, Steiner H (2004) Identification of distinct  $\gamma$ -secretase complexes with different APH-1 variants. *J Biol Chem* 279:41340–41345.
- Steiner H (2004) Uncovering  $\gamma$ -secretase. *Curr Alzheimer Res* 1:175–181.
- Steiner H, Duff K, Capell A, Romig H, Grim MG, Lincoln S, Hardy J, Yu X, Picciano M, Fichteler K, Citron M, Kopan R, Pesold B, Keck S, Baader M, Tomita T, Iwatsubo T, Baumeister R, Haass C (1999) A loss of function mutation of presenilin-2 interferes with amyloid  $\beta$ -peptide production and Notch signaling. *J Biol Chem* 274:28669–28673.
- Steiner H, Kostka M, Romig H, Basset G, Pesold B, Hardy J, Capell A, Meyn L, Grim MG, Baumeister R, Fichteler K, Haass C (2000) Glycine 384 is required for presenilin-1 function and is conserved in polytopic bacterial aspartyl proteases. *Nat Cell Biol* 2:848–851.
- Steiner H, Winkler E, Edbauer D, Prokop S, Basset G, Yamasaki A, Kostka M, Haass C (2002) PEN-2 is an integral component of the  $\gamma$ -secretase complex required for coordinated expression of presenilin and nicastrin. *J Biol Chem* 277:39062–39065.

- Struhl G, Adachi A (2000) Requirements for presenilin-dependent cleavage of Notch and other transmembrane proteins. *Mol Cell* 6:625–636.
- Takasugi N, Takahashi Y, Morohashi Y, Tomita T, Iwatsubo T (2002) The mechanism of  $\gamma$ -secretase activities through high molecular weight complex formation of presenilins is conserved in *Drosophila melanogaster* and mammals. *J Biol Chem* 277:50198–50205.
- Takasugi N, Tomita T, Hayashi I, Tsuruoka M, Niimura M, Takahashi Y, Thinakaran G, Iwatsubo T (2003) The role of presenilin cofactors in the  $\gamma$ -secretase complex. *Nature* 422:438–441.
- Thinakaran G, Borchelt DR, Lee MK, Slunt HH, Spitzer L, Kim G, Ratovitsky T, Davenport F, Nordstedt C, Seeger M, Hardy J, Levey AI, Gandy SE, Jenkins NA, Copeland NG, Price DL, Sisodia SS (1996) Endoproteolysis of presenilin 1 and accumulation of processed derivatives in vivo. *Neuron* 17:181–190.
- Tian G, Sobotka-Briner CD, Zysk J, Liu X, Birr C, Sylvester MA, Edwards PD, Scott CD, Greenberg BD (2002) Linear non-competitive inhibition of solubilized human  $\gamma$ -secretase by pepstatin A methylester, L685458, sulfonamides, and benzodiazepines. *J Biol Chem* 277:31499–31505.
- Tian G, Ghanekar SV, Aharony D, Shenvi AB, Jacobs RT, Liu X, Greenberg BD (2003) The mechanism of  $\gamma$ -secretase: multiple inhibitor binding sites for transition state analogs and small molecule inhibitors. *J Biol Chem* 278:28968–28975.
- Tomita T, Watabiki T, Takikawa R, Morohashi Y, Takasugi N, Kopan R, De Strooper B, Iwatsubo T (2001) The first proline of PALP motif at the C terminus of presenilins is obligatory for stabilization, complex formation and  $\gamma$ -secretase activities of presenilins. *J Biol Chem* 276:33273–33281.
- Wacker I, Kaether C, Kromer A, Migala A, Almers W, Gerdes HH (1997) Microtubule-dependent transport of secretory vesicles visualized in real time with a GFP-tagged secretory protein. *J Cell Sci* 110:1453–1463.
- Wang J, Brunkan AL, Hecimovic S, Walker E, Goate A (2004) Conserved “PAL” sequence in presenilins is essential for  $\gamma$ -secretase activity, but not required for formation or stabilization of  $\gamma$ -secretase complexes. *Neurobiol Dis* 15:654–666.
- Weihofen A, Binns K, Lemberg MK, Ashman K, Martoglio B (2002) Identification of signal peptide peptidase, a presenilin-type aspartic protease. *Science* 296:2215–2218.
- Westlund B, Parry D, Clover R, Basson M, Johnson CD (1999) Reverse genetic analysis of *Caenorhabditis elegans* presenilins reveals redundant but unequal roles for sel-12 and hop-1 in Notch-pathway signaling. *Proc Natl Acad Sci USA* 96:2497–2502.
- Wittenburg N, Eimer S, Lakowski B, Rohrig S, Rudolph C, Baumeister R (2000) Presenilin is required for proper morphology and function of neurons in *C. elegans*. *Nature* 406:306–309.
- Wolfe MS, Xia W, Ostaszewski BL, Diehl TS, Kimberly WT, Selkoe DJ (1999) Two transmembrane aspartates in presenilin-1 required for presenilin endoproteolysis and  $\gamma$ -secretase activity. *Nature* 398:513–517.
- Zhang Z, Nadeau P, Song W, Donoviel D, Yuan M, Bernstein A, Yankner BA (2000) Presenilins are required for  $\gamma$ -secretase cleavage of  $\beta$ APP and transmembrane cleavage of Notch-1. *Nat Cell Biol* 2:463–465.